

1 C 66 b

SLOVAK GEOLOGICAL MAGAZINE



DIONÝZ ŠTÚR PUBLISHERS, BRATISLAVA

2/96

SLOVAK GEOLOGICAL MAGAZINE

Periodical of Geological Survey of Slovak Republic is a quarterly presenting the results of investigation and researches in a wide range of topics:

- regional geology and geological maps
- lithology and stratigraphy
- petrology and mineralogy
- paleontology
- geochemistry and isotope geology
- geophysics and deep structure
- geology of deposits and metallogeny
- tectonics and structural geology
- hydrogeology and geothermal energy
- environmental geochemistry
- engineering geology and geotechnology
- geological factors of the environment

The journal is focused on problems of the Alpine-Carpathian region.

Editor in Chief: JOZEF VOZÁR

Editorial Board:

| INTERNAL MEMBER | | EXTERNAL MEMBERS | |
|-----------------|---------------|-----------------------|----------|
| Vladimír Bezák | Peter Kováč | Dimitros Papanikolaou | Athens |
| Dušan Bodiš | Jaroslav Lexa | Franz Neubauer | Salzburg |
| Michal Elečko | Ján Mello | Jan Veizer | Bochum |
| Milan Gargulák | Milan Polák | Franco Paolo Sassi | Padova |
| Pavol Grecula | Michal Potfaj | Niek Rengers | Enschede |
| Vladimír Hanzel | Miloš Rakús | Géza Császár | Budapest |
| Jozef Határ | Dionýz Vass | Miloš Suk | Brno |
| Michal Kaličiak | Anna Vozárová | Zdeněk Kukal | Praha |
| Alena Klukanová | | | |

Managing Editor: J. HRTUSOVÁ

Language review and translation: B. MOLÁK

Technical Editor: G. ŠIPOŠOVÁ

**Address of the publisher: GEOLOGICAL SURVEY OF SLOVAK REPUBLIC, MLYNSKÁ DOLINA 1,
817 04 BRATISLAVA, SLOVAKIA**

Typography: G. ŠIPOŠOVÁ

Printed at: DUAD-Print Bratislava

Price of single issue: USD12

Annual subscription rate: USD 48 (4 issues) The price include the postage

© Edition of Geological Survey of Slovak Republic, Mlynská dolina 1, 817 04 Bratislava, SLOVAKIA

Ústredná geologická knižnica SR
ŠGÚDŠ



3902001018569

SLOVAK GEOLOGICAL MAGAZINE



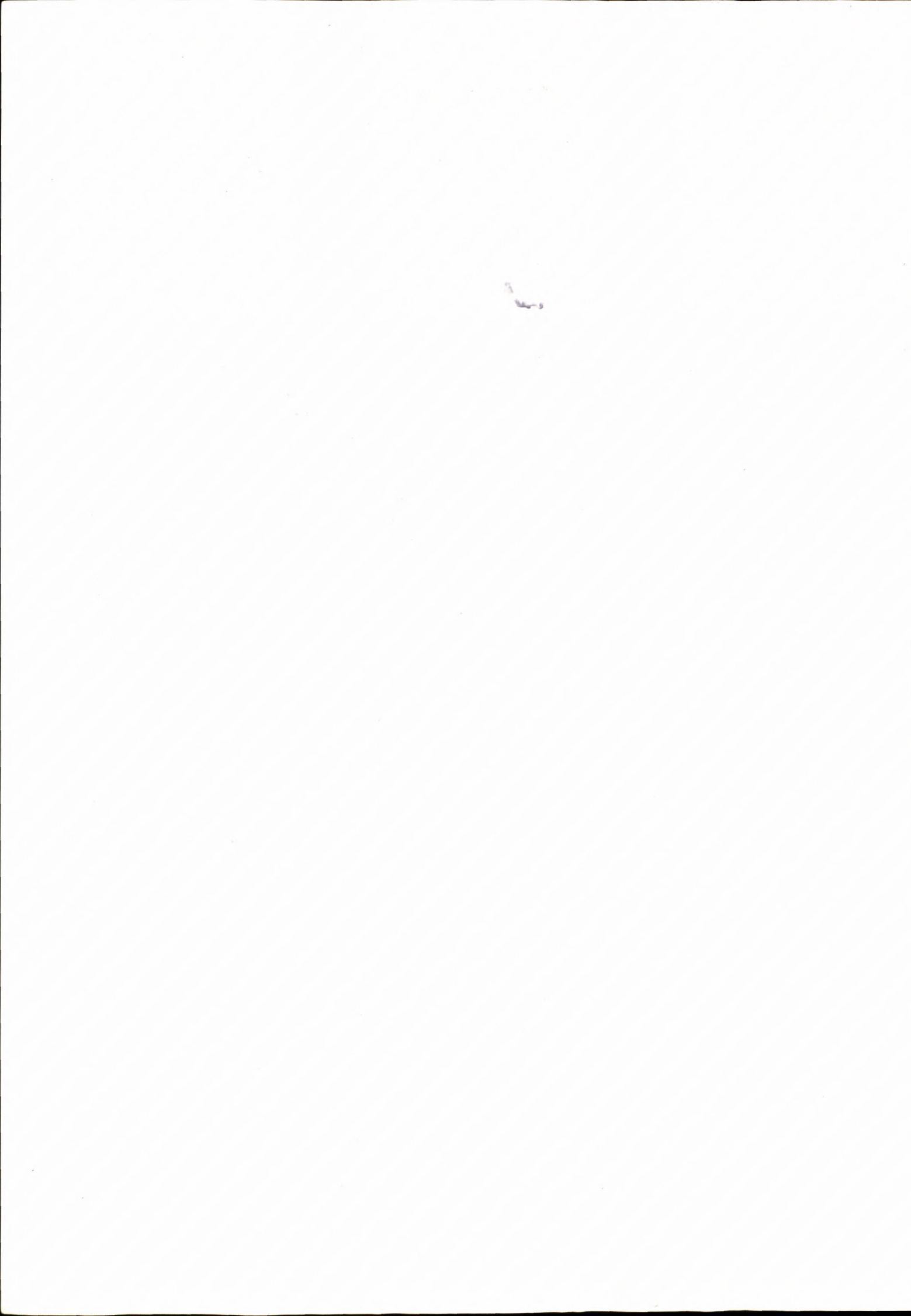
DIONÝZ ŠTÚR PUBLISHERS, BRATISLAVA

2/96



Contents

| | |
|--|-----|
| KATERINOPOULOS A., KOKKINAKIS A. and KYRIAKOPOULOS K.: Mineralogy, Petrology and Chemistry of the Fotino Granitic Rocks, Thessaly, Central Greece _____ | 87 |
| ŠIMON L. and HALOUZKA R.: Pútikov vršok volcano - the youngest volcano in the Western Carpathians _____ | 103 |
| HALÁSOVÁ E., HUDAČKOVÁ N., HOLCOVÁ K., VASS D., ELEČKO M. and PERESZLÉNYI M.: Sea ways connecting the Fiľakovo/Pétervására Basin with the Eggenburgian/Burdigalian open sea ____ | 125 |
| KOVÁČ P. and HÓK J.: Tertiary Development of the Western Part of Klippen Belt _____ | 137 |
| JACKO S., SASVÁRI T., ZACHAROV M., SCHMIDT R. and VOZÁR J.: Contrasting styles of Alpine deformations at the eastern part of the Veporicum and Gemericum units, Western Carpathians ____ | 151 |
| FENDEK M.: Distributed Parameter Model for the Laugarnes Geothermal Field - SW Iceland _____ | 165 |



Mineralogy, Petrology and Chemistry of the Fotino Granitic Rocks, Thessaly, Central Greece.

ATHANASSIOS KATERINOPOULOS¹, ANDREAS KOKKINAKIS¹ and KONSTANTINOS KYRIAKOPOULOS¹

Section of Mineralogy and Petrology, Department of Geology, University of Athens, Panepistimiopolis, Ano Ilissia, GR-15784.

Abstract. The studied plutonic rocks are granites, presenting S-type characteristics. The mineral constituents have been studied by optical and chemical methods. The whole rock chemistry is studied in terms of major, trace and REE analyses. The petrography of the granites is described and the crystallisation sequence is discussed.

Major and trace elements show continuous smooth variation trends and REE patterns, with high LREE/HREE ratios, indicating a distribution strongly controlled by the fractionation of feldspars. The mantle normalised patterns show high LIL/HFS element ratios and negative Nb, Ti and P anomalies.

Fotino granites yielded muscovite ages ranging from 273 to 225 Ma, while the geochemical features suggest an increased crustal involvement to the composition of the parental magma. These magmas should have been generated in a subduction-related geotectonic environment, which has been active during the formation of the Hercynian fold belt.

Key words: Granite, Petrology, Geochemistry, Greece.

Introduction

The granitic intrusion in Fotino area was mapped by STAMATIS (1987). In this map a quartz monzonite body appears near Fotino village (Fig. 1), another one exists near Deskati village, while small occurrences of granite, granodiorite and quartz diorite are spread in the area.

KILIAS & MOUNTRAKIS (1989) studied the geotectonic evolution of the area on the basis of field relationship data. STAMATIS (1987) gave a short description of the petrographic types and a reference to their mineral constituents in the relative map.

For the purposes of this study, rock samples from the Fotino granitic rocks have been collected, studied for their petrography and analysed for their mineral chemistry and their major, trace and rare earth element composition. Petrogenetic features of the plutonic rocks are depicted from the correlation of the above data.

Geologic setting

The Fotino plutonic rocks intrude the Pieria-Kamvounia crystalline massif, a structural element of the

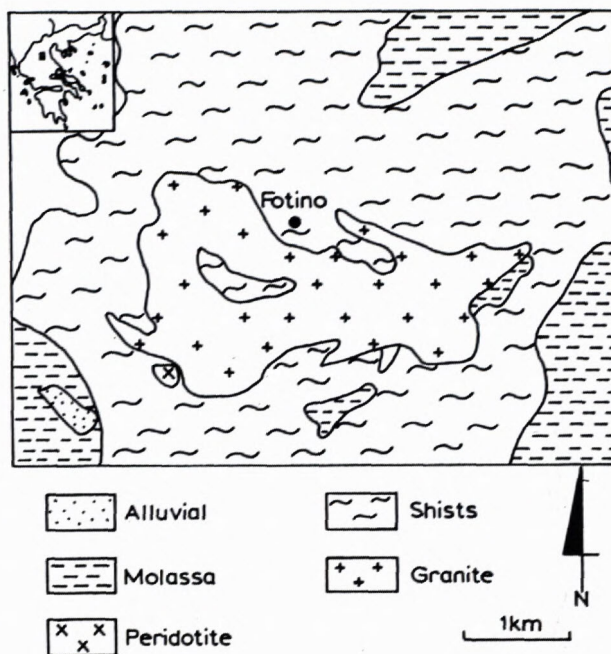


Fig. 1 Sketch map of the studied area

Pelagonian Nappe. According to KILIAS & MOUNTRAKIS (1989) the Pelagonian Nappe consists of:

- Limestones of Middle to Upper Cretaceous transgression and the Paleocene flysch.
- The western carbonate cover of Triassic to Jurassic age.
- The eastern carbonate cover of Triassic to Jurassic age.
- A metaclastic sequence of Late Permian - Early Triassic age.
- Three crystalline sequences (Vernon, Voras and Pieria-Kamvounia).
- Large granitic masses of different ages.

These crystalline sequences crystallised under similar conditions in the Paleozoic, but then they suffered different tectonic events as they present differences in their megastructure and their kinematics.

The Pieria-Kamvounia massif is characterised by a lower "Elassona" sequence, consisting of gneisses and amphibolites with migmatitic interpositions and an upper

Kefalovrysson" sequence consisting of schists with metabasite and marble intercalations.

According to KILIAS & MOUNTRAKIS (1989) the lithological and tectonic study indicates that the granites intruded the metamorphic rocks probably during Upper Jurassic-Lower Cretaceous.

In the Upper Cretaceous - Palaeocene the Pieria-Kamvounia crystalline massif overthrusts the blueschists of the Ambelakia unit and in Upper Eocene it is overthrust onto the carbonate masses of Olympos-Ossa, Rizomata and Krania carbonate sequences (MIGIROS 1983, KATSIKATSOS et al. 1986).

Sampling and analytical methods

Sampling was carried out with special care to collect unaltered samples from well preserved outcrops. The chemical analyses were made in the Department of Geology at the University of Leicester, England.

The mineral phases have been studied by polarised microscope and analysed by an automatic electron microprobe (JXA-8600 Superprobe) using the Energy Dispersive method. The standards used were of pure elements or natural compounds.

Major and trace element analyses were carried out by X-ray fluorescence method using a Philips PW 1400 series spectrometer. Details on the analytical procedure, precision and accuracy on the analytical techniques are given in MARSH et al (1983).

Rare earth elements were separated by chromatography and determined by inductive-couple plasma spectroscopy on an ICP Philips PW 8210 1.5 m.

Rb-Sr isotope analyses have been carried out at the Institute of Geochronology and Isotopic Geochemistry, CNR of Pisa, Italy, using a VG Isomass 54E mass spectrometer. The precision of the $^{87}\text{Rb}/^{86}\text{Sr}$ ratio determination has been estimated at $\pm 1\%$. The value of $1.42 \times 10^{-11} \text{ y}^{-1}$ was used for the ^{87}Rb decay constant. The mica ages were calculated adapting a $^{87}\text{Sr}/^{86}\text{Sr}$ correction of the corresponding whole rocks.

Mineralogy

a. Quartz: It is the most abundant mineral constituent, forming about 35 % of the studied samples. Primary quartz occurs in the form of irregular grains, as porphyroclasts or as aggregates consisting of randomly situated grains. Tectonism caused strong undulose extinction and biaxial optical character. Recrystallised quartz occurs in the form of small elongated grains, with irregular, interpenetrated edges, generally presenting a normal or a very weak undulose extinction.

b. Feldspars

b. 1. K-feldspar: Crosshatched microcline perthite is the dominant potassium feldspar forming about 35 % of the studied rocks. It is present in the form of porphyroclasts, or as allotriomorphic interstitial grains. Almost all large microcline grains present the tartan twinning, while the smaller ones are usually twinning free.

Vein-perthites are very common. In all cases, perthites and host microcline grains have the same optical orientation. Albite inclusions are usual, while zircon, apatite and allanite inclusions are rare. Results of representative chemical analyses of K-feldspars and their structural formulae recalculated on the basis of 32 (O) are shown in Tables 1 and 2.

b. 2. Plagioclase: It is present in the form of stressed grains and fragments, or in aggregates composed of allotriomorphic isodiametric porphyroclasts of albite or oligoclase. It is often replaced by K-feldspar and decomposed to quartz, sericite, epidote, titanite and garnet. Some of the chemical constituents of these secondary products result from the decomposition of neighbouring biotite crystals.

The larger grains present twinning according to the albite low and rarely to the pericline or karlsbad ones. Representative chemical analyses of Na-Ca-feldspars and their structural formulae recalculated on the basis of 22 (O) are listed in Tables 3 and 4.

b. 3. Inclusions: Both sodium and potassium feldspars are included in larger albite and microcline crystals. Chemical analyses of included feldspars and their structural formulae recalculated on the basis of 32 (O) are given in Table 5.

c. Micas

c. 1. Muscovite: It is present in all the studied samples, appearing in idiomorphic weakly pleochroic crystals, with an elongation ratio usually ranging from 2 to 4. In most cases it replaces biotite or plagioclase. This replacement of primary minerals by muscovite is usually developed parallel to the cleavage and twinning surfaces, or along cracks. The so formed fine sericite flakes are arranged parallel to the above mentioned surfaces.

Larger muscovite crystals bear on the outer surfaces, or along the cleavage and cracks, small isodiametric opaque mineral grains. Representative analyses of muscovite along with their structural formulae based on 22 [O] are shown in Table 6.

c. 2. Biotite: It occurs in small amounts, so it can be considered an accessory mineral in most cases. It usually appears as idiomorphic to hypidiomorphic flakes.

Most biotite crystals have been mechanically deformed so that the elongation ratio ranges from 10 to 20 and decomposed to sericite, epidote, titanite, magnetite apatite and garnet, pseudomorphically developed. The decomposition of adjacent feldspar crystals provided the necessary Ca, Si, Al, and K for these phases.

The biotite flakes are iron enriched, so their colour is dark brownish-red parallel to (001) and brown perpendicular to (001). Results of representative chemical analyses of biotites and their structural formulae recalculated on the basis of 22 (O) are listed in Table 6.

d. Accessory minerals: Accessory phases include titanite, epidote, allanite, zircon, garnet, apatite and opaque minerals.

d. 1. Titanite appears as fragments of unhexagonal crystals, honey-brown in colour. Analyses recalculated on the basis of 20 [O] are given in Table 7.

d. 2. Epidote appears in the form of allotriomorphic grains replacing mainly plagioclase and biotite, in association with muscovite, titanite and spinel. It also forms microcrystalline covers around allanite grains. They are weakly pleochroic, with Y intense yellow-green, Z yellow-green and X greenish-yellow. Chemical analyses recalculated on the basis of 25 [O] are given in Table 8, along with the composition expressed in terms of the theoretical end member Ps.

d. 3. Allanite grains occur as porphyroclasts, or as inclusions. The porphyroclasts are strongly pleochroic, parallel to Y dark brown, almost opaque, parallel to Z brownish-red and parallel to X yellowish-grey. They are usually surfaced by an epidote cover.

Table 1. Representative chemical analyses of K-feldspars.

| | FT10/104 | FT10/108 | FT10/111 | FT6/5 | FT6/6 | FT6/8 | FT6/11 |
|---------------------------------------|----------|----------|----------|-------|-------|-------|--------|
| SiO ₂ | 64.37 | 64.88 | 64.37 | 64.82 | 64.79 | 64.77 | 64.42 |
| Al ₂ O ₃ | 18.16 | 18.26 | 18.06 | 18.17 | 18.06 | 18.08 | 18.07 |
| FeO | 0.03 | 0.01 | 0.04 | 0.04 | 0.01 | 0.01 | 0.03 |
| CaO | 0.01 | 0.01 | 0.01 | 0.01 | 0.01 | 0.01 | 0.01 |
| Na ₂ O | 0.38 | 0.37 | 0.36 | 0.33 | 0.26 | 0.33 | 0.3 |
| K ₂ O | 16.39 | 16.61 | 16.5 | 16.61 | 16.84 | 16.59 | 16.69 |
| TOTAL | 99.34 | 100.14 | 99.34 | 99.98 | 99.97 | 99.79 | 99.52 |
| Z | 15.99 | 15.98 | 15.97 | 15.98 | 15.97 | 15.98 | 15.97 |
| X | 4.04 | 4.06 | 4.06 | 4.05 | 4.08 | 4.05 | 4.08 |
| Or | 96.44 | 96.64 | 96.59 | 96.87 | 97.62 | 96.98 | 97.18 |
| Ab | 3.40 | 3.27 | 3.20 | 2.93 | 2.29 | 2.93 | 2.65 |
| An | 0.17 | 0.09 | 0.20 | 0.20 | 0.09 | 0.09 | 0.16 |
| Number of ions on the basis of 32 [O] | | | | | | | |
| Si | 12.00 | 12.00 | 12.00 | 12.01 | 12.02 | 12.02 | 12.00 |
| Al | 3.99 | 3.98 | 3.97 | 3.97 | 3.95 | 3.95 | 3.97 |
| Fe | 0.00 | 0.00 | 0.01 | 0.01 | 0.00 | 0.00 | 0.00 |
| Ca | 0.00 | 0.00 | 0.00 | 0.00 | 0.00 | 0.00 | 0.00 |
| Na | 0.14 | 0.13 | 0.13 | 0.12 | 0.09 | 0.12 | 0.11 |
| K | 3.90 | 3.92 | 3.93 | 3.93 | 3.98 | 3.93 | 3.97 |

Table 2. Representative chemical analyses of zoned K-feldspars.

| | FT6/22c | FT6/22r | FT10/86c | FT10/86r | FT10/96c | FT10/96r |
|---------------------------------------|---------|---------|----------|----------|----------|----------|
| SiO ₂ | 64.92 | 64.86 | 65.07 | 63.52 | 62.63 | 64.11 |
| Al ₂ O ₃ | 18.2 | 18.17 | 18.3 | 17.78 | 17.33 | 18.05 |
| FeO | 0.03 | 0.05 | 0.03 | 0.04 | 0.22 | 0.04 |
| CaO | 0.01 | 0.01 | 0.02 | 0.04 | 0.12 | 0.01 |
| Na ₂ O | 0.32 | 0.29 | 1.19 | 1.03 | 0.39 | 0.41 |
| K ₂ O | 16.44 | 16.61 | 14.99 | 15.25 | 15.16 | 16.16 |
| TOTAL | 99.92 | 99.99 | 99.6 | 97.66 | 95.85 | 98.78 |
| Z | 15.99 | 15.98 | 16.00 | 15.97 | 15.99 | 15.99 |
| X | 4.00 | 4.04 | 3.97 | 4.07 | 3.93 | 4.02 |
| Or | 96.97 | 97.18 | 89.04 | 90.37 | 94.76 | 96.09 |
| Ab | 2.87 | 2.58 | 10.74 | 9.28 | 3.71 | 3.71 |
| An | 0.17 | 0.24 | 0.22 | 0.35 | 1.53 | 0.21 |
| Number of ions on the basis of 32 [O] | | | | | | |
| Si | 12.02 | 12.01 | 12.02 | 12.01 | 12.05 | 12.01 |
| Al | 3.97 | 3.97 | 3.98 | 3.96 | 3.93 | 3.98 |
| Fe | 0.00 | 0.01 | 0.00 | 0.01 | 0.04 | 0.01 |
| Ca | 0.00 | 0.00 | 0.00 | 0.01 | 0.02 | 0.00 |
| Na | 0.11 | 0.10 | 0.43 | 0.38 | 0.15 | 0.15 |
| K | 3.88 | 3.92 | 3.53 | 3.68 | 3.72 | 3.86 |
| SiO ₂ | 64.61 | 64.82 | 64.44 | 68.76 | 67.65 | 64.80 |
| Al ₂ O ₃ | 18.14 | 18.1 | 18.10 | 17.84 | 19.07 | 18.28 |
| FeO | 0.01 | 0.04 | 0.02 | 0.24 | 0.11 | 0.01 |
| CaO | 0.01 | 0.01 | 0.01 | 0.27 | 0.32 | 0.01 |
| Na ₂ O | 0.48 | 0.29 | 0.34 | 8.80 | 11.04 | 0.31 |
| K ₂ O | 16.24 | 16.4 | 16.53 | 3.82 | 1.15 | 16.62 |
| TOTAL | 99.49 | 99.66 | 99.44 | 99.73 | 99.34 | 100.03 |
| Z | 15.99 | 15.99 | 15.98 | 15.92 | 15.94 | 15.99 |
| X | 4.03 | 4.00 | 4.06 | 3.98 | 4.12 | 4.04 |
| Or | 95.62 | 97.18 | 96.85 | 21.73 | 6.29 | 97.16 |
| Ab | 4.30 | 2.61 | 3.03 | 76.08 | 91.84 | 2.75 |
| An | 0.09 | 0.21 | 0.13 | 2.19 | 1.87 | 0.09 |

Table 2, continue.

Number of ions on the basis of 32 [O]

| | | | | | | |
|----|-------|-------|-------|-------|-------|-------|
| Si | 12.01 | 12.03 | 12.00 | 12.19 | 11.97 | 12.00 |
| Al | 3.97 | 3.96 | 3.97 | 3.73 | 3.98 | 3.99 |
| Fe | 0.00 | 0.01 | 0.00 | 0.04 | 0.02 | 0.00 |
| Ca | 0.00 | 0.00 | 0.00 | 0.05 | 0.06 | 0.00 |
| Na | 0.17 | 0.10 | 0.12 | 3.02 | 3.79 | 0.11 |
| K | 3.85 | 3.88 | 3.93 | 0.86 | 0.26 | 3.93 |

c : core r : rim

Table 3. Representative chemical analyses of plagioclases.

| | FT10/103 | FT10/107 | FT6/40 | FT8/9 | FT8/10 | FT8/13 |
|--------------------------------|----------|----------|--------|-------|--------|--------|
| SiO ₂ | 67.48 | 68.73 | 68.15 | 67.04 | 69.32 | 68.33 |
| Al ₂ O ₃ | 19.64 | 19.15 | 19.32 | 19.84 | 19.64 | 19.46 |
| FeO | 0.02 | 0.11 | 0.05 | 0.41 | 0.04 | 0.02 |
| CaO | 0.5 | 0 | 0.24 | 0.45 | 0.21 | 0.18 |
| Na ₂ O | 10.05 | 11.99 | 11.79 | 11.36 | 12.1 | 11.44 |
| K ₂ O | 2.38 | 0.09 | 0.07 | 0.34 | 0.05 | 0.05 |
| TOTAL | 100.07 | 100.07 | 99.62 | 99.44 | 101.36 | 99.48 |

| | | | | | | |
|---|-------|-------|-------|-------|-------|-------|
| Z | 15.98 | 15.96 | 15.97 | 15.97 | 15.96 | 16.01 |
| X | 4.07 | 4.10 | 4.08 | 4.11 | 4.11 | 3.94 |

| | | | | | | |
|----|-------|-------|-------|-------|-------|-------|
| Or | 13.16 | 0.49 | 0.38 | 1.86 | 0.27 | 0.28 |
| Ab | 84.45 | 99.12 | 98.33 | 94.59 | 98.65 | 98.78 |
| An | 2.39 | 0.39 | 1.29 | 3.54 | 1.09 | 0.93 |

Number of ions on the basis of 32 [O]

| | | | | | | |
|----|-------|-------|-------|-------|-------|-------|
| Si | 11.90 | 12.01 | 11.97 | 11.84 | 11.97 | 11.99 |
| Al | 4.08 | 3.94 | 4.00 | 4.13 | 4.00 | 4.02 |
| Fe | 0.00 | 0.02 | 0.01 | 0.06 | 0.01 | 0.00 |
| Ca | 0.09 | 0.00 | 0.05 | 0.09 | 0.04 | 0.03 |
| Na | 3.44 | 4.06 | 4.01 | 3.89 | 4.05 | 3.89 |
| K | 0.54 | 0.02 | 0.02 | 0.08 | 0.01 | 0.01 |

Table 4. Representative chemical analyses of zoned plagioclases.

| | FT8/3r | FT8/3c | FT8/6r | FT8/6c |
|--------------------------------|--------|--------|--------|--------|
| SiO ₂ | 68.76 | 68.42 | 68.87 | 67.64 |
| Al ₂ O ₃ | 19.72 | 19.61 | 19.45 | 19.58 |
| FeO | 0.01 | 0.02 | 0.03 | 0.15 |
| CaO | 0.17 | 0.62 | 0.27 | 0.68 |
| Na ₂ O | 11.78 | 11.18 | 11.46 | 11.50 |
| K ₂ O | 0.06 | 0.05 | 0.08 | 0.05 |
| TOTAL | 100.50 | 99.90 | 100.16 | 99.60 |

| | | | | |
|---|-------|-------|-------|-------|
| Z | 16.01 | 16.01 | 16.01 | 15.96 |
| X | 4.01 | 3.91 | 3.94 | 4.08 |

| | | | | |
|----|-------|-------|-------|-------|
| Or | 0.33 | 0.28 | 0.45 | 0.27 |
| Ab | 98.84 | 96.68 | 98.16 | 96.05 |
| An | 0.82 | 3.04 | 1.39 | 3.68 |

Number of ions on the basis of 32 [O]

| | | | | |
|----|-------|-------|-------|-------|
| Si | 11.94 | 11.94 | 11.99 | 11.88 |
| Al | 4.07 | 4.07 | 4.02 | 4.09 |
| Fe | 0.00 | 0.00 | 0.00 | 0.02 |
| Ca | 0.03 | 0.12 | 0.05 | 0.13 |
| Na | 3.97 | 3.78 | 3.87 | 3.92 |
| K | 0.01 | 0.01 | 0.02 | 0.01 |

c : core r : rim

Table 5. Representative chemical analyses of feldspars included in microcline or albite crystals.

| | FT10/113 | FT10/114 | FT10/117 | FT10/120 | FT6/20 | FT6/122 |
|--------------------------------|----------|----------|----------|----------|--------|---------|
| SiO ₂ | 64.80 | 64.74 | 64.63 | 64.93 | 63.21 | 63.51 |
| Al ₂ O ₃ | 18.28 | 18.18 | 18.30 | 18.18 | 23.12 | 22.97 |
| FeO | 0.04 | 0.03 | 0.02 | 0.34 | 0.03 | 0.02 |
| CaO | 0.04 | 0.01 | 0.01 | 0.01 | 4.37 | 3.52 |
| Na ₂ O ₃ | 1.12 | 1.35 | 2.05 | 1.63 | 9.10 | 9.85 |
| K ₂ O | 14.52 | 15.03 | 14.08 | 14.65 | 0.08 | 0.05 |
| TOTAL | 98.80 | 99.34 | 99.09 | 99.74 | 99.91 | 99.92 |

| | | | | | | |
|---|-------|-------|-------|-------|-------|-------|
| Z | 16.04 | 15.99 | 15.99 | 15.96 | 16.01 | 16.02 |
| X | 3.85 | 4.04 | 4.07 | 4.08 | 3.97 | 4.05 |

| | | | | | | |
|----|-------|-------|-------|-------|-------|-------|
| Or | 89.18 | 87.84 | 81.78 | 84.40 | 0.45 | 0.28 |
| Ab | 10.45 | 11.99 | 18.10 | 14.27 | 78.58 | 83.22 |
| An | 0.37 | 0.16 | 0.12 | 1.33 | 20.96 | 16.51 |

Number of ions on the basis of 32 [O]

| | | | | | | |
|----|-------|-------|-------|-------|-------|-------|
| Si | 12.01 | 11.99 | 11.96 | 11.98 | 11.16 | 11.21 |
| Al | 4.03 | 4.00 | 4.02 | 3.98 | 4.85 | 4.82 |
| Fe | 0.01 | 0.00 | 0.00 | 0.05 | 0.00 | 0.00 |
| Ca | 0.01 | 0.00 | 0.00 | 0.00 | 0.83 | 0.67 |
| Na | 0.40 | 0.48 | 0.74 | 0.58 | 3.12 | 3.37 |
| K | 3.43 | 3.55 | 3.33 | 3.45 | 0.02 | 0.01 |

Table 7. Representative chemical analyses of titanites.

| | FT-8/243 | FT-8/238 | FT-6/124 |
|--------------------------------|----------|----------|----------|
| SiO ₂ | 33.12 | 32.86 | 32.56 |
| TiO ₂ | 29.19 | 28.55 | 31.57 |
| Al ₂ O ₃ | 7.35 | 7.12 | 6.82 |
| FeO | 1.36 | 2.91 | 1.54 |
| CaO | 28.76 | 28.13 | 27.43 |
| Total | 99.78 | 99.57 | 99.92 |

Number of ions on the basis of 20 [O]

| | | | |
|----|------|------|------|
| Si | 4.27 | 4.27 | 4.19 |
| Ti | 2.83 | 2.79 | 3.06 |
| Al | 1.12 | 1.09 | 1.03 |
| Fe | 0.15 | 0.32 | 0.17 |
| Ca | 3.97 | 3.92 | 3.78 |

| | | | |
|---|-----|-----|-----|
| Z | 4.3 | 4.3 | 4.2 |
| Y | 4.1 | 4.2 | 4.3 |
| X | 4.0 | 3.9 | 3.8 |

Table 8. Representative chemical analyses of epidote crystals.

| | FT10/105 | FT10/105a | FT6/211 |
|--------------------------------|----------|-----------|---------|
| SiO ₂ | 38.81 | 38.04 | 38.12 |
| TiO ₂ | 0.23 | 0.10 | 0.14 |
| Al ₂ O ₃ | 20.48 | 20.77 | 21.81 |
| Fe ₂ O ₃ | 14.82 | 15.07 | 13.5 |
| Mn ₂ O ₃ | 0.76 | 0.48 | 0.64 |
| CaO | 22.10 | 22.83 | 23.37 |
| Total | 97.20 | 97.29 | 97.58 |

Number of ions on the basis of 25 [O]

| | | | |
|------------------|-------|-------|-------|
| Si | 6.241 | 6.137 | 6.108 |
| Ti | 0.028 | 0.012 | 0.017 |
| Al | 3.882 | 3.949 | 4.119 |
| Fe ³⁺ | 1.793 | 1.829 | 1.628 |
| Mn ³⁺ | 0.093 | 0.059 | 0.078 |
| Ca | 3.808 | 3.946 | 4.012 |

| | | | |
|------------|-------|-------|-------|
| Pistacite% | 31.60 | 31.66 | 28.33 |
|------------|-------|-------|-------|

| | | | |
|---|------|------|------|
| Z | 6.24 | 6.14 | 6.11 |
| Y | 5.80 | 5.85 | 5.84 |
| X | 3.81 | 3.95 | 4.01 |

Table 6. Representative chemical analyses of micas.

| | FT8/19 | FT8/22 | FT8/24 | FT6/1 | FT6/2 | FT6/3 | FT10/91 | FT6/9 | FT10/115 | FT10/99 | FT6/27 | FT6/27a | FT6/14a | FT6/32a |
|--------------------------------|--------|--------|--------|-------|-------|-------|---------|-------|----------|---------|--------|---------|---------|---------|
| SiO ₂ | 47.29 | 47.34 | 48.99 | 54.53 | 48.6 | 48 | 48.83 | 49.91 | 50.18 | 49.9 | 38.56 | 38.69 | 38.85 | 38.73 |
| TiO ₂ | 0.13 | 0.69 | 0.21 | 0.24 | 0.43 | 0.4 | 0.29 | 0.27 | 0.04 | 0.07 | 0.08 | 0.08 | 0.13 | 0.12 |
| Al ₂ O ₃ | 29.67 | 28.86 | 25.56 | 21.66 | 27.32 | 28.4 | 25.15 | 23.6 | 22.47 | 21.93 | 20.04 | 19.62 | 18.32 | 18.98 |
| FeO | 4.76 | 5.1 | 6.65 | 6.11 | 5.24 | 5.15 | 6.6 | 5.82 | 7.71 | 8.84 | 17.21 | 17.72 | 20.47 | 20.82 |
| MnO | 0.05 | 0.06 | 0.06 | 0.04 | 0.06 | 0.06 | 0.07 | 0.07 | 0.08 | 0.09 | 0.25 | 0.26 | 0.26 | 0.22 |
| MgO | 1.4 | 1.53 | 1.53 | 2.45 | 2.11 | 1.85 | 2.41 | 2.88 | 2.68 | 2.39 | 8.59 | 8.84 | 8.32 | 8.27 |
| Na ₂ O | 0.28 | 0.34 | 0.13 | 0.08 | 0.21 | 0.21 | 0.14 | 0.08 | 0.09 | 0.1 | 0.06 | 0.06 | 0.08 | 0.11 |
| K ₂ O | 10.92 | 10.95 | 10.67 | 9.3 | 10.62 | 10.87 | 10.87 | 11.17 | 11.05 | 10.83 | 9.35 | 9.52 | 9.68 | 9.63 |
| Total | 94.5 | 94.87 | 93.8 | 94.41 | 94.59 | 94.94 | 94.36 | 93.8 | 94.3 | 94.15 | 94.14 | 94.79 | 96.11 | 96.88 |

Number of ions on the basis of 22 [O]

| | | | | | | | | | | | | | | |
|----|-------|-------|-------|-------|-------|-------|-------|-------|-------|-------|-------|-------|------|------|
| Si | 6.479 | 6.483 | 6.808 | 7.382 | 6.653 | 6.556 | 6.765 | 6.933 | 6.996 | 7.005 | 5.806 | 5.809 | 5.84 | 5.78 |
| Ti | 0.013 | 0.071 | 0.022 | 0.024 | 0.044 | 0.041 | 0.03 | 0.028 | 0.004 | 0.007 | 0.009 | 0.009 | 0.01 | 0.01 |
| Al | 4.791 | 4.658 | 4.187 | 3.456 | 4.408 | 4.572 | 4.107 | 3.864 | 3.692 | 3.629 | 3.557 | 3.472 | 3.25 | 3.34 |
| Fe | 0.545 | 0.584 | 0.773 | 0.692 | 0.6 | 0.588 | 0.765 | 0.676 | 0.899 | 1.038 | 2.167 | 2.225 | 2.57 | 2.60 |
| Mn | 0.006 | 0.007 | 0.007 | 0.005 | 0.007 | 0.007 | 0.008 | 0.008 | 0.009 | 0.011 | 0.032 | 0.033 | 0.03 | 0.03 |
| Mg | 0.286 | 0.312 | 0.317 | 0.494 | 0.431 | 0.377 | 0.498 | 0.596 | 0.557 | 0.5 | 1.928 | 1.978 | 1.87 | 1.84 |
| Na | 0.074 | 0.09 | 0.035 | 0.021 | 0.056 | 0.056 | 0.038 | 0.022 | 0.024 | 0.027 | 0.018 | 0.017 | 0.02 | 0.03 |
| K | 1.909 | 1.913 | 1.892 | 1.606 | 1.855 | 1.894 | 1.921 | 1.979 | 1.965 | 1.94 | 1.796 | 1.823 | 1.86 | 1.83 |

| | | | | | | | | | | | | | | |
|---|------|------|------|------|------|------|------|------|------|------|------|------|------|------|
| Z | 8 | 8 | 8 | 8 | 8 | 8 | 8 | 8 | 8 | 8 | 8 | 8 | 8.00 | 8.00 |
| Y | 4.12 | 4.12 | 4.11 | 4.05 | 4.14 | 4.14 | 4.17 | 4.11 | 4.16 | 4.19 | 5.5 | 5.53 | 5.58 | 5.60 |
| X | 1.98 | 2 | 1.93 | 1.63 | 1.91 | 1.95 | 1.96 | 2 | 1.99 | 1.97 | 1.81 | 1.84 | 1.88 | 1.87 |

d. 4. Zircon appears in hypidiomorphic crystals, with an elongation ratio averaging 2. Some crystals present zoning and darker core.

d. 5 Garnet occurs as small isodiametric isotropic crystals. It was usually found in secondary mineral aggregates, as a product of biotite and feldspar alteration. Representative analyses recalculated on the basis of 12 [O] are given in Table 9 along with the composition expressed in terms of the theoretical end members.

d. 6. Only a few apatite crystals were observed.

d. 7. Magnetite was found in hypidiomorphic grains, usually in contact with muscovite, epidote and other biotite alteration products. Small goethite grains were ob-

Table 9. Representative chemical analyses of garnets.

| | FT-8/233 | FT-8/235 | FT-6/122 |
|--------------------------------|----------|----------|----------|
| SiO ₂ | 36.42 | 36.81 | 37.8 |
| TiO ₂ | 1.37 | 1.47 | 1.52 |
| Al ₂ O ₃ | 21.44 | 20.39 | 21.36 |
| FeO | 25.16 | 26.62 | 24.11 |
| MnO | 0.21 | 0.2 | 0.36 |
| MgO | 0.14 | 0.02 | 0.04 |
| CaO | 15.38 | 14.65 | 15.22 |
| Na ₂ O | 0.06 | 0.02 | 0.02 |
| K ₂ O | 0.05 | 0.01 | 0.03 |
| Total | 100.23 | 100.19 | 100.46 |

Number of ions on the basis of 12 [O]

| | | | |
|------------------|-------|-------|-------|
| Si | 2.892 | 2.938 | 2.968 |
| Ti | 0.082 | 0.088 | 0.090 |
| Al ^{IV} | 0.000 | 0.000 | 0.000 |
| Al ^{VI} | 2.023 | 1.933 | 1.992 |
| Fe | 1.671 | 1.777 | 1.583 |
| Mn | 0.014 | 0.014 | 0.024 |
| Mg | 0.017 | 0.002 | 0.005 |
| Ca | 1.309 | 1.253 | 1.280 |
| Na | 0.009 | 0.003 | 0.003 |
| K | 0.005 | 0.001 | 0.003 |

| | | | |
|---|------|------|------|
| Z | 2.89 | 2.94 | 2.97 |
| Y | 2.10 | 2.02 | 2.08 |
| X | 3.01 | 3.05 | 2.89 |

| | | | |
|-------|------|------|------|
| Pyr | 0.6 | 0.1 | 0.2 |
| Alm | 55.5 | 58.3 | 54.7 |
| Spess | 0.5 | 0.4 | 0.8 |
| Andr | 0.0 | 0.0 | 0.0 |
| Gross | 43.5 | 41.1 | 44.3 |

served as an alteration product of magnetite. Representative analyses of magnetite crystals are given in Table 10.

Table 10. Representative chemical analyses of magnetite crystals.

| | FT10/100 | FT6/15 | FT6/16 |
|--------------------------------|----------|--------|--------|
| TiO ₂ | 0.04 | 0.17 | 0.17 |
| Al ₂ O ₃ | 0.11 | 0.04 | 0.02 |
| Cr ₂ O ₃ | 0.01 | 0.02 | 0.02 |
| Fe ₂ O ₃ | 67.74 | 68.14 | 67.96 |
| FeO | 31.72 | 31.91 | 31.83 |
| MnO | 0.07 | 0.04 | 0.10 |
| MgO | 0.01 | 0.02 | 0.01 |
| Total | 99.70 | 100.35 | 100.11 |

Number of ions on the basis of 4 [O]

| | | | |
|------------------|-------|-------|-------|
| Ti | 0.001 | 0.005 | 0.005 |
| Al | 0.005 | 0.002 | 0.001 |
| Cr | 0.000 | 0.001 | 0.001 |
| Fe ³⁺ | 1.973 | 1.972 | 1.972 |
| Fe ²⁺ | 1.027 | 1.026 | 1.026 |
| Mn | 0.002 | 0.001 | 0.003 |
| Mg | 0.001 | 0.001 | 0.001 |

| | | | |
|---|------|------|------|
| Z | 1.98 | 1.98 | 1.98 |
| X | 1.03 | 1.03 | 1.03 |

| | FT6/19 | FT8/8 | FT8/11 |
|--------------------------------|--------|-------|--------|
| TiO ₂ | 0.14 | 0.10 | 0.12 |
| Al ₂ O ₃ | 0.03 | 0.03 | 0.00 |
| Cr ₂ O ₃ | 0.03 | 0.04 | 0.01 |
| Fe ₂ O ₃ | 68.15 | 67.76 | 68.38 |
| FeO | 31.91 | 31.73 | 32.02 |
| MnO | 0.03 | 0.12 | 0.03 |
| MgO | 0.01 | 0.01 | 0.04 |
| Total | 100.31 | 99.79 | 100.61 |

Number of ions on the basis of 4 [O]

| | | | |
|------------------|-------|-------|-------|
| Ti | 0.004 | 0.003 | 0.003 |
| Al | 0.001 | 0.001 | 0.000 |
| Cr | 0.001 | 0.001 | 0.000 |
| Fe ³⁺ | 1.973 | 1.973 | 1.974 |
| Fe ²⁺ | 1.027 | 1.027 | 1.028 |
| Mn | 0.001 | 0.004 | 0.001 |
| Mg | 0.001 | 0.001 | 0.002 |

| | | | |
|---|------|------|------|
| Z | 1.98 | 1.98 | 1.98 |
| X | 1.03 | 1.03 | 1.03 |

Petrography

Granite is the only rock type of the intrusion. It is light grey, dark grey to greenish-grey in colour, with a partly porphyritic structure and strong foliation. Late magmatic, or hydrothermal activity has affected the plutonic rocks causing decomposition of primary feldspar and biotite. Modal analyses of the studied rocks are given in Table 11.

In thin section the rock, though strongly tectonised, it still preserves its original granitic texture. It is composed of K-feldspar quartz, plagioclase biotite and allanite porphyroclasts, surrounded by fine fragments of the same minerals and other primary phases such as zircon, apatite and titanite, along with recrystallised and secondary formed minerals such as quartz, muscovite and epidote.

Table 11. Modal analyses of representative samples

| | FT-3 | FT-9 | FT-8 | FT-10 | FT-11 | FT-12 |
|-------------|--------|--------|--------|--------|--------|--------|
| | n=2582 | n=1953 | n=2841 | n=2255 | n=2161 | n=1646 |
| Quartz | 32.7 | 37.8 | 37.4 | 37.3 | 34.4 | 30.4 |
| Plagioclase | 18.5 | 17.3 | 7.7 | 14.1 | 14.2 | 14.5 |
| Microcline | 40.5 | 38.2 | 40.2 | 41.1 | 35.2 | 41.3 |
| Muscovite | 7.0 | 4.5 | 12.3 | 5.7 | 8.5 | 3.3 |
| Biotite | 0.2 | tr | 0.8 | 0.4 | 5.3 | 8.2 |
| Epidote | tr | 0.7 | 0.1 | 0.5 | 0.5 | 0.5 |
| Titanite | 0.1 | 0.5 | 0.4 | 0.4 | 0.8 | 1.2 |
| Opaque | 1.0 | 0.7 | 1.1 | 0.1 | 0.5 | 0.4 |
| Garnet | - | tr | - | tr | - | - |
| Allanite | tr | 0.3 | tr | 0.4 | 0.6 | 0.1 |
| Zircon | tr | tr | tr | tr | tr | tr |
| Apatite | - | tr | tr | - | tr | - |

n = counts tr = traces

Vein-like aggregates composed of fine grained recrystallised quartz, small fragments of K-feldspar, muscovite flakes and secondary mineral grains, cross the rock parallel to foliation surfaces, arching around the porphyroclasts. All the intermediate grain sizes between the large porphyroclasts and the cryptocrystalline fragments are present, with no dominant size, so that the structure of the rock relative to the grain size can be characterised as successive porphyroclastic.

Chemical results

The major element analytical results along with the CIPW norms of representative analyses are given in Table 12 and the trace along with the rare earth element results are given in Tables 13 and 14.

In Figs. 3 and 4 the geochemical trend is shown in the plots of various major and trace elements v. SiO₂. Mantle and ORG normalised plots, as well as trace element diagrams for the discrimination of the geotectonic environment are shown in Figs. 5 - 7. Finally, chondrite normalised REE patterns are drawn in Fig 8.

Age determination

Rb-Sr whole rock and mica analyses were carried out on 2 samples. The Rb-Sr analytical results as well as age determinations of the studied rocks are listed in Table 15. The long-time reproducibility for the ⁸⁷Sr/⁸⁶Sr ratio

gave a mean value of 0.71033·5 (1σ, n=29). Rb and Sr contents have been measured by isotopic dilution method, using 98 % ⁸⁷Rb and 99.9 % ⁸⁴Sr spikes, respectively.

Age determinations from muscovite concentrates and the corresponding whole rocks gave values ranging from 273 to 225 Ma (Table 15).

Some ages obtained by mica concentrates represent rejuvenated Rb-Sr systems of muscovites, affected by various tectonic events. Considering the high whole rock Rb/Sr ratio we can assume that these strongly differentiated granites reacted probably as an open system to these events regarding their Rb and Sr contents. For this reason, in addition to the high Rb/Sr values, the (⁸⁷Sr/⁸⁶Sr)_i values diverge significantly from the relative values of other neighbouring plutonic rocks (Verdikoussa, Diava and Deskati plutonic complexes) and they are not reported. In any case it seems reliable that its emplacement took place during Variscan orogenesis.

Discussion - Conclusions

From the mineral chemistry we can reveal some essential features of the plutonic rocks.

The K-feldspar is essentially microcline (Or = 97.62 - 96.44 %) and plagioclase is represented by albite and acid oligoclase (Ab = 99.12 to 84.45 %). There is a lack of calcium rich plagioclase in the studied granitic rocks, due to the decomposition of the primary plagioclase.

Table 12 Representative major element analyses of the studied rocks.

| | FT8 | FT5 | FT3 | FT7 | FT1 | FT2 | FT16 |
|--------------------------------|--------|--------|--------|--------|--------|--------|-------|
| SiO ₂ | 78.48 | 78.45 | 78.39 | 78.26 | 78.22 | 78.08 | 77.62 |
| TiO ₂ | 0.20 | 0.18 | 0.17 | 0.20 | 0.20 | 0.22 | 0.24 |
| Al ₂ O ₃ | 11.20 | 11.46 | 11.47 | 11.95 | 11.70 | 11.82 | 11.72 |
| FeO | 1.19 | 1.16 | 1.14 | 1.29 | 1.43 | 1.62 | 1.31 |
| MnO | 0.01 | 0.00 | 0.00 | 0.01 | 0.01 | 0.01 | 0.00 |
| MgO | 0.22 | 0.21 | 0.20 | 0.25 | 0.27 | 0.22 | 0.18 |
| CaO | 0.41 | 0.12 | 0.20 | 0.37 | 0.17 | 0.17 | 0.12 |
| Na ₂ O | 3.62 | 2.62 | 2.38 | 2.69 | 2.87 | 2.49 | 2.46 |
| K ₂ O | 4.94 | 5.64 | 5.46 | 5.58 | 5.23 | 5.17 | 5.57 |
| P ₂ O ₅ | 0.04 | 0.03 | 0.02 | 0.04 | 0.04 | 0.03 | 0.02 |
| L.O.I. | 0.53 | 0.31 | 0.65 | 0.44 | 0.52 | 0.27 | 0.45 |
| Total | 100.84 | 100.18 | 100.10 | 101.07 | 100.65 | 100.09 | 99.69 |

Norm wt %

| | | | | | | | |
|------|-------|-------|-------|-------|-------|-------|-------|
| Ap | 0.07 | 0.05 | 0.04 | 0.07 | 0.07 | 0.05 | 0.04 |
| Il | 0.32 | 0.29 | 0.27 | 0.32 | 0.32 | 0.36 | 0.39 |
| Or | 26.89 | 30.99 | 30.13 | 30.43 | 28.66 | 28.41 | 30.87 |
| Ab | 29.95 | 21.89 | 19.98 | 22.30 | 23.85 | 20.84 | 20.70 |
| An | 0.05 | 0.39 | 0.81 | 1.47 | 0.56 | 0.62 | 0.45 |
| C | 0.00 | 0.57 | 0.84 | 0.57 | 0.70 | 1.19 | 0.94 |
| WoDi | 0.81 | 0.00 | 0.00 | 0.00 | 0.00 | 0.00 | 0.00 |
| EnDi | 0.22 | 0.00 | 0.00 | 0.00 | 0.00 | 0.00 | 0.00 |
| FsDi | 0.58 | 0.00 | 0.00 | 0.00 | 0.00 | 0.00 | 0.00 |
| EnHy | 0.48 | 0.67 | 0.64 | 0.79 | 0.86 | 0.70 | 0.58 |
| FsHy | 1.24 | 1.79 | 1.79 | 2.01 | 2.27 | 2.57 | 1.99 |
| Q | 39.40 | 43.36 | 45.50 | 42.02 | 42.72 | 45.25 | 44.05 |

| | FT4 | FT6 | FT9 | FT10 | FT12 | FT11 | FT13 |
|--------------------------------|-------|--------|--------|-------|--------|-------|-------|
| SiO ₂ | 77.44 | 77.02 | 76.82 | 76.73 | 75.26 | 74.92 | 74.08 |
| TiO ₂ | 0.26 | 0.20 | 0.19 | 0.28 | 0.32 | 0.30 | 0.32 |
| Al ₂ O ₃ | 11.72 | 12.23 | 11.89 | 12.35 | 12.33 | 12.48 | 12.40 |
| FeO | 1.13 | 1.28 | 1.58 | 1.40 | 1.89 | 1.67 | 2.25 |
| MnO | 0.00 | 0.00 | 0.01 | 0.01 | 0.02 | 0.01 | 0.22 |
| MgO | 0.19 | 0.25 | 0.24 | 0.26 | 0.44 | 0.38 | 0.55 |
| CaO | 0.15 | 0.12 | 0.46 | 0.53 | 0.52 | 0.50 | 0.63 |
| Na ₂ O | 2.89 | 2.97 | 2.93 | 2.73 | 2.93 | 3.61 | 2.85 |
| K ₂ O | 5.40 | 5.55 | 5.42 | 5.18 | 5.81 | 5.32 | 5.19 |
| P ₂ O ₅ | 0.03 | 0.03 | 0.04 | 0.04 | 0.07 | 0.05 | 0.08 |
| L.O.I. | 0.47 | 0.86 | 0.43 | 0.45 | 0.54 | 0.65 | 0.65 |
| Total | 99.69 | 100.51 | 100.00 | 99.95 | 100.12 | 99.89 | 99.20 |

Norm wt %

| | | | | | | | |
|------|-------|-------|-------|-------|-------|-------|-------|
| Ap | 0.05 | 0.05 | 0.07 | 0.07 | 0.13 | 0.09 | 0.15 |
| Il | 0.42 | 0.32 | 0.31 | 0.45 | 0.52 | 0.49 | 0.52 |
| Or | 29.91 | 30.67 | 29.89 | 28.61 | 32.18 | 29.55 | 29.03 |
| Ab | 24.28 | 24.97 | 24.56 | 22.91 | 24.70 | 30.48 | 24.20 |
| An | 0.53 | 0.39 | 1.90 | 2.23 | 2.02 | 1.99 | 2.50 |
| C | 0.59 | 0.75 | 0.30 | 0.88 | 0.27 | 0.00 | 0.73 |
| WoDi | 0.00 | 0.00 | 0.00 | 0.00 | 0.00 | 0.04 | 0.00 |
| EnDi | 0.00 | 0.00 | 0.00 | 0.00 | 0.00 | 0.01 | 0.00 |
| FsDi | 0.00 | 0.00 | 0.00 | 0.00 | 0.00 | 0.02 | 0.00 |
| EnHy | 0.61 | 0.80 | 0.77 | 0.84 | 1.41 | 1.21 | 1.78 |
| FsHy | 1.64 | 1.99 | 2.58 | 2.11 | 2.95 | 2.54 | 4.00 |
| Q | 41.97 | 40.05 | 39.62 | 41.89 | 35.82 | 33.58 | 37.09 |

Table 13. Representative trace element analyses in ppm.

| | FT1 | FT2 | FT3 | FT4 | FT5 | FT6 | FT16 |
|----|-----|-----|-----|-----|-----|-----|------|
| Sc | 10 | 8 | 6 | 3 | 11 | 9 | 7 |
| V | 13 | 17 | 12 | 11 | 16 | 13 | 15 |
| Cr | 7 | 21 | 7 | 1 | 7 | | -- |
| Co | 53 | 62 | 72 | 49 | 46 | 47 | 47 |
| Cu | 2.5 | 2.8 | 0.6 | 0.1 | 1.6 | 3 | -- |
| Ba | 294 | 288 | 252 | 264 | 269 | 270 | 251 |
| La | 31 | 32 | 14 | 37 | 26 | 28 | 24 |
| Ce | 38 | 45 | 23 | 79 | 41 | 54 | 57 |
| Nd | 23 | 28 | 11 | 30 | 18 | 23 | 26 |
| Nb | 18 | 20 | 13 | 14 | 13 | 14 | 13 |
| Zr | 166 | 194 | 123 | 132 | 122 | 135 | 138 |
| Y | 46 | 21 | 23 | 41 | 29 | 33 | 36 |
| Sr | 34 | 37 | 31 | 20 | 29 | 29 | 27 |
| Rb | 263 | 278 | 273 | 267 | 246 | 245 | 240 |
| Th | 22 | 25 | 21 | 28 | 22 | 26 | 25 |
| Ga | 16 | 17 | 15 | 15 | 16 | 17 | 17 |
| Zn | 35 | 41 | 12 | 15 | 15 | 20 | 16 |

| | FT7 | FT8 | FT9 | FT10 | FT11 | FT12 | FT13 |
|----|-----|-----|-----|------|------|------|------|
| Sc | 6 | 6 | 6 | 7 | 5 | 4 | 3 |
| V | 17 | 15 | 14 | 13 | 21 | 19 | 29 |
| Cr | -- | 3 | 0.3 | 1 | 14 | 20 | 7 |
| Co | 46 | 48 | 31 | 32 | 21 | 30 | 26 |
| Cu | -- | 1.6 | 3.1 | 1.4 | 0 | 0 | 0 |
| Ba | 320 | 258 | 305 | 289 | 238 | 227 | 260 |
| La | 32 | 31 | 32 | 31 | 33 | 37 | 40 |
| Ce | 57 | 66 | 63 | 62 | 68 | 78 | 79 |
| Nd | 23 | 25 | 23 | 25 | 27 | 30 | 33 |
| Nb | 13 | 15 | 13 | 13 | 15 | 14 | 13 |
| Zr | 153 | 155 | 143 | 151 | 210 | 229 | 221 |
| Y | 38 | 42 | 43 | 42 | 46 | 56 | 54 |
| Sr | 43 | 30 | 39 | 42 | 61 | 43 | 63 |
| Rb | 282 | 288 | 274 | 269 | 312 | 275 | 292 |
| Th | 23 | 23 | 21 | 23 | 36 | 33 | 33 |
| Ga | 16 | 16 | 16 | 16 | 19 | 18 | 18 |
| Zn | 21 | 18 | 44 | 63 | 16 | 26 | 25 |

Table 14. Representative REE analyses in ppm.

| | La | Ce | Pr | Nd | Sm | Eu | Gd | Dy | Er | Yb | Lu |
|------|------|------|------|------|-----|------|------|------|------|------|------|
| FT8 | 10.9 | 21.1 | 3.42 | 13 | 2.6 | 0.23 | 2.5 | 3.05 | 1.97 | 1.96 | 0.28 |
| FT10 | 33.2 | 68.4 | 8.5 | 33.6 | 5.3 | 0.68 | 5.32 | 5.34 | 3.23 | 3.13 | 0.41 |
| FT13 | 26.4 | 55.5 | 7.3 | 27 | 4.8 | 0.56 | 4.93 | 5.56 | 3.59 | 3.59 | 0.47 |

Table 15. Rb-Sr geochronological data of the studied plutonic rocks.

| Sample | Material | Rb ppm | Sr ppm | $^{87}\text{Rb}/^{86}\text{Sr}$ | $^{87}\text{Sr}/^{86}\text{Sr}$ ($\pm 2\sigma$) | Age Ma ($\pm 2\sigma$) |
|--------|-----------|--------|--------|---------------------------------|---|--------------------------|
| FT-5 | W.ROCK | 231 | 29.8 | 22.638 | 0.84951 \pm 3 | |
| | MUSCOVITE | 946 | 9.1 | 335.652 | 1.85192 \pm 6 | 225 \pm 2 |
| FT-8 | W.ROCK | 87 | 62 | 4.106 | 0.76916 \pm 2 | |
| | MUSCOVITE | 682 | 15.1 | 138.342 | 1.2913 \pm 2 | 273 \pm 3 |

Normal zoning of the sodium feldspar is common. As an example, sample FT8/6 (Table 4) presents an Ab content of 96.05 % in the core (analysis FT8/6c), while the rim composition is sodium enriched with an Ab content 98.16 % (analysis FT8/6r).

This plagioclase zoning cannot be considered indicative of its origin, as it is not exclusively a primary characteristic of the mineral. It is also the result of the extended decomposition that it is not uniform, but advances progressively from the edges of the crystal towards the core, along cracks, or cleavage and twinning surfaces.

Normal zoning is also common in K-feldspar. As an example, sample FT10/96 (Table 2) presents in the core an Or % content of 94.76 (analysis FT10/96c), while the rim is potassium enriched (Or % 96.09 analysis FT10/96r). A common feature is the development of a thin albite rim around microcline crystals (analyses FT10/118c, FT10/118r, Table 2), while the development of a thin K-feldspar rim around plagioclase crystals is less common (analyses FT10/109c, FT10/109r Table 2). The smaller K-feldspar crystals are usually twinning free, indicating a selective recrystallisation of the neighbouring grains.

Both, sodium (Ab % = 78.58 - 83.22) and potassium (Or % = 81.78 - 89.18) feldspars grains up to 0.5 mm in length are included in larger albite and microcline crystals. Plagioclase inclusions have more calcic composition than the host albite crystals, while K-feldspar inclusions are potassium depleted and sodium richer, compared to the large microcline crystals.

The analysed biotites can be considered Ti depleted, as TiO₂ percentage is always lower than 0.1. But the small anatase and hematite grains, that can be observed along the biotite cleavage, are exsolution products indicative of an originally Fe, Ti rich biotite. The high elongation ratios measured indicate a crystallisation at low temperatures.

Muscovite must have been crystallised meta-tectonically as there are small muscovite flakes that are enclosed in recrystallised quartz grains, while there are not any muscovite inclusions in primary phases such as K-feldspar.

There are a few large muscovite crystals protected among the porphyroclasts so that they are not tectonically affected. The development of these large muscovite crystals is probably due to a selective crystallisation of fine sericite grains. The majority of muscovite flakes have an orientation and they are strongly affected by a late tectonism.

Epidote composition is usually expressed in terms of the theoretical pistacite end member: $P_s = 100 \cdot Fe^{3+} / (Fe^{3+} + Al)$. Natural epidote composition rarely exceeds P_{s33} (DEER et al. 1986). Epidotes of the studied samples present P_s % value 31.6.

Garnet is almandine (Alm = 54.7 - 58.3 %) containing appreciable amounts of the grossularite molecule (Gross. = 41.1-44.3 %). Both, garnet and titanite are partly primary and partly the result of biotite and plagioclase decomposition.

Magnetite is the only spinel present in the rocks studied. In some cases it is oxidised to hematite.

From the mineralogical characteristics described above, the successive crystallisation can be depicted. The oldest authigenic mineral phases of the studied rocks are zircon, apatite, allanite and partly titanite, which were formed during a primary stage of the magma crystallisation. Plagioclase and K-feldspar crystallised consequently. The formation of the latter is partly over-

lapped and followed by the primary quartz and biotite crystallisation. At the same time the Na-component of the alkali feldspar was separated causing the perthite formation. During tectonism a recrystallisation of quartz took place, while from the existing liquid phase crystallised fine quartz, K-feldspar and muscovite, filling the cracks and the fissures among the porphyroclasts.

Hydrothermal alteration caused the biotite and plagioclase decomposition, giving rise to secondary quartz, muscovite, titanite, garnet and magnetite.

In Fig. 2 the possible crystallisation sequence for the Fotino granitic rocks is presented.

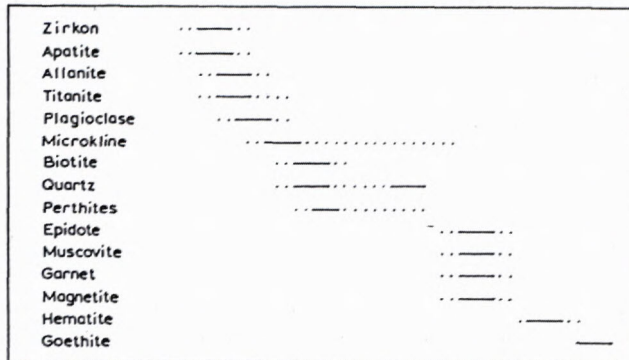


Fig. 2 Possible crystallisation sequence for the Fotino granitic rocks

From the rock chemistry some important petrogenetic features of the studied rocks can also be depicted.

All the studied samples of the Fotino granite show S type characteristics, as muscovite is the main mica present, plagioclase is albite and acid oligoclase (Ab = 99.12 to 84.45 %), CaO content is low, the Rb/Sr ratio is high (4.6 - 13.4), normative anorthite content is low, ranging from 0.05 - 2.50, Na₂O content ranges from 2.4 to 3.6 and for K₂O averaging 5.4.

The molar ratio $Al_2O_3 / (CaO + Na_2O + K_2O)$ ranges from 0.93 to 1.19, so as normative C values range from 0.0 to 1.2.

S-type granitoids in Greece have been reported in Macedonia (N. Greece) and in Paros island, (Aegean Sea). In N Greece the Sochos plagiogranite and the Arnea leucogranite, both belonging to the Circum Rhodope belt of the Hellenides, show typical S-type characteristics (BALATYIS & al. 1992). In Paros island, which belongs to the Attico-Cycladic unit, ALTHER (1981) and ALTHER et al. (1982) reported a granitic body also presenting S-type properties. Typical S-type characteristics are also described for the Deskati plutonic rocks (KATERINOPOULOS et al. 1994)

The major element analytical results of the Fotino granites, plotted in Harker variation diagrams (Fig. 3), depict a negative correlation for FeO, MgO, TiO₂ and CaO in relation to SiO₂, while Al₂O₃ and total alkalis do not show any significant variation.

Concerning the trace elements, a positive correlation for Ba and a negative one for Nd, Y, Rb, Sr, V and Zr are shown in the plots of the trace elements v. SiO₂ (Fig. 4). Probably, part of the mobile elements was washed away during the tectonism and the hydrothermal alteration, bringing about the S type characteristics mentioned.

In terms of the criteria proposed by PEARCE et al. (1984) the studied samples exhibit the geochemical

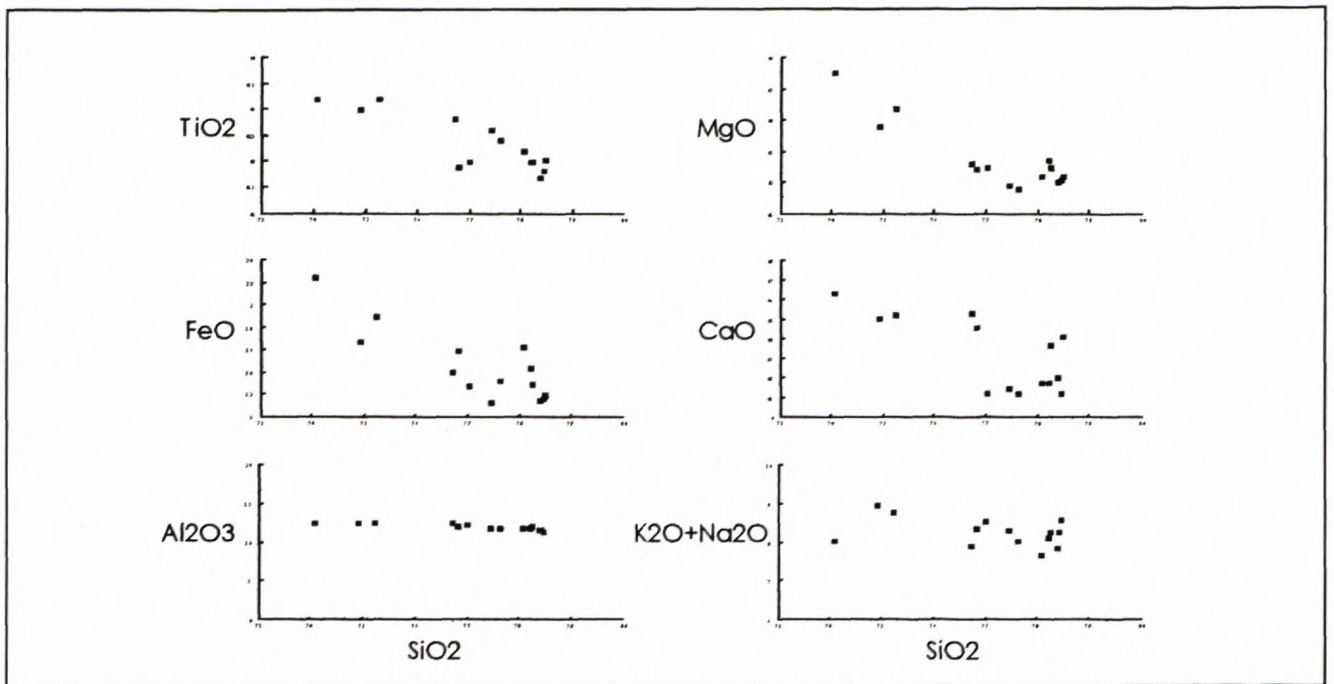


Fig. 3 Major element variation diagrams.

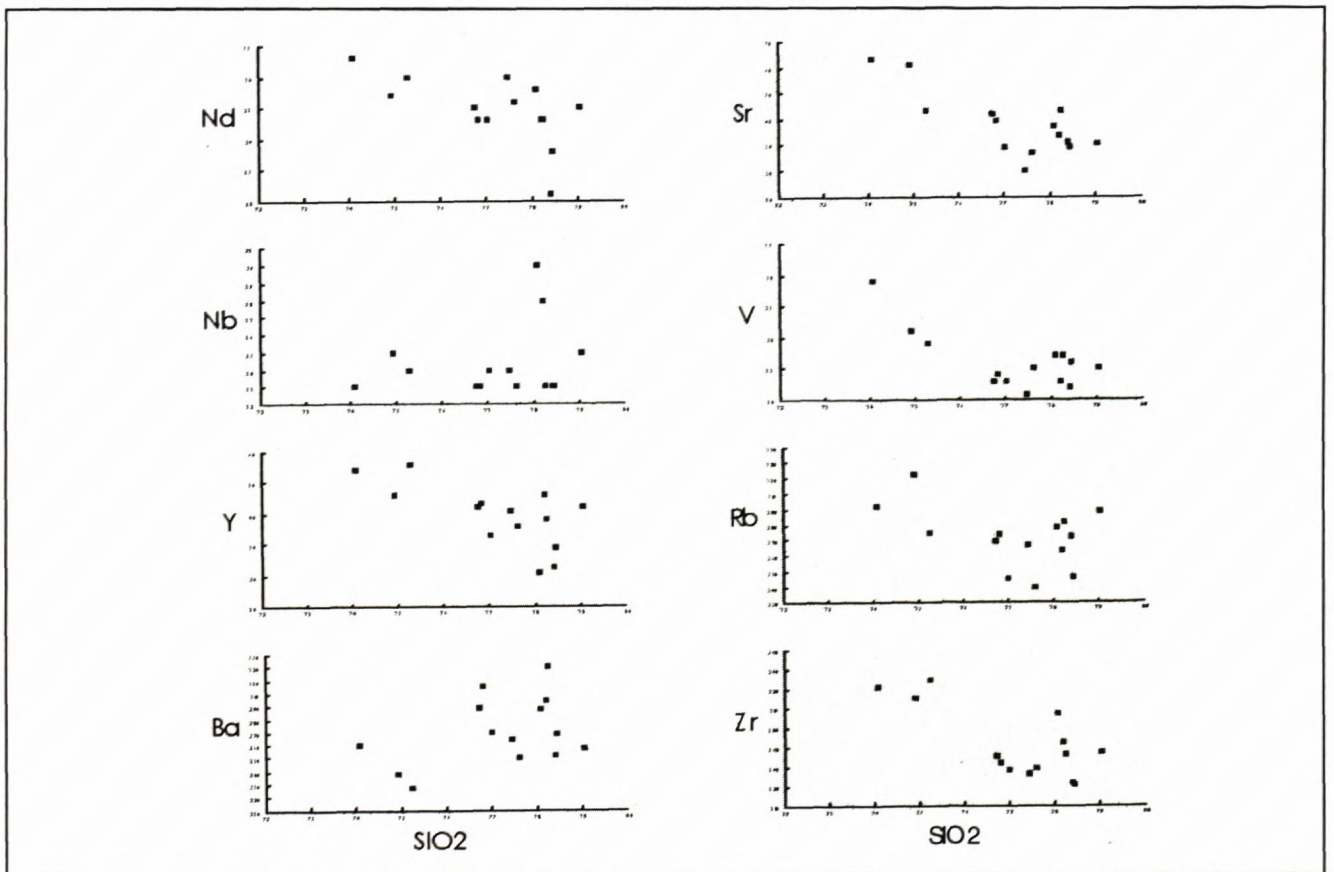


Fig. 4 Trace element variation diagrams.

characteristics that can be attributed to both granites formed in a Volcanic Arc environment, or Within Plate granites. The ORG normalised geochemical diagrams for representative samples (Fig. 5) have shapes similar to the plots of typical Volcanic Arc granites and especially

the granite from Chile (PEARCE & al. 1984). They are characterised by strong enrichment in K, Rb, Ba, and Th, relative to Nb, Ce, Zr, Sm, Y, and Yb, negative anomalies for Nb, Ba and Zr and low Y and Yb values relative to the normalising compositions.

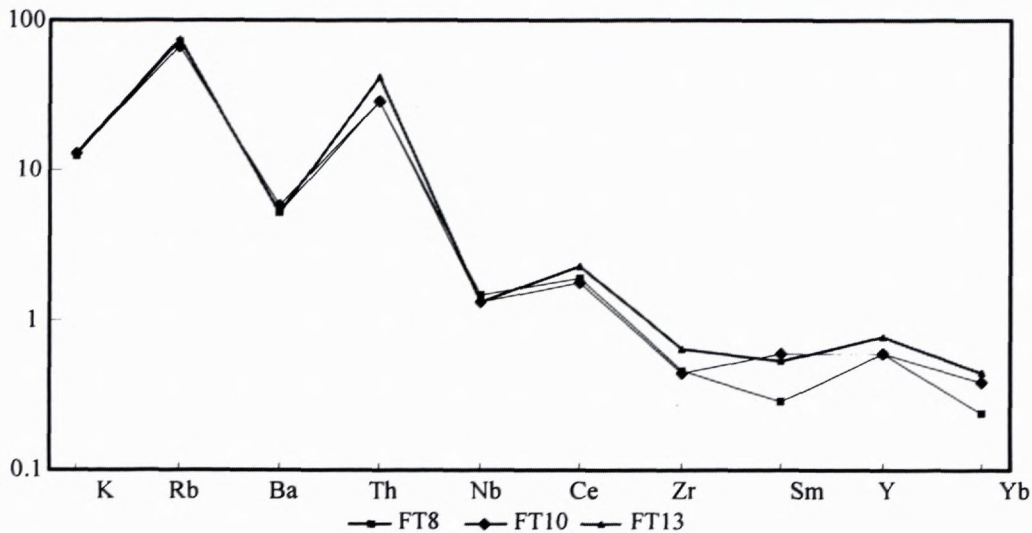


Fig. 5 Ocean Ridge Granites normalised plots of representative samples (after PEARCE et al. 1984).

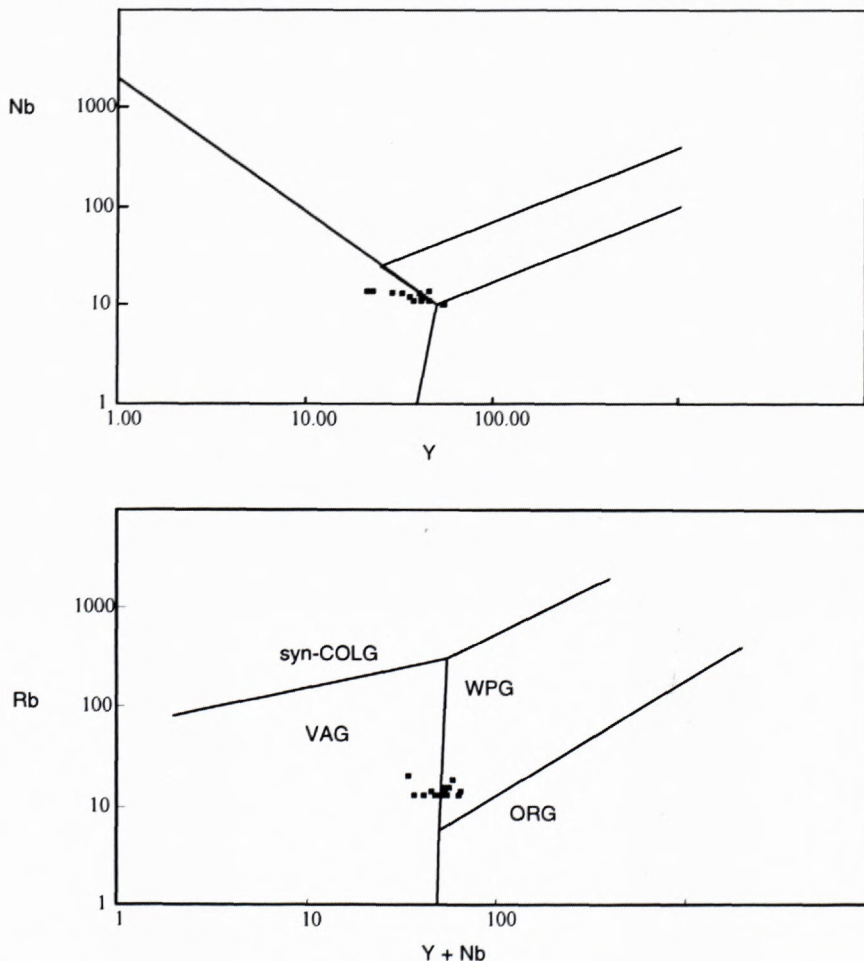


Fig. 6 Nb v. Y and Rb v. (Y + Nb) plots (after PEARCE et al. 1984).

At the same time the studied rocks could be considered Within Plate granites, according to the criteria proposed by PEARCE et al. (1984), as their ORG normalised geochemical patterns are similar to that of Skaergaard granite, which is considered a typical Within Plate intrusion. They have high ratios of Rb and Th relative to Nb, a characteristic of "crust dominated" pattern and flat trends from Zr to Yb with values close to the normalising ones. Figure 6 shows the Nb v. Y and the Rb v. (Y+Nb) plots (proposed by PEARCE et al. 1984) for the discrimination of the geotectonic environment of granitic rocks. The studied samples plot in both the VAG and the WPG fields.

The same geochemical characteristics are depicted from the relative diagrams of the Deskati granitic rocks (KATERINOPOULOS et al. 1994)

In Fig. 7 the mantle normalised large ion lithophile and high strength element spider-diagrams (WOOD & al. 1979) for representative samples are shown. All of them present geochemical characteristics such as high

LIL/HFS element ratios and marked negative Nb, P and Ti anomalies, typical of all subduction zone magmas, precluding the within-plate genesis partly indicated by the diagrams in Figs. 5 and 6.

Those characteristics indicate a relation of the studied plutonic rocks to a subduction geotectonic environment, in accordance with the petrographic observations mentioned, which indicate a syn-tectonic intrusion.

The same characteristics are depicted from the relative diagrams of the Verdikoussa and Deskati granites (KATERINOPOULOS 1994, KATERINOPOULOS et al. 1994)

The plot of some samples in the WPG field of the Nb v. Y and Rb v. (Y+Nb) plots may be attributed to various types of alteration (PEARCE et al., 1984), which are common in the studied rocks.

In relation to other granitic rocks in Greece (BALTAZIS et al 1992, KATERINOPOULOS et al 1992) the studied samples have larger Ba, Sr, Nb, P and Ti negative anomalies. Average continental crust has quite significant nega-

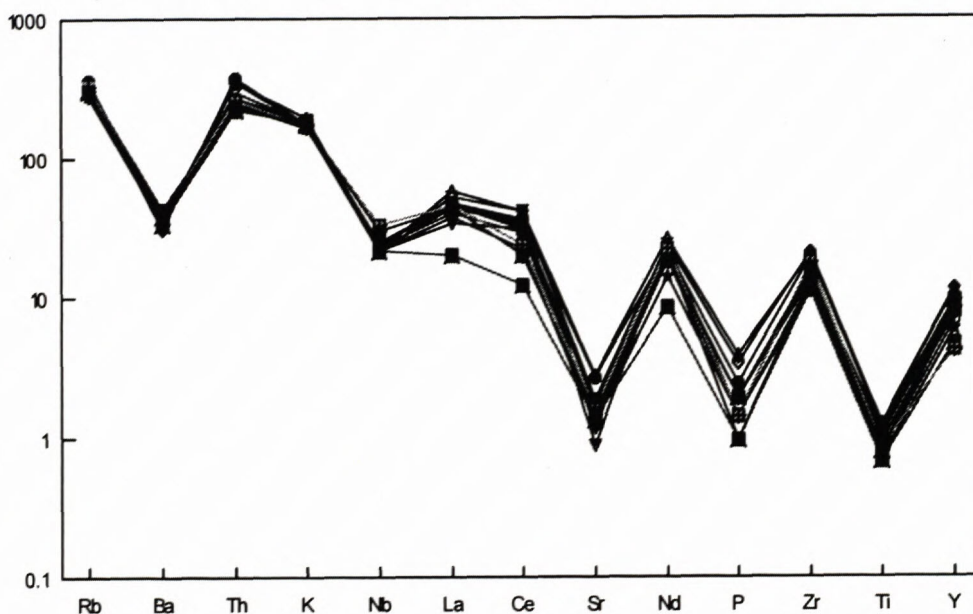


Fig. 7 Mantle normalised LIL and HFS element plots of representative samples (after WOOD et al. 1979).

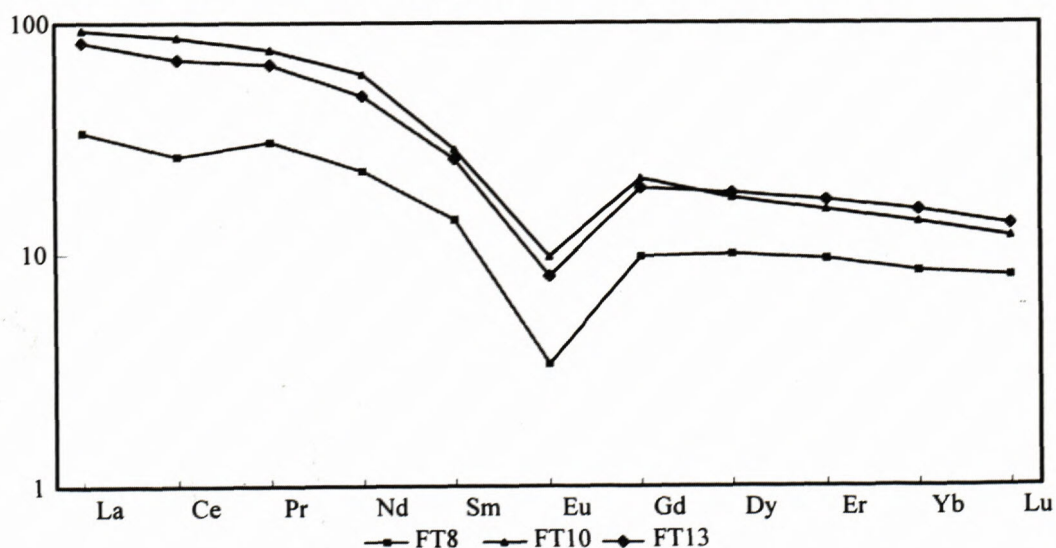


Fig. 8 Rare Earth Element patterns of selected samples (normalisation after HASKIN & al. 1968).

tive anomalies for these elements (JONES et al. 1992), so we can assume an increased crustal involvement to the composition of the parental magma.

The chondrite normalised (HASKIN et al 1968) REE patterns of selected samples (Fig. 8) show relatively high LREE/HRRE ratios and strong Eu negative anomalies, indicating that the distribution of the REE was strongly controlled by the fractionation of feldspars.

In the case of the Deskati and Fotino plutons their formation can be due to a number of diverse mechanisms including crustal anatexis and fractional crystallisation, either, or not combined with assimilation. However, there are several indications that they derived from different parental magma(s) originating the Diava and Verdikoussa magmatic suite, while they probably have a common origin with the Deskati plutonic rocks.

Concerning the age of the emplacement, we can conclude it took place during the Variscan time, according to the analytical data. The same age has been determined for the Deskati plutonic rocks occurring north of the studied area, the Verdikoussa and Diava plutons situated E of the studied pluton, the Varnoundas and Baba mountain plutonic rocks lying NW of the studied area (KATERINOPOULOS et al. 1992) as well as for Pieria granites, situated NE of the studied plutons (SCHERMER et al. 1989).

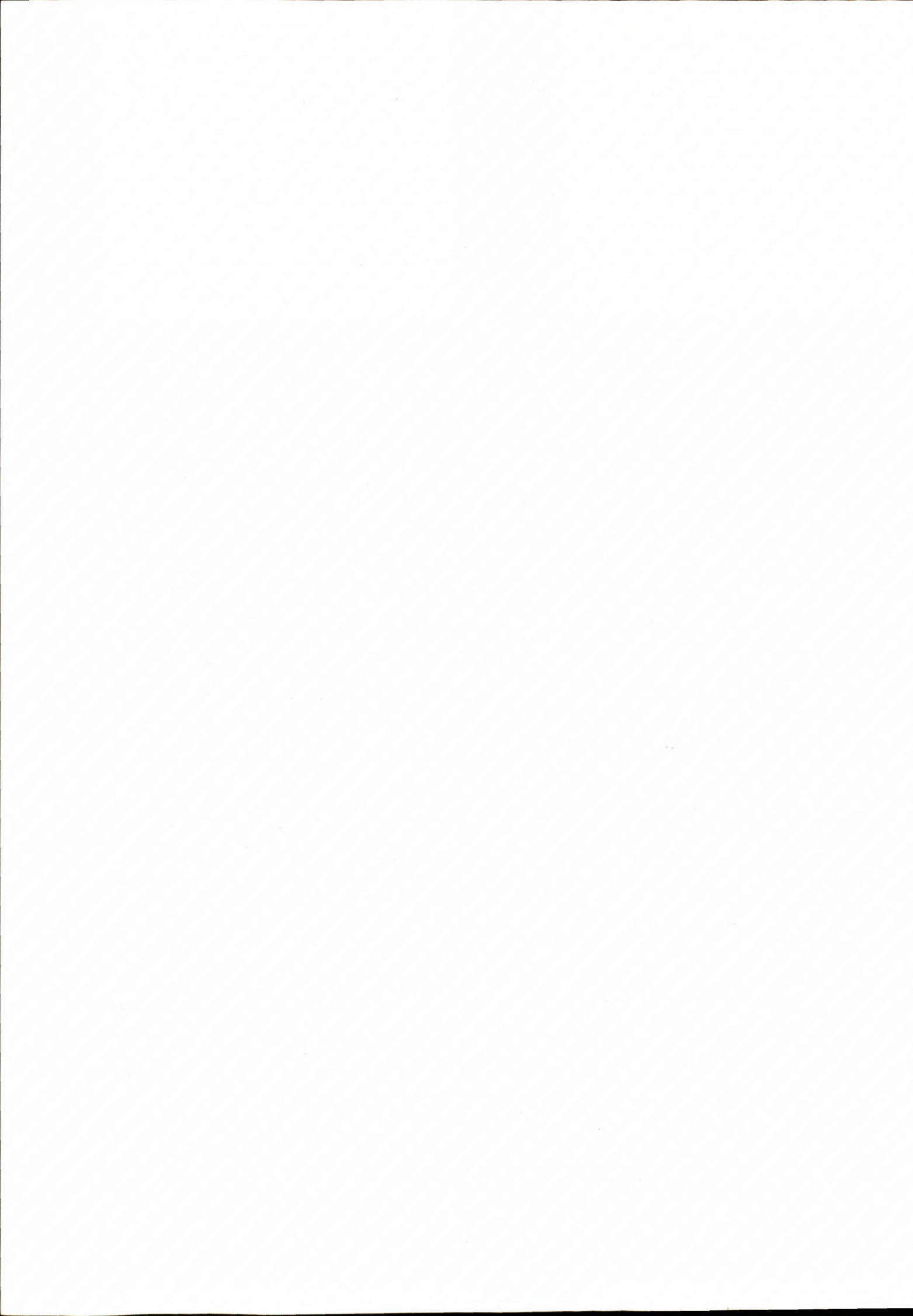
Since the Permian period the Palaeo-Tethys ocean started to develop between Eurasia and Gondwana. During Permo-Triassic, the Cimmerian continent had been separated and broke into smaller pieces (MOUNTRAKIS 1983), so that the Palaeo-Tethys and Neo-Tethys oceans were created at both sides of the North Pelagonian zone, possibly representing the north-western part of the Cimmerian continent (KORONEOS 1991). During that period a subduction zone should have been developed in the area, giving rise to an extended calc-alkaline plutonism.

Acknowledgements

The authors are grateful to Prof. J. TARNEY, University of Leicester, for making available the analytical facilities in the Department of Geology.

References

- ALThER, R. (1981). Zur petrologie der miozanen granitoiden der zentralagais (Griechenland). *Habil-Schrift Techn.Univ. Braunschweig*, 218 p.
- ALThER, R., KREUZER, H., WENDT, I., LENZ, H., WAGNER, G.A., KEKKER, J., HARRE, W. & HOHNDORF, A. (1982) A Late Oligocene/Early Miocene high temperature belt in the Attic-Cycladic crystalline complex (SE Pelagonian, Greece). *Geol. Jb.*, E23, 97-164.
- ANDERSON, L. J. (1980). Mineral equilibria and crystallisation conditions in the Late Precambrian Wolf River Rapakivi massif, Wisconsin., *Am. J. Sci.*, 280, p. 289-332
- BALTATZIS, E., ESSON, J. & MITROPOULOS, P. (1992) Geochemical characteristics and petrogenesis of the main granitic intrusions of Greece: an application of trace element discrimination diagrams. *Min. Mag.*, 56, p. 487 - 501.
- DEER, W. A., HOWIE, R. A. & ZUSSMAN, J. (1986). *Rock forming minerals*, 1B. Longman S & T, New York, 629 p.
- HASKIN, L.A., HASKIN, M.A., FRAY, F.A. & WILDEMAN, D. R. (1968). Relative and absolute terrestrial abundances of the rare earths. In L.A. Ahrens ed. *Origin and distribution of the elements*. Pergamon, Oxford, p. 889 - 912.
- JONES, C.A., TARNEY, J., BAKER, J. & GEROUKI, F. (1992). Tertiary granitoids of Rhodope, N. Greece: magmatism related to extensional collapse of the Hellenic orogen?. *Tectonoph.*, 210, p. 1 - 21.
- KATERINOPOULOS, A. (1994) *Petrology and Chemical Characteristics of the Verdikoussa Granitic Rocks, Thessaly, Greece*. *Ann. Geol. Pays Hell.* (In print)
- KATERINOPOULOS, A., KYRIAKOPOULOS, K. & MARKOPOULOS, T. (1992) Distribution in time and space of the acid plutonic complexes in Greece. *International IGCP Congress No 276. Paleozoic Geodynamic Domains and their Alpidic Evolution in Tethys*. Granada.
- KATERINOPOULOS, A., KOKKINAKIS, A. & KYRIAKOPOULOS, K. (1994) *Petrology and Chemical Characteristics of the Deskati Granitic Rocks, Thessaly, Greece*. 7th Congress. *Geol. Soc. Greece, Thessaloniki*.
- KATSIKATSOS, G. & MIGOIS, G., Triantaphyllis, M., Mettos, A., (1986). Geological structure of internal Hellenides. *Geol. Geoph. Res.*, Sp. issue, p. 191-212.
- KILIAS, A. & MOUNTRAKIS, D. (1989). The Pelagonian Nappe. Tectonics, metamorphism and magmatism. *Bull. Geol. Soc. Greece*, 23/1 p. 29-46.
- KORONEOS, A. (1991). *Mineralogy, Petrology and Geochemistry of the East Varnoundas plutonite (N. W. Macedonia)* Ph.D. Thesis, University of Thessaloniki, 414pp.
- MARSH, N. G., TARNEY, J. & HENDRY, G. L. (1983). Trace element geochemistry of basalts from Hole 504B, Panama Basin, DSDP Legs 69 and 70. *Init. Rept. Deep Sea Drilling Project. 69, 747-764*. (U.S. Govt. Printing Office, Washington).
- MIGOIS, G. (1983). *Geological study of the Kato Olympos area, Thessaly*. Ph.D. thesis, Patra, p.204.
- MOUNTRAKIS, D. (1983). *Structural geology of the North Pelagonian Zone s. l. and the geotectonic evolution of the Internal Hellenides*. Docent thesis, University of Thessaloniki, 289 pp.
- PEARCE, J. A., HARRIS, N.B.W. & TINDLE, A. J. (1984) Trace elements discrimination diagrams for the tectonic interpretation of the granitic rocks. *J. Petrol.*, 25, p.956-983
- SCHERMER, E. R., LUX, D. R. & BURCHFIEL, B. C. (1989). Age and tectonic significance of metamorphic events in the Mt. Olympos region, Greece. *Bul. Geol. Soc. Greece*, 23/1 p. 13-27.
- STAMATIS, A. (1987). *Geological map of Greece, (1:50000) Deskati sheet*, Publication IGME.
- TULLOCH, A.J. (1979). Secondary Ca-Al silicates as low-grade alteration products of granitoid biotite. *Contr. Min. Petr.*, 69, p. 105-117.
- WONES, D. R. & EUGSTER, H. P. (1965). Stability of biotite: experiment, theory and application. *Am. Min.*, 50, p. 1228 -1278.
- WOOD, D. A., JORON, J. L., TREUIL, M. & TARNEY, J. (1979). Elemental and Sr isotope variations in basic lavas from Iceland and the surrounding ocean floor. *Contrib. Min. Petr.*, 70, p. 319-339.



Pútikov vršok volcano - the youngest volcano in the Western Carpathians

LADISLAV ŠIMON and RUDOLF HALOUZKA

Geological Survey of Slovak Republic, Mlynská dolina 1, 817 04 Bratislava

Abstract: As an independent space- and time-bound volcano, composed of a succession of lava flows and pyroclastic rocks, the Pútikov vršok volcano marks the latest volcanic activity in the Western Carpathians spanning the time between 140 000 and 130 000 years ago (Late Riss, Pleistocene stage). The lava flows, predominated by the Aa types of lava, churned out of the central volcanic crater, while the pyroclastic rocks, generated during the processes of Stromboli, Hawai and/or freatomagmatic kinds of eruptions, have been piled up to form a cinder cone. The volcanic rocks have been classified as alkali basalts and/or basanites.

Key words: Pútikov vršok volcano, Quaternary, lava flows, pyroclastics.

Introduction

As the earlier studies have not addressed the volcano proper the authors have carried out co-operative petrologic studies and compiled all available information obtained during previous investigations with the objective to classify and to characterise both, the volcanic and the Quaternary rocks of the Pútikov vršok volcano and its surroundings. The volcanologic classification and the description are based on geologic map at a scale 1:10 000 (sheet 35-44-20), constructed during past few years by L. ŠIMON, V. KONEČNÝ and J. LEXA and on detailed lithological studies of the volcanic rocks underlying the area between Tekovská Breznica and Nová Baňa/Brehy. The interpretations related to Quaternary rocks are based on geologic maps of the Pohronie (Hron valley) area at scales 1:25 000 and 1:10 000, completed recently by R. HALOUZKA. Most detailed investigations (in the context of the whole alluvial terrace system) were made in the areas of the Hron River terrace accumulations.

Prior to defining the Pútikov vršok volcano as a unit its lithologic-petrographic content and stratigraphic position had to be established. The volcano is a discrete, space- and time-bound volcanic body (see geological map and section) situated in the south-western part of the Central Slovakian volcanic region (Fig 1, Photo 1 and 2). It is, in fact, the youngest volcanic feature in the Western Carpathians and if it was not for the volcanoes

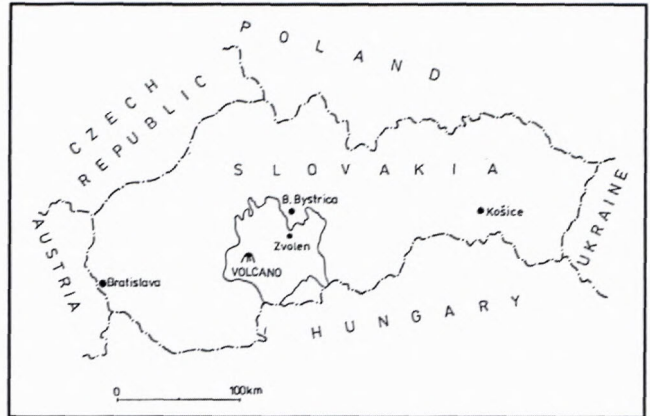


Fig.1. Location of the Pútikov vršok volcano in the Middle Slovakian volcanic area

of the southern end of the Hargita Mts. in Romania it would be second to none in the whole Carpathian-Pannonian region. This paper also describes character of volcanism, lithologic features, origin of rocks, their tectonic position and relation to Quaternary sediments, with the objective to define the stratigraphic features and the age of volcanism.

Review of previous investigations

The volcanic rocks exposed in the surroundings of the locality were first referred to as basalts by JONAS (1820 in FIALA 1952). In addition to these basalts BEUDANT (1822, in FIALA 1952) described tuffs and volcanic bombs. FIALA (1952) was the first to make a detailed petrographic analysis of rocks in the surroundings of the Pútikov vršok (the name Pútikov vršok, used in older maps, coincides with the existing triangulation point 477 m), classifying them as alkaline basalts (basanites) and recognising three main lava flows, cinder accumulations and volcanic bombs. He assigned them Neogene age. KUTHAN (in KUTHAN et al 1963, pp. 122-123) in his explanations to geologic overview map at a scale 1: 200 000, M-34-XXXI, Nitra sheet used the drill hole logging, prospection reports and geologic map of a basalt deposit, made by KAROLUS. He was the first to assign the basalt at Brehy Late Quaternary age, which he believed was in agreement with its position in the "lowest Hron

River terrace". ŠÍMOVÁ (1965) and MIHÁLIKOVÁ and ŠÍMOVÁ (1989) brought forward a detailed account of petrographic and petrochemical features of the basalts (including the Brehy and Pútikov vršok localities (points 1,7,8 in Table 1). The results of long run mapping in the broader surroundings of the locality are summarised in the geologic map of Central Slovakian volcanics on the scale 1:100 000 (KONEČNÝ, LEXA et al. 1984), as well as in the monography of KONEČNÝ, LEXA and PLANDEROVÁ (1983), in which the Brehy locality appears as a cindercone

with crater breccias. Three nepheline basanite lava flows of Quaternary age (this age is indicated in the map, too) are shown to have extruded from the crater. According to K-Ar dating of BALOGH et al. (1981) the age of basaltic rocks of Brehy is 0.53 ± 0.16 Ma. However, previous K-Ar dating of BAGDASARJAN (BAGDASARJAN, KONEČNÝ and VASS, 1970) gave less than 0.4 Ma, a value below the detectability limit of the method. The results of measurements and the assessment of positive polarity of paleomagnetism (see NAIRN and KAROLUS, 1965) are not contradictory to this dating.

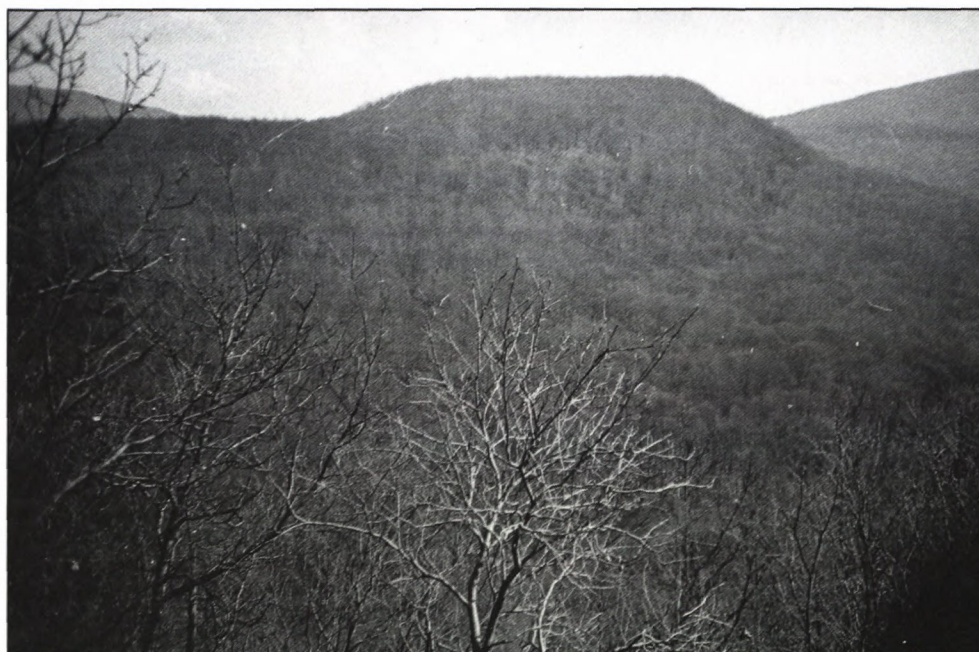
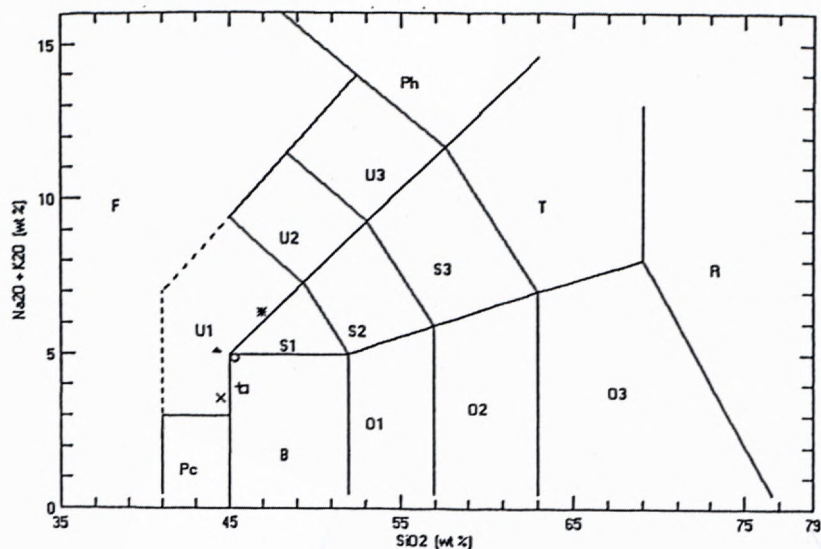


Photo 1. Pútikov vršok volcano- cinder cone, 477 m t.p. and surroundings



Photo 2. Lava plateau of the Pútikov vršok volcano.

Table 1 TAS classification diagram according to LE BAS et al. (1986)



x - Plp-1, Pútikov vršok, ŠIMON; + - PV-1, Pútikov vršok, ŠIMON; Δ - FIALA (1952); O - 1, Brehy, MIHÁLIKOVÁ - ŠÍMOVÁ (1989); □ - 7, Chválenská dolina, MIHÁLIKOVÁ - ŠÍMOVÁ (1989); * - 8, Chválenská dolina, MIHÁLIKOVÁ - ŠÍMOVÁ (1989);

Major oxides

| | Plp-1 | PV-1 | 1 | 7 | 8 | Fiala |
|--------------------------------|-------|-------|-------|-------|-------|-------|
| SiO ₂ | 44.47 | 45.54 | 45.30 | 45.85 | 46.90 | 44.22 |
| TiO ₂ | 2.57 | 2.48 | 2.79 | 2.53 | 3.45 | 2.62 |
| Al ₂ O ₃ | 13.26 | 12.54 | 12.52 | 11.42 | 14.94 | 12.02 |
| Fe ₂ O ₃ | 3.14 | 3.80 | 5.91 | 2.60 | 3.72 | 4.05 |
| FeO | 7.26 | 6.87 | 6.47 | 8.84 | 7.83 | 7.54 |
| MnO | 0.18 | 0.15 | 0.15 | 0.16 | 0.13 | 0.23 |
| MgO | 11.63 | 11.52 | 10.71 | 12.33 | 5.36 | 10.74 |
| CaO | 10.93 | 10.36 | 9.44 | 10.68 | 9.56 | 10.23 |
| Na ₂ O | 2.40 | 2.58 | 3.38 | 2.85 | 4.47 | 3.43 |
| K ₂ O | 1.18 | 1.33 | 1.49 | 1.00 | 1.90 | 1.69 |
| P ₂ O ₅ | 0.64 | 0.68 | 0.81 | 0.58 | 0.76 | 0.72 |
| | 97.66 | 97.85 | 98.97 | 98.84 | 99.02 | 97.49 |
| CIPW norms | | | | | | |
| Or | 6.97 | 7.86 | 8.81 | 5.91 | 11.23 | 9.99 |
| Ab | 14.19 | 18.19 | 20.56 | 16.10 | 22.36 | 11.64 |
| An | 21.93 | 18.71 | 14.59 | 15.42 | 15.09 | 12.41 |
| Ne | 3.31 | 1.97 | 4.36 | 4.34 | 8.38 | 9.42 |
| Di | 22.35 | 22.41 | 21.19 | 27.07 | 22.08 | 26.79 |
| Ol | 17.99 | 16.92 | 13.72 | 20.08 | 6.17 | 14.73 |
| Mt | 4.55 | 5.51 | 8.57 | 3.77 | 5.39 | 5.87 |
| Il | 4.87 | 4.71 | 5.30 | 4.80 | 6.55 | 4.98 |
| Ap | 1.53 | 1.61 | 1.92 | 1.37 | 1.80 | 1.71 |

Since mid-sixties the Quaternary research of Tekovská Breznica - Brehy localities (important in stratigraphic terms) has been repeatedly carried out in several projects realised within the framework of systematic mapping of the Pohronie (or, more precisely, Central Pohronie) area. One of two principal sections running through the Tekovská Breznica village (drill hole HŠ-15, ŠKVARKA, KAROLUS and HALOUZKA) has been made in 1971 as a co-operation venture. Apart from the detailed macroevaluation of Quaternary section, a sedimentary-petrographic evaluation has also been made (MINAŘIKOVÁ, non refereed manuscript). The second section running through Brehy (loesses and their derivatives resting on the basalts), which was presented as an excursion locality during the international geomorphological symposium held in 1992 (section through loess with fossil soils, prepared by HALOUZKA), has also been investigated. An alternative section of the Brehy locality, in which the litological features and molluscan fauna have been studied in 1995 (HALOUZKA and KERNÁTSOVÁ), is exposed in an outcrop of loess derivatives.

Finally, we note that a detailed geophysical research using electric-resistivity method has been made throughout the Hron River valley (1:5 000 maps with geological-geophysical sections published in thematic atlas sets). An expert in Quaternary geology (HALOUZKA in JANÍK, Kanda et.al., 1986) also evaluated the section Tekovská Breznica-Brehy. RAČKO's remarkable geomorphologic publication (1990), which addresses the same problems, must also be mentioned in this context. Most recent information related to the locality was published by present authors in other papers, or in lectures. ŠIMON (1991) described the succession of several lava flows, overlain by cinder cone with pyroclastic rocks.

In their detailed description of the Nová Baňa -Brehy excursion locality, published as part of the excursion guide to the international symposium on dating in geomorphology (held in Tatranská Lomnica, Stará Lesná, in June 1992), HALOUZKA and ŠIMON (1992a,b) presented a concept of the so called refined interpretation of the Quaternary position of lava flows (end of Middle Pleistocene - late glacial stage) during Late Riss (by HALOUZKA inferred approx. age range from 160 000 to 130 000 y. B.P.), which they base mainly on the results of own detailed lithologic and stratigraphic studies of volcanic and sedimentary rocks, as well as on the above mentioned data. And finally, the same interpretation of the stratigraphic position of lava flows and sediments was presented by HALOUZKA and ŠIMON (1992) as an unpublished lecture at the mentioned symposium. Notably, their concept was appreciated by the participants in the following discussion and during the excursion to the locality.

The Pútikov vršok volcano

The rocks making up the volcano represent a discrete volcanic unit referred to as the Pútikov vršok volcano. Below we present the definition of the volcano.

Name: After the Pútikov vršok hill, located on the map sheet No. 4661 Nová Baňa (old grid), on the sheet No. 35-44-20 (new grid). It corresponds to triangulation point 477 m, located between the Nová Baňa and Tekovská Breznica villages, on western slopes of the Štiavnické pohorie Mts.

Definition: The cinder cone and a set of alkaline basalt and/or basanite lava flows, located between this cone and the Brehy and Tekovská Breznica villages, named the Pútikov vršok volcano.

The stratotype (type section): The volcano has stratotype outcrops in the Chválenská dolina, below the triangulation point 477 m (photos 5, 6, 7, 8, 9, 11, 12, 13, 14, 15, 16), near the triangulation point 432 m (photo 4) and in the quarry near Nová Baňa/Brehy (photo 10).

Extension, thickness, boundaries: Located between the Tekovská Breznica - Chválenská dolina sites, below the triangulation point 477 m - Nová Baňa/Brehy, the volcano outcrop covers an area of some 4 sq. km.

Stratigraphic data: Volcano is a product of the latest volcanic activity in the Western Carpathian territory. The basement of this formation is made of gravels dating back to latest Riss stage (Middle Pleistocene) (HALOUZKA and ŠIMON 1992a,b), (Fig.2). Most recent update of this dating gave an age of basalt ranging between 140 000 and 130 000 y. B. P. , while the final extrusions were dated roughly at 125 000 y.B.P. ago (HALOUZKA l.c.). The problems of dating will be further discussed in an independent paper, now under preparation.

Rock lithology of the Pútikov vršok volcano

The volcano is made of 2 lithogenetic types of volcanic rocks, represented by:

- 1) lava flows and 2) pyroclastic rocks.

1. Lava flows

Lava flows are products of effusive volcanic activity. The extrusions have been discharged from the central volcanic crater. The flows emplaced over the cone are arrayed in a fan-shaped fashion around its centre. Some 90% of the lava mass have flowed in NNW direction towards the Tekovská Breznica and Nová Baňa, part Brehy (the passage of descending flows was controlled by both, the geomorphologic features and the gravity). Lava flows have variable lengths and thicknesses ranging from short, through medium long to very long. The short ones, situated in the crater's surroundings, may be as long as 10 m and up to 30 cm thick. The medium thick flows are 10 - 100 m long (Photo 4) and their thickness ranges between 10 cm and 10 m. The longest flows encroach as far afield as the area of Brehy village. With total length of up to 3.2 km and maximum thickness of 15 m (Fig.10) the individual flows of variable thickness and length overlap and/or intermingle with each other, making the distinction of individual lobes, or counting precisely their numbers, impossible. The main flows are

emplaced in the wash-outs, from which the side lava lobes branch out (Fig.3) to make, what we call, the lava plateau sequence. The entire mass of the lava flows extends over an area of roughly 4 sq. km. It fills some 500 m wide valley (originally the Chváleňská dolina stream?) located below the cinder cone and overlies Quaternary deposits in the valley, which opens downwards to form a

plateau measuring as much as 1.5 km across. The flows represent the products of volcanic activity with variable eruptions and low degree of eruptivity. The eruptions produced lavas of the Aa type and the pahoehoe type (according to WILLIAMS - MCBIRNEY, 1979). The Aa - lavas (photo 3, 4, 5, 8A) are the main types of lava generated during the eruptions. The difference between Aa

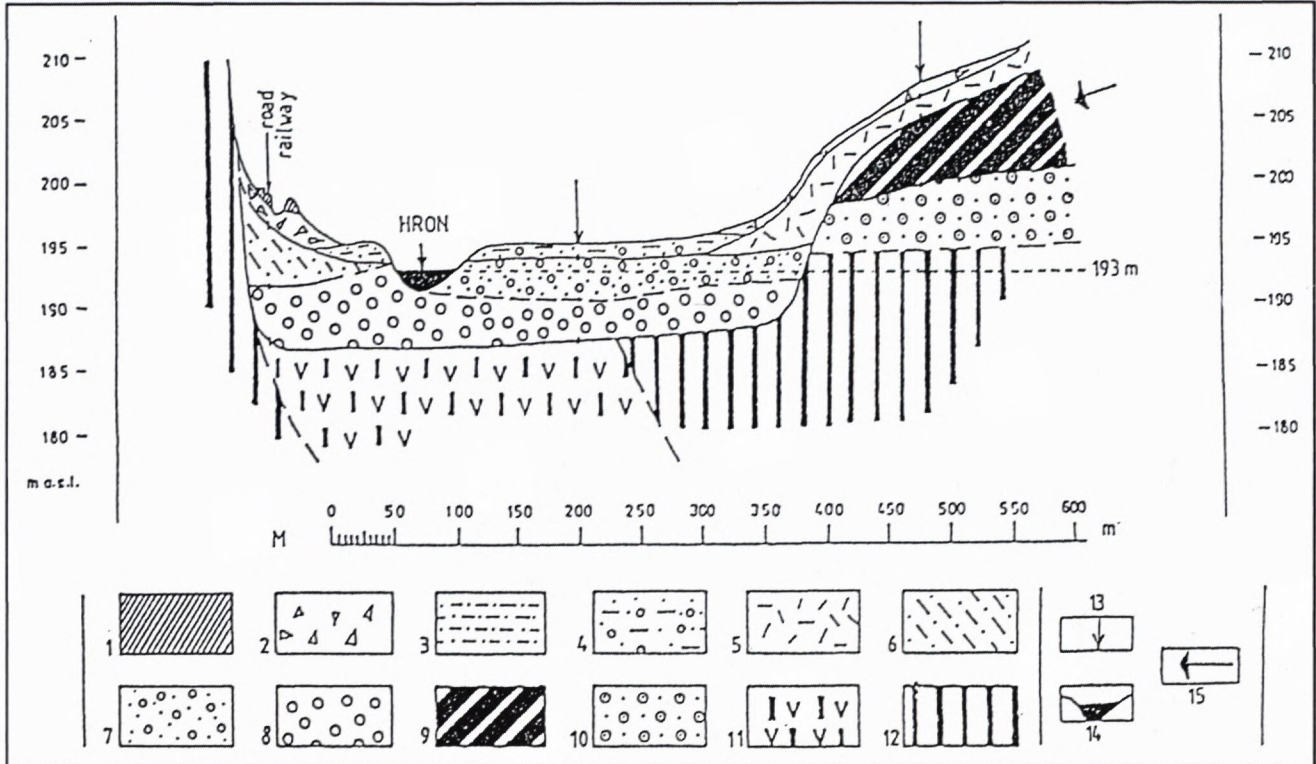


Fig. 2 Geological section through the Hron River valley near Nová Baňa-Brehy (HALOUZKA 1992 - compiled according profile in map 1:5000 - in KANDA et al. 1986)

1. man-made ground deposits, 2. debris, 3. fluvial sandy loams, 4. fluvial sandy loams with gravel, 3-4. alluvium in the flood plain, 5. polygenetic slope loams (surface wash), 6. polygenetic slope sandy loams (surface wash). 2,5,6. deluvial (slope) sediments, 1 to 6. Holocene, 7. fluvial gravel and sands, 8. fluvial sandy gravel, 7. to 8. Late (Upper) Pleistocene, Wurm (bottom accumulation), 9. nepheline basalts, 10. fluvial sandy gravel (terrace accumulation), 9 to 10. Middle Pleistocene, Late Riss, 11. andesitic volcanoclastics (tuff), 12. andesites, 11. to 12. Miocene (Badenian), 13. resistivity sounding probes (geophysical survey), 14. river channel, 15. lava flow direction

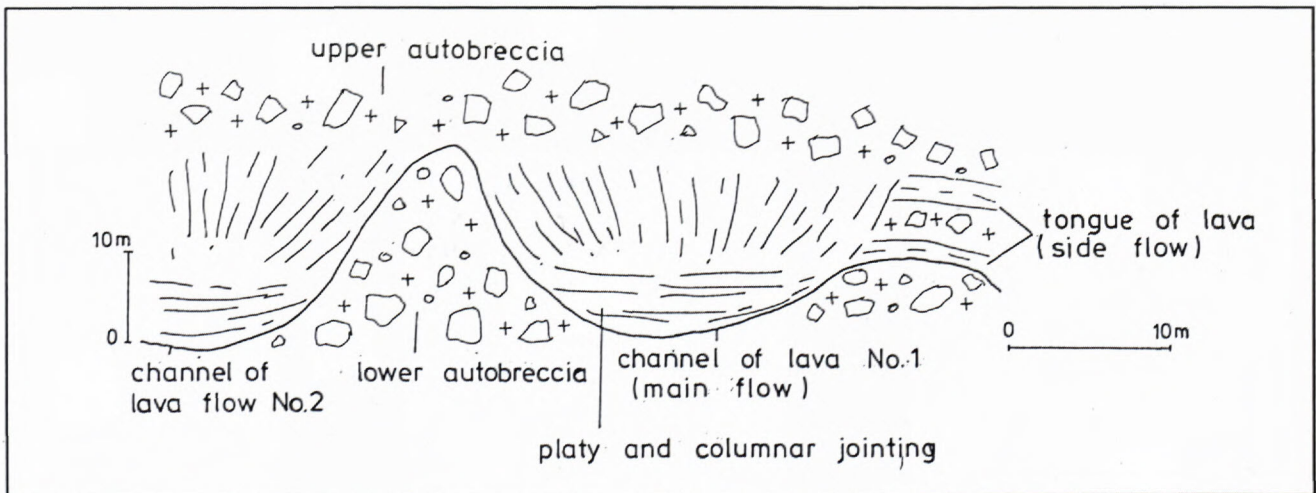


Fig. 3. Sketch of geological setting in the Brehy quarry (to be compared with photo 10 A. - 10H.).

and pahoehoe lavas is demonstrated by the surfaces of their bodies (Fig. 4). Besides, no breccias form in the pahoehoe lava flows. Their surfaces are fine, smooth and porous, although, the porosity may vary. Some of the pahoehoe lava flows have become subject of bubble cracking processes, similar to those described by BLACKBURN (1976), involving accumulation of gas bub-

bles inside the lava body and subsequent bursting of small local eruptions outside the central crater of the volcano, accompanied by destruction of the surficial crust of the flow, followed by churning of lava over a short distance around it. The fragments accumulate next to the sites of bursting (deformation), on top of the lava flow. Essential part of the lava mass, which makes up the lava



Photo 3. Medium long lava flow - measuring 100 m in diameter and 10 m thick.



Photo 4. Lower part of the Aa type lava flow with traces of brecciation with cauliflower surface.

plateau, is represented by the lava flows of the Aa type. The Aa lavas are composed of massive lava and lava breccias and have coarse surfaces. As a consequence of movements and subsequent cooling of the lava mass the lava breccias develop mainly within the lower and upper parts of the lava flow. Their colour is red, pink, or brown-red, although, some red-yellowish, or ochre-yellow-

pink portions can also be found, particularly in the lower parts. The red, brown-red, or even yellow-red coloured breccias, consisting of angular, spherical or cindery fragments, measuring 1 to 60 cm across, are cemented with brecciated ground material from the above quoted variegated lavas. Yellow tint of a breccia is indicative of the presence of water during eruption. Having originated

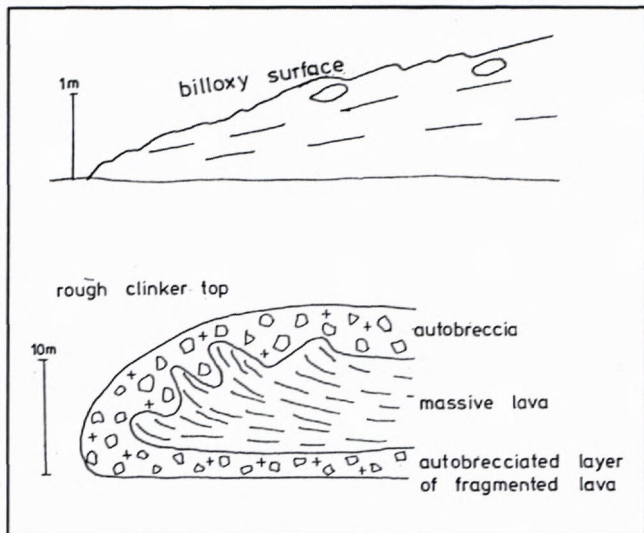


Fig. 4. Differences between pahoehoe and Aa lavas: adapted, after LOCKWOOD, I.P., LIPMAN, P.W. 1980

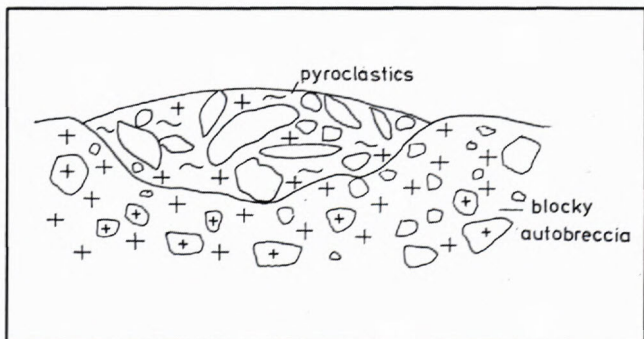


Fig. 5. Pocket filled with pyroclastics in the Brehy quarry.



Photo 5. Massive lava flow in the central zone of the volcano.

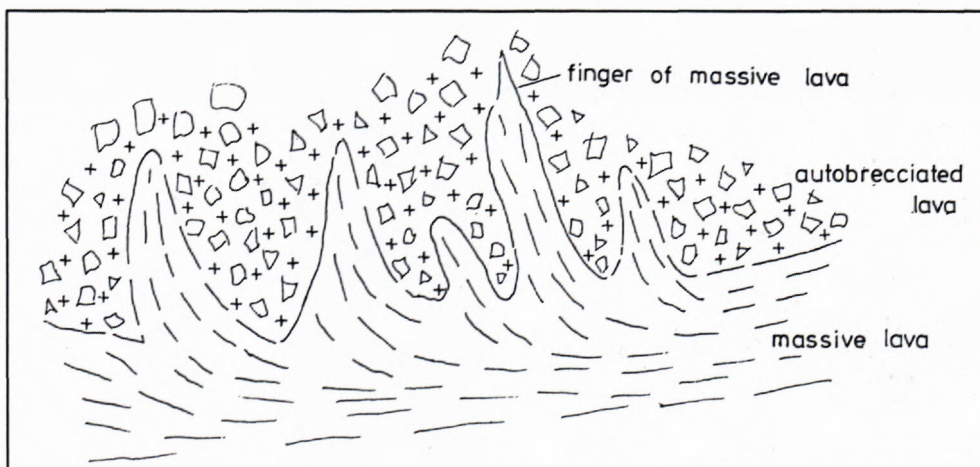


Fig 6. Injection of lava into the lava breccia (Brehy quarry).

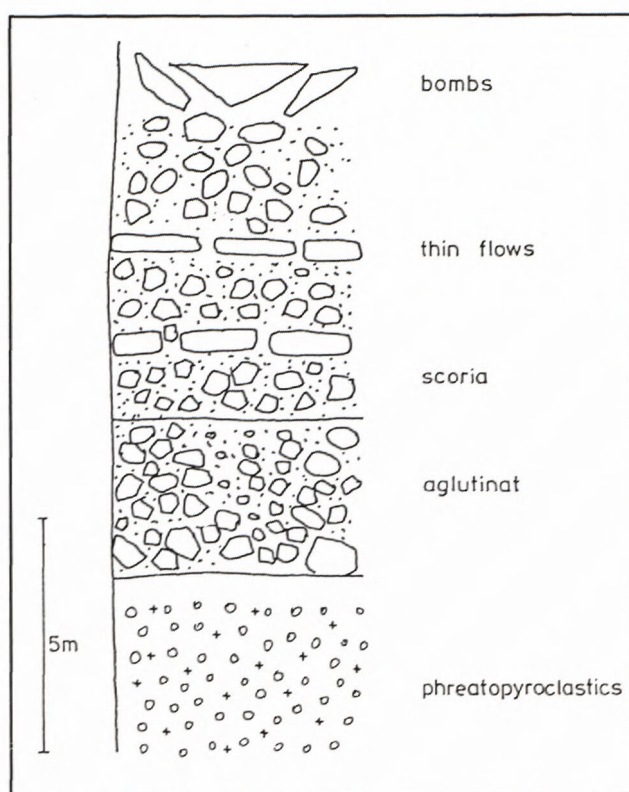
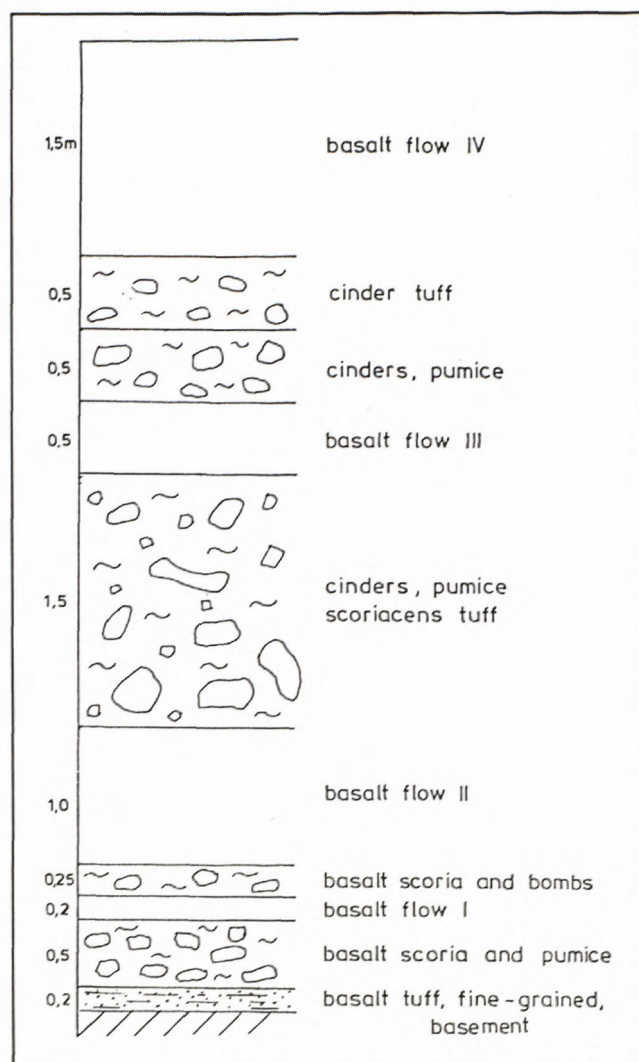


Fig. 8. Sketch section through a cinder cone

Fig. 7. Alternation of lava flows with pyroclastics at the 303 m triangulation point: adapted, after FIALA (1952).



Photo 6. Lava flow - an example of "sonnen brand" type of weathering - pea-shape -spherical desintegration of the body.

either underground, or at the surface (the Hron paleoriver), the water causes weak freatomagmatic eruptions, which take place at the contacts with lava, as indicated by the change-over from red-hot lava desintegrating into red (+tints of red) and yellow (+ tints) fragments. Yellow-growing colours are characteristic of the palagonitisation processes. Occurrence of pyroclastic

pockets, found on tops of lava flows (on the upper lava breccia) (Fig.5), testify that the lava flow eruptions are syngenetic with the explosive pyroclastic eruptions. The pockets filled with pyroclastics developed as the flows run down the slope. Cinder material produced during the Stromboli type eruptions has been strewn over the surrounding grounds whilst a part of it landed on the flowing

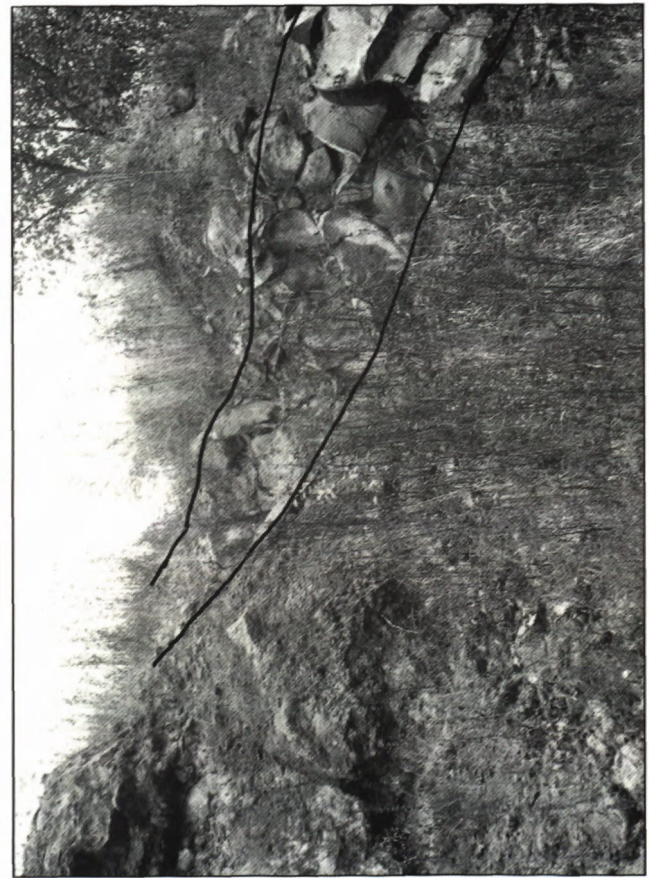
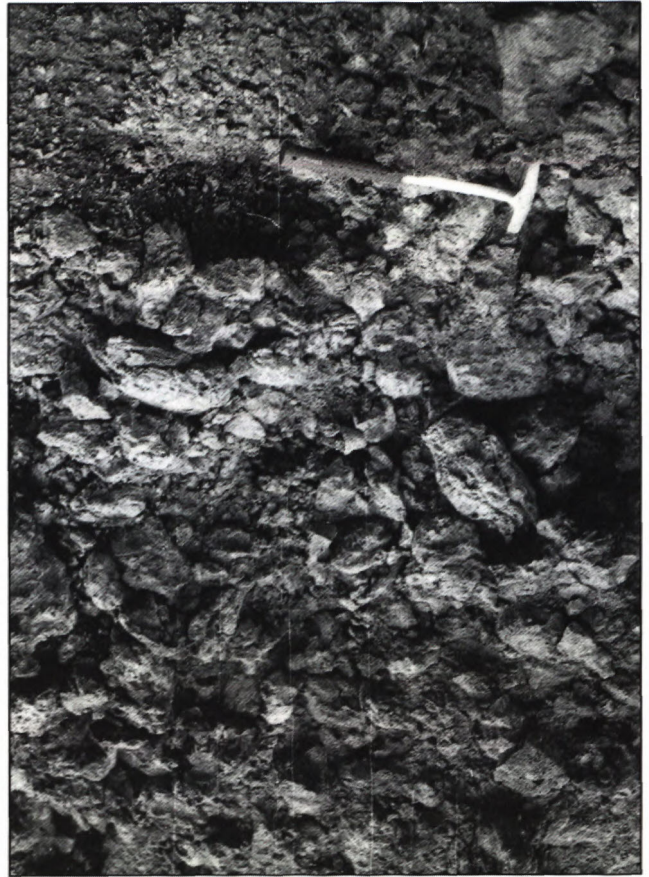


Photo 7. Fragments of broken thin lava flows in pyroclastics of the cinder cone (central zone of volcano).



Photo 8 A-8E. Lava flows in Nová Baňa - Brehy quarry.

Photo 8A. Lava plateau - lava wash-out No. 1, overall view - see Fig.3.



lava (see in the Brehy quarry). Syngenetic origin of both eruptions can best be demonstrated in the surroundings of the 303 m triangulation point. FIALA (1952) described alternation of thin flows (0.5-1.5 m thick) with pyroclastics (0.2-1.5 m thick) (see FIALA p. 17, Fig. 7, 8). The signs of grinding and the development of quasi brecciated texture with cauliflower features in both, the lower and the upper parts of the flows, have been observed on the surfaces of some of thin Aa lava types of flows (Photo 4). If located in the upper parts of the volcano these types of lava flows have tabular jointing and show signs of columnar jointing. Irregularly columnar, fan-shaped tabular and tabular-bench-like jointing was observed in peripheral zone of the volcano (e.g. in the quarry near Brehy) (photo 8A, 8C). The lava injections into the upper lava breccias (Fig.6) have also been observed. The lava flow bodies, which spilled over the upper and middle parts of the volcano, impounded and diverted existing streams. These events had favourable effects upon Quaternary sedimentation. Quaternary paleolakes formed along the southern and south-eastern margin of the volcano (see geologic map).

2. Pyroclastic rocks

Pyroclastic rocks (= pyroclastics) of the Pútkov vršok volcano developed in a process of explosive eruptions described by FISHER-SCHMINCKE (1984), BLACKBURN et. al. (1976), Self et. al. (1974) and WALKER (1973). The cinder cone, situated in the central zone and composed predominantly of fallen freatomagmatic pyroclastics, has been piled up during intense Stromboli-type to Hawaiian-type eruptions (Fig. 4). The deposited cinder cone is made of non-consolidated to ignimbritic pyroclastic rocks. We presume that the cone, composed of well defined beds commencing in its lower part with palagonitised yellow-ochre lapilli tuffs (= freatopyroclastics - defined by ŠIMON, 1995) (photo 9), has been partially eroded away and that these rocks were produced during a freatomagmatic eruption, when the magma came into contact with water coming either from the Chválenký potok, or from a lake created due to impoundment of the Chválenká dolina valley. This contact triggered a strong, principal eruption and initiated subsequent formation of the cone. FIALA (1952) reported the occurrence of similar rocks in the area around the triangulation point 303 m. These rocks, composed of fine grained basaltic tuffs (FIALA, 1952, p.17, Fig.7) deposited on the slope of the volcano are termed, using modern terminology, as

base surge freatopyroclastics. They overlie a thin (20 cm) sandstone unit at the base of the volcanic complex. On the other hand, the above quoted palagonitised lapilli tuffs are represented by conspicuous freatopyroclastics, deposited near the crater of the volcano. Strongly ignimbritic agglutinates and red to brick-red spatter rocks (photo 10) occur in the overlier. There are coarse ignimbritic agglutinates with textures of flowage and massive, crust-free, very thin lava flows, deposited in the upper part of the cone (photo 8, 23, Fig.8). The dip angle of the beds in the cone ranges between 6° and 30°. Larger and smaller, brick-red, dark-red, brown-black, or black volcanic bombs measuring 1 to 50 cm across (photo 12-16) are randomly emplaced in the cone. Their shapes are spherical, fish-like, amygdaloidal, cylindrical, cow's stool-like, or shell-like with a tail. In the cone there predominate medium to strongly ignimbritic, massive and herogeneous agglutinates (photo 10-11), composed of irregular, spindle-shaped and spherical spatter rocks, large and small bombs and cinder lapilli (as fallen pyroclastics). The agglutinates, composed of fallen pyroclastics of the size of lapilli and agglomerates, have porous structure. Although some cindery may rarely occur, it is most likely completely absent. Rare blocks and megablocks, measuring 70 to 120 cm across, also occur in them. Strongly ignimbritic variety contains scarce beds of ignimbritic, elongated and flattened bombs, which could have formed as the agglutinate flew down the slope (gravitation effect). This could, however, have only taken place when the agglutinate was hot enough and the slope of its deposition was steep and nonstable. Flattening of the fragments could have been produced as the flying objects hit the volcanic mass. Due to their fancy shapes the volcanic bombs, attracted the attention of old geologists. The bombs represent lava fragments which, after having been blown out of the volcanic crater, landed on the ground. Following genetic types of bombs were distinguished: type 1 - bombs blown out from the crater in rigid state - fragments from older lava flows (block bombs), type 2 - bombs blown high enough into the air to allow for their cooling before hitting the ground, or flown in a form of comet bombs attaining, at the moment of landing, amygdaloidal, shelly, or similar shapes (stromboli eruptions), type 3 - bodies blown to small heights due to weak eruption, forming fish-like, cow stool-like bombs, some of which are twisted, cracked and broken due to the impact (Hawaiian eruptions - lava fountains).

B C
D E

Photo 8B. Detail of lava breccias in a hump.

Photo 8C. Upper part of the lava wash-out - massive lava with transitions to lava breccias.

Photo 8D. Left hand side of the quarry - lava injection into the lava breccias. 8D. The uppermost, right-hand side of the quarry - thin, 1 m thick lava flow between lava breccias in the lava plateau.

Photo 8E. Pockets filled with pyroclastics in the uppermost left hand side of the quarry - they overlie the lava breccias - geological hammer indicates the boundary between lithofacies.

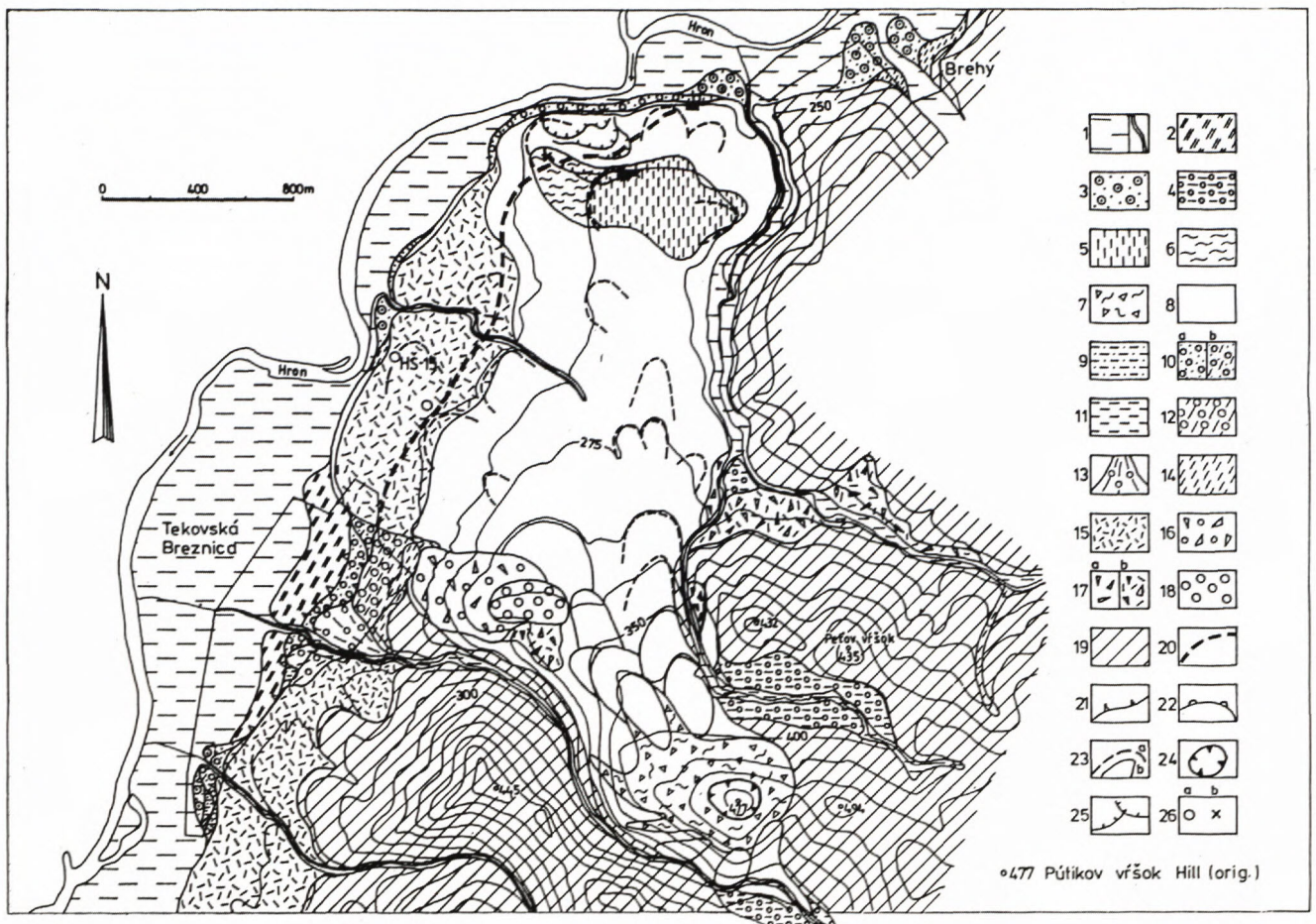
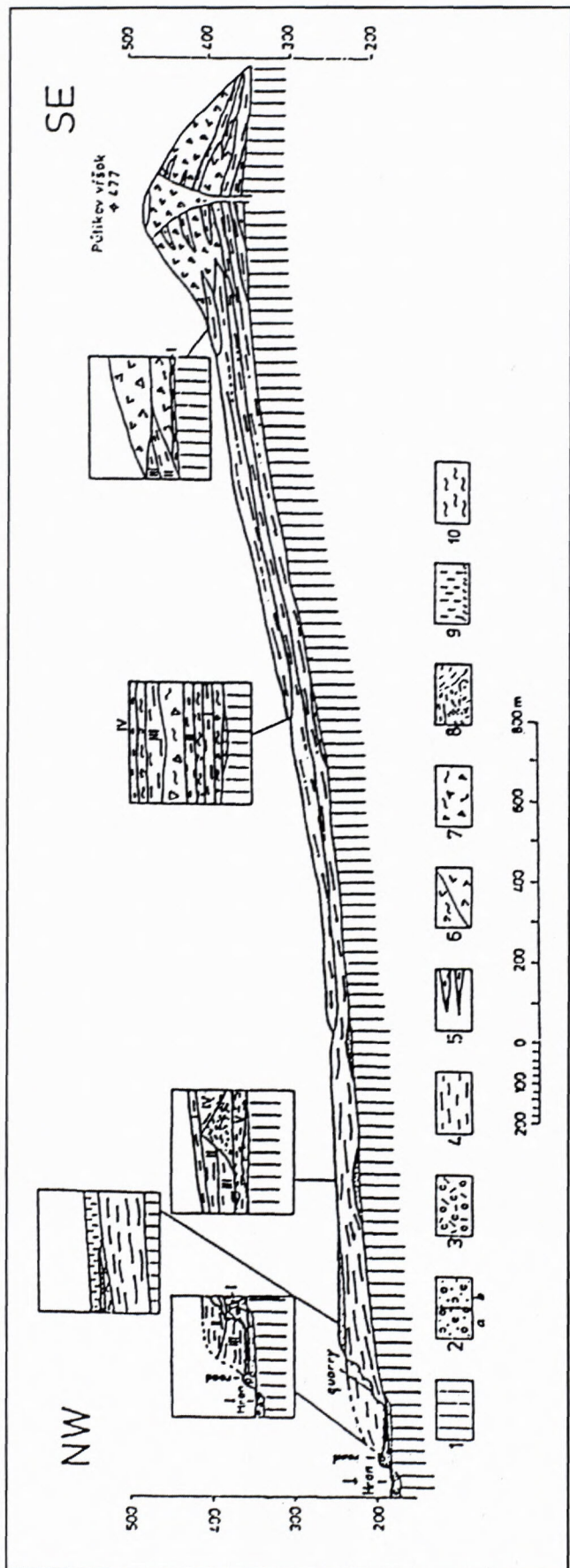


Fig. 9 Geologic map of the Tekovská Breznica - Brehy area (compiled by HALOUZKA and ŠIMON 1995)

1. fluvial and alluvial plain loams and sandy loams, loamy gravelly sediments (Holocene) in stream alluviums; 2. deluvial-fluvial, predominantly loamy outwash and rainwash sediments (Wurm/Holocene) in the overlier of fluvial sandy gravels (Wurm); 3. fluvial sandy gravels and sandy (Wurm); 4. fluvio-limnic loams with gravels (Riss/Wurm-Wurm); 5. Aeolian loessy fossil soils, loessy loams at the base; 6. a series of loessy loams, limy, or lime-free (resedimented loess and fossil soils); 5.-6. Upper Pleistocene; 7. pyroclastic volcanic rocks - undifferentiated; 8. alkaline basalt to nephelinitic basanite lava flows; 7.-8. final period of late Riss - basal part of Riss/Wurm; 9. fluvial aleuritic loams and/or sands; 10. fluvial sandy gravels (a without cover, b - with a younger outwash loam cover); 9.-10. Late Riss; 11. fluvial loams to sandy loams; 12. fluvial gravels and sandy gravels, with younger outwash loam cover; 13. proluvial gravels and loams with semirounded clastics (alluvial fan); 11.-13. early Riss; 14. deluvial-fluvial, predominantly loamy outwash and rainwash sediments; 15.-17. deluvial sediments; 15. polygenetic deluvial loams; 16. gravelly-blocky stony screes to periglacial solifluction flows; 17. screes a) stony and b) loamy-stony. 14.-17. Quaternary undifferentiated; 18. fluvio-limnic desintegrating conglomerates and gravels, polymict (Banská Bystrica, or Hron gravel formation, Upper Pleistocene); 19. underlying andesitic volcanics - undifferentiated (Middle Miocene - Badenian); 20. concealed geologic boundary (with Quaternary fluvial sediments); 21. boundary of riverine terrace; 22. terminal boundary of the alluvial fan front; 23. lava flows a) volcanologically identified b) geomorphologically identified; 24. Quaternary of the volcano; 25. Brehy quarry wall; 26. drill holes study sections.



Petrographic a petrochemic characteristics of volcanic rocks

FIALA (1952) and MIHALIKOVÁ - ŠIMOVÁ (1989) characterised petrographic features of volcanic rocks in detail. We supplement their elaborate results by our petrographic description of to date unknown, once southwards running lava flows (see geological map) with characteristic black, or grey-black colour and compact, or porous texture. They are composed of macroscopic phenocrysts of green amphibole, black pyroxene and glassy lustrous feldspar needles and the matrix, made of plagioclase, olivine, pyroxene and ore pigment and nepheline. Alacime and volcanic glass occur in only accessory amounts. In petrogeochemical terms the Pútikov vršok volcano is made of rocks ranging from alkali basalts to nephelinitic basanites (Table 1).

Discussion and comparison with the global volcanism

1. The volcanic activity of the Pútikov vršok volcano is the youngest of its kind in the Western Carpathians. The volcano was formed during Pleistocene stage (Late Riss) between 140 000 and 130 000 years ago, this time span having been inferred from detailed lithostratigraphy of Quaternary sediments, overlapped by the lava flows of the volcano. The above age cannot be supported by radiometric dating (as none of the methods allows for reliable dating of volcanic materials younger than 200 000 y. B. P., KRÁL pers. comm.). The first of two recent age determinations made on basalts from the volcano (BALOGH et al. 1981), gave the radiometric age of 530 000 years, while the second (RAČKO, 1990), based on geomorphological features, gave an age ranging from 50 000 to 70 000 years (early Würm). An independent and complex study (relation analysis) is needed to solve this problem.

2. Stratigraphic division and dating of the Pútikov vršok volcanism is compatible with the youngest volcanic activity of other volcanoes in the Central European realm. We refer to the dating using pedostratigraphic method of a silty tuff located in the sequence of loesses in Komjatice, Lower Nitra region (VAŠKOVSKÝ and KAROLUSOVÁ, 1969), which gave Mindelian age. Although the

Fig.10. Longitudinal geological section through the area studied (Pútikov vršok-Brehy quarry, compiled by ŠIMON, HALOUZKA, 1995).

1. Underlying andesite volcanics undifferentiated (Middle Miocene - Badenian). 2. fluvial sandy gravels (a - Würm, b - late Riss). 3. fluvial loamy sandy stream gravels (on the bed of initial old valley) - late Riss. 4. lava flows in transitional and peripheral zone of the volcano. 5. thin lava flows in central zone of the volcano. 6. pyroclastics a) in transitional zone of the volcano b) in central zone of the volcano. 7. freatopyroclastics. 8. lava flows in the lava plateau (lava flows and their breccias - lava wash-outs and tongues). 4. -8. late Riss (final part) -Riss/Wurm (basal part). 9. aeolian loess and loessy fossil soils. 10. loessy loams (resedimented loess). 9. -10. Upper Pleistocene.

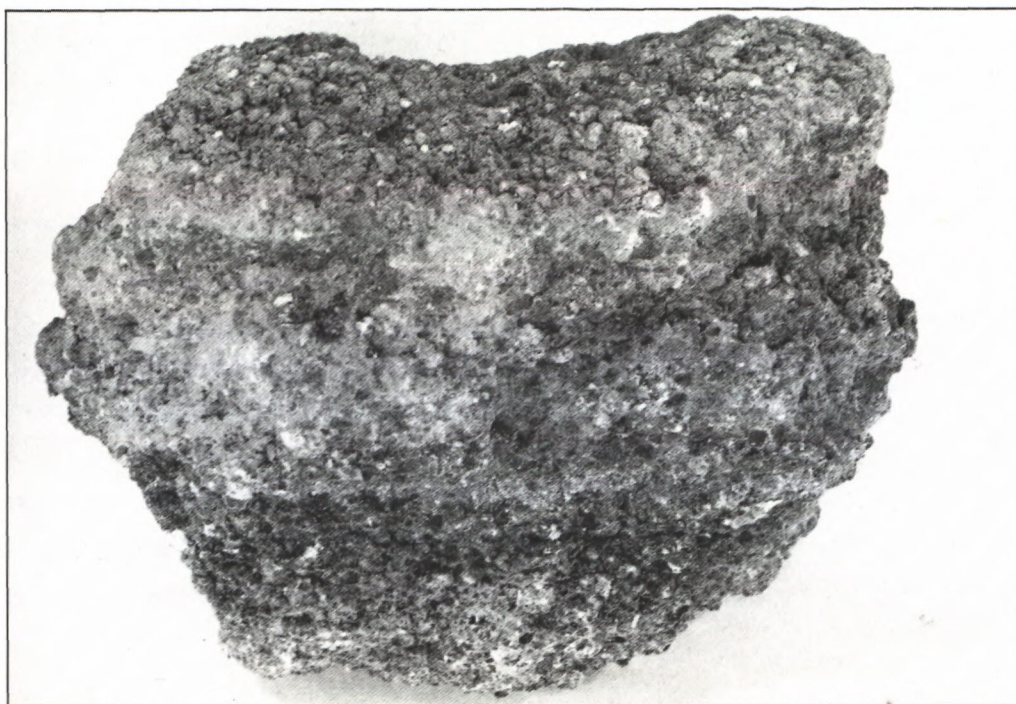


Photo 9. Deposited down fallen pyroclastics - lapilli tuff (freatopyroclasticum).



Photo 10. Agglutinates with scarce megablocks (75 cm).



Photo 11. Strongly ignimbritised agglutinates composed of irregular, spindle-like and spherical bombs and spatter rocks.

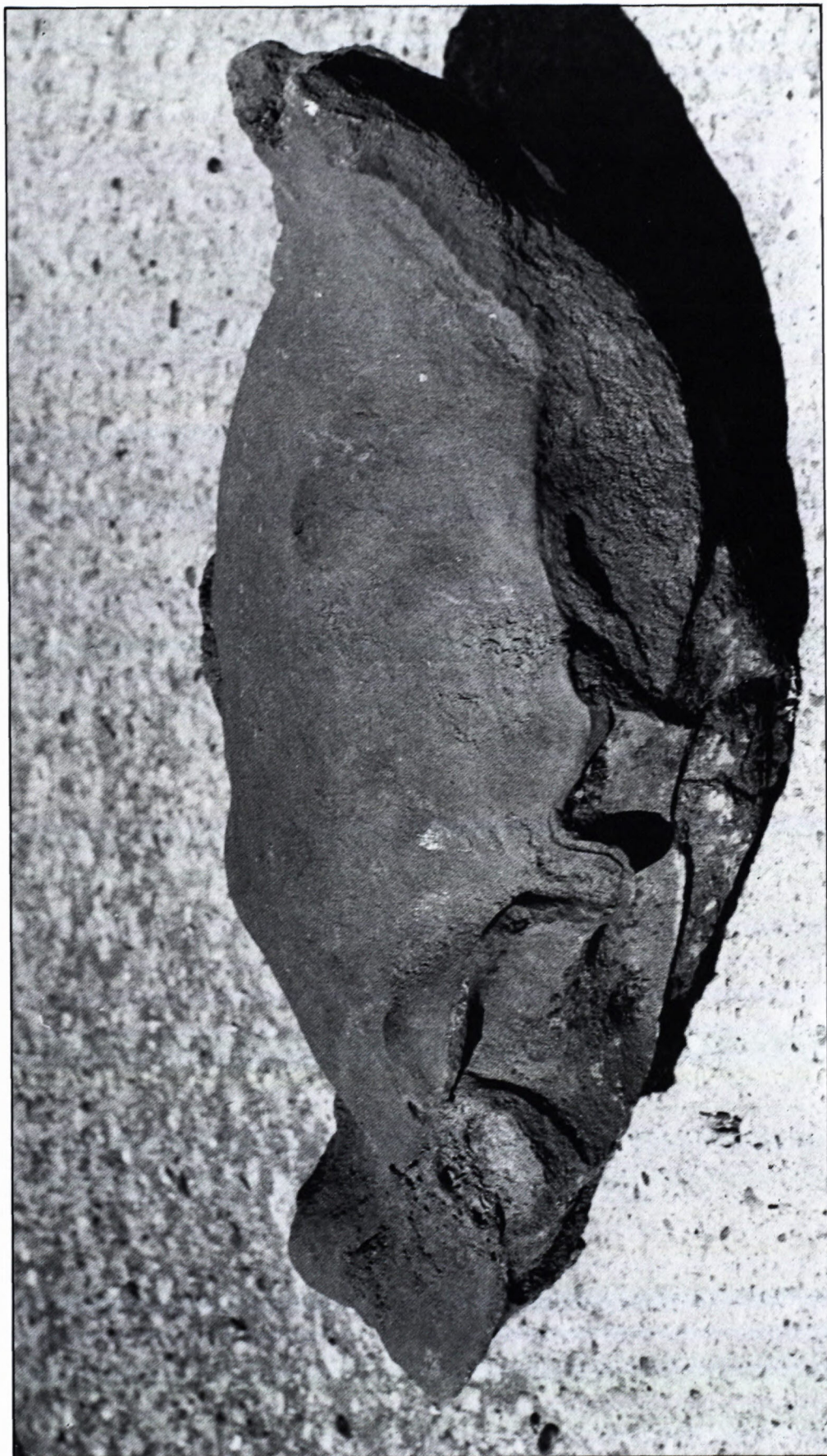


Photo 12. Shell bomb - a side view.

analysis of molluscan fauna found in Komjatice section (SCHMIDT, 1973) does not contradict this dating, a younger, Rissian age of the loessy bed with tuff seems to be more plausible. Moreover, KAROLUSOVÁ found out that the origin of the Komjatice tuff should be sought in vol-

canic regions of northern Hungary, near the Austrian border, where there occur isolated basaltic bodies of the latest (even Quaternary) volcanism, for which the Pleistocene age has been indicated by several authors (corresponding roughly to Riss). We also note that a tuff



Photo 13. Amygdaloidal bomb.

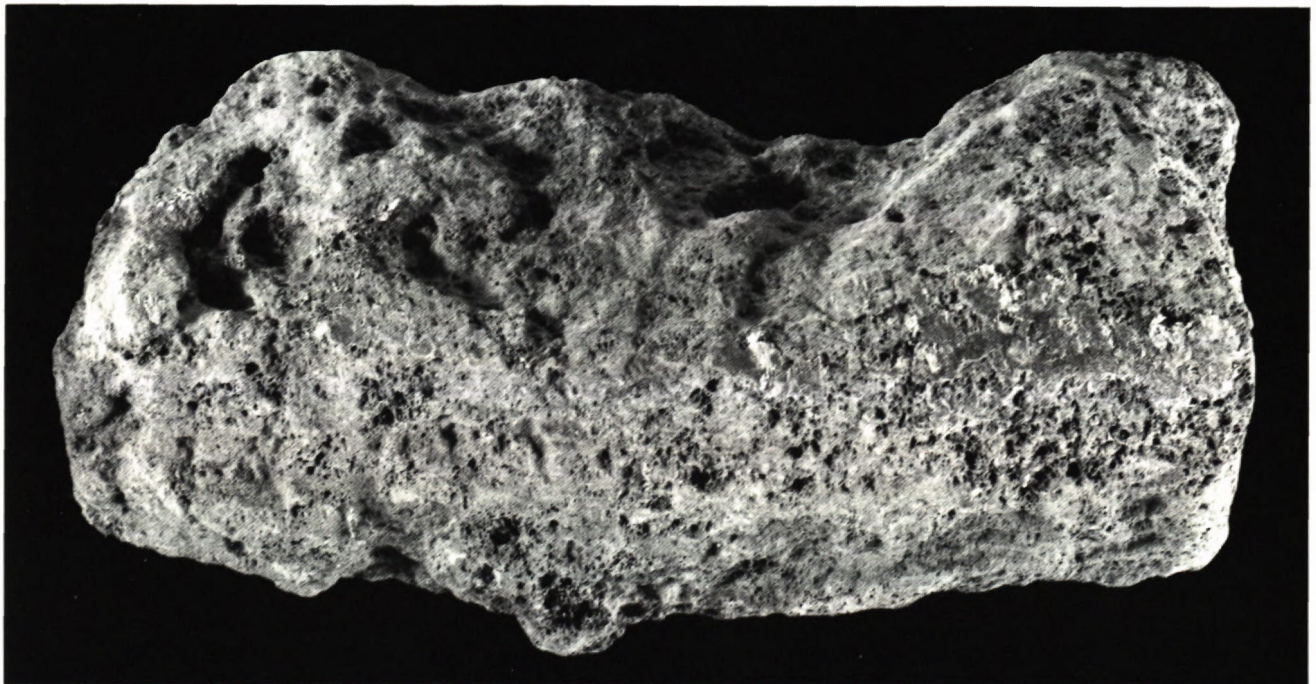


Photo 14. Block bomb - elongated shape

bed similar to that encountered in Komjatice, for which Mindelian age was assigned before (Kukla), has been found in loess near Levice (brick kiln Monako). Thanks to progress in geologic mapping a revision of the section and re-dating of the loessy bed in Levice to Riss age

(HALOUZKA,1982) could be made. As far as the age and the origin of the tuff are concerned, the most likely association was with the latest maar basaltic volcanism in Fíľakovo (Cerová vrchovina upland). Anyway, to compare the age of the Pútikov vřšok volcano with the other

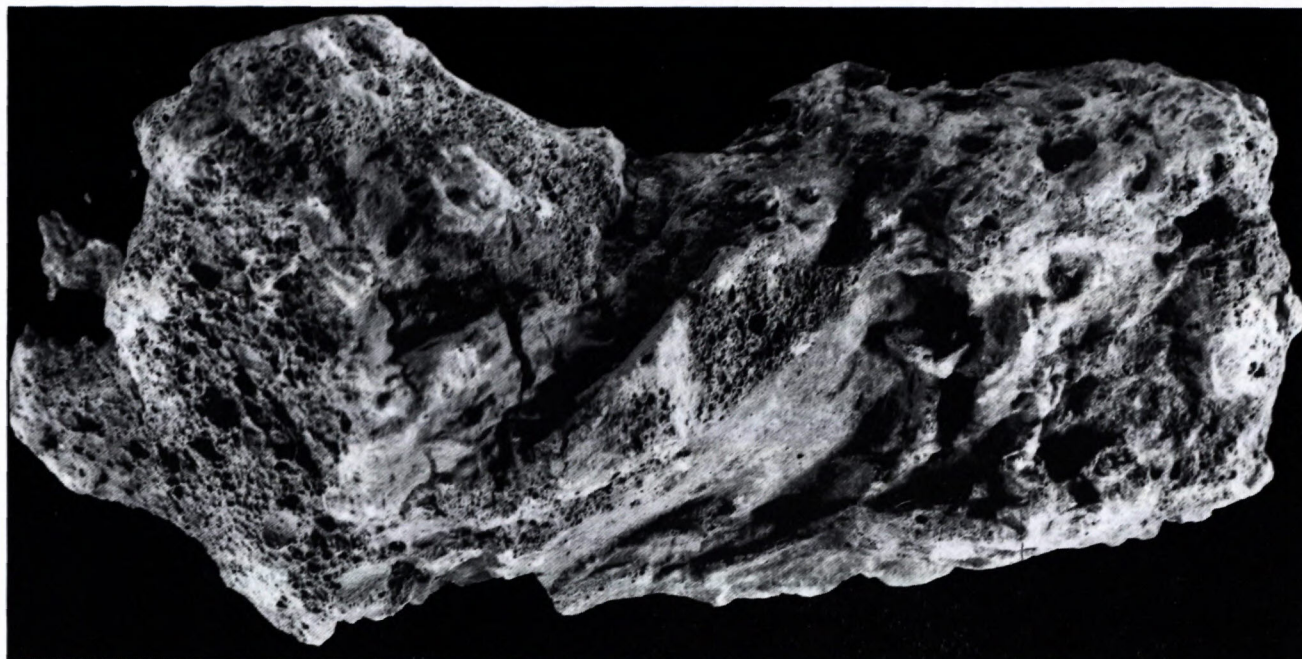


Photo 15. Spindle-like bomb.

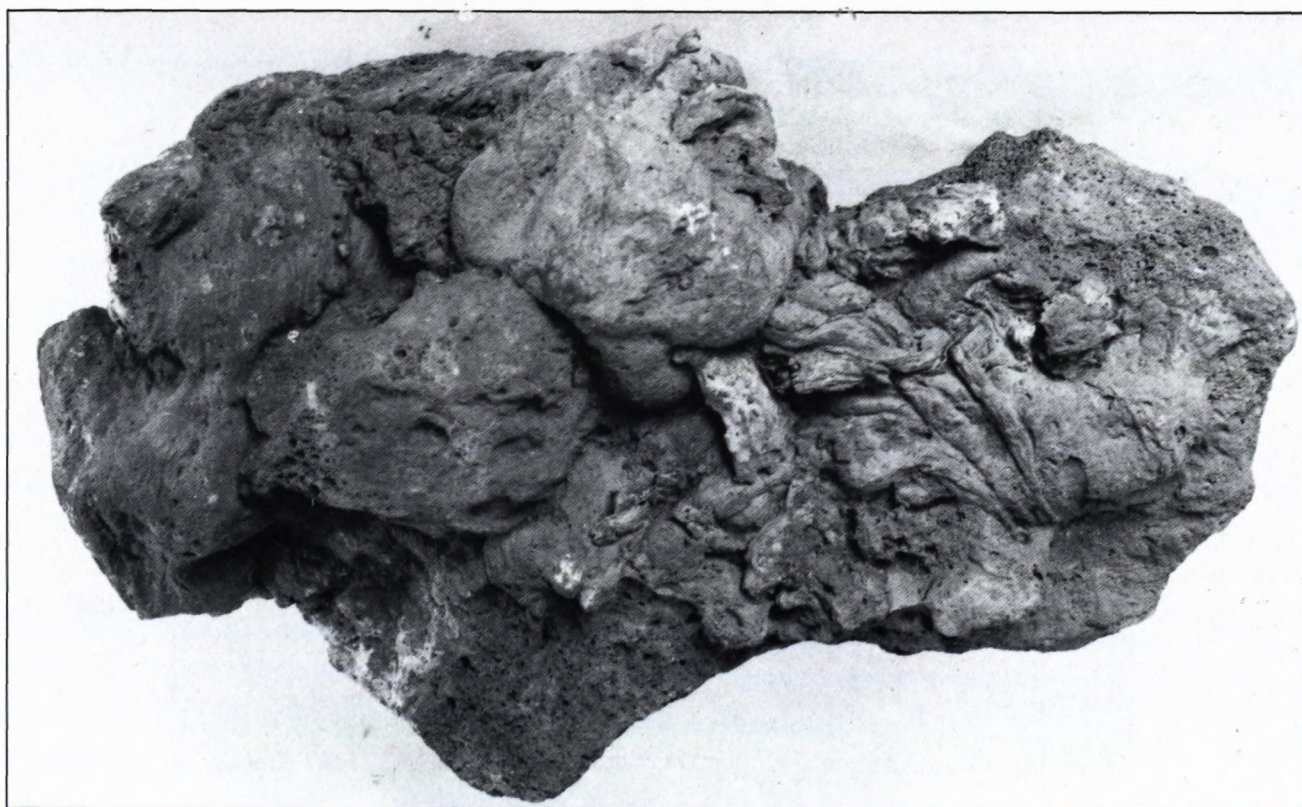


Photo 16. Cow's stool bomb.



Photo 17. Lava flow 1992, Etna - a lava tongue of Aa lava type (coarse surface) with scarce pahoehoe lava tongues (smooth surface), separated from the lava plateau

Photo 19. Recent cinder cones - western slope of the Etna volcano.

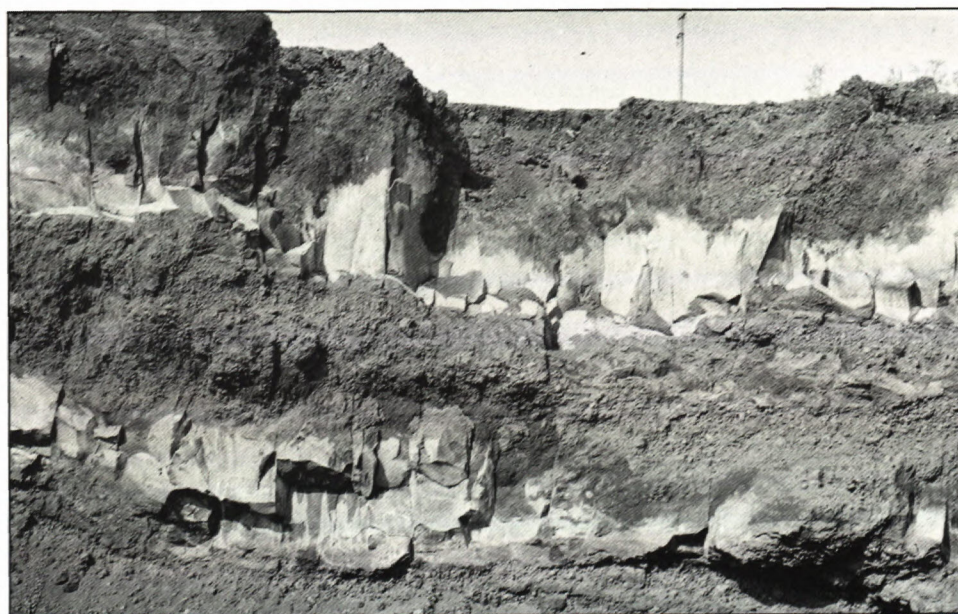


Photo 18. Lava flows Etna 1983 Etna, Aa -type made of massive lava with lava breccias (2 flows).

European volcanoes, the only reliable younger fossil remnant of volcanism dating back to Pleistocene, is in the Eifel region of western Germany (late Pleistocene -Wurm).

3. The crater of Pútikov vršok volcano surrounded the 477 m triangulation point (called Pútikov vršok). Although the cinder cone has developed in its centre, most of the volcanic material have churned from the centre NW, filling up a paleovalley. A feature analogical to that of the Parícutin volcano in Mexiko, (1943 - 1945, see topographic maps showing the situation before and after the eruption) has been reported by FOSHAG and

GONSALES (1959). The lava flows have poured down to fill in suitable depression (paleovalleys, trenches, gullies).

4. The Pútikov vršok volcano produced mainly the lava flows = effusive eruptions. Two types of lava flows occur - the Aa lavas and pahoehoe lavas. The lava flows join together to form a lava plateau. The position and character of flows is reminiscent of that of the Hawai islands (USA) volcanoes, described by WALKER (1990). A similar feature has been observed (ŠIMON) during the Etna (Sicily) eruption in May 1992. Starting on 14 December 1991 this eruption produced anastomosing lava



Photo 20. A view into the Etna cinder cone crater.



Photo 21. Volcanic bomb from Etna - recent.

flows running through channels and forming lava tongues. Out of the mixture of lava masses (plateau) the Aa lavas made up to 90 - 95 % (photo 17,18), while the pahoehoe lavas (tongues) were of scarce occurrence (photo17). The eruption produced the rocks of hawaite composition strewn over an area of 7 sq. km (before 31 October 1992, BARBERI et al.1993).

5. Investigation into volcanic features of the Pútikov vŕšok volcano allowed to distinguish three types of explosive eruptions: the Stromboli, the Hawai and the freatomagmatic ones. As medium explosive types of the Hawai - Stromboli eruptions the Pútikov vŕšok volcano produced the basaltic magma material and the Stromboli and Hawai type pyroclastic rocks, both being deposited side by side depending on the eruption dynamics. These eruptions were responsible for piling up of the cinder cone composed of poorly bedded cinders and volcanic bombs (Stromboli type) and spatter rocks, thin lava flows and clinkers (Hawai). SELF et al., 1974 described the Heimaey Island - eruption (1973), lava fountain eruption (Hawai type), with transitions to Stromboli type explosions, which produced a cinder cone. The klinker cones developed on slopes of the Etna stratovolcano. The cones are made of Stromboli type pyroclastics (photo 19 - author's observation). The shape of the 20th century cones are well preserved. Some of the 19th century (or older) cones are, on the other hand, more or less affected by erosion (photo 20). The third type of eruptions, the freatomagmatic ones, are less widespread in the structure of the Pútikov vŕšok volcano. The eruption products are made of thin beds situated in the centre, and on slopes of the volcano. These explosions were either caused by waters coming from the Chválenský potok creek, or from a paleolake (which formed due to impoundment of the above creek by streams at the southern side of the volcano), or by groundwaters from underlying rocks. HOUGHTON and SCHMINCKE (1989) described the Rotherberg volcano (Eifel, Germany) as a complex of Stromboli and freatomagmatic eruption. The volcano is made predominantly of Stromboli type pyroclastics with thin beds of freatomagmatic eruption products, and the freatomagmatic eruption, as part of the Stromboli type eruption, was initiated due to suitable hydrogeologic conditions in the environment.

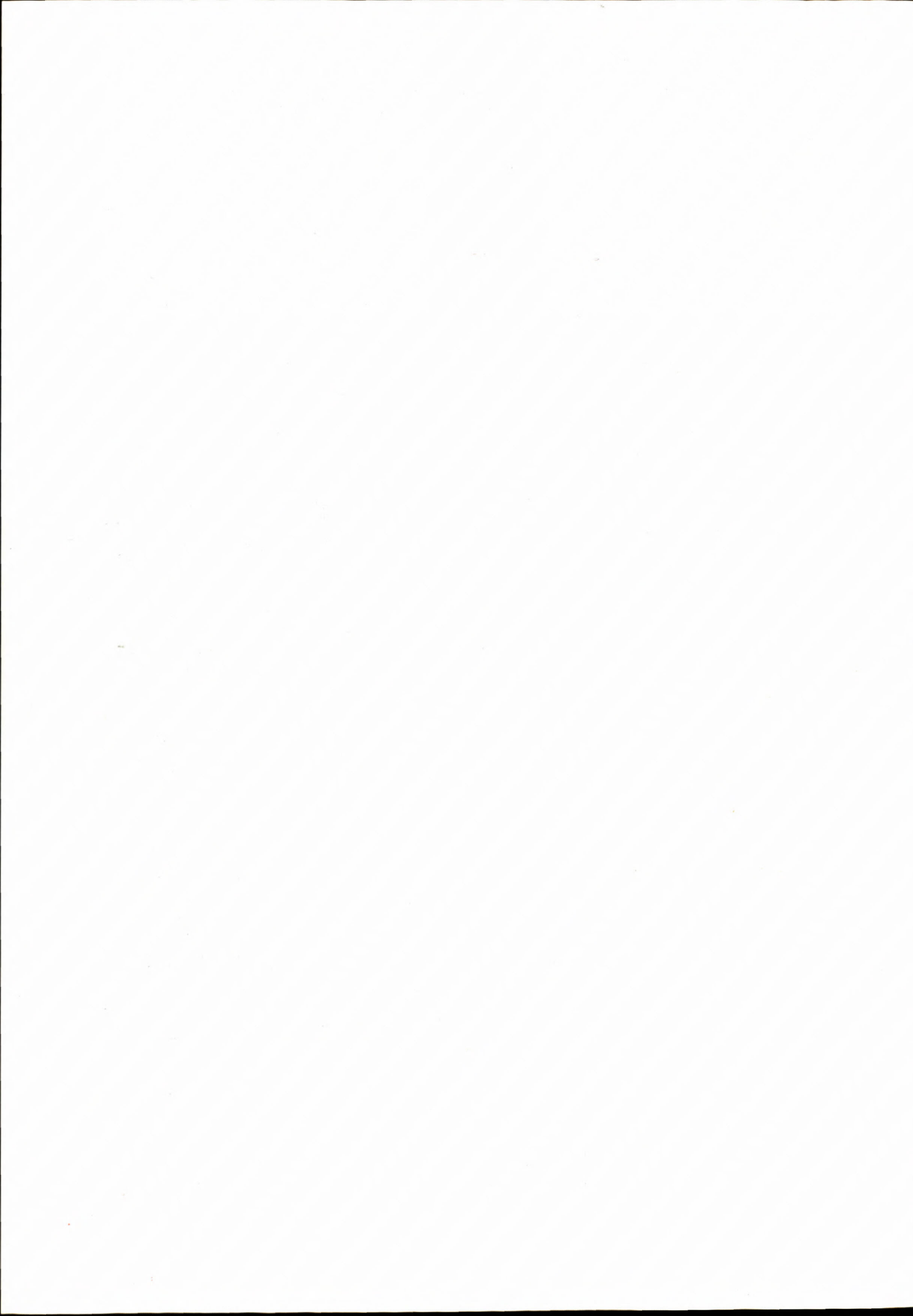
References

- BALOGH, K., MIHALIKOVÁ, A. & VASS, D. et al. 1981: Radiometric dating of basalts in southern and central Slovakia. *Západné Karpaty*, sér. Geol. 7, Bratislava, 113-126.
- BAGDASARJAN, G. P., KONEČNÝ, V. & VASS, D. 1970: Príspevok absolútnych vekov k vývojovej schéme neogénneho vulkanizmu stredného Slovenska. *Geol. Práce, Správy* 51, Bratislava, s. 47-69.
- BARBERI, F., CARAPEZZA M. L., VALENZA, M. & VILLARI, L. 1993: The control of lava flow during the 1991 - 1992 eruption of Mt. Etna. *Jour. of Volcanology and Geother. Reseach*, 56, 1-34.
- BLACKBURN, E., WILSON, L. & SPARKS, R. S. J. et al. 1976: Mechanism and dynamics of strombolian activity. *J. Geol. Soc. London* 132, 429-440.
- CAS, R. A. F., WRIGHT, J. V., 1987: *Volcanic succesions*. Unwin Hyman, London, 528.
- FIALA, F. 1952: Alkali basalt (basanitoids) from Tekovská Breznica and Brehy near Nová Baňa in Slovakia. *Acta Musei Nationalis Prague*, Vol. VIII. B, No. 5, Geol. et paleon. No. 2, 1-44.
- FISHER, R. V., SCHMINCKE, H. U. 1984: *Pyroclastic rocks*. Springer Verlag, Berlín, 472.
- FOSHAG, W. F., GONZÁLEZ, R. J. 1956: *Birth and Development of Paricutin Volcano, Mexico*. Geological Survey Bulletin 965-D, 355-485 pp., plates.
- HALOUZKA, R. 1982: *Dolné Pohronie - kvartér a morfológia*. Kandidátska dizert. práca. Manuscript, GÚDŠ, Bratislava, 148 pp.
- HALOUZKA, R., ŠIMON, L. 1992a: Locality No. 11, Nová Baňa - Brehy. *Geology of Quaternary; Determination of stratigraphy and age of basalts ...* In (74-76): M. Stankoviansky - J. Lacika (edits) - R. Halouzka et al. *Excursion guide-book (of) International Symposium of Time, Frequency and Dating in Geomorphology (STIFDIG)*, Tat. Lomnica/Stará Lesná, 1992. Bratislava, Institute of Geography of the Slovak Academy of Sciences, 83 pp.
- HALOUZKA, R., ŠIMON, L. 1992b: *Dating report about quaternary latest volcanic activity in Czecho - Slovakia (basalt near Nová Baňa - Brehy)*. STIFDIG, Abstract, Bratislava.
- HOUGHTON, B. F., SCHMINCKE, H. U. 1989: Rotherberg scoria cone, East Eifel: a complex strombolian and phreatomagmatic volcano. *Bull. Volcanol* (1989) 52. 28-48.
- JANÍK, S., KANDA, J. 1986: *Hydromorfologický výskum slovenských riek - Hron*. Atlas účelových máp kvartéru a jeho podložia v dolinnej nive rieky, 1:5 000, časť 2 (Stredný Hron). ÚVUH Bratislava (in Geodézia Žilina), Bratislava.
- KONEČNÝ, V., LEXA, J. & PLANDEROVÁ, E. 1983: *Stratigraphic division of neovolcanics of Central Slovakia (in Slovak)*. *Záp. Karp.*, sér. Geol. 9, Bratislava, 203 pp.
- KONEČNÝ, V., LEXA, J. 1984: *Geologická mapa stredoslovenských neovulkanitov, 1:100 000*. Geol. Úst. D. Štúra, Bratislava.
- KUTHAN, M. (edit.) 1963: *Vysvetlivky k prehľadnej geologickej mape ČSSR 1:200 000, M-34-XXXI Nitra*. Geofond - Vydavateľstvo, Bratislava, 172 s.
- LE BAS, M. J., LE MAITRE, R. W. STRECKEISEN, A. & ZANETTIN, B. 1986: *A chemical classification of volcanic rocks based on the total alkali - silica diagram*. *Jour. of petrology*, Oxford, vol. 27, 745-750.
- LOCKWOOD, J. P., LIPMAN, P. W. 1980: *Recovery of datable charcoal beneath tounge lavas: lessons from Hawaii*. *Bull. Volcanol*. 43, 609-615.
- MIHALIKOVÁ, A., ŠIMOVÁ, M. 1989: *Geochemistry and petrology of Miocene-Pleistocene alkaline basalts of central and southern Slovakia (in Slovak)*. *Záp. Karp.*, sér. min., geoch., metalog., Bratislava 12, 7-142.
- NAIRN, A. E. M., KAROLUS, K. 1965: *A preliminary paleomagnetic study of the rocks of the Central Slovakian igneous province*. *Geologické práce, Zprávy* 36, 1965, Bratislava, s. 149-172.
- Principles of Czechoslovakian stratigraphic commission, 2. edition (in Slovak) 1978: Věst. ÚÚG.*, 6, roč. 53, Praha.

- RAČKO, J. 1990: Geomorphologic situation in broader background of the final volcanism of south-western part of the SELF, S., SPARKS, R. S. J., BOOTH, B. & WALKER, G. P. L. 1974: The 1973 Heimay Strombolian scoria deposit, Iceland. *Geol. Mag.* 111, 539-548.
- Schmidt, Z. 1973: Fosilne mäkkýše sprašového komplexu v Komjaticiach v Podunajskej nížine. *Geol. Práce, Správy* 61, Geol. Úst. D. Štúra, Bratislava, s. 305-313.
- ŠIMON, L. 1991: Púťkov vršok - a Quaternary basanite volcano nearby Nová Baňa in central Slovakia. SCEAVR, Abstract, Praha.
- ŠIMON, L. 1995: Phreatopyroclastics in the Northern Vtáčnik Mts. *Geologické práce, Správy* 100, Geol. Úst. D. Štúra, Bratislava, 81-85.
- ŠIMOVA, M. 1965: Final basalt volcanism of Slovak Mídmountains (in Slovak). *Acta geol. geog. Univ. Comen.* 9, Bratislava, 1-125.
- VÁŠKOVSKÝ, I., KAROLUSOVÁ, E. 1969: Prvý nález vulkanického popola v sprašiach komjatickej tehelne. *Geol. Práce, Správy* 50, Geol. Úst. D. Štúra, Bratislava, s. 192-198.
- Hodruša hornatina upland (in Slovak). Dipl. práca, Katedra fyzickej geografie PrF UK, Bratislava.
- WALKER, G. P. L. 1973: Explosive volcanic eruption - a new classification scheme. *Geol. Rund.* 62, 431-446.
- WALKER, G. P. L., 1990: Geology and Volcanology of the Hawaiian Island. *Pacific Science* (1990), vol. 44, no. 4. 315-347.
- WILLIAMS, H., MCBIRNEY, A. R. 1979: *Volcanology*. Freeman, Cooper and Company, San Francisco, 397.

Acknowledgements

Authors take this opportunity to thank for invaluable expertly advice and consulting in the field, as well as during preparaton of this paper to Dr. J. Lexa and Dr. V. Konečný. Dr. Kohlerová is thanked for her help in assembling Table 1. The figures have been re-drown by Mrs. Žilavá. This paper is based on the results of national geological research projects, undertaken by the GUDŠ. Photographs from the Etna volcano were made by Dr. L. Šimon.



Sea ways connecting the Fiľakovo/Pétervására Basin with the Eggenburgian/Burdigalian open sea

EVA HALÁSOVÁ¹, NATÁLIA HUDAČKOVÁ¹, KATARINA HOLCOVÁ², DIONÝZ VASS³, MICHAL ELEČKO³
and MIROSLAV PERESZLÉNYI⁴

¹Department of Geology and Paleontology, Faculty of Science Comenius University, Mlynská dolina G, 842 15 Bratislava, Slovakia

²Institute of Geology and Paleontology, Faculty of Science, Charles University, Albertov 6, 128 43 Praha, Czech Republic

³Geological Survey of Slovak Republic, Mlynská dolina I, 817 04 Bratislava, Slovakia

⁴Oil Company for Research, Exploration and Production, Votrubova 11/a, 825 05 Bratislava, Slovakia

Abstract: The Fiľakovo/Pétervására Basin of Eggenburgian age is situated in southern Slovakia and northern Hungary. Physiographically, the basin was configured as a bay closed towards south. As regards present day erosional extent of basinal marine deposits the foraminifera and calcareous nannoplankton assemblages from the marginal sites indicate that the bay was connected with open sea, i.e. with the marine basins located on the back of the Magura nappe and in front of the ascending Carpathians, by a northeast sea way via East Slovakian - Transcarpathian Basin and by a north - north-west sea way (recent coordinates) via west Carpathian intramontaneous depressions, through Vienna Basin to Alpine - Carpathian foredeep.

Key words: Western Carpathians, Fiľakovo-Pétervására Basin, Eggenburgian/Burdigalian paleogeography, Eggenburgian sea ways in Central Europe, foraminifers, calcareous nannoplankton.

A number of authors have addressed the problems related to distribution of original sedimentary basins in the Central Paratethys area during the Eggenburgian (22-19 Ma B.P., VASS et al., 1987). DÉPÉRET (1892) defined the range of Burdigalian chronostratigraphical stage as corresponding approximately to the Eggenburgian (compare STEININGER and SENEŠ et al., 1971). The Burdigalian was later redefined to include the Helvetian stage and to combine Eggenburgian, Ottnangian and Karpatian stages of the Central Paratethys in new definition.

Déperet presented "faluns" (lumachelles) from Saucats and Léognan (département Gironde, Southwest France) and calcareous sandstones with *Pecten prescabriusculus* in Rhône valley as typical Burdigalian sediments. He considered faluns the sediments of the Miocene first phase transgression, which progressed from Rhône valley to the valley of Drôme. Calcareous sandstones with *Pecten prescabriusculus* are the sediments of the following transgression phase, which progressed into Dauphiné and farther to Savoy, Switzerland (Molasse du Plateau), Bavaria and to "Outer Vienna Basin", where the Alpine Foredeep passes into the Carpathian one. Later papers also describe the Burdigalian (Eggenburgian) sediments in the Carpathian Foredeep near Ostrava, and

eastwards and below the Outer Carpathians nappes (OSZCZYPKO and SLACZKA, 1985, Fig. 5). More eastwards in the Carpathian Foredeep the marine Eggenburgian sediments are missing, but the Eggenburgian marine transgression progressed into the sedimentary basins of Stebnica, Boryslav-Pokuty, Skola and partially also into Subsilesian and Silesian units (OSZCZYPKO and SLACZKA l.c., KOVÁČ et al., 1989). Afterwards, these units were folded to form nappes of the Outer Carpathians (Fig. 5). The Eggenburgian sea progressed eastwards (using recent coordinates) into the Central Western Carpathians area, through sedimentary basins of Pouzďfany and Ždánice units (now folded into the Outer Western Carpathians front) into the Vienna Basin and farther eastwards through the Brezová and Vaďovce depressions to the Váh River valley (Trenčín and Ilava depressions) to Bánovce, Horná Nitra and Turiec depressions. From these sedimentary areas could, e.g. Turiec depression communicate through the Mid-Slovakian fault zone and Zázrivá - Budapest fault Belt, respectively, with piggy back marine basin situated on the Magura nappe unit (north of the present day Vysoké Tatry Mts.). To the east the mentioned basin communicated with the marine basin of the Skole unit. The basin was later folded to form the Outer Carpathian Magura Unit (CZIESZKOWSKI, 1992). Other marine sedimentary basin, today parallel with the axis of the Outer Carpathians, existed in the Transcarpathian Basin, which communicated (e.g. through a channel near Modra nad Cirochou, KÁROLI-pers. com.) with NE sedimentary basins of the present Outer Carpathians frontal units (Fig.5)

From the above mentioned it follows that for Central Europe the Alpine and Carpathian Foredeeps were important, if not vital sea ways, through which the marine Eggenburgian (or Burdigalian, respectively) transgression progressed (PAPP et al., in STEININGER, SENEŠ et al. 1971; RÖGL and STEININGER, 1983; BÁLDI, 1986; HÁMOR et al., 1988; KOVÁČ et al., 1989 and others).

Due to various reasons the reconstruction of paleogeographic sea ways with the areas of marine sedimentation in northern Hungary and southern Slovakia (Fiľakovo-Pétervására Basin in sense of VASS, 1995, or the North Hungarian marine bay, respectively, SZTANÓ, 1994) is still problematic. Several authors have proposed a southward communication with open sea (it means with

the Mediterranean sea) through the Transdinaric straits via Budapest - Zagreb (PAPP et al. in STEININGER and SENEŠ et al., 1971, Fig. 1) for this basin, situated

excentrically relative to the Alpine and Carpathian Foredeeps, as well as for the basins inside Central Western Carpathians. However, this concept has been

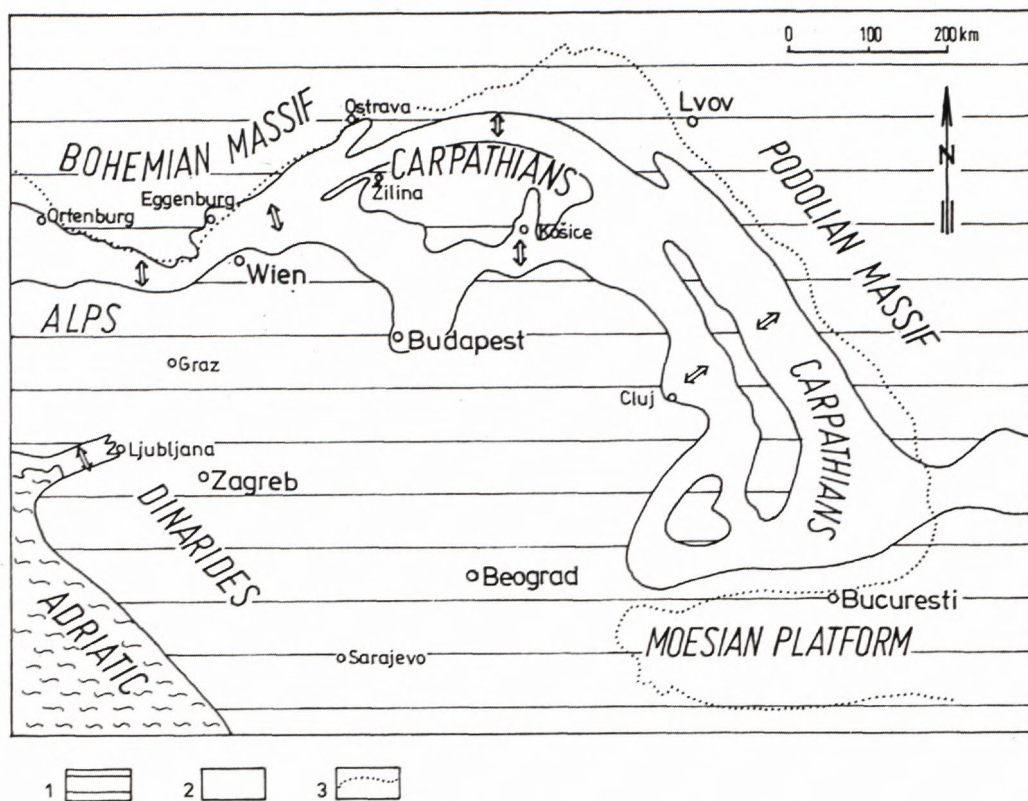


Fig. 1: Scheme of on distribution and mutual connection of marine sedimentary basins in Central Europe during Eggenburgian (Early Burdigalian) according to PAPP et al., in STEININGER, SENEŠ et al. 1971.

1. Dry land; 2. sea and sea ways; 3. recent front of the Eastern Alps and Carpathians.

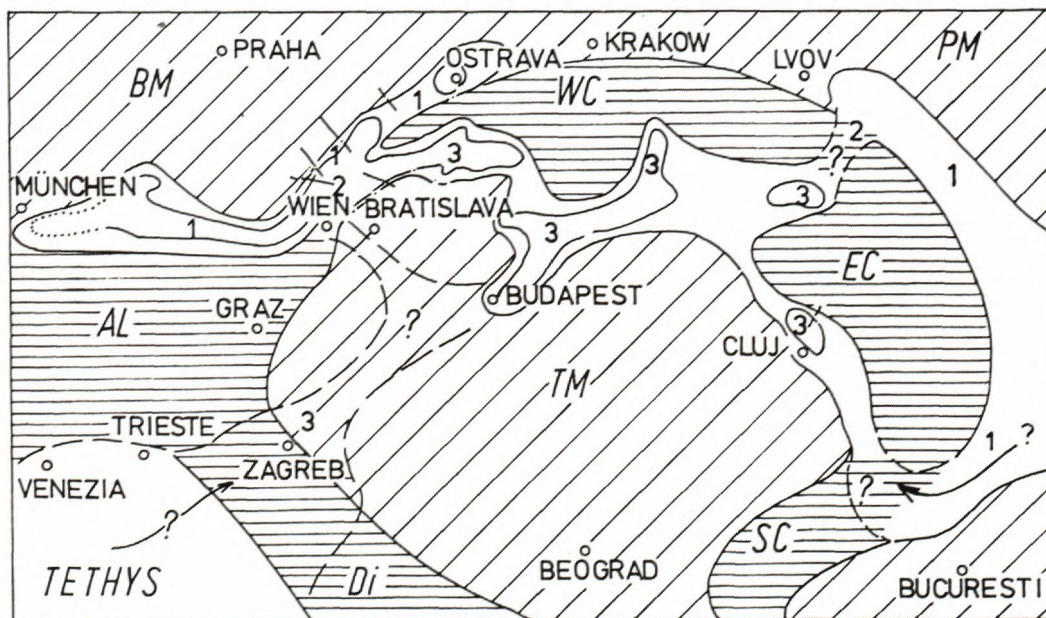


Fig. 2: Scheme of distribution and mutual connections among Central and Eastern European sedimentary basins at the beginning of Eggenburgian (22 Ma B.P. Rögl and STEININGER 1983).

BM - Bohemian Massif; AL Alps; WC, EC, SC West, East, South Carpathians; TM Tisia Massif; PM - Podolian massif DI - Dinarides; 1 - Alpine - Carpathian fore deep; 2 - Vienna Basin; 3 - Intra-Carpathian basins

later refused (RÖGL and STEININGER, 1983, see Fig. 2; BÁLDI, 1986; HÁMOR et al., 1988; SZTANÓ, 1994). Migration paths of the terrestrial mammals, sedimentation in the south Alpine and Dinaric Foredeeps and evidences for the syn-Eggenburgian erosion in southern Hungary indicate that the Transdinaric corridor has been closed (SZTANÓ, 1994). Another possible sea way from Vienna Basin south-east (using recent coordinates) through the Danube Basin is presumed by RÖGL and STEININGER (1983, see Fig. 2). However, the oldest known Miocene sediments in the Danube Basin are those of Ottnangian, (e.g. Brenberg Formation) or of Karpatian age, respectively, (e.g. Ligederdö Formation) thus, they are younger than Eggenburgian. Communication across the Central Western Carpathians was postulated by PAPP et al. (in STEININGER and SENEŠ et al., 1971) regardless of the fact that no occurrences of marine Eggenburgian sediments in either the Central Slovakian Neogene volcanic basement, or in the area between the Fífakovo-Pétervására and the East Slovakian Basins were known at that time. This absence was explained by post-Eggenburgian erosion as a consequence of the Central Carpathians uplift. BÁLDI (1986) has later resumed an idea of a connection between the Fífakovo-Pétervására, the Intracarpathian basins and the Transcarpathian Basin. Moreover, SZTANÓ (1994) emphasized the role of the sea way between the Transcarpathian Basin, the residual Magura Basin (the basin in piggy-back position on the Magura

nappe northwards from Vysoké Tatry Mts.; CIEZSKOWSKI, 1992) and other contemporary sedimentary basins, respectively, (folded today in front of the Outer Carpathians), as the only possible way for marine tide waves to progress into northern Hungarian bay. The tide significantly influenced sedimentation there. Especially the Pétervására sandstones and sandstones of the Fífakovo Formation display sedimentary structures typical for tide dominated coastal deposits. The energy of tidal flood was amplified by the physiography of North Hungarian bay as is the case of today's Bay of Fundy, Canada. Huge cross-stratified sets of the Jalová member and their equivalents in the Pétervására sandstones have been formed due to tidal ebb, which was stronger than tidal flood (SZTANÓ, 1994).

VASS and ELEČKO et al. (1989, enclosure Nr 4) presumed that the extent of early Eggenburgian Fífakovo Formation of Southern Slovakia was greater than that of present day. They have not drawn any conclusion since this presumption was based only on rare occurrence of the molluscs *Clio triplicata* and *Latemula fuchsi* described by ONDREJČIKOVÁ (1977) from the borehole VCH-1 near Chanava in the Rimavská kotlina Depression. According to ONDREJČIKOVÁ the species are not older than the Eggenburgian, or Ottnangian, respectively. But the Eggenburgian elements have not been found in foraminiferal and calcareous nannoplankton assemblages.

The presence of Eggenburgian in the NE corner of the Rimavská kotlina Depression was recently confirmed

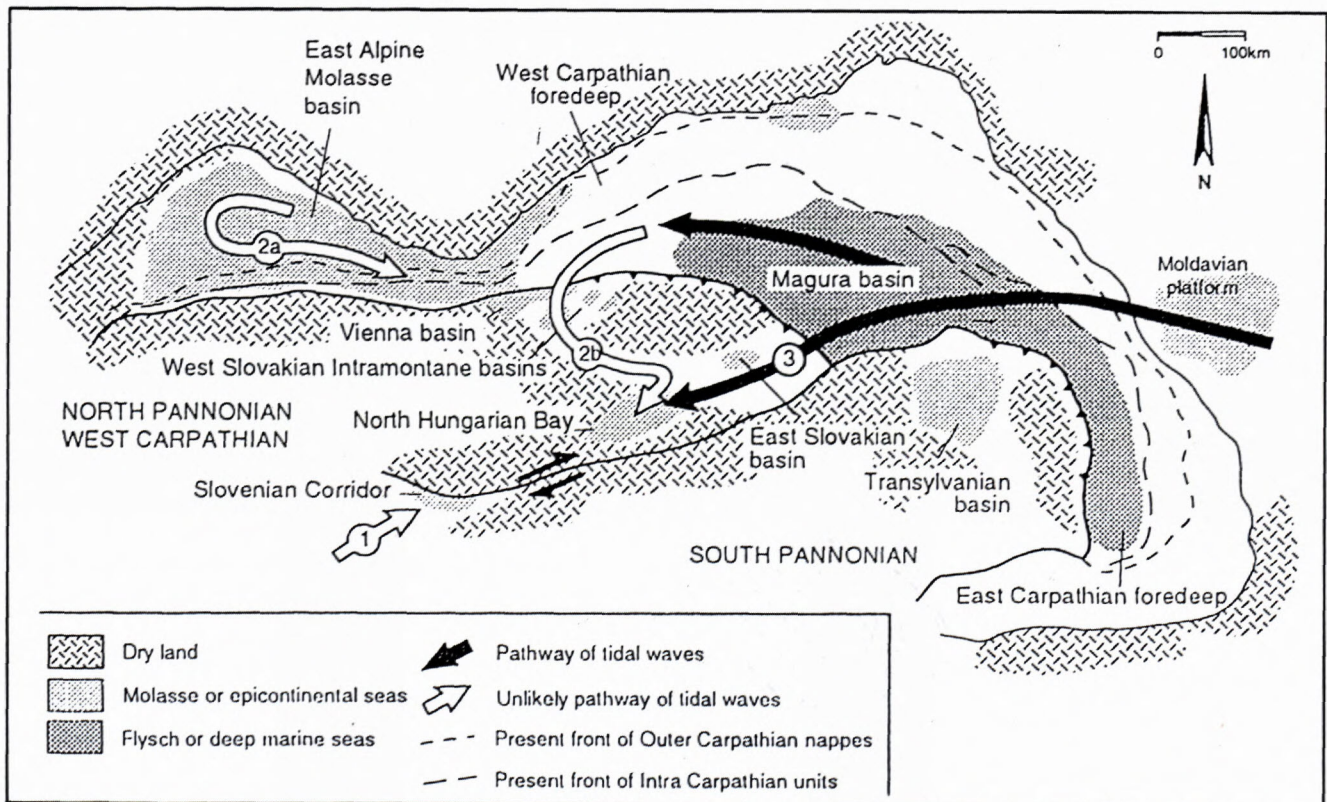


Fig. 3: Paleogeographic reconstruction of the Intra - Carpathian area during the Early Eggenburgian (22-20 Ma B.P.) and the sea-ways connecting the North Hungarian Bay and/or Fífakovo/Pétervására basin with open sea of the Alpine-Carpathian fore-deep and of Flysch seas via West Carpathian intramontainous basins (according to SZTANÓ 1994).

by findings of Eggenburgian foraminifers and nannoflora of the NN2 zone, found in a shallow well in the village of Gemerská Panica (Fig. 4, 5, 6). Rich foraminiferal assemblages of Eggenburgian age were found in the calcareous siltstone. The age of mentioned sediments was determined on the basis of Globigerinoides trilobus finds, (first appearance datum: the Eggenburgian; RÖGL, 1986) and Haplophragmoides vasiceki pentacameratus (C. et Z.), which occurs in the Eggenburgian (CICHA et al., 1982) exclusively. Agglutinated forms prevailed (28 %) in the well-diversified assemblage, with the most frequent Bathysiphon sp., Cyclamina acutidorsata (HANT.), C. aff. praecancelata VOLOSH. (Plate 1). Except for the above mentioned foraminifers the assemblage also contains numerous Angulogerina angulosa (WILL.) species. The observed taxa indicate a neritic to bathyal environment

(plankton/benthos ratio of 1.6) with cold water and slight oxygen deficit at the bottom (MURRAY, 1991). The occurrence of calcareous nannoflora also confirms this age of the sediment. The Helicosphaera ampliapertura BRAM. & WILC., H. scissura MILLER, H. kamptneri HAY & MOHLER, Sphenolithus belemnos BRAM. & WILC., Discoaster druggi BRAM. & WILC. species indicate the upper part of the NN2 - NN3 biozone, defined by MARTINI (1971), corresponding to stratigraphical range - Egerian to Lower Ottnangian. Ascertained thanatocoenosis resembles the calcareous nannofossil assemblages determined by LEHOTAYOVÁ (1982) in Eggenburgian sediments of the Western Carpathians (Bánovce, Horná Nitra depressions). Apart from the mentioned Neogene nannofossils the reworked Cretaceous, Eocene and Oligocene calcareous nannoplankton was also determined.

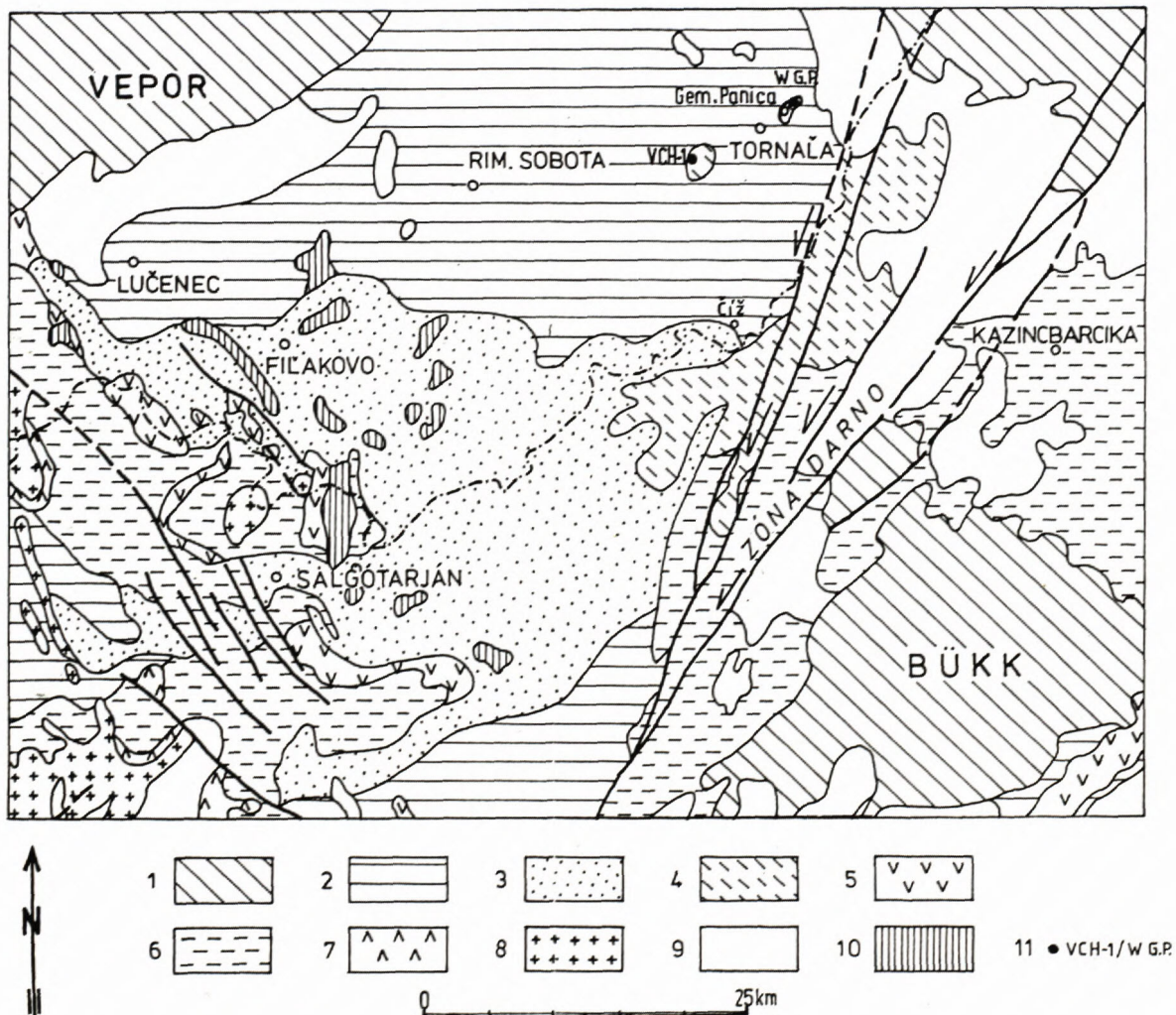


Fig. 4: Recent distribution of the Putnok Schlier. Due to left lateral strike-slips in the Rimavská kotlina Depression there are only erosional remnants of the Putnok Schlier equivalents
 1 pre-Cenozoic rocks; 2 Hungarian Paleogene Basin; 3 Fiľakovo - Pétervására formation partly covered by upper Szécsény Schlier; 4 upper Szécsény and Putnok Schlier; (3-4 Eggenburgian); 5 Gyulakézi rhyolite tuff (Eggenburgian - Ottnangian) and/or rhyodacite tuff in Bukovinka formation (Eggenburgian); 6 Nógrád /Novohrad Basin (Ottnangian and Karpathian); 7 "middle rhyolite tuff" and/or Tarr tuff; (Upper Karpathian - Lower Badenian); 8 Middle (and Upper) Miocene volcanics; 9 Middle to Upper Miocene sediments; 10 Upper Miocene to Pleistocene basalts; 11 borehole /well (WG.P.-well in the village of Gemerská Panica; VCH-1 : borehole)

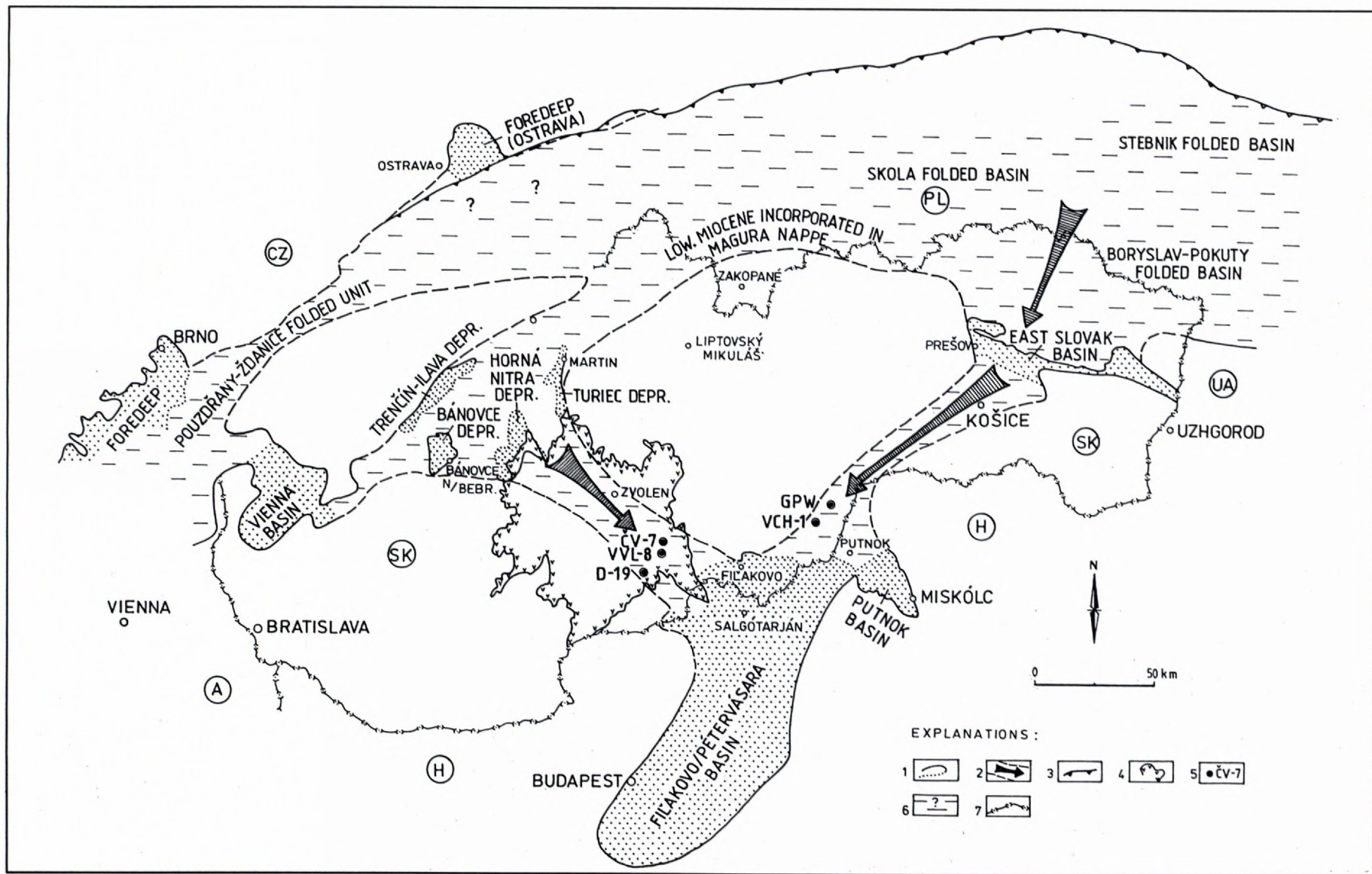


Fig. 5: Sea ways of the Eggenburgian sea in the Western Carpathian territory.

1 Recent distribution of areas with Eggenburgian deposits (deposits incorporated into Outer Carpathian nappe units are not shown); 2 Eggenburgian sea-way inferred; 3 Recent front of Outer Flysch Carpathians; 4 Central Slovakian Neogene volcanics; 5 Borehole and/or well with the Eggenburgian deposits intersected and/or hit; 6 Area covered by sea inferred; 7 National boundary

The occurrence of dinoflagelata assemblages also supports the Lower Miocene age of the sediments from Gemerská Panica (could it be the *Ectosphaeropsis burdigalensis* zone?). Occurrence of heterotrophic *Deflandrea* spp. could indicate an existence of nutrient currents in the basin (ESHET, 1994). Most likely, this calcareous siltstone could be the equivalent of Putnok Schlier, which, in the past, evidently continued farther NE, beyond present day border of the Rimavská kotlina Depression.

Since the Eggenburgian fauna and flora assemblages in the Rimavská kotlina Depression are very rare, repeated geological and biostratigraphical campaigns to verify the presence of the sediments Eggenburgian stage in the Rimavská kotlina Depression have all failed. SLAVÍKOVÁ (1953) failed to find the Eggenburgian foraminifers in the wells near the village of Číž, as did Kantorová (fide VASS and ELEČKO, 1989) and later ŠUTOVSKÁ (1990) in the borehole material from the whole depression. Not even Eggenburgian calcareous nannoflora was found in studied samples (LEHOTAYOVÁ in VASS and ELEČKO l.c.). Sporadic findings of molluscs postdating Eggenburgian, and recently also of the Eggenburgian microfauna and nannoflora assemblages show that the Eggenburgian rocks occur as but small occurrences in the Rimavská kotlina depression, namely in its NE part. Original larger extension of Eggenburgian deposits was reduced due to erosion, aided by wrench tectonics. The Darnó tectonic zone (Darnó line accompanied by numerous parallel faults) runs along the eastern margin of the Rimavská kotlina Depression. During Middle Miocene the left strike-slip faults of the Darnó line displaced the bulk of Eggenburgian sediments southwards. Therefore, the Eggenburgian sediments now occur presumably in the Hungarian territory. In the Rimavská kotlina Depression there are only small erosional remnants near the villages Chanava and Gemerská Panica (Fig. 4). These erosional remnants are lithological equivalents of calcareous siltstones of the Szécsény Schlier and/or of the Putnok Schlier, widespread eastwards of the Darnó zone.

The presence of erosional remnants of pelitic, therefore, basinal sediments of the open deeper sea and shortage of the littoral ones at the present basin's margin suggest their erosional amputation. The Fífakovo-Péteřvására Basin occupied originally an area more to the NE and was probably connected by a sea way with the Transcarpathian (East Slovakian) Basins. Mentioned sediments were eroded away as a consequence of an uplift of the Slovakian Karst and the whole Slovenské rudohorie Mountains area during Neogene.

Another possible sea way linking the Fífakovo-Péteřvására Basin with the open sea was through present Western Carpathian intramountainous depressions: Turiec, Horná Nitra, Bánovce, Ilava and Trenčín and through Vienna Basin into the Carpathian Foredeep (Fig. 5). This communication postulates a sea way across the area of present day Central Slovakian Neogene volcanics. In spite of the fact that the western and north-western margin of recent Fífakovo Formation, located below the

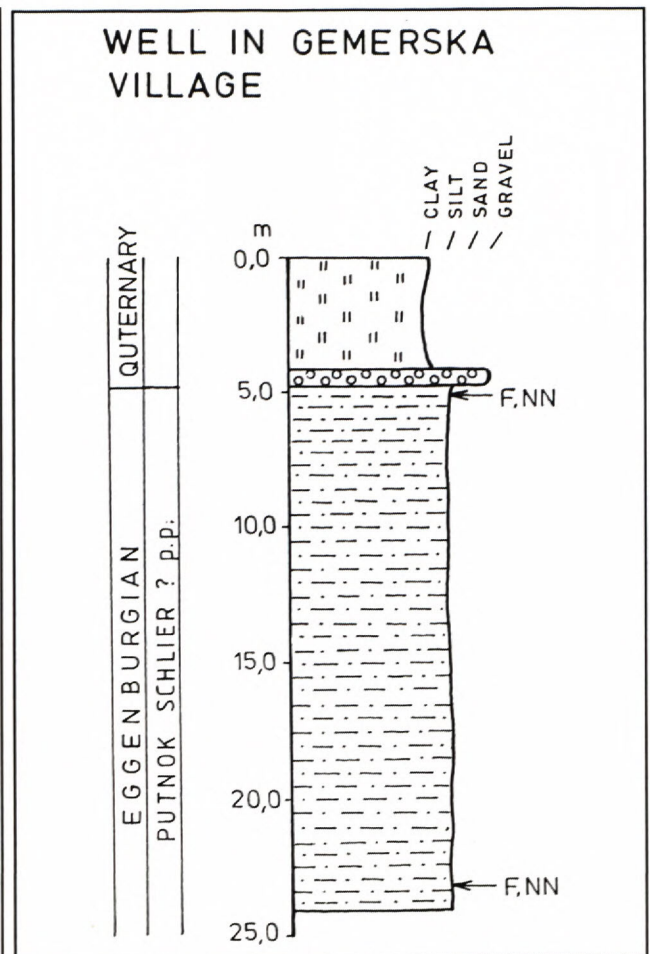


Fig. 6 Lithological section through the well in the village of Gemerská Panica NE of the town of Rimavská Sobota (S. Slovakia). For situation see Fig. 5; for lithology see Fig. 7.

volcanics of the Krupina Plateau and in the Ipeřská kotlina Depression, has been subject to intra-Eggenburgian erosion (its erosional margin is well confirmed by many boreholes), the erosional remnants of Eggenburgian sediments have been found W and NW from the mentioned erosional margin (VASS and ELEČKO et al. in lit.) and in the Ipeřská kotlina depression (SENEŠ, 1952; VASS et al, 1979), where they are known as the Ďarmoty Member (VASS et al., 1983). But they were also ascertained to underlie the Badenian Neogene volcanics and Lower Miocene rocks beneath the Krupina Plateau. The Eggenburgian marine sediments were found in several wells: D-19 nearby the village of Horné Suváre, ČV-7 nearby Červeňany and recently in the well VVL-8 nearby the village of Veľký Lom (Fig. 7).

A foram assemblage with prevailing stenohaline epifytic foraminifers has been found in the sandy sediments in the borehole D-19 at depth of 665 m (Fig. 7). Dominant taxa of *Asterigerinata planorbis* indicates a normal marine environment, with sufficient oxygen supply. A relatively deep water foram assemblage: *Cibicides pseudoungerianus*, *Heterolepa dutemplei*,

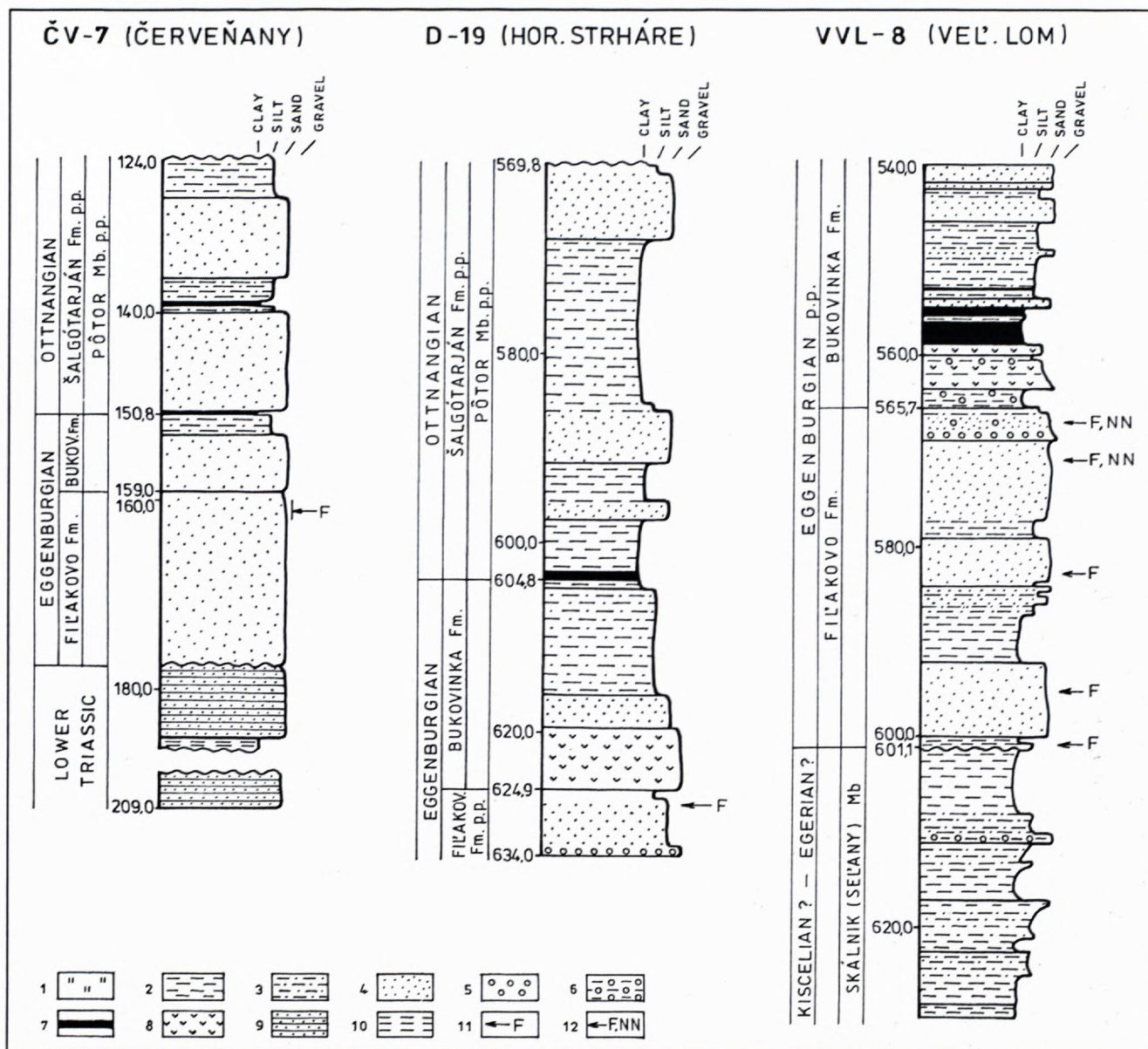


Fig. 7: Lithological scheme of the Eggenburgian deposits intersected by the boreholes ČV-7 (Červeňany), D-19 (Horné Strháre) and VVL-8 (Veľký Lom).

1 Quaternary deposits; 2 clay/claystone; 3 silt/siltstone; 4 sand/sandstone; 5 gravel/conglomerate; 6 pebbly mudstone; 7 coal seam; 8 rhyodacite tuff; 9 quarcite (Triassic); 10 red shales (Triassic); 11 Foraminiferal assemblage; 12 NN calcareous nannoplankton assemblage

Bolivina antiqua, *Bulimina elongata*) (Plate 3), also indicating normal salinity and good aeration, has been found in the well ČV-7 at a depth of 160-162 m, in the sandstone overlying transgressively the Lower Triassic basement (Fig. 7). A significant feature of the assemblages from both wells is large size of the foram individuals, indicating optimal living conditions. Friable calcareous sandstone with marine foram assemblage (ZLINSKÁ in VASS and ELEČKO 1995) was intersected in the well VVL-8 at depth of 565.7-601.1 m (Fig. 7). It is interesting to note that foraminifers from the Tachty and Lipovany sandstones and the Čakanovce Member of the Fifakovo

Formation in the Cerová vrchovina Upland are small sized, suggesting stressing living conditions (large and sudden supply of clastic material in case of Tachty sandstone, oxygen shortage in case of Lipovany sandstone and Čakanovce Member, respectively). Assemblages of large epiphytic and cibicidoid foraminifers, described from the Horná Nitra Depression by LEHOTAYOVÁ (in STEININGER and PAPP et al., 1971), and by GAŠPARIKOVÁ (1970), and from the Ilava Depression by ZLINSKÁ and SALAJ (1991) prove that good open sea living conditions existed in the mentioned intra-mountainous depressions. This could have been due to

proximal position of the depressions relative to open sea of the Vienna Basin, while the Fíľakovo-Péťervására Basin represented physiographically a bay in distal position relative to the open sea.

Eggenburgian age of sandstones from the boreholes D-19 and ČV-7 is proved by findings of *Globigerinoides trilobus* (its first occurrence is in the Eggenburgian RÖGL, 1986) and its common occurrence with the *Almanea osnabrugensis*, the latter marking the end of Eggenburgian (CICHA et al., 1982). Eggenburgian age is further supported by the fact that the sandstones with described microfauna in two wells (D-19, VVL-8) are situated below rhyodacite tuff (Fig. 7), a member of the Bukovinka Formation. Radiometric age of the rhyodacite tuff in the southern Slovakia is 20.1 and 19.7 Ma respectively, (REPČOK and/or DURKOVIČOVÁ et al., in VASS and ELEČKO et al., 1992), corresponding to the Eggenburgian (comp. VASS et al., 1987).

Conclusion

The Alpine and Carpathian Foredeeps were probably the most significant communication ways for the Eggenburgian marine transgressions to progress from the Mediterranean and/or Atlantic Ocean into the Central Paratethys area of the Middle Europe.

From the Carpathian foredeep and/or from the marine basins in front of ascending Carpathians the sea entered the Western Carpathian intramontane depressions and,

crossing the area covered presently by Mid-Slovakian Neogene volcanics, the sea reached as the Fíľakovo/Péťervására Basin, situated nowadays in Southern Slovakia and Northern Hungary.

Connection between the Fíľakovo-Péťervására Basin with the Transcarpathian Basin and between the residual Magura Basin and other contemporary marine basins situated in front of the rising Carpathians is proved by:

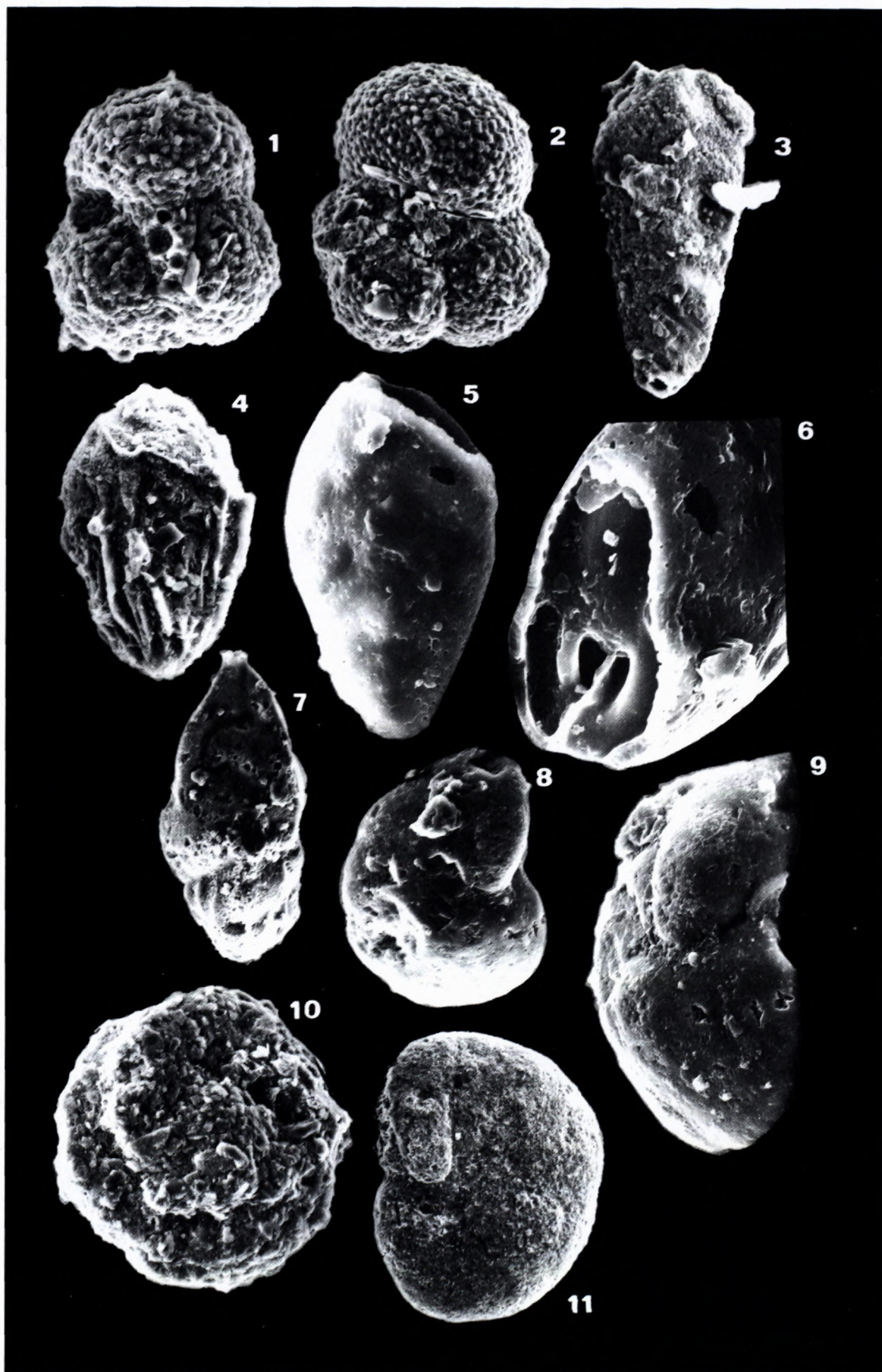
1. impressive tidal sedimentary structures of Péťervására sandstones and sandstones of the Fíľakovo Formation. The tide was coming from NE (SZTANÓ, 1994).

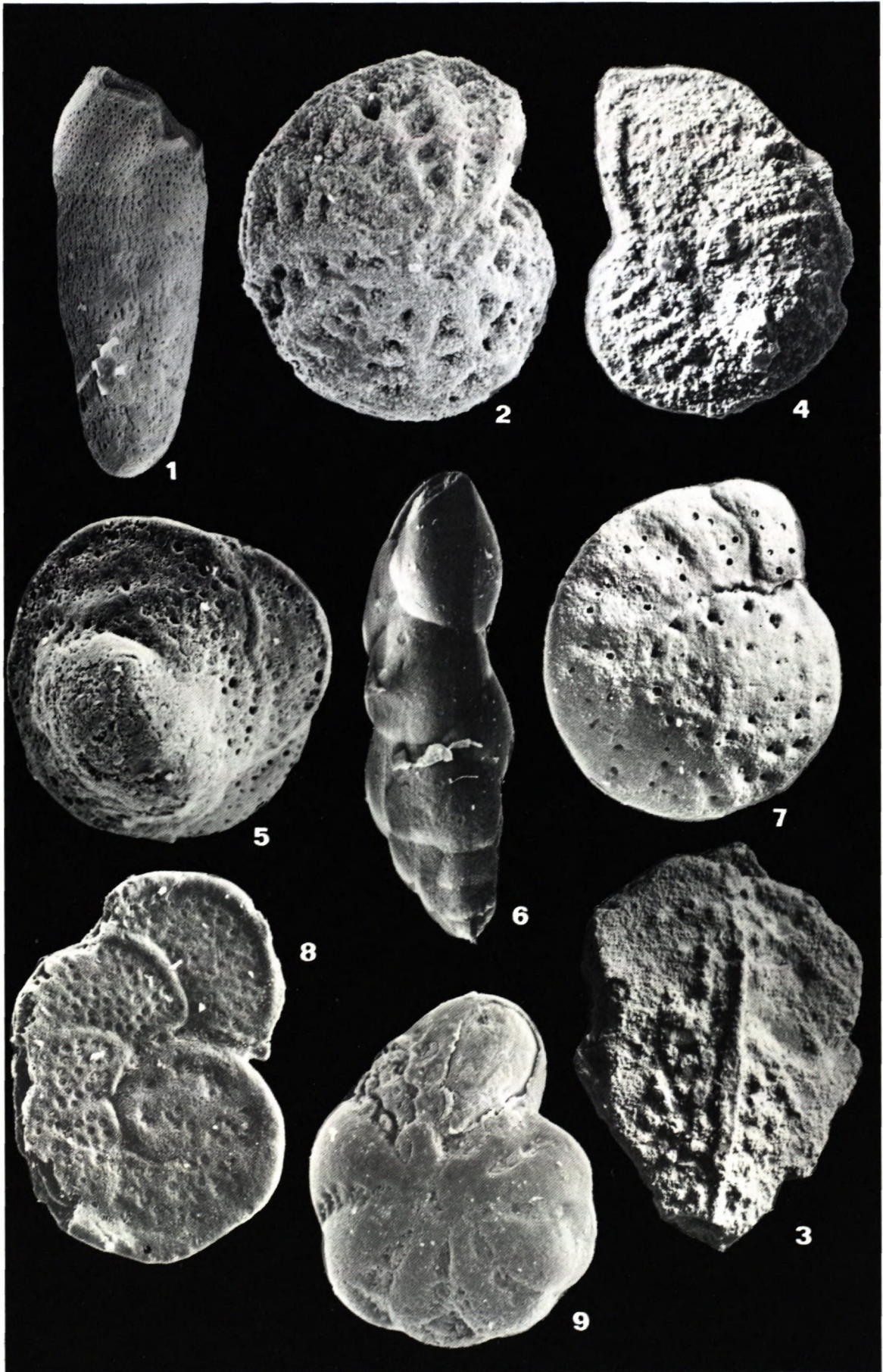
2. presence of open marine, relatively deep sea forams in the erosional sediments remnants near the NE border of the present day Rimavská kotlina depression. This gives an impression of originally much larger extent of the Eggenburgian marine deposits in the recent Rimavská kotlina Depression, especially in NE direction, where from the sea way, connecting both Fíľakovo/Péťervására and Transcarpathian (East Slovakian) Basins, can be inferred.

Another possible sea way was through the Western Carpathians intramontaneous depressions into the Vienna Basin and through this into the Carpathian Foredeep. This is proved by 1) erosional remnants of Eggenburgian deposits in the Ipeľská kotlina depression - Ďarmoty Member (VASS et al., 1983) and by 2) occurrence of marine Eggenburgian deposits beneath the volcanics of the Krupina Plateau, as confirmed by the wells D-19, ČV-7 and VVL-8.

Plate 1 Foraminiferal assemblage from the well in the Gemerská Panica village

1. *Globigerinoides trilobus* (RSS.), magn. 280X; 2. *Globigerina praebulloides* BLOW, magn. 180X; 3. *Bolivina antiqua* ORB., magn. 240X; 4. *Bolivina scalprata retiformis* CUSH., magn. 380X; 5. *Bolivina dilatata brevis* (C. et Z.), magn. 320X; 6. *Bolivina dilatata brevis* (C. et Z.), magn. 667X; 7. *Trifarina bradyi* CUSH., magn. 210X; 8. *Hanzawaia boueana* (ORB.), magn. 350X; 9. *Hanzawaia boueana* (ORB.), magn. 600X; 10. *Glomospirella* sp., magn. 150X; 11. *Haplophragmoides vasiceki* (C. et Z.) magn. 60X





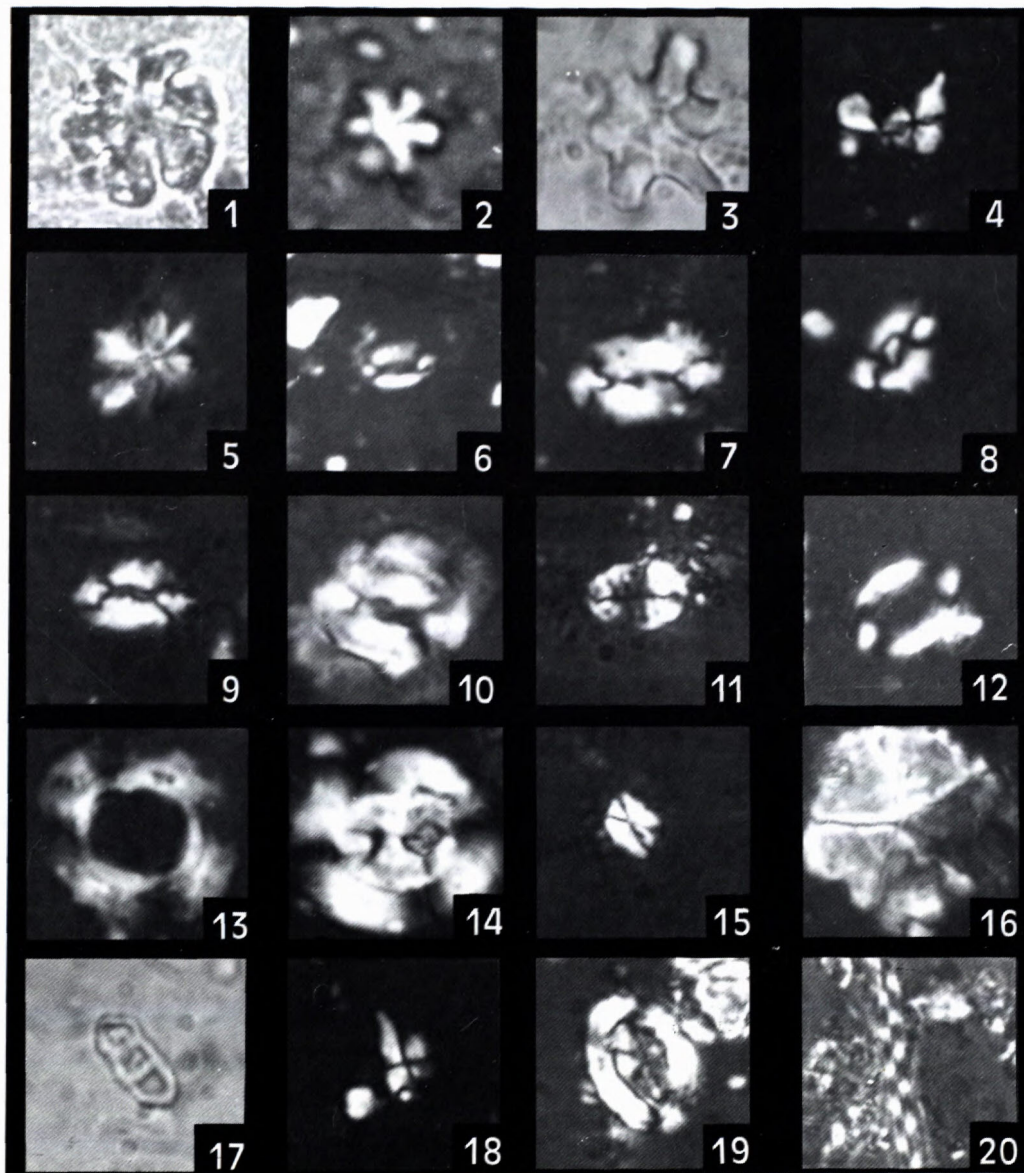


Plate 3 Calcareous nannoplankton assemblage from the well in the village Gemerská Panica (magn. 1900x).

1.-2. *Discoaster deflandrei* BRAMLETTE & RIEDEL; 3. *D. druggi* BRAMLETTE & WILCOXON; 4. *Sphenolithus conicus* BUKRY; 5. *S. moriformis* (BRONNIMANN & STRADNER) BRAMLETTE & WILCOXON; 6. *Helicospaera ampliperta* BRAMLETTE & WILCOXON; 7. *H. carteri* (WALLICH) KAMPTNER; 8. *H. euphratis* HAQ; 9. *H. scissura* MILLER; 10. *Coccolithus eopelagicus* (BRAMLETTE & RIEDEL) BRAMLETTE & SULLIVAN; 11. *Pontosphaera multipora* (KAMPTNER) ROTH; 12. *P. latelliptica* (BALDI-BEKE & BALDI) PERCH-NIELSEN; 13. *Reticulofenestra umbilica* (LEVIN) MARTINI & RITZKOWSKI; 14. *Dictyococcites bisectus* (HAY, MOHLER & WADE) BUKRY & PERCIVAL; 15. *Zygrhablithus bijugatus* (DEFLANDRE) DEFLANDRE; 16. *Braarudosphaera bigelowii* (GRAN & BRAARUD) DEFLANDRE; 17. *Isthmolithus recurvus* DEFLANDRE; 18. *Sphenolithus radians* DEFLANDRE; 19. *Arkhangelskiella cymbiformis* VEKSHINA; 20. *Microrhabdulus decoratus* DEFLANDRE

Plate 2 Foraminiferal assemblage from the boreholes ČV-7 and D-19

1. *Bolivina elongata* HANTKEN, ČV-7-161m, magn. 100X; 2. *Elphidium* ex gr. *macellum* (L.), ČV-7-161m, magn. 180X; 3. *Almaena osnabrugensis* (ROEM), ČV-7-161m, magn. 30X; 4. *Asterigerinata planorbis* (ORB.), D-19-665m, magn. 250X; 5. *Bulimina elongata* (ORB.), D-19-665m, magn. 140X; 6. *Cibicides pseudoungerianus* (CUSH.) D-19-665m, magn. 170X; 7. *Lobatula lobatula* (W. et J.), D-19-665m, magn. 240X; 8. *Elphidium rugulosum* (CUSH. et WIECKEN.) D-19-665m, magn. 240X; 9. *Bolivinella rugosa* HOWE, D-19-665m, magn. 130X

References

- BÁLDI T., 1986: Mid-tertiary stratigraphy and paleogeographic Evolution of Hungary. Akadémia kiadó Budapest, 1-201
- CICHA I., ZAPLETALOVÁ I., MOLČÍKOVÁ V. & BRZOBOHATÝ P., 1983: Stratigraphical range of Eggenburgian - Badenian foraminifera in West Carpathian Basins. - Knihovna Zem. Plyn. Nafta, Miscellanea micropaleont. 4, Hodonín, 99-144
- CIEZSKOWSKI M., 1992: Marine miocene deposits near Nowy Targ, Magura nappe Flysch Carpathians (South Poland). *Geologica Carpathica*, 43, Bratislava, 33-346
- DEPÉRET M., 1892: Note sur la classification et le parallélisme du Systéme Miocéne. C.R. somm. seances Soc. Géol. France, n.13, PP. CXLV-CLVI, Paris
- ESHET Y., LABIN A. & BEIN A., 1994: Dinoflagellate cysts, paleoproductivity and upwelling systems: A Late Cretaceous example from Israel. *Mar. Micropaleont.* 23, 231-240
- GAŠPARIKOVÁ V., 1970: Rozšírenie spodného miocénu v hornonitrianskej kotline a príľahlej časti Vťáchnika. Distribution of the Lower Miocene in Horna Nitra Depression and adjacent Vťáchnik Mts.(English abstract). *Geol. Práce*, Spr. 52, Bratislava, 345-349
- HÁMOR G., (edit.) 1988: Neogene paleogeographic atlas of Central and Eastern Europe. Hungarian Geological Institute, Budapest, Map 1-7
- KOVÁČ M., CICHA J., KRÝSTEK I., SLACZKA A., STRÁNIK Z., OSZCZYPKO N. & VASS D., 1989: Palinspastic Maps of the Western Carpathian Neogene, scale 1:1 000 000. *Geol. Surv. Prague*
- LEHOTAYOVÁ R., 1982: Miocene Nannoplankton Zones in West Carpathians. *Záp. Karpaty, Ser. Paleontol.* 8, Bratislava, 91-110
- MARTINI, E., 1971: Standart Tertiary and Quaternary calcareous nannoplankton zonation. - *Proc. Iind. Planktonic Conf.*, Roma 1970, 2: 739-785, pls. 1-4, Rom.
- MURRAY J.W., 1991: Ecology and Paleoecology of bentic foraminifera. *Longman Sc. Tech.* London 1-396
- ONDREJČKOVÁ A., 1977: Makrofauna vrťov VCH-1 a VCH-2 z Rimavskej kotľiny (in Slovak). Manuscript, Geofond, Bratislava.
- OSZCZYPKO N., SLACZKA A., 1985: An Attempt to Palinspastic Reconstruction of Neogene Basins in the Carpathian Fore-deep. *Ann. societat Geologorum Polonine, Rocn. Polsk. Towar. Geologicznego*, 55-1/2, Kraków, 55-75
- RÖGL V. F., STEININGER F.F., 1983: Vom zerfall der Tethys zu Mediterran und Paratethys. *Ann. Naturhist. Mus. Wien*, 85/A, 135-163
- RÖGL F., 1986: Late Oligocene and Miocene Planktonic Foraminifera of the Central Paratethys - In: Bolli H. M., Sanders J. B., Perch Nielsen K., Planktonic Stratigraphy - Cambridge Univ. Press, Cambridge, 315-328
- SALAJ J., ZLINSKÁ A., 1991: Spodnomiocénne sedimenty slienitej fácie od Považskej Teplej. (English abstract). *Min. Slov.* 23, Bratislava, 173-178
- SENEŠ J., 1952: Štúdiu o akvitánskom stupni. (English abstract). *Geol.Práce*, Zoš.31, Bratislava, 1-75
- SLAVÍKOVÁ K., 1953: Hlubinná opěrná vrťba Cakov-1. (in Czech). *Archív Čs. naft. dolov Hodonín*
- STEININGER F., SENEŠ J., et al., 1971: Chronostratigraphie und Neostatotypen Miozán der Zentralen Paratethys Bd. II. Eggenburgian. Vydavateľstvo SAV, Bratislava, 1-827
- SZTANO O., 1994: The Tide - influenced Péťervására Sandstone, Early Miocene, Northern Hungary: Sedimentology, Paleogeography and Basin Development. *Geol. Ultraieictina Mededelingen von de Faculteit Aardwetenschappen Universiteit Utrecht N.* 120, 7-155
- ŠUTOVSKÁ K., 1990: Paleoeológia bentózných foraminifer oligocénu a miocénu tylovej a vnútornej molasy Západných Karpát. (in Slovak). Dissertation thesis, Manuscript, archive PF UK Bratislava.
- VASS D., KONEČNÝ V., ŠEFARA J., et al., 1979: Geologická stavba Ipeľskej kotľiny a Krupinskej planiny. *Geology of Ipeľská kotlina Depression and Krupinská planina Mts.* (English abstract). *Geol. Úst. D. Štúra*, Bratislava, 1-280
- VASS D., KONEČNÝ V. & PRISTAŠ J., 1983: Vysvetlivky ku geologickej mape Ipeľskej kotľiny a Krupinskej planiny 1:50 000. (in Slovak). *Geol. Úst. D. Štúra*, Bratislava, 7-126
- VASS D., REPČOK I., BALOGH K., HALMAI J., 1987: Radiometric time scale of Central Paratethys Neogene revised. *Ann. Inst. Geol. Publ. Hung. vol. LXX.*, Budapest, 423-434.
- VASS D., ELEČKO M., PRISTAŠ J., LEXA J., HANZEL V., MODLITBA I., JÁNOVÁ V., BODNÁR J., HUSÁK L., FILO M., MÁJOVSKÝ J. & LINKEŠ V., 1989: Geológia Rimavskej kotľiny. *Geology of Rimavska kotlina Depression.* *Geol.* (English abstract) *Úst. D. Štúra*, Bratislava, 1-160
- VASS D., ELEČKO M., BEZÁK V., BODNÁR J., PRISTAŠ J., KONEČNÝ J., LEXA J., MOLÁK B., STRAKA P., STANKOVIČ J., STOLÁR M., ŠKVARKA L., VOZÁR J., & VOZÁROVÁ A., 1992: Vysvetlivky ku geologickej mape Lučenskej kotľiny a Cerovej vrchoviny 1:50 000. (in Slovak). *Geol. Úst. D. Štúra*, Bratislava, 5-196
- VASS D., 1995: The Origin and Disappearance of Hungarian Paleogene Basins and short term Lower Miocene Basins in Northern Hungary and Southern Slovakia. *Slovak Geol. Mag.* 2/1995, *Geol. Úst. D. Štúra*, Bratislava, 81-95.

Tertiary Development of the Western Part of Klippen Belt

PETER KOVÁČ and JOZEF HÓK

Geological Survey of Slovak Republic, Mlynská dolina 1, 817 04 Bratislava, Slovak Republic

Abstract: The scope of this work was to find Tertiary changes in orientation of the strain field in the western part of the Klippen belt, to study the kinematic character of faults and to date their activity.

Structural interpretation of data obtained from the western part of the Klippen belt (up to the Orava section) indicates that it was affected by several phases of deformation. As observed in the field the compression of Klippen belt, oriented perpendicular to its strike, occurred during the first phase, responsible for the development of slip-fault and fold structures. This stage dates back to Oligocene? - Lower Miocene. Gradual reorientation of the stress field resulted in the development of strike faults and shear folds. The evolution of the Klippen belt between Lower and Middle Miocene has been influenced by transpressional regime. Generally, the maximum strain σ_1 was oriented N-S to NNE-SSW. Subsequently, the extensional regime, characterised by the development of randomly oriented downslip faults, prevailed in the area of the Klippen belt during Upper Miocene.

Introduction

The Klippen belt (Pieniny Klippen belt), situated between the Western Carpathian externides and internides (sensu Mišík et al., 1986), represents a narrow independent structural belt with extraordinarily complicated structure. It stretches from Vienna through central Považie (Váh River valley) to Orava and extends via Polish Pieniny to eastern Slovakia, Ukraine and Romania (Fig. 1). The following features are characteristic for Klippen belt: primary absence of pre-Mesozoic rock, scanty representation of Triassic rocks, variable developments of Jurassic and Cretaceous rocks and klippe-type tectonic style (Pieniny type klippen - ANDRUSOV and SCHEIBNER, 1968). Most of the klippen have tectonic origin. The klippen are represented by lenses of predominantly Jurassic and Lower Cretaceous limestones, detached from more plastic formations, composed mainly of Middle and Upper Cretaceous marls (klippen envelope). These lentiform, or isometric bodies, are situated in marlstone, or in flysch rocks of the klippen envelope. Although the envelope units were originally placed in normal stratigraphical superposition on top of rocks representing the klippen, their contacts were generally tectonic (ANDRUSOV 1974).

The Klippen belt was affected by several deformational events whose effects suggest multistage brittle - ductile and brittle deformation and relatively small depth, at which the tectonic deformations have taken place. Paleogeographic analysis indicates that the sedimentation area of the Pieniny geosyncline was considerably broad, the estimations being within the range from 30 (SCHEIBNER 1963) to 100 km (SWIDZIŃSKI 1962). In seismic sections the Klippen belt appears as indistinct, sub-vertically oriented suture belt situated between the blocks of Outer and Inner Western Carpathians

Methods

Structural analysis of the western section of the Klippen belt (Fig. 2) included a study of its deformational effects and of their timing. Field studies of individual sections of the Klippen belt (Fig. 3, 4) and surrounding units included a statistic evaluation of mesoscopic manifestations of Tertiary deformation represented mainly by faults, fissures and folds.

Direct inversion method (ANGELIER 1994) has been applied to evaluate the fault planes and movement indicators. This method assesses the orientation of the main stress field tensors on the basis of fault plane orientation and slide vectors of the movement indicators on discrete fault planes. Statistic sets of measured elements allowed to assess (together with the study of geologic map) the courses of faults, their kinematic character and, if the stratigraphic datings of investigated localities were available, also the times spanning their activity.

The fault planes are plotted using stereographic projections (Schmidt net, lower hemisphere). The fault plane projections are represented by large arcs and the striations on them by dots. The arrows assigned to dots show the sense of movement, while large arrows indicate the strike of compression, or extension, respectively (Tables 1, 2, 3, 4).

Structural development of the Klippen belt during Tertiary

Structural interpretation of data obtained from western section of the Klippen belt (up to the Orava section) indicates that several phases of deformation have taken place.

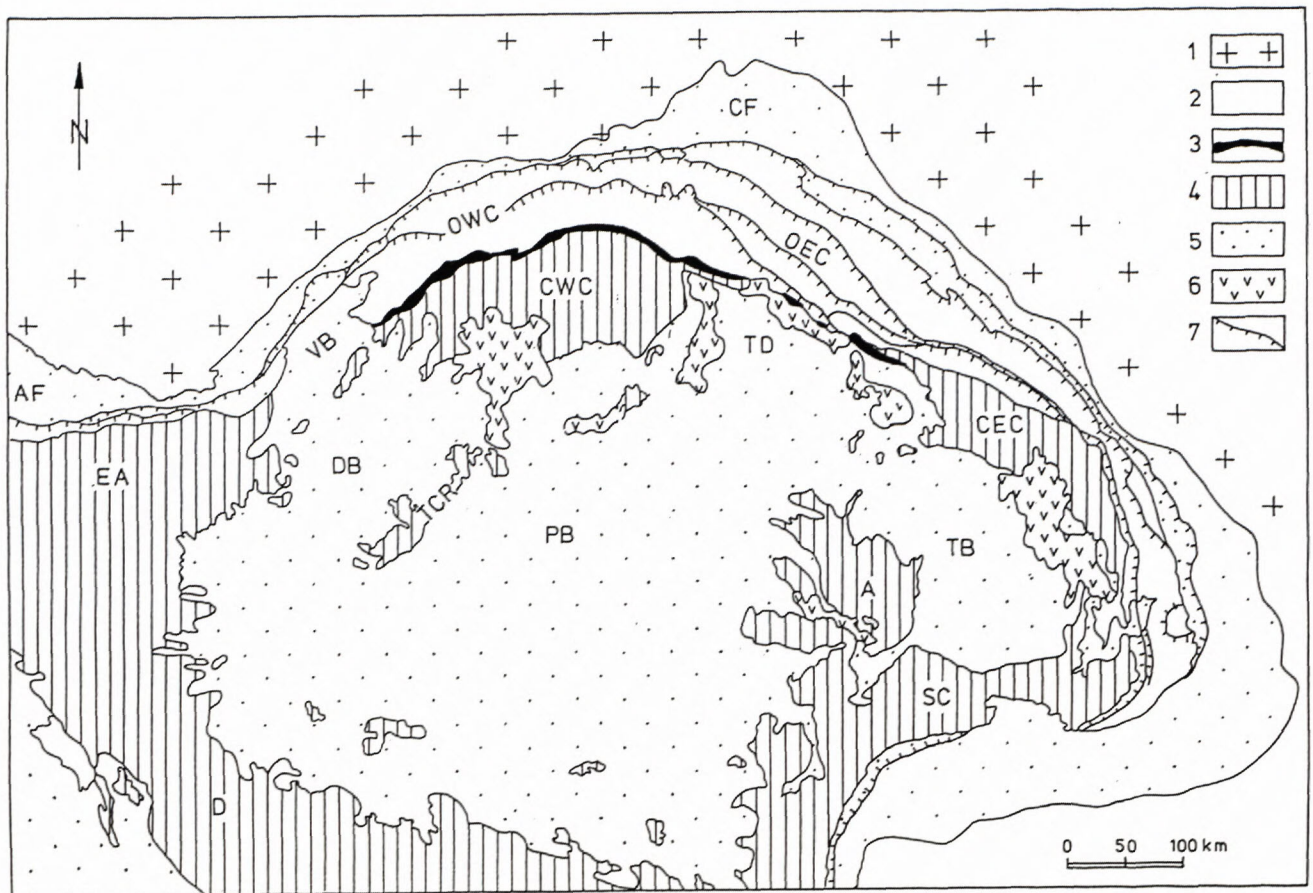


Fig. 1 Geological sketch of Carpathian arc and Pannonian basin system (KOVÁČ *et al.* in press).

1 - North- and East-European platform, 2 - flysch zone of externides, 3 - Klippen belt, 4 - Inner Carpathians, 5 - Neogene basins, 6 - Neogene volcanics, 7 - thrust lines, AF - Alpine foredeep, CF - Carpathian foredeep, OWC - Outer Western Carpathians, CWC - Central Western Carpathians, CEC - Central Eastern Carpathians, SC - Southern Carpathians, EA - Eastern Alps, A - Apuseni, D - Dinarides, VB - Vienna Basin, DB - Danube Basin, PB - Pannonian Basin, s.s., TB - Transylvanian Basin, TD - Trans-Carpathian Depression.

As observed in the field, during the first phase, the rocks which now form the Klippen belt, became subject of a compression oriented perpendicularly to the belt's strike. In most klippen there are shear thrusts (Table 1) and folding structures accompanied by strike slips (Table 2). At the northern fringe of the Inner Carpathian Paleogene, at the contact with Klippen belt, southvergent back thrusts and imbricated systems of partial thrusts (seen e.g. at the Gácel locality - part Dolný Kubín) have been formed. This phase which, we presume, was coeval with the overthrusting of flysch nappes in the western part of Carpathians (Vienna Basin area), dates back to Oligocene? - Lower Miocene. Cessation of nappe overthrusting processes in the western part of Carpathians in Karpatian stage marked an end of compressional phase. Succession of tectonic events and change of strain field in the area of Brezovské Karpaty were characterised by a clock-wise rotation of compressional process, i.e. from NW - SE to NE - SW (MARKO *et al.*, 1991; FODOR, 1995). At the same time the paleogeographic situation at the end of Otnangian, when the sedimentation area of the

Western Carpathian sea has been connected with the Alpine foredeep and during Karpatian there developed a new marine connection with the Mediterranean area in the south, indicates that important changes in tectonic regime with activation of strike slips have taken place.

Progressive reorientation of the strain field gave way to gradual formation of strain slips and shear folds. A sinistral shear zone has been formed in the area of Klippen belt (Table 3). This transpressional regime influenced the development of Klippen belt between Lower and Upper Miocene. Maximum strain σ_1 was oriented generally in NNE - SSW direction.

Subsequent extensional regime, characterised by randomly oriented downslip faults, predominated in the Klippen belt area during the Upper Miocene (Table 4). The downslip faults can be observed at all investigated localities in the Klippen belt's area.

The effects of successive individual deformational stages can clearly be observed at many places. At the Podbielsky Cickov locality (abandoned quarry in the valley with homonymous name, some 2 km from Podbiel)

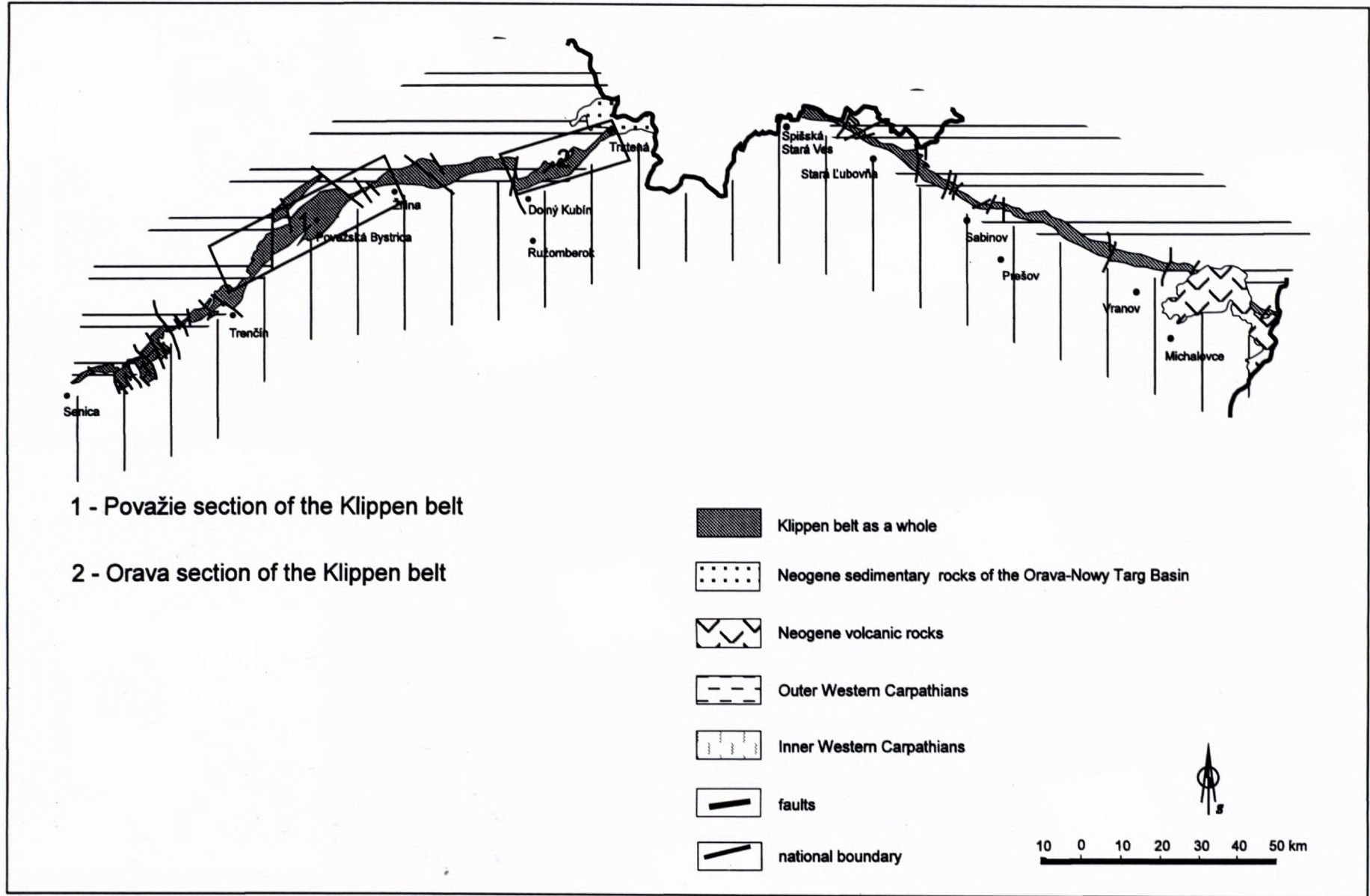


Fig. 2 Schematic tectonic sketch map showing Klippen belt and the areas investigated

the mesoscopic faults, which formed due to bend gliding in a process of pure compression, can be observed. The course of axial planes of faults indicates that the strike of maximum compression was oriented perpendicularly to the strike of the Klippen belt. Ensuing deformational process was responsible for formation of shear folds (Fig. 5).

Data on magnetic anisotropy and paleomagnetic data

As indicated by magnetic anisotropy data from the western section of the Klippen belt the deformation has taken place predominantly under brittle conditions (HROUDA et al., 1992), whereas plastic deformation was here weaker compared to Sliezská, Bystrická and Rača Units (HROUDA, 1993a). However, we can contend that generally, the deformational effects within the Klippen belt were stronger compared to marginal units of the Flysch belt, but weaker relative to Inner Carpathian units (HROUDA, 1993b). As regards the intensity of deformational effects in individual sections of the Klippen belt proper, it was generally about equal, excepting the Žilina

section, which was characterised by relatively stronger effects (HROUDA, 1993b).

The results of research into orientation of magnetic foliation and lineation in the investigated section of the Klippen belt indicate that some differences exist between this and the adjoining section of the Flysch belt. In fact, the Klippen belt was affected by events which have no equivalent in the Flysch belt. (HROUDA et al., 1992). Although not as clear-cut as they should be, the courses of poles and magnetic foliation (HROUDA 1993a Fig. 5-11) suggest NE-SW direction of the compression and complicated deformational history of the Klippen belt and adjoining sections of the Flysch belt.

Interpretation of paleomagnetic data (Fig. 6) evidences a counterclockwise (CCW) rotation of rigid blocks along the margin of moving block of Western Carpathians. Measured values show approximately 40-60° CCW rotation of the Sliezská Unit, 60° CCW of the Magura Unit in NW part of the Flysch belt (KRS et al., 1982, 1991) and 28-43° in NE part of Vienna Basin (TÚNYI and KOVÁČ, 1991, KOVÁČ and TÚNYI, 1995). While the maximum CCW rotation in the western part of Central Western Carpathians could have reached between Eocene

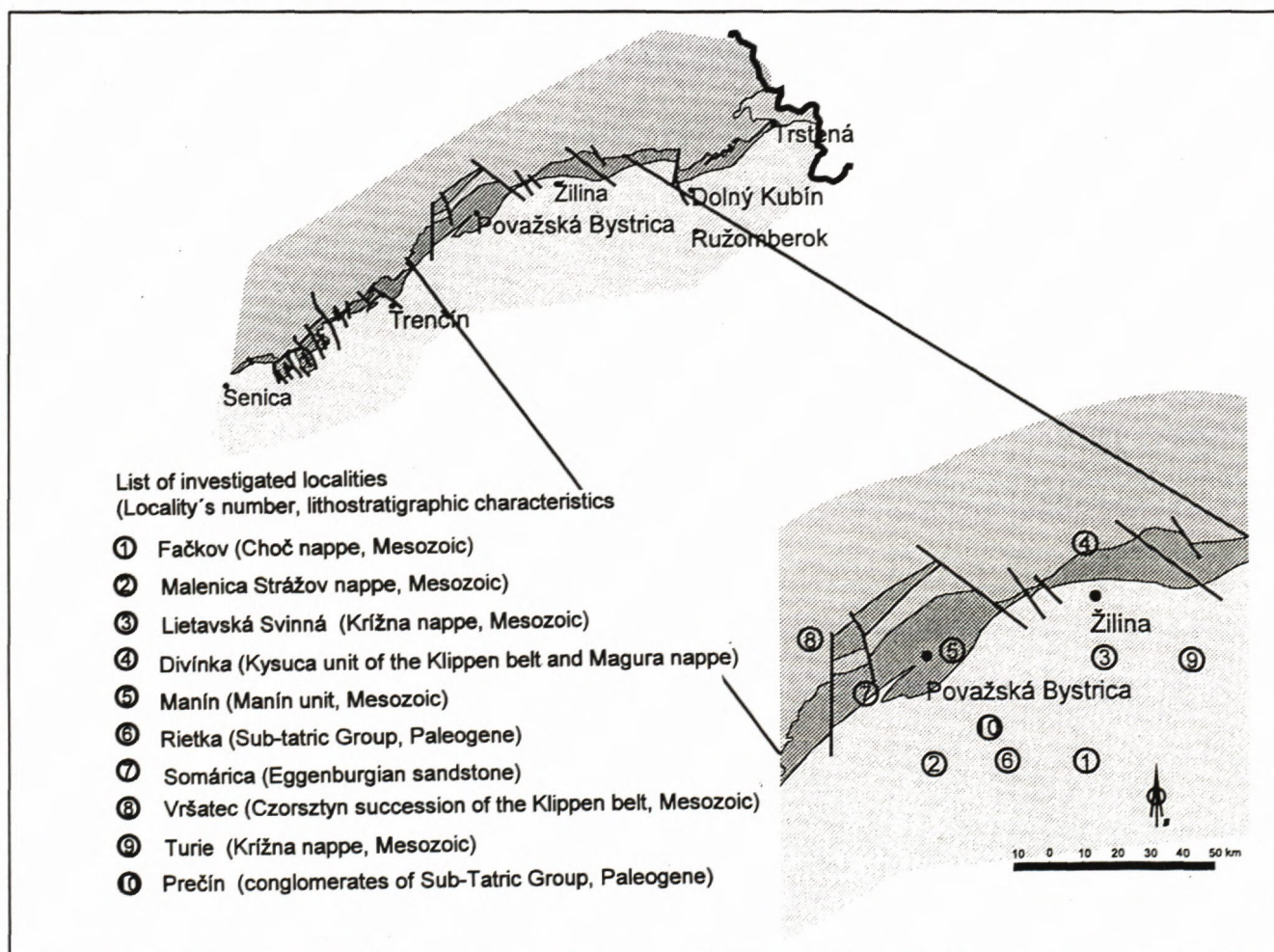


Fig. 3. Schematic tectonic sketch map showing Považie section of the Klippen belt and the localities with structural measurements in broader surroundings

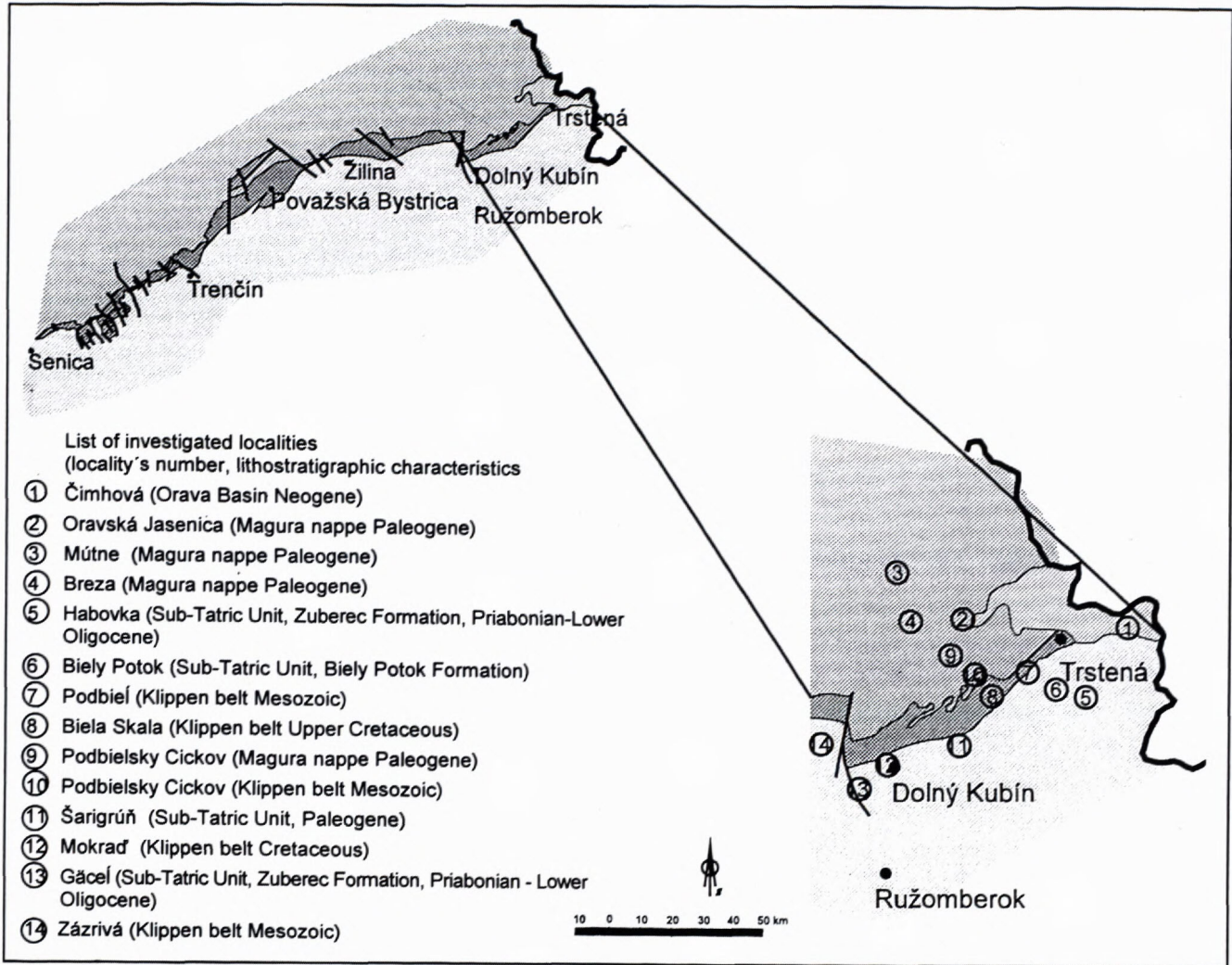


Fig. 4. Schematic map of Orava section of the Klippen belt showing the localities with structural measurements

and Oligocene 40-60° (KOVÁČ and TŮNYI, 1995), at the end of Lower Miocene it probably reached only 30-40° (KOVÁČ and TŮNYI, 1995).

The paleomagnetic rotation data together with the results of orientation of pole courses and magnetic foliation clearly record transpressional tectonic regime in the area of the Klippen belt.

Paleotectonic development

As the opening prograded during Lower Jurassic the sea bed relief in the "sedimentation area of the Klippen belt" became dissected. Jurassic transgression proceeded from west to east (BIRKENMAJER 1986). Between Middle Jurassic and Lower Cretaceous there prevailed sedimentation of pelagic sediments. The Middle Cretaceous times have seen an equilibration of sedimentation conditions in a process of deepening. There are records that the onset of the flysch "trench" sedimentation occurred in the Upper Cretaceous and continued with

gradual tectonic spatial shortening and piling of both, the Klippen belt units and overthrust units of the Central Western Carpathians, to form north-vergent fold-nappe belt, the present-day Klippen belt (MAHEL, 1978; MIŠIK 1978, PLAŠIENKA, 1995).

Formation of the fold-nappe belt continued during Paleogene. Partial emersion has taken place. Thrusting of the Pieniny and Kysuca sequences over the Czorsztyn sequence occurred during Paleocene, while during Eocene the deep water sedimentation has been initiated. At the contact with Central Carpathian block the Klippen belt has been strongly deformed during Oligocene and the Klippen belt formations have been erected and locally reworked to form south-vergent structures (ANDRUSOV, 1938). The along-strike movements between Miocene and Pliocene were associated with the faults and fissures developed mainly in competent rocks, while the incompetent rocks became subject of folding. Uneven transport of individual blocks of Central Western Carpathians resulted in the development of sigmoidal bends in the Klippen belt (ANDRUSOV, 1927).

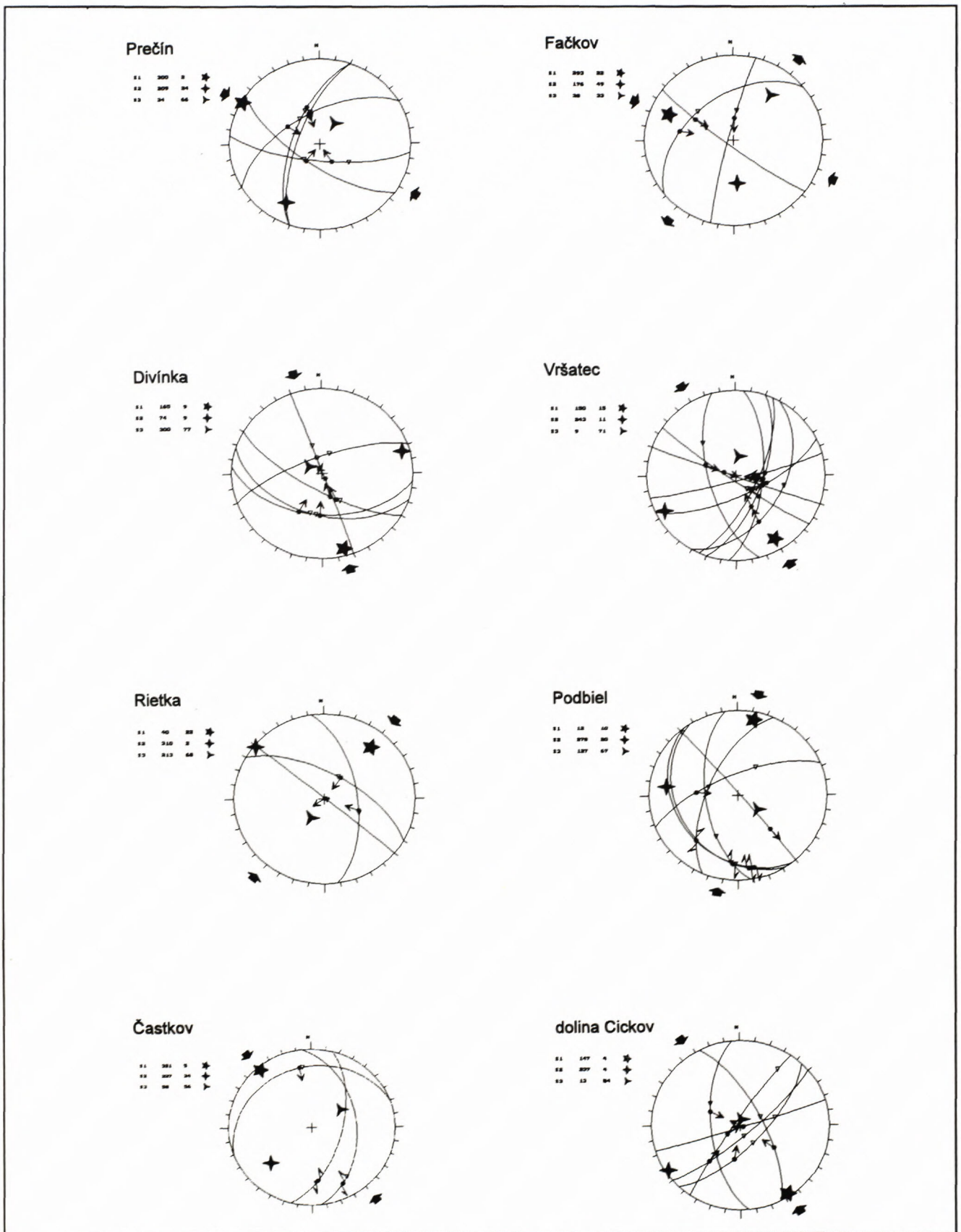


Table 1. Structural measurements in the area of Klippen belt and surrounding units Cickov valley

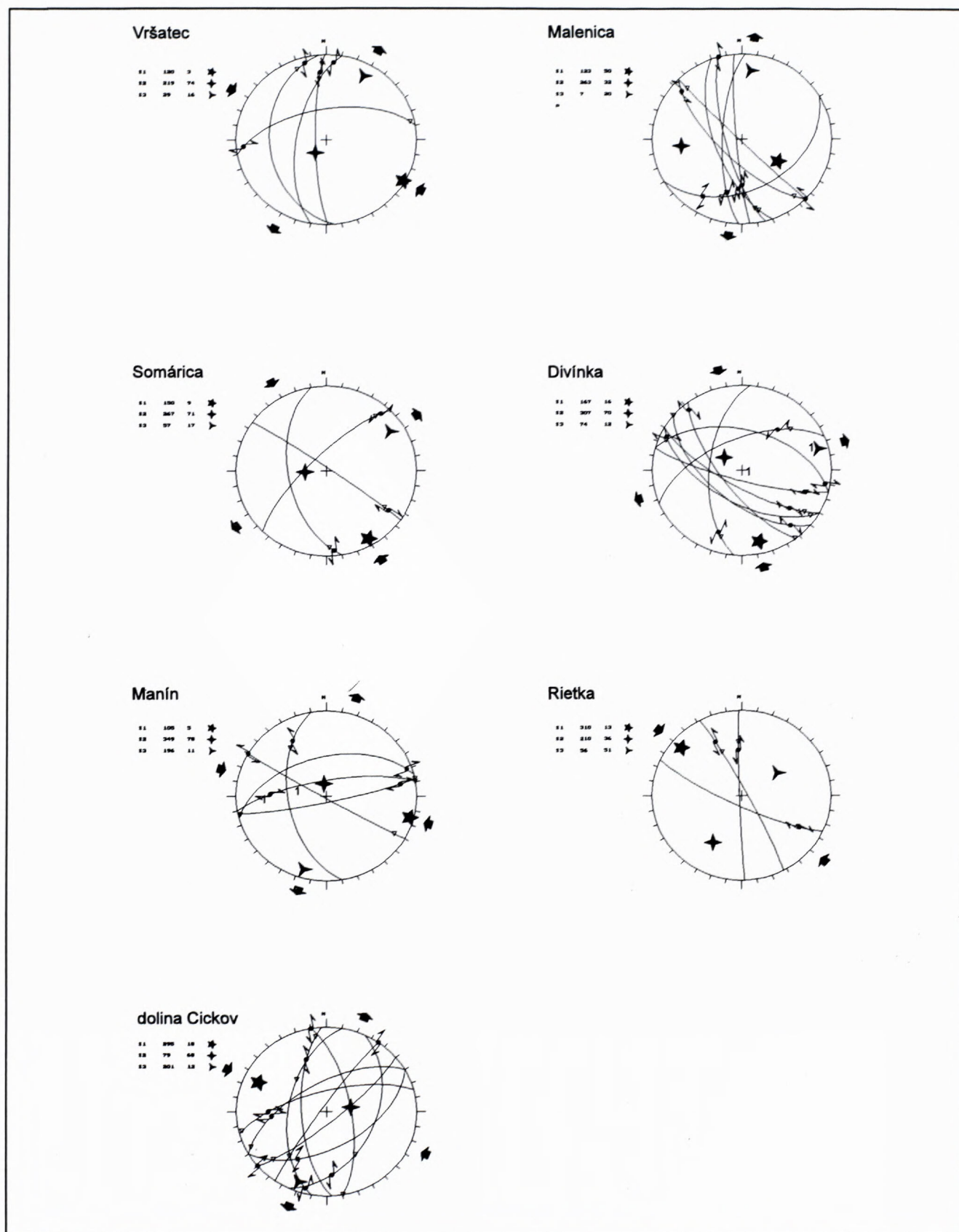


Table 2. Structural measurements in the area of Klippen belt and surrounding units Cickov valley

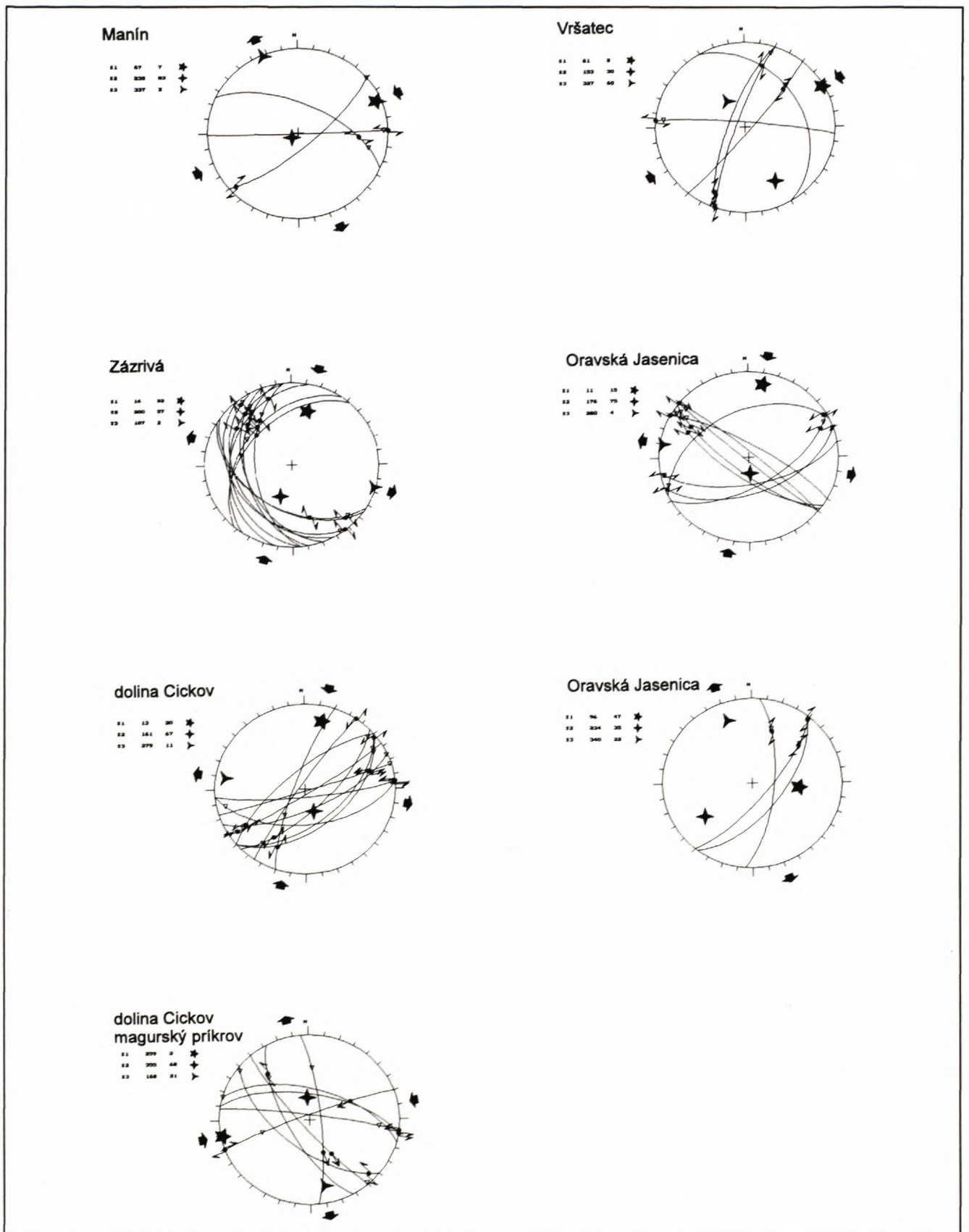


Table 3. Structural measurements in the area of Klippen belt and Magura Unit Cickov valley, Cickov valley Magura nappe

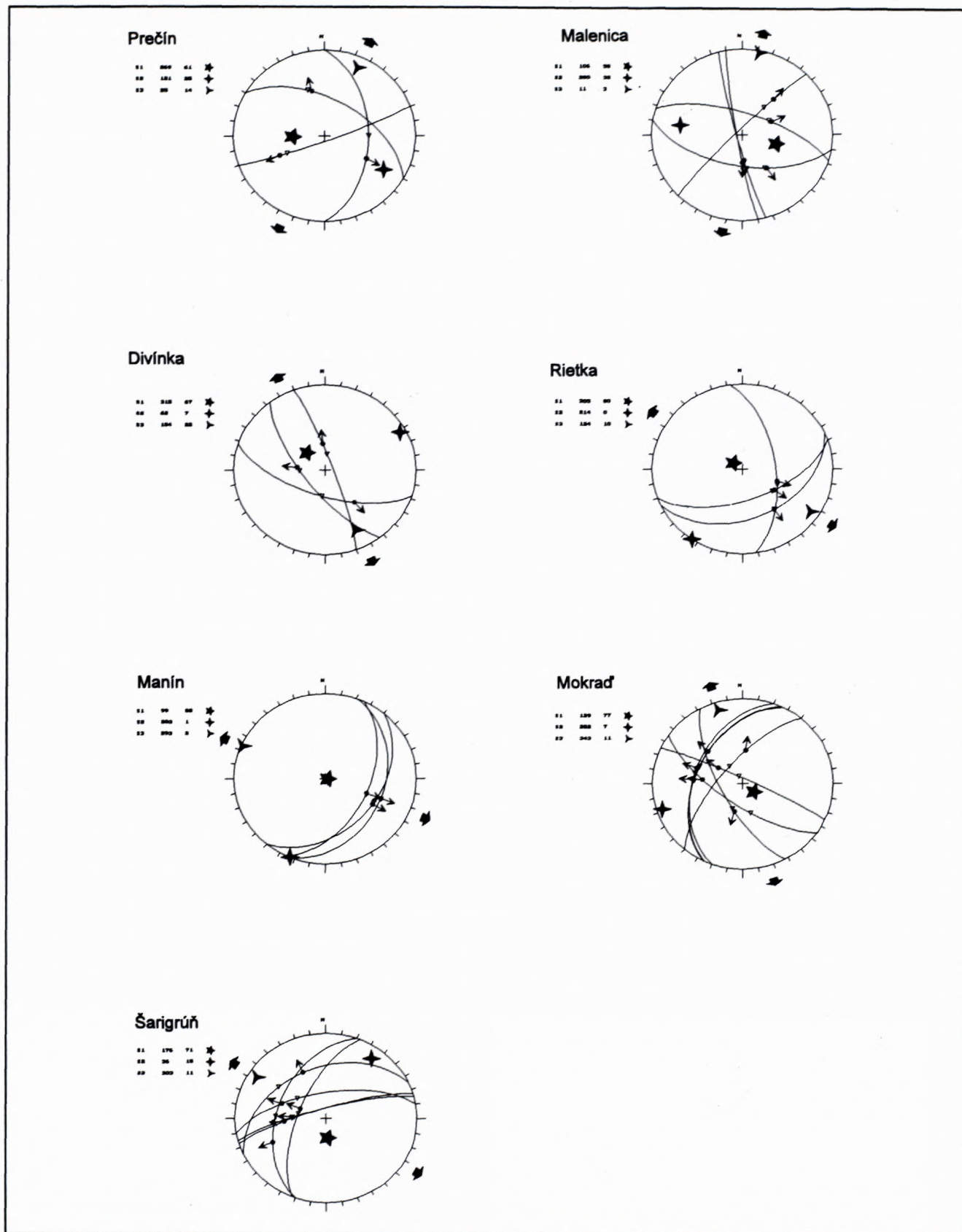


Table 4. Structural measurements in the area of Klippen belt and surrounding units

Discussion

Present shape of the Klippen belt is a result of its long term, continuous deformation brought about by convergence and later collision of the Inner Western Carpathians with the European platform (Fig. 7).

Structural analysis made in the western section of the Klippen belt allows to characterise Tertiary stage and its deformational development. The whole expanse of Klippen belt displays a very complicated internal structure. The bend gliding type folds observed as well in the rocks of the Klippen belt proper as in the rocks of the Magura nappe (ALEXANDROWSKI, 1989) speak in favour of a compressional stage spanning the time from Eocene-Oligocene to Lower Miocene, characterised by spatial shortening oriented perpendicularly to its course. The then Klippen belt was probably situated more to the south-west relative to its recent position and it was oriented NW-SE (OSZCZYPKO and ŚLACZKA, 1985, KOVÁČ et al 1994). Compressional regime is also evidenced by frequent south-vergent (recent situation) reverse faults. Gradual rotation of the western part of Klippen belt went on until the end of Lower Miocene (KRS et al. 1982, 1991, TÚNYI a KOVÁČ, 1991, KOVÁČ a TÚNYI 1995). Transpressional regime, predominant in the western part of Klippen

belt since Lower Miocene, have progressively gained the ground. A sinistral shear zone have formed. The orientation of maximum stress was generally NNE-SSW. The transition from compressional to transpressional regime was presumably diachronous, as substantiated by subsequent waves of overthrusting of east-vergent flysch nappes (JIŘÍČEK, 1979).

Timing of tectonic events in the area of Outer Carpathians is also evidenced by stratigraphic divergence of the foredeep's filling, composed in the Polish and Ukrainian parts of the Badenian and Sarmatian sediments, while in the Romanian side the sedimentation continued until Quaternary (ROURE et al., 1995). The molasse sediments usually directly overlie the Mesozoic, or crystalline basement of the foreland, as evidenced by a distinct erosional event, which took place between Upper Cretaceous and Paleogene as a possible consequence of Laramian phase. In contrast to diachronous tectonic events, which occurred during Late Oligocene to Miocene, the records of Upper Cretaceous to Paleocene Laramian inversion tectonics indicate its synchronous course along the whole perimeter of the Klippen belt.

The above facts evoke a concept of a compact block of Inner Western Carpathians, whose mobility between Upper Cretaceous and Paleogene resulted in a collision

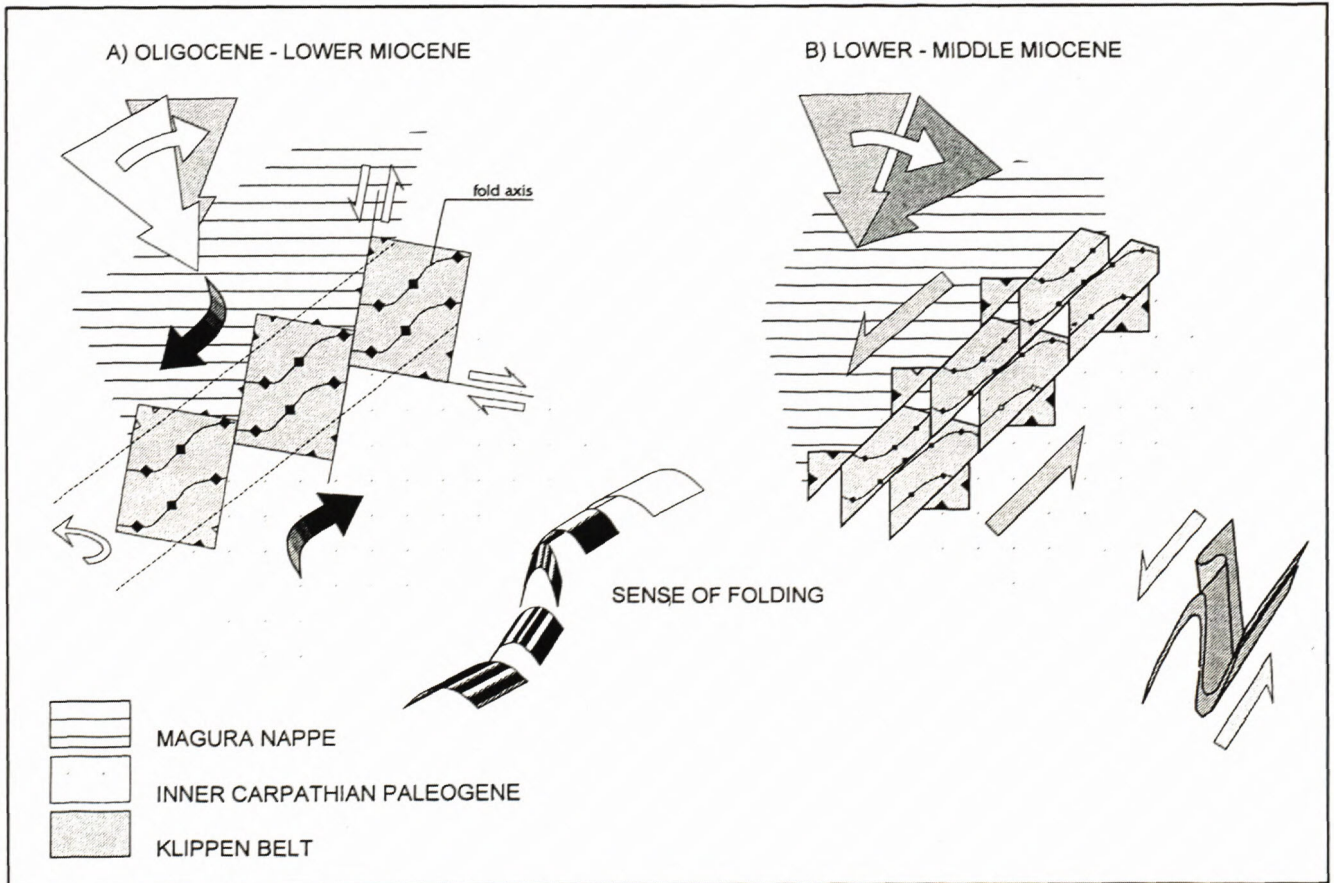


Fig. 5. Deduced kinematic development of the western part of Klippen belt

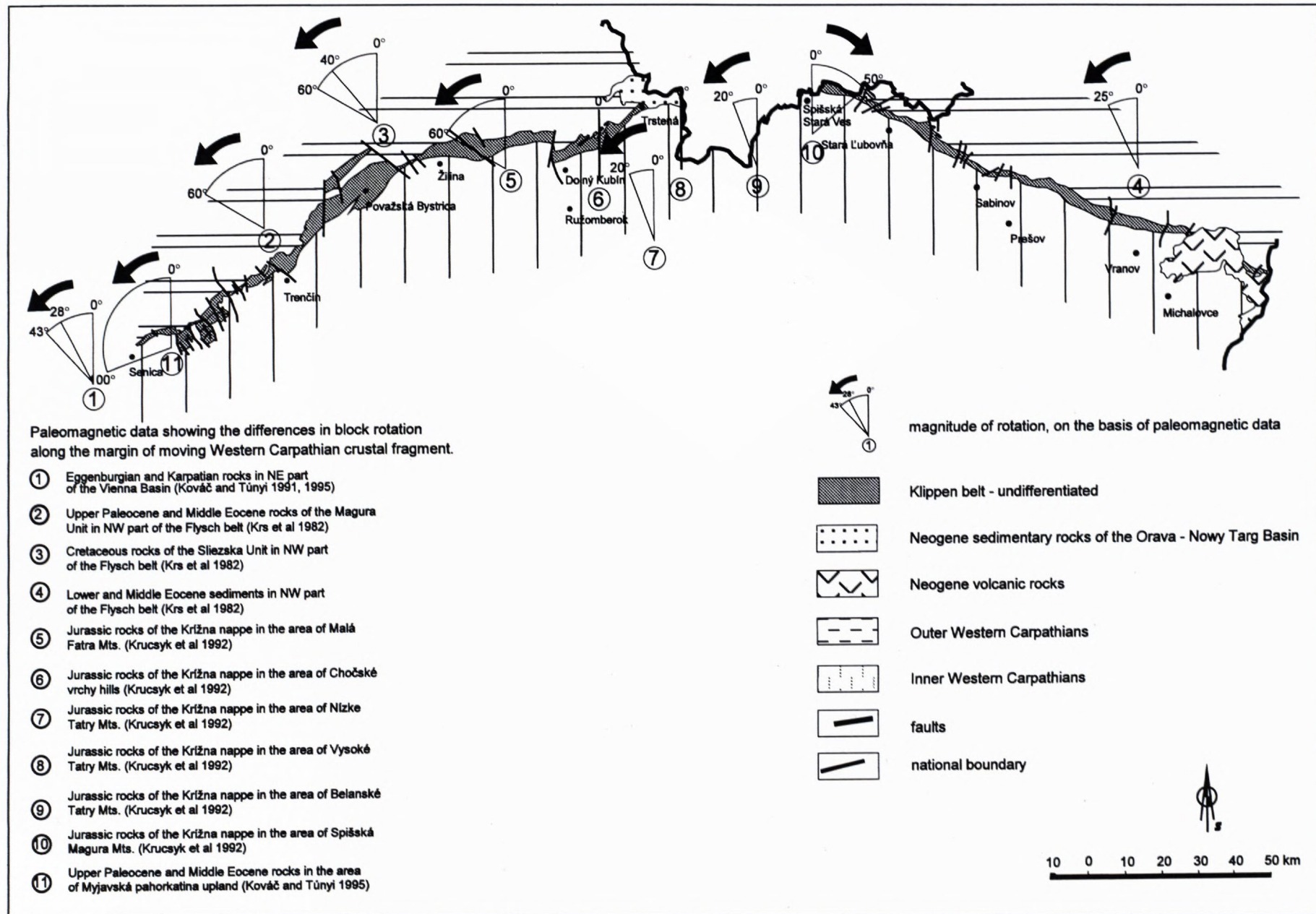


Fig. 6. Simplified map of the Klippen Belt with values with values of paleomagnetic measurements

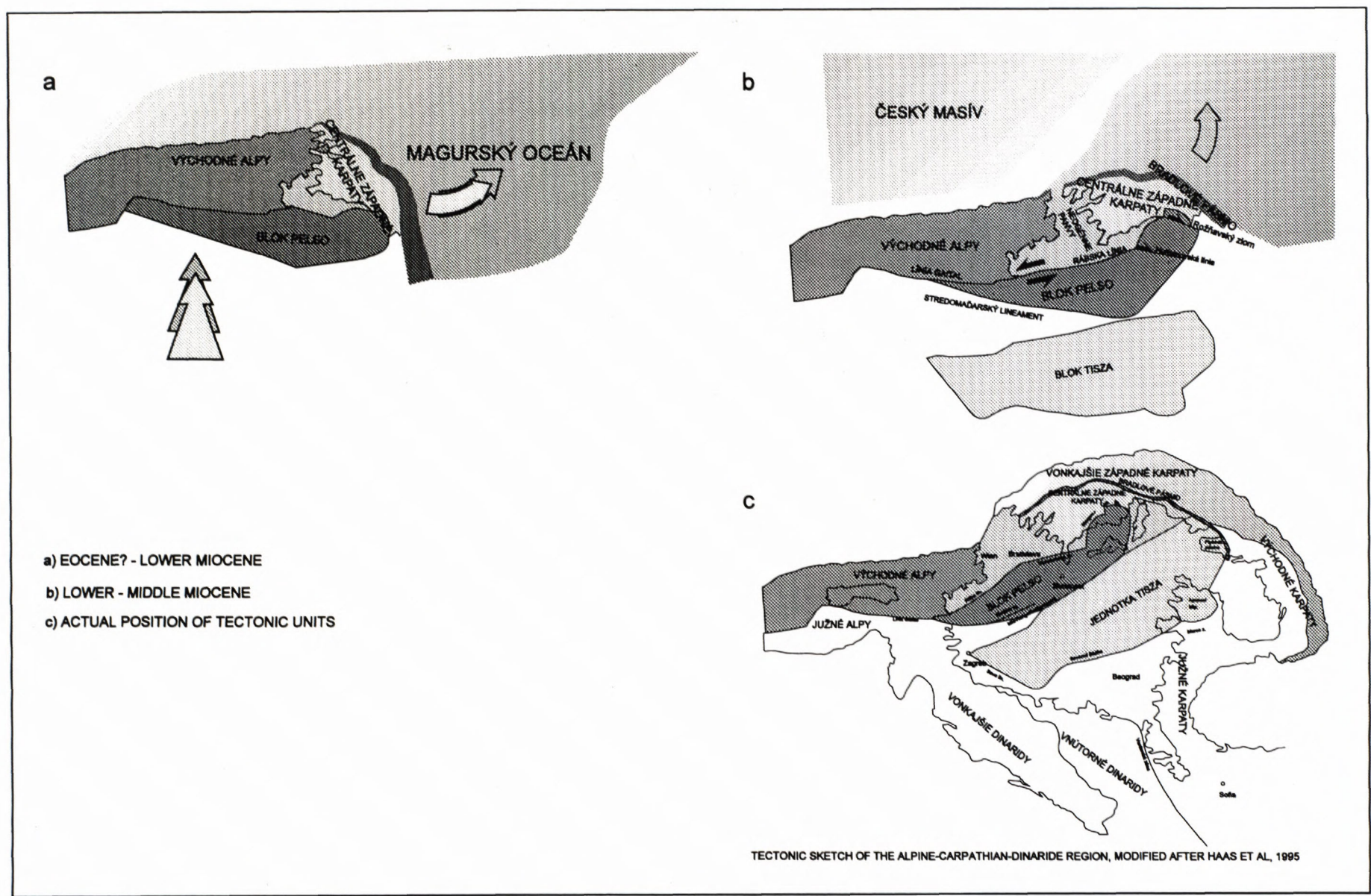


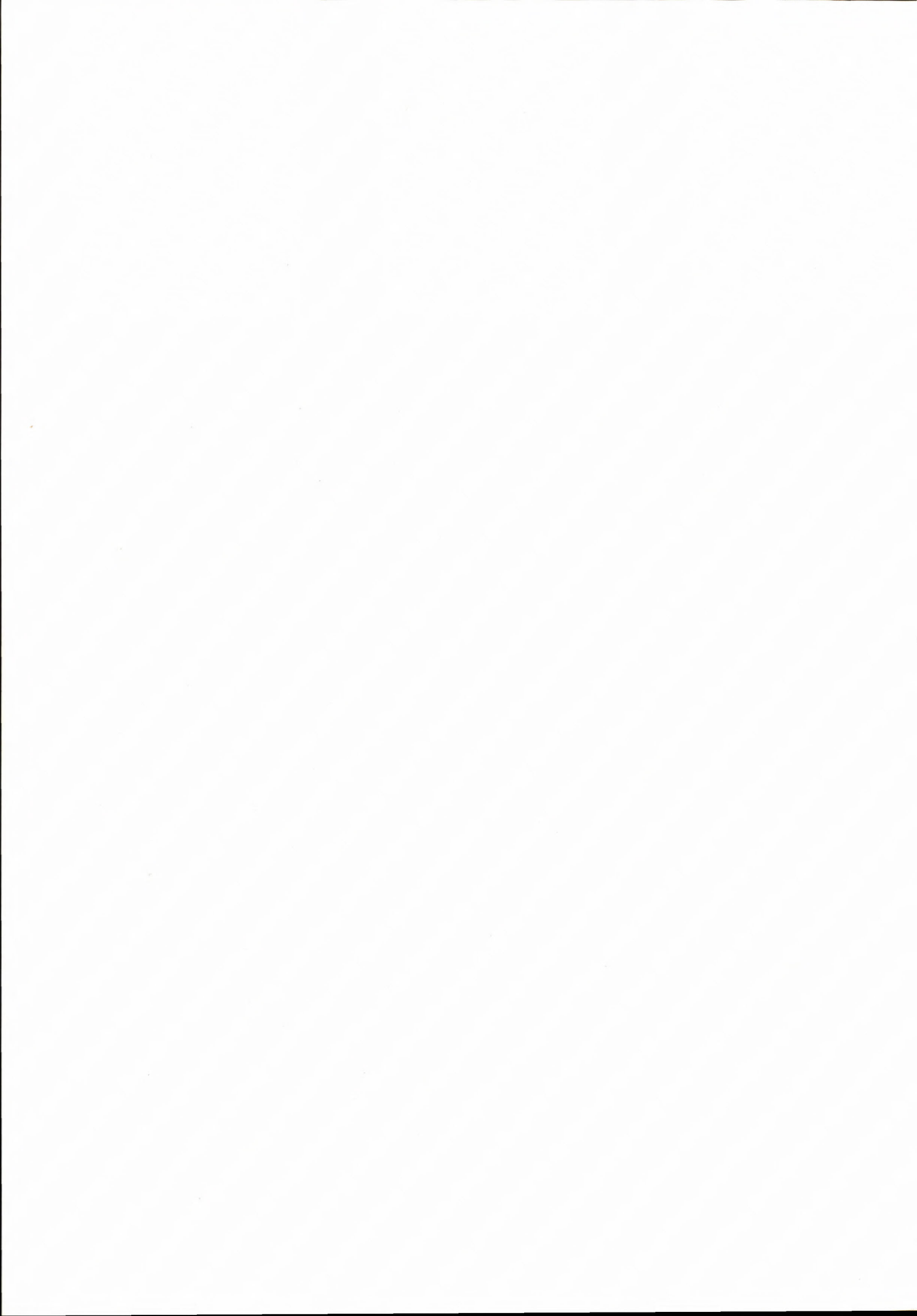
Fig. 7 A model of tertiary development of the Alpine-Carpathian-Pannonian region

along its western margin with the margin of the European platform at the end of Oligocene and during Lower Miocene (Fig. 7). The area of collision shifted gradually eastwards. In structural terms, the deformation process is expressed by gradual transition from compressional to transpressional regime.

The fact that the intensity of compression gradually decreased is vividly demonstrated by overall Post-Oligocene shortening of the Romanian part of the Flysch belt reduced between Badenian and Sarmatian by approximately 108 km, as compared to the reduction between Pliocene and Quaternary, which reached only 22 km (ROURE et al. 1993). In the Polish and Ukrainian parts the compressional events were terminated at the end of Sarmatian.

Literature

- ALEXANDROWSKI, P. 1989: Structural geology of the Magura nappe in the Mt. Babia góra region, western outer Carpathians. *Stud. Geol. Pol.*, 96, 7-134.
- ANDRUSOV D. 1927: Sur les inflexions de la zone Klippes internes entre la vallée de la Kysuca et de la vallée de l'Orava en Slovaquie. *Věst. st. geol. úst. Roč. 2* (č. 4-6). Praha. 1-12.
- ANDRUSOV D. 1938: Étude géologique de la zone des klippes internes des Carpathes occidentales. Illieme part. *Rozpr. St. geol. úst. V9*. Praha. 1-135.
- ANDRUSOV D. 1974: The Pieniny Klippen Belt. Tectonic of the Carpathian Balkan Regions (Edit: M. MAHEL) GUDŠ, Bratislava, 174-158.
- ANDRUSOV D. & SCHEIBNER E. 1960: Outline of the present state of knowledge about of the Klippen belt between R. Vlára and T. Tvrdošín. *Geol. Sborn. 11* (2). Bratislava. 239-279.
- ANGELIER J. 1994: Fault slip analysis and paleostress reconstruction. *Continental deformation*. (Edit: Hancock P.L.) Pergamon Press, 53-101.
- BIRKENMAJER K. 1986: Stages of structural evolution of the Pieniny Klippen Belt, carpathians. *Studia geol. Polonica*, 88, 7-32
- FODOR, L. 1995: From transpression to transtension: Oligocene - Miocene structural evolution of Viena basin and East Alpine - Western Carpathian junction. *Tectonophysics*, 242, 151 - 182.
- HASS J., KOVÁCS L., KRYSZYN L. & LEIN R. 1995: Significance of Late Permian - Triassic facies zones in terrane reconstructions in the Alpine - North Pannonian domain. *Tectonophysics*, 242, 19-40.
- HROUDA F., ONDRA P. & HANÁK J. 1992: Petrofyzikální korelace souvrství paleogenního a křídového flyše vnějších Karpát a vnitrokarpatického paleogénu. Manuscript. *Geofyzika*, s. p., Brno, 52.
- HROUDA F. 1993a: Magnetická anizotropie a duktilní deformace pískovců bradlového pásma (Hlbinná stavba a geodynamický model Západných Karpát - Geofyzika, varínsky úsek bradlového pásma. Manuscript, *Geofyzika s.p.*, Brno, 47.
- HROUDA F. 1993b: Magnetická anizotropie a duktilní deformace pískovců bradlového pásma (Hlbinná stavba a geodynamický model Západných Karpát - Geofyzika, varínsky úsek bradlového pásma. Manuscript, *Geofyzika s. p.*, Brno, 36.
- JIRÍČEK R. 1979: Structural evolution of the carpathian arc during the Oligocene and Neogene. (In MAHEL M ed.) *Tektonické profily Západných Karpát*. GUDŠ Bratislava, 205-215
- KOVÁČ M., KRÁL J., MÁRTON E., PLAŠIENKA D. & UHER P. 1994: Alpine uplift history of the central Western Carpathians: geochronological, paleomagnetic sedimentary and structural data. *Geologica Carpathica*, 45, 2, 83 - 96.
- KOVÁČ M. & TÚNYI I. 1995: Interpretácia paleomagnetických údajov zo západnej časti Centrálnych Západných Karpát. (Eng. abstr.) *Mineralia slov.*, 27, 3, 213-220.
- KOVÁČ M., KOVÁČ P., MARKO F., KAROLI S. & JANOČKO J. (in press): The East Slovakian Basin - a complex back arc basin history. *Tectonophysics*.
- KRS M., MUŠKA P. & PAGÁČ P. 1982: Review paleomagnetic investigations in the West Carpathians of Czechoslovakia. *Geol. Práce, Správy*, 78, 39-58.
- KRS M., KRISOVÁ M., CHVOJKA R. & POTFAJ M. 1991: Paleomagnetic investigation of the flysch belt in the Orava region, Magura unit, Czechoslovak Western Carpathians. *Geol. Práce, Správy*, 92, 135-151.
- MAHEL 1978: Manínska jednotka - čiastkový príkrov skupiny krížňanského príkrovu. (Eng. abstr.) *Mineralia slov.*, 10, 289 - 309.
- MARKO F., FODOR L. & KOVÁČ M. 1991: Miocene strike - slip faulting and block rotation in Brezovské Karpaty Mts. (Western Carpathians). *Mineralia slov.*, 23, 189 - 200.
- OSZCZYPKO N. & SLACZKA A. 1985: An attempt to palinspastic reconstruction of Neogene basins in the Carpathian foredeep. *Ann. Soc. Geol. Pol.*, 55 (1/2), 55 - 75.
- PLAŠIENKA D. 1995: Mesozoic evolution of tatic units in the Malé Karpaty and považský Inovec Mts.: implications for the position of the Klape and related units in Western Slovakia. *Geologica Carpathica*, 46, 2, 101 - 112.
- ROURE F., ROCA E. & SASSI W. 1993: The Neogene evolution of the outer Carpathian flysch units (Poland, Ukraine and Romania): kinematics of a foreland/fold-and-thrust belt system. *Sedimentary Geology*, 86, 177-201
- SCHEIBNER E. 1963: The possibility of paleogeographical reconstructions in the Klippen Belt on the basis of analysis of tectonic building. *Geol. sbor.*, 14, 1, Bratislava.
- SWIDZIŃSKI H. 1962: Sur la forme structurale de la zone des Klippes Pienines des Carpates. *Bull. Acad. polon. sci., sér. sci. géol. et géogr.*, 10, 3, Warszawa.
- TÚNYI I. & KOVÁČ M. 1991: Paleomagnetic investigation of the Neogene sediments from Malé Karpaty Mts. (Lower Miocene of the SW part of the Western Carpathians). *Contr. Geophys. Ins. Slov. Acad. Sci., Veda*, 21, 125-150. (Bratislava).



Contrasting styles of Alpine deformations at the eastern part of the Veporicum and Gemericum units, Western Carpathians

STANISLAV JACKO¹, TIBOR SASVÁRI¹, MICHAL ZACHAROV¹, ROBERT SCHMIDT¹ and JOZEF VOZÁR²

¹Department of Geology and Mineralogy Faculty of Mining, Ecology, Control and Geotechnologies (B.E.R.G), Technical University, Park J. A. Komenského 15, 043 84 Košice, Slovakia

²Geological Survey of Slovak Republic, Mlynská dolina 1, 817 04 Bratislava, Slovakia

Abstract: Contrasting styles of Alpine deformations at the eastern margin of the Western Carpathian Internides are the result of a poly-stage process comprising progressive modification of the deformation regime, from thrusting to wrenching, and corresponding downward reworking of pre - Upper Carboniferous basement. The Alpine reworking of the Veporic basement complexes has been significantly influenced by a flat shear zone located at the base of the Late Variscan nappe pile.

AD₁ deformation stage is related to the development of recumbent folds of E - W axial direction and to pre - Senonian top - to - the N - NNE nappe stacking of the Choč and Silica nappes carrying, in the last case, the Meliata Unit slices at the base. The expressive NW - SE lithostratigraphic zonation of the area marked by regionally penetrative AF₂ folds development and corresponding south-westerly dipping reverse fault shear zones, have been formed during subsequent AD₂ deformation stage.

Local AD₃ fault/fold structures have opened AD₂ shear planes for either hydrothermal vein mineralisation or for a local thermal ascent in the Veporic Unit. NW - SE trending sinistral strike - slip zones of the AD₄ stage have been most probably created due to the eastward escape of the Western Carpathians from the Eastern Alps.

Introduction

The boundary between the Gemericum and Veporicum units belongs to the most important structures of the Alpine convergence within the Western Carpathian Internides. Its territory, known for decades as the Margecany - Lubeník line (scar, fan, etc.), was regarded to be both a remnant root zone and a homeland area for the Choč nappe (ANDRUSOV 1968, BIELY & FUSAN, 1967, MAHEL, 1967, 1986) and/or for the Silica nappe (ANDRUSOV, 1975, KOZUR & MOCK, 1973), respectively.

In a wider area of the eastern, i.e. Margecany part of this collisional structure, not only cover and crystalline sequences of the Gemericum, Veporicum and Tatricum units, but also nearly complete profiles of the Western Carpathians superficial nappes are present. The men-

tioned units stretch NE-SW, parallel to the Margecany shear zone. Structural data reveal a poly-stage evolution of the regional structure evolving from the Late Variscan and Alpine nappe stacking, continuing to pre - Upper Cretaceous fold/upthrust spatial reduction and the Tertiary wrenching, respectively. The aims of this contribution are: (1) to clarify the imprint role of the Late Variscan nappe structures to the formation of the Alpine ones within particular crystalline complexes. (2) to demonstrate the contrasting style of Cretaceous deformations among them, (3) to explain the Tertiary strike-slip phenomena within the structure of the region.

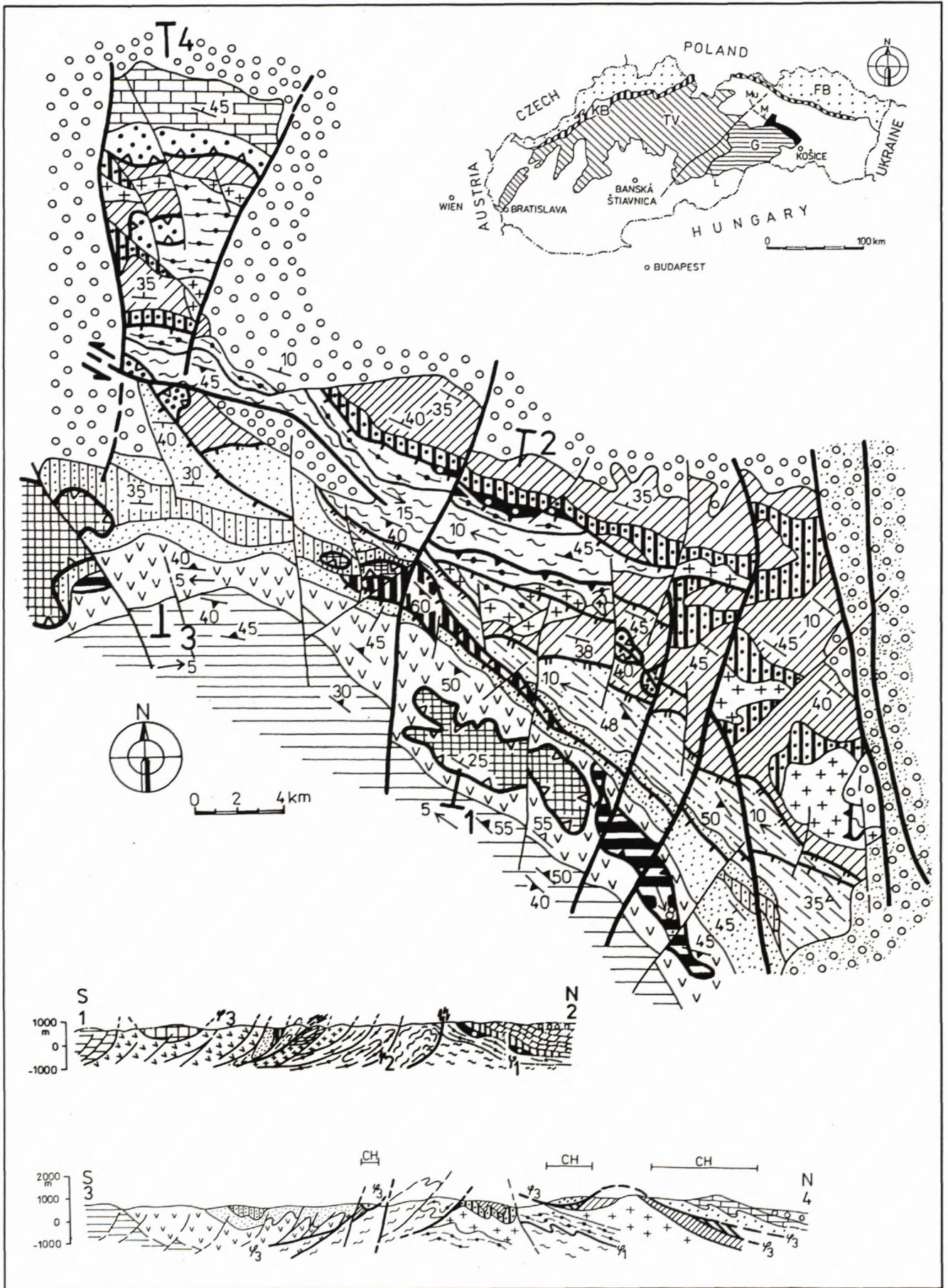
Main lithotectonic units

Six principal pre-Tertiary lithostratigraphical units, differing in metamorphic grade and style of Alpine deformations, form the extremely reduced east-western part of the Western Carpathian Internides (WCI). From top to bottom (or from south to north) these are: the Silica nappe, the Meliata Unit, the Gemericum Unit, the Hronicum Unit, the Veporicum Unit and the Tatricum Unit (Figs. 1a,b,c, 2.). All these units are more or less incorporated into the NW-SE regionally expressive zoning (Fig. 1a), which culminates by the development of directionally related, NE vergent imbricate structures of the Gemericum and the Veporicum contact zone. (Fig. 1c).

The Silica nappe - the highest tectonic unit of the WCI, is composed mainly of shallow water Triassic carbonates forming isolated flatly deposited klippe on both the Meliata and the Gemericum units (KOZUR & MOCK, 1973, MELLO & REICHWALDER, 1979).

Allochthonous - **the Meliata Unit** consists of Triassic to Jurassic LT-HP metamorphosed psammo-pelites, limestones, radiolarites, glaucophanitized basalts and serpentinitised ultramafic rocks (KOZUR & MOCK, l. c., REICHWALDER, 1982). The unit is folded and stretched in SE direction, acquiring south-westerly inclined monoclinical position and finally elongated out along this strike (Fig. 1a).

The Gemericum Unit, composed mainly of slightly metamorphosed Paleozoics volcanosedimentary sequences, is divided into four lithotectonic groups. From the bottom to the top they are: The Gelnica group, the



Rakovec group, the Klatov group, and the Late Paleozoic to Early Triassic successions.

The *Gelnica Group* is represented by a thick volcanogenic flysh formation (SNOPKO & IVANIČKA, 1978, IVANIČKA et al., 1989) of Late Cambrian to Early Devonian age (SNOPKOVÁ & SNOPKO, 1979). Among volcanogenic interlayers the acid to calc-alkaline differentiates predominate. The sequence is regionally deformed by both, tight N-NE vergent folds and successive steeply dipping axial plane reverse faults.

The *Rakovec Group*, overlaying the northern part of the *Gelnica group*, has the same structural pattern as the former. It consists mainly of metabasalts, their volcanoclastics and phyllite intercalations. This ill-dated sequence is probably of Middle Devonian to Early Carboniferous age (BAJANÍK et al. 1983).

The *Late Paleozoic and Early Triassic successions* form NW-SE stretching syncline at the NE part of the *Gemicum Unit* (Fig.1c). The basal part of this pile consists of *Dobšiná Group*, a Carboniferous suite - starting with flysh sequence containing volcanites and volcanoclastics and continuing with shallow marine carbonate - clastic formations (VOZÁROVÁ in BAJANÍK et al. 1981).

Unconformably deposited Permian suite of the *Krompachy Group* (Fig. 2) comprises continental clastic formations interlayered with rhyolite dacite volcanites and volcanoclastics, capped by clastic - evaporite formation (VOZÁROVÁ & VOZÁR, 1988). The suite transits into *Early Triassic shales*, forming the core of the mentioned syncline.

The *Klatov Group*. This tabular nappe unit (Fig. 2), comprising isoclinally folded gneisses, amphibolites (sporadically interlayered with limestones) and serpen-

tinities, is thrust onto the *Rakovec Group* (ROZLOŽNÍK, 1965, HOVORKA et al., 1984). Presence of clasts of this unit within unconformably overlaid Westphalian conglomerates (VOZÁROVÁ, 1973) reveals the upper displacement limit of the nappe.

The *Hronicum Unit* is represented by its partial, the *Choč nappe* sequence (Figs.1 b,c,2). This north vergent nappe pile, coming most probably from homeland area between the *Gemicum* and *Veporicum* units (ANDRUŠOV 1968, BIELY & FUSÁN, 1967, MAHEL, 1967, 1986), comprises Late Paleozoic clastic formations and Triassic, mostly carbonate successions. Within the area of outcrop of the *Veporicum Unit* only the first ones are preserved.

The *Veporicum Unit*, exemplified by its *Čierna hora Mts.* segment, consists of crystalline basement and Late Paleozoic to Mesozoic cover formations. The crystalline basement is made of three lithotectonic complexes. From the bottom to the top these are (Figs.1 b, c, 2), the *Lodina Complex*, the *Miklušovce Complex* and the *Bujanova Complex* (JACKO, 1985). The first one is composed of strongly diaphoritised gneisses, micaschists and tiny intrafolial amphibolite bodies, the *Miklušovce Complex* is formed by migmatites and intrafolial aplitic granites and the *Bujanova Complex* consists of gneisses, migmatites, amphibolites and Variscan granodiorites.

The cover sequence of the unit starts with Late Carboniferous and Permian clastic formations, comprising rhyolitic volcanics within the latter. Triassic to Late Jurassic part of the sequence is mainly composed of carbonates.

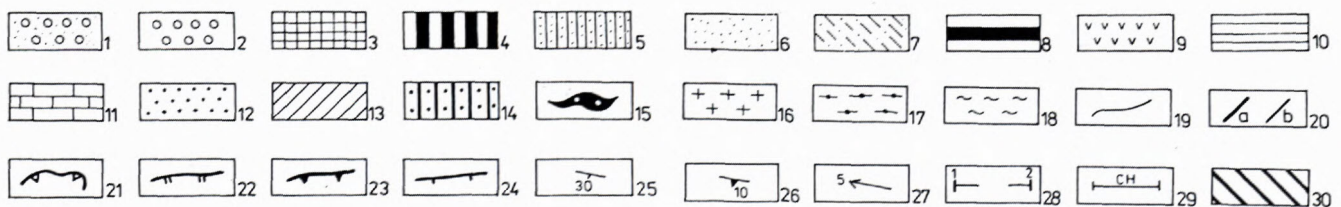


Fig. 1. (a) Position of the studied area in the Western Carpathians. FB - Flysh Belt, KB - Klippen Belt, TV - Tatric and Veporic units, G - Gemicum unit, Mu - Murán fault, L - Lubeník shear zone, M - Margecany shear zone, black strip - Studied area position

Fig.1 (b-c) Geological map and cross sections of the area. 1 - Neogene molasse sediments, 2 - Flysh successions of the Intra Carpathian Paleogene, 3 - Silica nappe limestones, 4 - Sediments and metabasites of the Meliata Unit, 5 - 10 Gemicum Unit, 5 - Early Triassic shales, 6 - Permian greywackes, rhyolitic volcanites and evaporites, 7 - Carboniferous flysch metabasite sequence with conglomerate and carbonate intercalations, 8 - Klatov Group gneisses and amphibolites, 9 - Metabasalts and phyllites of the Rakovec Group, 10 - Sandstones, phyllites and rhyolite volcanites of the Gelnica Group, 11 - 12 - Choč nappe of the Hronicum Unit, 11 - Late Carboniferous shales, sandstones and conglomerates, 12 - Triassic and Jurassic carbonates, 13 - 18 Veporicum and Tatricum units, 13 - Triassic to Late Jurassic cover - prevailing carbonate, successions, 14 - Permian greywackes, shales and rhyolite volcanites, 15 - Late Carboniferous conglomerates and shales, 16 - Veporicum (Bujanova Complex) and Tatric (Branisko Mts.) granodiorites, 17 - migmatites gneisses and amphibolites of the Tatric and Veporic (Bujanová and Miklušovce complexes) units, 18 - diaphoritised gneisses and amphibolites of the Lodina Complex (Veporicum Unit), 19 - Geological boundaries, 20 - Normal faults, a - regionally significant, 21 - Soles of the Alpine nappes (ϕ_3 in cross sections only), 22 - Margecany shear zone, 23 - Alpine reactivated sole of the Late Variscan nappe (ϕ_2 in cross sections only), 24 - others important shear zones, 25 - bedding position, 26 - Alpine schistosity orientation, 27 - Alpine fold axes orientation, 28 - Cross sections lines, 29 - Choč nappe extent (in cross sections only), ϕ_1 - sole of the Late Variscan nappe (in cross sections only).

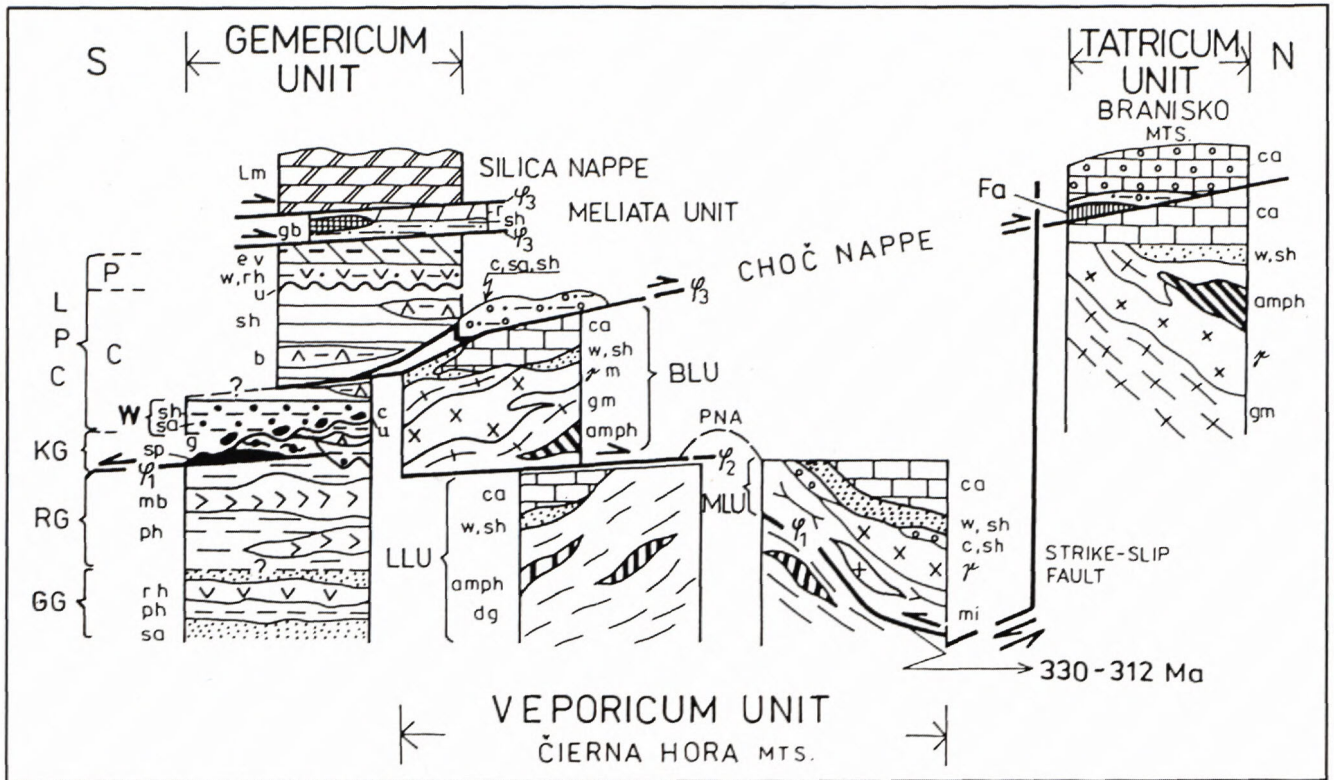


Fig. 2. The Alpine post-nappe position of lithotectonic units at the eastern part of the Western Carpathian Internides. LPC - Late Paleozoic complexes, P - Permian, C - Carboniferous, KG - Klatov Group, RG - Rakovec Group, GG - Gelnica Group, BLU - Bujanová lithotectonic Unit, MLU - Miklušovce lithotectonic Unit, LLU - Lodina lithotectonic Unit, Lm - limestones, r - radiolarites, gb - glaucophanitized basalts and serpentinites, sh - shales, ev - evaporites, w - greywackes, rh - rhyolites and their volcanoclastics, b - basalts, c - conglomerates, sa - sandstones, g - gneisses and amphibolites, sp - serpentinites, mb - metabasalts and their volcanoclastics, ph - phyllites, ca - dolomites and limestones, γ - mylonitised granodiorites, gm - gneisses and migmatites, amph - amphibolites, γ - granodiorites, mi - migmatites, dg - diaphoritised gneisses, Fa - Fatric unit, u - unconformities, PNA - post-nappe anticline, ϕ_3 - soles of Alpine nappes, ϕ_2 - Alpine reactivated sole of the Late Variscan nappe, ϕ_1 - sole of the Late Variscan nappe.

Mesozoic sequences of the **Fatricum Unit** likely underlie buried parts of the Hronicum nappe in the Branisko Mts. (POLÁK, 1987)

The **Tatricum Unit**, forming the Branisko Mts. (Figs. 1 b,c,2), is composed of crystalline basement, corresponding compositionally and in age to the Bujanova Complex of the Veoporikum Unit, and to Permian to Late Jurassic cover formations, comparable to the cover sequence of the Veoporikum Unit.

Pre-Tertiary sequences of the region are in the northern and north-eastern part roofed by flatly deposited flysch formation of the Intra Carpathian Paleogene suite. Their S-SE continuation is covered by Neogene molasse formations (Figs. 1 b,c).

Outline of essential Features of Tectonic development of the region

Principal aspects of structural development of the Gemic part of the area were evaluated by REICH-WALDER & SNOPOKO (in BAJANÍK et al., 1983). They consider

the overall NW-SE zoning of the north-eastern part of the unit to be a result of an extensive and polyphase tangential shortening between the Gemic and Veoporikum units, which had caused both a reduction of the homeland area of the Hronicum Unit and nearly complete obliteration of pre-Alpine structures within the Gemic basement.

JACKO (1979) described typological features of two Variscan and four Alpine deformation stages within the Veoporikum Unit. Their adjusted modification, based on structural, petrological and geochronological data, is outlined in Fig. 3.

According to the mentioned data the crystalline basement of either the Miklušovce and Bujanova complexes, or the Branisko Mts., corresponds to the Upper basement unit of the Western Tatra (FRITZ et al., 1992) and/or to the Upper unit (BEŽÁK, 1994) of the Late Variscan nappe structure of the Western Carpathian Tatra and Veoporikum basement. The underlying Lodina crystalline complex is, in the mentioned sense, complementary to either the Lower basement unit of the Western Tatra

(FRITZ et al., l.c.), or to the Middle unit (BEZÁK, l.c.) of the cited nappe structure.

The Late Variscan nappe cleavage set played a significant role in the formation of Alpine structures within the Veporic crystalline complexes. The same function for the evolution of contrasting styles of Cretaceous deformations within the region have had different mechanical properties of particular lithotectonic suites and their structural position, respectively. Kinematic analysis of the most pronounced shear zones confirms a connection of their prominent, sinistral, strike-slip activity to the AD₄-the post - Paleogene evolution stage of the area. (Fig. 3.).

| Orogenic cycle | phase | Deformational (metamorphic, * plutonic) | | Directional orientation | Metamorphic facies and their extent | Representative parageneses |
|----------------|-------|---|-------|-------------------------|-------------------------------------|---|
| | | stage | style | | | |
| ALPINE | St ? | AD ₄ | | N-S NE-SW NW-SE | Gr. sch. local | Chl + Ser ± Q ± Ep |
| | La? | AD ₃ | | N-S | Gr. sch. local | Bi + Mu + Q ± Ab ± Chl |
| | Me? | AD ₂ | | NW-SE | Gr. sch. regional | Cal + Chl ± Q ± Ser ± Pl (J) Ser + Chl + Q ± Ab ± Il ± m ± Ep ± Zo (C + γ) Chl + Ser + Q ± Ab ± Il ± m ± Ep ± Zo (L + M) |
| | | | | NW-SE | Gr. sch. regional | Chl + Mu + Q ± Pl ± Tour ± Il ± m ± Ep ± Zo (L) |
| | Au? | AD ₁ | | E-W | Gr. sch. regional | Chl + Ser + Q ± Ep ± Zo ± Ab |
| E-W | | | | Gr. sch. local | Chl + Ser + Q ± Ep ± Zo | |
| VARISCAN | S? | VD ₂ | | E-W | Gr. sch. local | Chl + Mu + Q ± Ab ± Ep ± Zo (L + B) |
| | Br. | * | | E-W | Amph. local | Ksp + Mu + Q ± Bi + Pl (B) |
| | | | | E-W | Amph. regional | Pl + Q + Ksp ± Bi ± Mu ± Sill (B) Hrb ± Bi ± Pl ± Q ± Sph (B) Mu + Ksp + Q ± Sill (M) |
| | | | | E-W | Amph. regional | Bi + Pl + Q ± Mu ± Ksp ± Ga ± Il ± m (B + L) Hrb + Pl ± Bi ± Q ± Ga ± Clz ± Sph (B + L) Hrb + Px + Pl ± Srp ± Carb (B) St ± And + Ga + Bi + Mu ± Q ± Pl (L) Bi + Pl + Q ± Ksp ± Ga ± Mu (M) |

Fig. 3. Tectonometamorphic development scheme of the Veporic Unit of the area. 1 - gneisses and amphibolites, 2 - biotite granodiorites, 3 - granites, 4 - Late Variscan nappe sole and its tectonites, 5 - Alpine nappe sole, 6 - Axial plane of the post - nappe recumbent folds, 7 - reverse fault shear zones of the Margecany type, 8 - normal faults and contemporaneous upright folds, 9 - strike - slips and normal faults. St - Styrian, La - Laramian, Me - Mediterranean, Au - Austrian, S - Sudetian, Br - Bretonian, J - Jurassic cover stratates, C - Carboniferous cover stratates, γ - biotite granodiorite of the Bujanova Complex, B - metamorphics of the Bujanova Complex, M - metamorphics of the Miklušovce Complex, L - metamorphics of the Lodina Complex, Gr. sch. - green schist metamorphic facies, Amph. - amphibolite metamorphic facies, Chl. - chlorite, Ser. - sericite, Q - quartz, Ep. - epidote, Zo. - zoisite, Clz - clinozoisite, Cal. - calcite, Ab. - albite, Pl. - plagioclase, Il. - ilmenite, Carb - carbonates, Mu - muscovite, Bi - biotite, Ga - garnet, Sph - sphene, Hrb - hornblende, Px - pyroxenes, Ksp. - kalifeldspar, St - staurolite, And - andalusite, Sill. - sillimanite, Crd - cordierite.

Imprint of the Late Variscan nappe stacking to Alpine structures formation

The Late Variscan nappe emplacement of Miklušovce and Bujanová crystalline complexes onto the Lodina one (Figs. 2,3), dated between 330 and 312 Ma (R.D. DALMAYER, pers. commun, 1993), has caused a significant reworking of their rock successions. The nappe sole of the overthrust pile is subparallel to the cleavage set of the oldest recognizable, the Variscan VF₁ folds (Fig. 3.). Their similar cm - m rootless remnants, belonging to 3C & 4D category of HUDLESTON'S (1973) classification, have generally the southern vergency and they are distingly modified throughout the nappe pile (JACKO et al. 1995).

Significant nappe emplacement reworking of rather homogenous and more rigid migmatites of Miklušovce Complex - forming the base of the Late Variscan nappe, is restricted to their norther flank only. In this zone the moderately N-NE dipping penetrative cleavage set contains tight SSW vergent asymmetric folds with brittle-ductile stretching lineations of micas, quartz and feldspars indicating top- to-the SSW transport direction. The southern part of the suite, namely its basal margin, is strongly overprinted by Alpine structures, indicating a more effective emplacement shearing of the basal edge of the migmatite slice.

A lack of the Miklušovce Complex migmatites at the southern flank of the Veporic basement of the area suggests a partial delamination of the nappe pile during its emplacement. The Bujanova Complex has been, at this part of the basement, prevailingly thrust over the metamorphics of the Lodina Complex. Two regionally significant shear zones have developed as a consequence

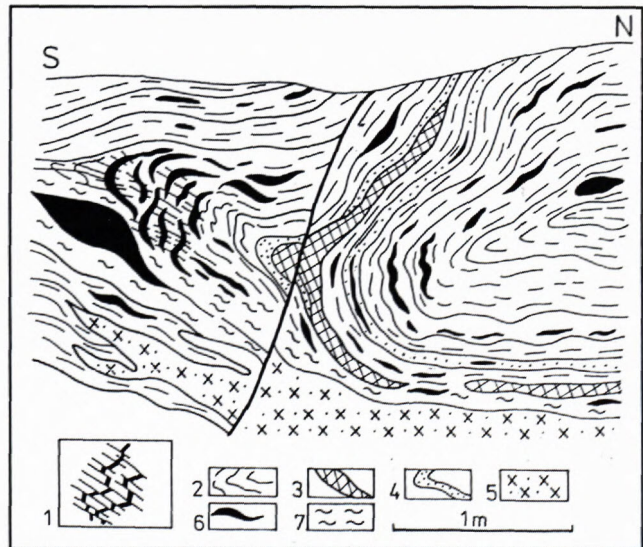


Fig. 4. Brittle - ductile modification of the pre - Carboniferous folds in the Bujanova Complex metamorphites due to the Alpine - nappe delamination of the complex. 1 - detail of the modified fold closure, 2 - biotite gneisses, 3 - amphibolites, 4 - quartz - biotite gneisses, 5 - biotite granodiorites, 6 - quartz segregations, 7 - mylonites.

of the Bujanová Complex emplacement, the basal one and the shear zone, following the synformal closure of the Bujanova metamorphics. Both are several 10 m thick and dip moderately south-westwards (Figs. 1,c).

A strongly foliated, over 100 m thick shear zone, rimming either the northern edge of the Bujanova, or the southern margin of the Miklušovce Complex, follows the top part of subautochthonous diaphoritised gneisses of the Lodina Complex. The zone has typically an extremely high content of intrafolial quartz segregations, deformed by Alpine structures.

The foregoing relationships indicate that the emplacement of the Late Variscan nappe pile within the Veporic basement of the area have caused the most significant reworking, either within the basal zone of the overthrust suite, or in the central part of Bujanova Complex. Both mentioned shear zones are accentuated by involvement of cover strata in them, namely, the typological structures of all Alpine deformation stages of the area are observable in the latter. Following geological and structural criteria show that the discussed shear zones have played a catalytic role for both, the Alpine delamination of the Veporic basement slices, and the penetrative development of the Alpine structures, namely within the Lodina Complex metamorphics.

First Alpine Deformation stage (AD₁)

Structures of this pre-Upper Cretaceous deformation stage are directly related to the Alpine nappe shortening in the region. Striation remnants, preserved on contemporaneous AS₁ cleavage set, indicate top-to-the N - NE movement of the nappes.

AD₁ deformations in the Veporicum Unit

Two closely related tectonometamorphic events of the AD₁ stage are recognizable in the Lodina and Bujanová crystalline complexes and their cover formations (Fig.3). Recumbent isoclinal AF₁ folds of both, parallel and similar geometry with axial plane dipping gently south, to - south-westwards, are typical for the first event (JACKO, 1979).

The AF₁ folds are regularly developed either in tectonites of the Late Variscan nappe emplacement zone of the Lodina basement rocks, or within relatively less competent cover strata. In the mentioned basement shear zone, cm - dm remnants of AF₁ folds are preserved only in quartz medium segregations (Fig. 6). A common occurrence of AF₁ folds of the order of m - 10 m, observed in the Liassic limestones at the south-western



Fig. 5. Recumbent paleo - Alpine AF₁ folds with axial plane cleavage developed in the Liassic cover limestones due to ramp effect of the more rigid Veporicum Unit. (cf. Fig.3. for corresponding deformation stage).

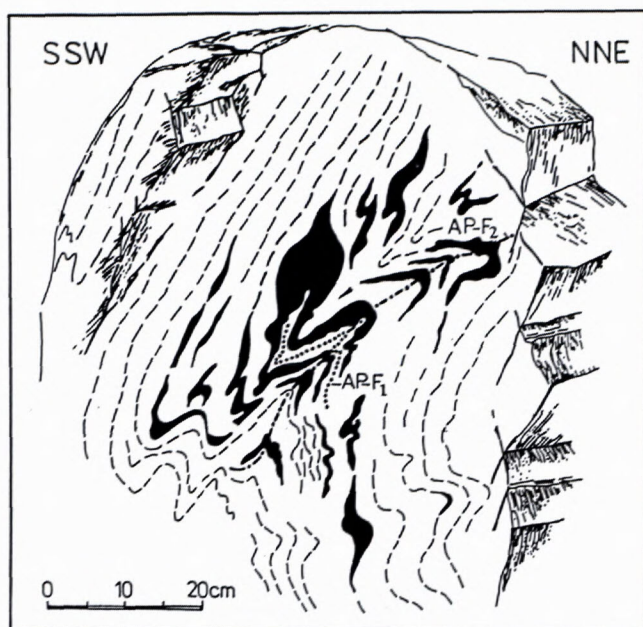


Fig. 6. Refolding of paleo Alpine recumbent AF_1 folds by post-nappe AF_2 folds at quartz segregation lenses of the Lodina Complex diaphoritised metamorphites, APF_1 - axial plane of AF_1 folds, APF_2 axial plane of AF_2 folds.

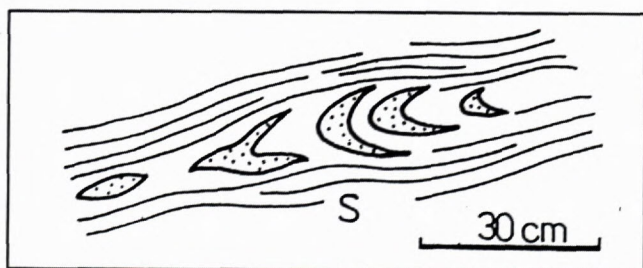


Fig. 7. Rootless remnants of paleo - Alpine AF_1 folds at the reactivated base of the Bujanova Complex fixed by quartz segregations.

margin of the Veporicum Unit (Fig. 7), marks a hinge zone of an asymmetric recumbent fold structure developed in the cover formations due to ramp effect of the Veporicum Unit, during nappe shortening of the area. More rigid overturned segments of Triassic dolomites regionally overlayers Jurassic strata of the zone to stress the regional extent of this structure (Fig. 1c).

Some 100 m thick penetrative zones of AS_1 axial plane cleavage set of AF_1 folds spatially correspond with soles and cleavage position of paleo - Alpine nappe units of the region. They are probably a product of the second tectonometamorphic event of the more or less continuous AD_1 deformation stage. In the basement complexes (except of Miklušovce one) the cover strata (prevailingly Early Triassic quartzites) are incorporated into these zones. No other than successively contemporaneous or superimposed structures have been found in these markers.

Subhorizontally lying AS_1 cleavage plane set, occurring within 450 m of the vertical profile of the Lodina complex diaphoritised gneisses, has been most probably developed due to reverse, (top-to-the northeast) overthrusting of the Bujanova Complex suite along reactivated the Late Variscan sole. According to extent of the superimposed AF_2 folds within tectonics of corresponding shear zone in the central part of the Bujanova Complex metamorphics, the thickness of the zone reached over 100 meters.

A penetrative set of AS_1 cleavage developed in cover formations is rather restricted to either less rigid media of Jurassic limestones (Fig.7) or nearly to the sole of overlying Choč nappe.

AD_1 deformations in the Gemicum Unit

Within the lithotectonic groups of the Gemicum Unit the structures of the AD_1 deformation stage have been nearly completely obliterated by superimposed ones (BAJANIK et al., 1983, MAHEL, 1986). Remnants of AF_1 folds of the same geometry as in the Veporic part of the area, measuring few dm, have been found by JACKO & REICHWALDER (1992, unpubl. data).

A flatly lying cleavage set, corresponding to AS_1 cleavage of the Gemicum Unit, scarcely occurs above the soles of the Silica nappe klippees. A similar, few dm thick, planar set, partly deformed by AF_2 folds, has been observed in serpentinised ultramaphics of the Klatov group (JACKO et al., 1995).

AD_2 deformation stage

Regionally developed NW - SE trending AF_2 folds and subsequently formed monoclinally SW dipping reverse shear zones are typical products of the AD_2 deformation stage. AF_2 folds deform the soles of the Silica and Choč nappes, as well as the structures of the AD_1 deformation stage (JACKO, 1979). Their AS_2 axial plane cleavage set, and corresponding reverse fault shear zones occur nearly throughout the exposed vertical profile of both the Gemic and Veporic units.

Structural reworking of the units was accompanied by a low grade progressive metamorphism of cover formations and by a retrogressive metamorphism in the basement complexes (Fig.3). A successive evolution of two tectonometamorphic events of the AD_2 deformation stage (Fig. 3) is indicated by: (i) - a progressive flattening and shearing of AF_2 folds towards and inside shear zones, (ii) - absence of corresponding mineral parageneses of the second tectonometamorphic event in folded domains, located besides shear zones. The fact that the Middle Eocene conglomerates of the overlying Intra Carpathian Paleogene contain the tectonites of the reverse shear zones of both, the basement and cover formations, confirms that the upper limit of the last event predates the Paleogene.

AD₂ in Veporicum Unit

The intensity of the first tectonometamorphic event of the AD₂ deformation stage was heterogenous throughout the unit. It was controlled mainly by the rock mechanics, including the distribution of earlier tectonic zones within the basement suites. The AF₂ folds are regularly developed in the cover formations, except of more rigid Triassic dolomites. These occur as remnants in the phyllonite zone at the base of Miklušovce and Bujanova basement complexes, as well as in the central tectonite zone of the latter. Diaphthorised gneisses of the underlying Lodina complex are nearly penetratively refolded by AF₂ folds throughout the exposed profile (JACKO, 1979).

Overall geometric pattern and style of the AF₂ folds, fixed by representative rock suites of the unit (Fig.8a) indicates a significant flattening of originally open, upright and mostly parallel AF₂ folds. Majority of AF₂ folds in the Veporicum Unit are close to tight folds with significant thinning of the fold limbs and distinct AS₂ cleavage set, inclined monoclinaly (at 40° - 60°) to SW.

Distinct modification and shearing of AF₂ folds reflect a progressive shortening of the Veporicum Unit during a subsequent, the second tectonometamorphic event of the AD₂ deformation stage. Modified AF₂ folds have stronger NE vergency than original open ones, but their shallow hinge line dips (i.e. 5°-10° either to NW or to SE, cf. Fig. 1b.) are identical in both mentioned evolution types.

According to the distribution of typological parameters of AF₂ folds in ZAGORCEV'S (1993) diagram (Fig.8a) the dominant part of AF₂ folds of the Veporicum Unit belong to 2-nd class and/or to 1C and 3A subclasses, respectively. The layer parallel (or oblique) compression is regarded to be the dominant folding mechanism for the development of such fold types (l.c.), which agrees with the orientation of striation observed on folded bedding planes in the Jurassic limestones. Open to close folds with changing layer morphology, projected around 1A₂ subclass line (Fig. 8a), most probably reflect a change of the strain field during repeated reactivation of the shear zones.

A continuous shortening of the area, which took place probably in the same stress field orientation, led to delamination of the Veporicum Unit according to NW-SE trending, moderately (45°-65°) SW dipping reverse fault zones (Fig.1b,c). The shear zones either reactivated the lithostratigraphical formation boundaries, or the early developed tectonite zones in the basement of the unit and they progressively climbed into the cover strata in the latter case. The most pronounced of them, the Margecany shear zone, strongly reactivates the boundary between the Gemericum and Veporicum units. It has no earlier kinematic indicators than the top-to-northeast motion striations (JACKO, 1979), which are consistent, as regards the sense of their movement, with the mica fish orientation (LISTER & SNOKE, 1984) in the biotite granodiorite S-C mylonites of the Bujanova basement complex.

The same sense of movement is indicated by displacement of the reverse fault sets in the diaphthorised gneisses of the Lodina complex (Fig.10). The displace-

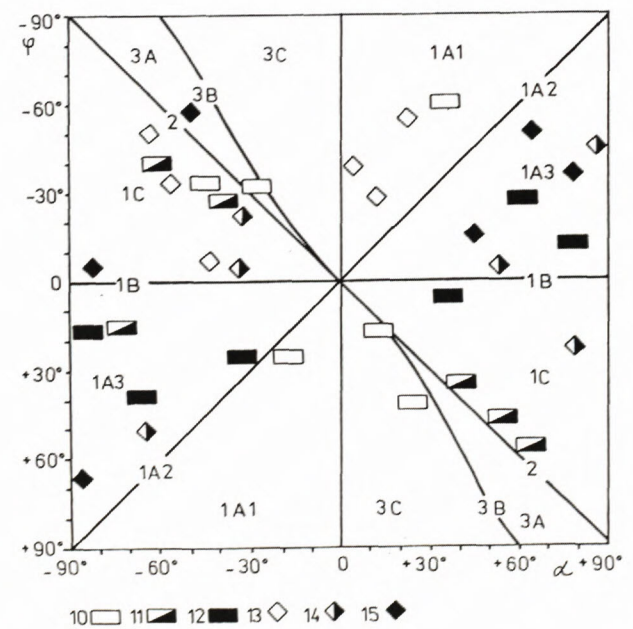
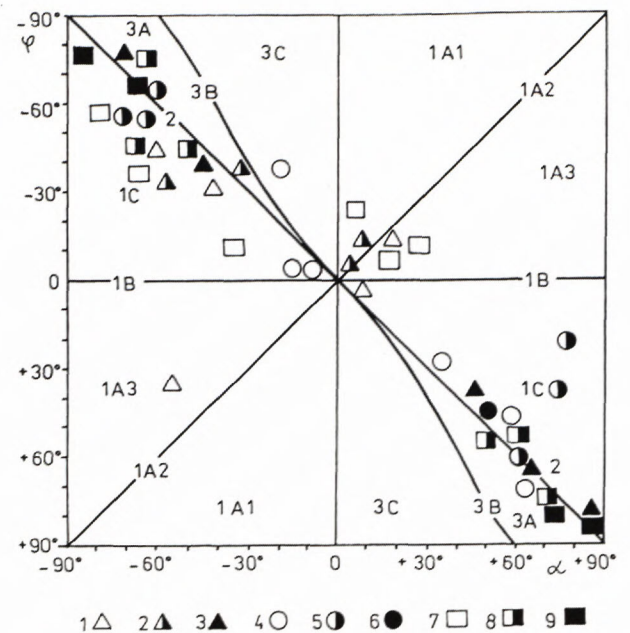


Fig. 8.a,b. Geometrical relationships of the Alpine AF₂ folds (cf. Fig.3 for the complementary deformation stage) within competent layers of the Veporicum and Gemericum units, as results from ZAGORCEV'S (1993) modified diagram of HUDLESTON'S (1973) and RAMSAY'S (1967) classification. φ - dip isogon angle, α -dip angle, empty symbols - open folds, half filled symbols - close folds, full filled symbols - tight folds, Fig. 8a., modification trend of AF₂ folds of the Veporicum Unit: 1-3, in the Lodina complex diaphthorised gneisses, 4 - 6, in the Early Triassic quartzites, 7-9, in the Jurassic limestones. Fig. 8 b., modification trend of AF₂ folds of the Gemericum Unit: 10-12, in the Carboniferous limestones, 13 - 15 in the Carboniferous basalts and their volcanoclastics.

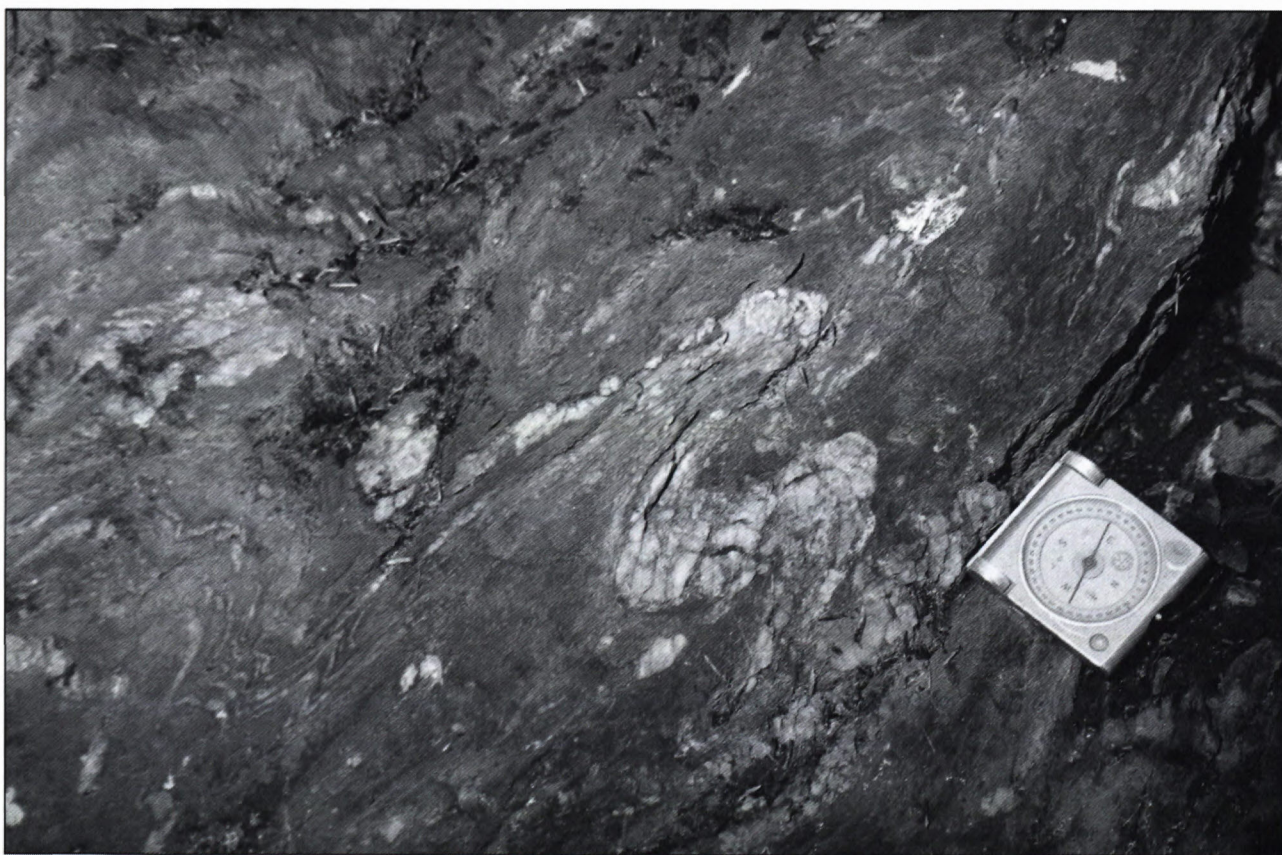


Fig. 9. Monoclinally south-westerly dipping cleavage set developed due to shearing of AF_2 folds in the Gemic Carboniferous basalt volcanoclastics nearby the Margecany shear zone.

ment in the discussed shear zones has been accompanied by synchronous growth of lower greenschist facies metamorphic assemblages (Fig.3).

AD₂ in Gemicum Unit

Due to extensive shearing in the repeatedly activated AS₂ cleavage planes the AF₂ folds irregularly occur only in more competent layers of both the Gelnica group and the Carboniferous formations of the unit. To compare these folds with folds of the same deformation stage in the Veporicum Unit, the AF₂ folds of the adjacent Gemicum Carboniferous formations have been plotted in the ZAGORCEV'S (1993) diagram (Fig.8b). Except for clear common features with a general modification trend of the AF₂ folds in the Veporicum Unit (Fig. 8a), much more evaluated folds belong to 1A₁, 1A₂ and 1A₃ fold types fields i.e. into the field of supratenuous 1A subclass of RAMSAY'S (1967) classification. Relatively great number of these folds with strongly convergent isogons and thickened limbs at the NE margin of the Gemicum Unit, were probably produced during superimposed deformations in this strongly mobile contact zone of two rheologically contrasting units.

For analogous reasons as in the Veporicum Unit the extensive shearing of AF₂ folds in their AS₂ axial plane cleavage set (Figs. 9a,b), and the development of corresponding reverse fault shear zones are the result of the second tectonometamorphic event of the AD₂ deformation stage. Generally, both structures are moderately inclined to SW ward (Figs. 1b,c) and they are an original cause of monoclinaly imbricated structure of the contact zone of the Gemicum and Veporicum units (JACKO, 1979).

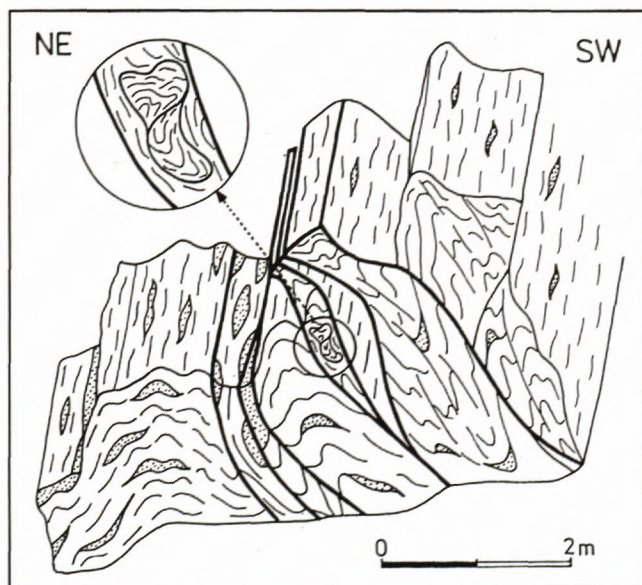


Fig. 10. Axial plane reverse fault shearing of AF₂ folds and contemporaneous mullions development within the Lodina Complex diaphoritised gneisses. Lenses of segregation quartz are dotted.

AD deformation stage

Locally developed N - S trending fault/AF₃ fold structures of this deformation stage (Fig. 3) are clearly superimposed on structures of previous deformation stages (JACKO, 1979). Very scarce AF₃ folds of metric order, which originally accompanied normal fault zone, occur only in the cover formations of the Veporicum Unit. These open, upright folds, slightly similar in geometry, have well developed AS₃ axial plane crenulation cleavage, subparallel to corresponding fault zone. Fold axis and parallel crenulation cleavage dip gently (5°-10°) to S - SSW.

AD₄ deformation stage

This stage comprises an expressive, post - Paleogene wrenching of the previous structure of the area. Dominant strike-slip zones within all the units of the region are several 10 m thick, they have NW-SE orientation and moderate to steep dip to SW (Figs. 1b,c, 11,12). Three significant - sinistral strike-slip zones developed either within the Veporicum Unit, or at its south-western boundary with the Gemicum Unit (Fig.11). Brittle deformations in all of them reactivated tectonic zones produced during earlier deformation stages. The overall paleostress field, determined from the fault slip data analysis, reveals a subhorizontal, roughly E-W oriented compression for these wrenching deformations (Fig.11).

Both the fault slip data (Figs. 12B, D, E, F) and the average stress ratio of about 0,5, confirm the subhorizontal motion component (GUIRAUD et al. 1989) within the most pronounced, the Margecany strike - slip zone. The stress ratio (above 0,5) (Figs. 12J, K, L), calculated for the strike - slip zone running along NE boundary of the Miklušovce basement rocks with cover formations (Fig.11), indicates prevailingly inclined normal faulting in the zone (Fig.12 M). An analogous movement pattern has been obtained from corresponding data (Fig.12 G,H,I) for the central strike-slip zone of the Veporicum Unit (Fig.11), which reactivated the phyllonite zone at the to boundary of the Bujanova and the Lodina crystalline complexes, respectively.

Steeply SW dipping normal fault zone, developed at the NW edge of the unit, (Figs.11,12 A) along which the Intra Carpathian Paleogene strata submerged into the pre-Tertiary complexes, reveal a composite movement pattern in the strike-slip zones of the area. GRECULA et al. (1990) described dextral shearing in directionally analogous shear zones in the Gemicum Unit.

Discussion and conclusions

Alpine deformations of the studied area have developed in a poly-stage process, influenced by either rock formations anisotropy, or by a change of bulk strain regime during its evolution.

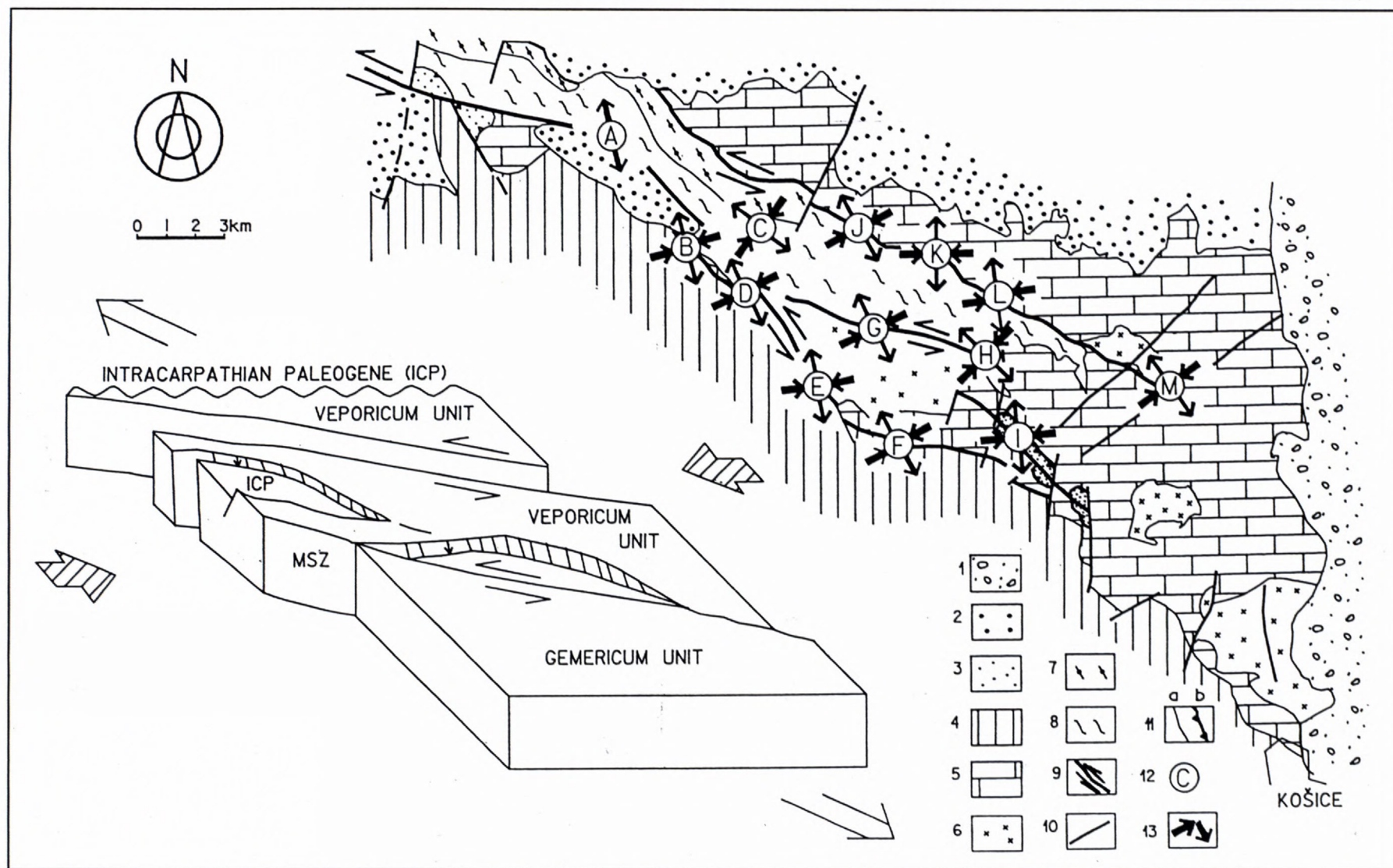


Fig. 11. Map scheme and the kinematic model of dominant post-Paleogene strike - slip zones in the Veporicum Unit of the area.

1 - Neogene molasse sediments, 2 - Intra Carpathian Paleogene flysch, 3 - Late Carboniferous of the Choč nappe, 4 - the Gemericum Unit (undivided), 5 - Veporic cover formations, 6 - Bujanova Complex (undivided), 7 - Miklušovce Complex, 8 - Lodina Complex, 9 - strike-slip zones, 10 - normal faults, 11 a - geological boundaries, 11b - sole of the Choč nappe, 12 - Location of paleostress analysed strike - slip zones sites plotted in Fig. 12.

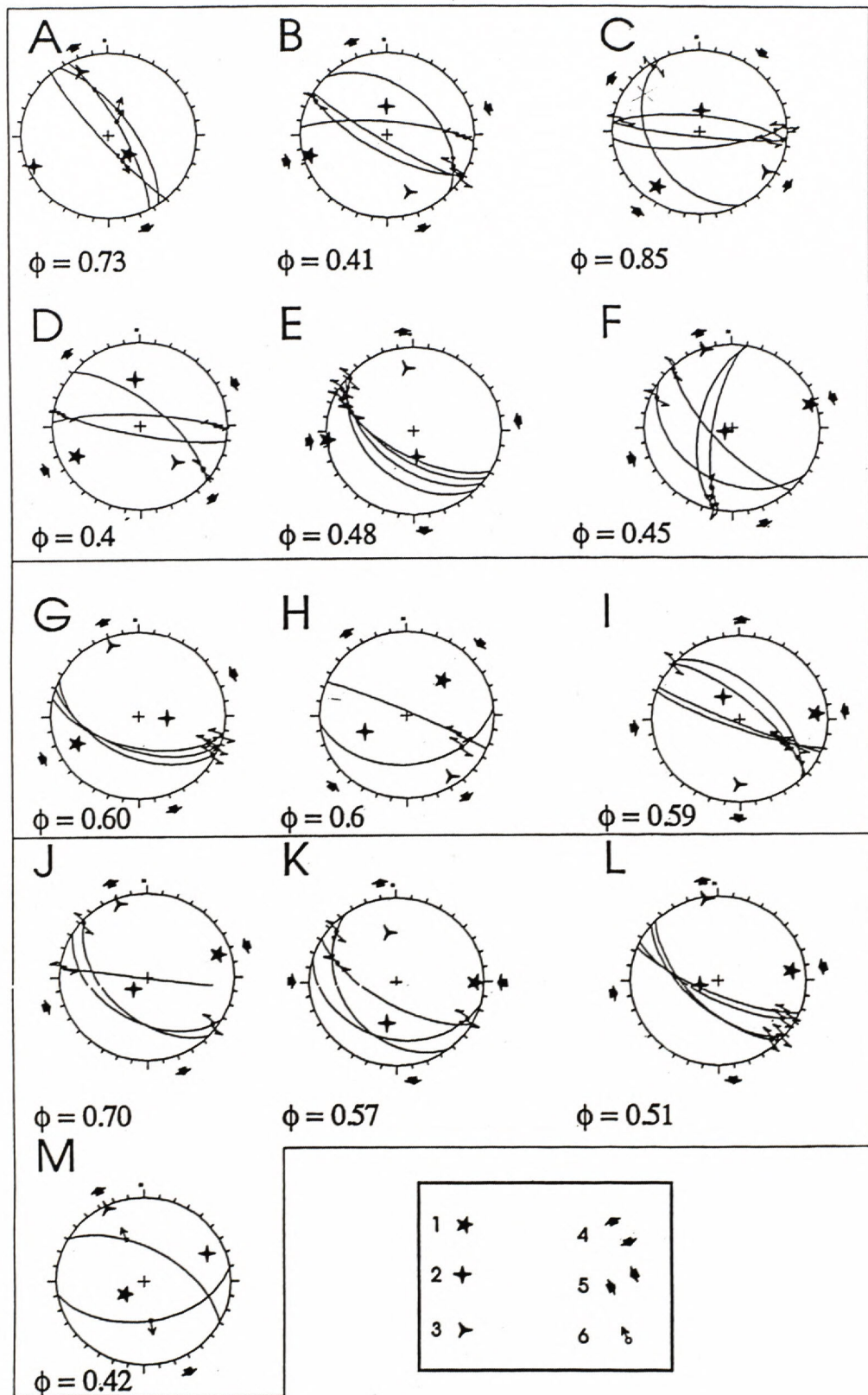


Fig. 12. Stereogram of paleostress analyse sites of strike - slip zones drawn in Fig. 11. 1 - σ_1 (maximum compressive stress), 2 - σ_2 , 3 - σ_3 , 4 - direction of extension, 5 - direction of compression, 6 - direction and sense of slip, ϕ - stress ratio.

Tectonite zones of the Late Variscan nappe stacking developed at the base and within the nappe slices of the Veporicum Unit crystalline complexes have played a catalytic role in the Alpine structural reworking of the basement complexes of this unit. Remnants of structural and mineral assemblages of AD₁ - AD₄ deformation stages occur in all these zones (Figs.3, 4, 5). The Late Variscan top - to - the SE nappe stacking of the Western Carpathian basement, recognized by FRITZ et al., (1992) in the Western Tatra basement has been confirmed to have occurred in the Veporicum Unit (geochronological dating 330-312 Ma, DALLMEYER, pers. commun., 1993) and by occurrence of clasts from the diaphthorised gneisses of Lodina Complex in the Upper Carboniferous cover conglomerates (KORIKOVSKIJ et al., 1989).

The pre - Senonian AD₁ shortening of the area is characterised by formation of AF₁ recumbent folds, limited to either the less competent cover strata at the SW edge of the more rigid Veporicum Unit, or to analogous media at the top of Lodina basement complex and to the Gelnica Group of the Gemicum Unit, respectively. A successive top - to - the N - NNE emplacement of the Alpine nappes led to the closure of the Choč nappe homeland area and to thrusting of the nappe over a frontal Veporic ramp northwards, over the Tatric area of the WCI (Fig.2). In the Veporic basement this nappe shortening caused a reverse-thrusting of two delaminated slices of Bujanova basement complex onto the Lodina complex, along reactivated Late Variscan shear zones (Figs.1b,c, 2). The remnants of AF₁ axial plane cleavage, occurring in over 400 m of Lodina Complex diaphthorised gneisses, indicate an extensive shearing of this basal, subachtonous (?) sequence of the Veporic crystalline complexes of the region.

Corresponding cleavage sets in the Gemicum Unit occur scarcely in more competent strata of both the Silica nappe klippe and the Late Variscan Klatov Group nappe pile (JACKO, et al., 1995). Analogous, i.e. flat position of about 6 km thick, strongly reflective zone, is also seen in the recently shot deep seismic profile G (VOZÁR et al., 1995), which intersects the area nearby the lines 3 - 4 of the cross - section (Fig.3c). This highly sheared northern Gemic zone, followed within of the depth interval of 6 - 10 km, is regarded to be the root zone of both, the Križna and the Choč superficial nappes (l.c.).

The AF₂ folds and complementary reverse fault shear zones control the main features of the recent NW-SE lithostratigraphic zoning of the area (Fig.1b,c). The AF₂ folds are penetratively developed throughout the lowest unit of the Veporic basement, i.e. throughout the Lodina diaphthoritic gneisses. Axes of the AF₂ folds, superimposed on the earlier structures, make an angle of about 60° with the Alpine nappe emplacement striations, which are preferred on corresponding cleavage set. These data, as well as unlike mineral assemblages of both the AD₁ and AD₂ stages (Fig.3) either indicate a change in bulk strain orientation, or slightly different low temperature metamorphic conditions during the AD₂ deformation stage.

A close spatial connection between flattening intensity of AF₂ folds and reverse fault shear zones suggests a successive development of the latter. An extensive brittle- ductile shearing in the these shear zones, which reactivate the rheological boundaries of both the Gemicum and Veporicum units, transposed the majority of lithostratigraphical units into monoclinical, south-west dipping position (Fig.1c). The Meliata Unit slice in the core of the Northern Gemic syncline is strongly stretched and finally sheared in NE direction, along one of these structures (Fig.1b,c). According to recent geochronological investigations carried out in the central part of the Veporicum Unit of the WCI, the discussed zones have formed between 85 - 86 Ma (Ar-Ar, DALLMEYER et al., 1993), which corresponds with occurrence of their tectonics in the Intra-Carpathian Paleogene conglomerates in the area.

Subsequently developed AD₃ structures have opened the shearing planes of the AD₂ stage for both, hydrothermal vein mineralisation in the Gemic and Veporic units, and for the local post - kinematic thermal ascent (Fig.3) in the latter unit (JACKO, 1979, 1983, ROZLOŽNÍK, 1990).

Sinistral AD₄ strike - slip zones, following the most weakened zones between and inside the units of the area (Figs. 1b, 11), are directionally, as well as in terms of paleostress orientation, compatible with the Badenian - Sarmatian widening of the Eastern Slovakian molasse basin (KALIČIAK et al., 1991). We suggest that their origin was primarily caused by the eastward escape of the Western Carpathians from the Alps (NEUBAUER & GENSER, 1990, RATSCHBACHER et al., 1991). The Margecany strike - slip zone, detected in the above mentioned deep seismic profile G₁ to dip at an angle of 45° down to the depth of 7 kms, continues as a flat tectonic zone below this depth horizon, at an angle of approximately 20° - 25° to a depth of 25 km (VOZÁR et al. 1995).

References

- ANDRUSOV D., 1968: Grundriss der Tektonik der Nördlichen Karpaten. SAV, Bratislava, 188 p.
- ANDRUSOV D., 1975: Aperçu bref du bati des Carpathes occidentales. X.th Congress of the Carpathian - Balkan geological association, 95-108.
- BAJANÍK S., VOZÁROVA A. & REICHWALDER P., 1981: Litostratigrafická klasifikácia rakoveckej skupiny a mladšieho paleozoika v Spišsko-gemerskom rudohorí. Geologické práce, Správy 75, 19-53. (Engl. res.)
- BAJANÍK S., HANZEL V., IVANIČKA J., MELLO J., PRISTAŠ J., REICHWALDER P., SNOPKO L., VOZÁR J. & VOZÁROVA A., 1983: Vysvetlivky ku geologickej mape Slovenského rudohoria, východná časť. GÚDŠ, Bratislava, 223 p. (Engl. res.)
- BEZÁK V., 1994: Návrh nového členenia krystalinika Západných Karpát na základe rekonštrukcie hercynskej tektonickej stavby. Miner. slov., 26, 1, 1-6. (Engl. res.)
- BIELY A. & FUSAN O., 1967: Zum Problem der Würfelzonen der subtatrischen Decken. Geol. Práce, Správy 42, 51-64.
- DALLMEYER R. D., NEUBAUER F. & PUTIŠ M., 1993: ⁴⁰AR/³⁹AR mineral age controls for the Pre-Alpine an Alpine tectonic evolution of nappe complexes in the West-

- ern Carpathians. In: P. PITOŇÁK & J. SPIŠIAK (Editors), Pre-Alpine Events in the Western Carpathians Realm. PAEWCR Conf., Stará Lesná, Excursion Guide: 12-20.
- FRITZ H., NEUBAUER F., JANAK M. & PUTIŠ M., 1992: Variscan midcrustal thrusting in the Carpathians. Part II: Kinematics and fabric evolution of the Western Tatra basement. Abstr. supplement, NO. 2 to TERRA nova, 4, 24 p.
- GRECULA P., NAVESŇÁK D., BARTALSKÝ B., GAZDAČKO L., NÉMETH Z., IŠTVAN J. & VRBATOVÍČ P., 1990: Shear zones and arc structure of Gemerikum, the Western Carpathians. Mineralia slov., 22, 2, 97 - 110.
- GUIRAUD M., LABORDE O. & PHILIP H., 1989: Characterization of various types of deformation and their corresponding deviatoric stress tensors using microfault analysis. Tectonophysics, 170, 289-316.
- HOVORKA D., IVAN P. & SPIŠIAK J., 1984: Nappe with amphibolite facies metamorphites in the Inner Western Carpathians its position, origin and interpretation. Miner. slov., 16,1, 73-86.
- HUDLESTON P. J., 1973: Fold Morphology and some geometrical implications of theories of fold development. Tectonophysics, 16, 1-46.
- IVANIČKA J., SNOPKO L., SNOPKOVÁ P. & VOZÁROVÁ A., 1989: Gelnica group - Lover Unit of Spišsko - gemerské rudohorie Mts. (West Carpathians), Early Paleozoic. Geol. Zborník, Geol. Carpathica, 40, 4, 483-501.
- JACKO S., 1979: Geologický profil pásmom Čiernej hory a jeho styku s gemerikom. In: M. MAHEL (Ed.) Tektonické profily Západných Karpát. 185-192. (Engl. res.)
- JACKO S., 1983: Vplyv geologickeho prostredia na vývoj zrudnenia v pásme Čiernej hory. In: J. Gubač (Ed.) Vplyv geologickeho prostredia na zrudnenie. 125-134. (Engl. res.)
- JACKO S., 1985: Litostratigraficke jednotky kryštalinika Čiernej hory. Geol. Práce, Správy 82, 127 - 133.
- JACKO S., SASVÁRI T., ZACHAROV M. & PUTIŠ M., 1995: Variscan pre-granitoid fold paragenesis of the Western Carpathians. Krystalinikum, 22, 1-11. (In print).
- KALIČIAK M., BAŇACKÝ V., JACKO S., JANOČKO J., KAROLI S., MOLNÁR J., PETRO L., PRIECHODSKÁ Z., SYČEV V., ŠKVARKA L., VOZÁR J., ZLINSKÁ A. & ŽEC B., 1991: Vysvetlivky ku geologickej mape severnej časti Slanských vrchov a Košickej kotliny, GÚDŠ Bratislava, 231 p. (Engl. res.)
- KORIKOVSKIJ S. P., JACKO S. & BORONICHIN V. A., 1989: Alpine anchimetamorphism of Upper Carboniferous sandstones from the sedimentary mantle of the Cierna hora Mts. crystalline complex (Western Carpathians). Geol. Zborník, Geol. Carpathica, 40, 5, 579-598.
- KOZUR H. & MOCK R., 1973: Zum Alter und zur tektonischen Stellung der Meliata - serie des Slovakischen Karstes. Geol. Zborník, Geol. carpathica, 25, 1, 113-143.
- LISTER G. S & SNOKE A.W., 1984: S-C mylonites. Journal of Structural Geology, 6, 617-638.
- MAHEL M., KAMENICKÝ J., FUSAN O. & MATEJKA A., 1967: Regionální geologie CSSR, díl II. Západní Karpáty, sv.1., UUG, Praha, 486 p.
- MAHEL M., 1986: Geologická stavba československých Karpát. Palealpínské jednotky. Veda, SAV, Bratislava, 503 p.
- MELLO J. & REICHWALDER P., 1979: Geologicke profily JV. časťou Spišsko gemerskeho rudohoria a príľahlou časťou Slovenského krasu. In: M. Mahel' (Ed.), Tektonické profily Západných Karpát, 199-202. (Engl. Summ.)
- NEUBAUER F. & GENSER J., 1990: Architektur und Kinematik der Östlichen Zentralalpen - eine Übersicht. Mitt.naturwis. Ver. Steiermark, 120, 203-219.
- POLÁK M., 1987: Litofaciálna charakteristika jury Braniska a zapadnej casti Čiernej hory. Geol. Práce, Správy 87, 7-17.
- RAMSAY J. G., 1967: Folding and Fracturing of Rocks. Mc Graw-Hill, New York, 568 pp.
- RATSCHBACHER, L., FRISCH, W. & LINZER, G., 1991. Lateral extrusion in the Eastern Alps, part 2: structural analysis. Tectonics, 10, 257-271.
- REICHWALDER P., 1982: Structural characteristic of root zones of some nappes in innermost parts of West Carpathians. In: M. Mahel (Editor), Alpine structural elements: Carpathian - Balkan - Caucasus - Pamir orogene zone. Problem Commission Multilateral coop. of Sciences of soc. countries "Geosynclinal process and evolution of Earth crust", 43-56.
- ROZLOŽNÍK L., 1965: Petrografia granitizovaných hornin rakoveckej série v okolí Dobšinej. Zborník geologických vied, rad ZK, 4, 95-144. (German res.)
- ROZLOŽNÍK V., 1990: Strižná zóna gemerika - nositeľka sideritovej formácie: Mineralia slov., 22, 1, 47-54.
- SNOPKO L. & IVANIČKA J., 1978: Uvahy o paleografii v staršom paleozoiku Spišsko-gemerskeho rudohoria. In: J. VOZÁR (Ed.) Paleogeografický vývoj Západných Karpát, 269-279. (Eng. res.)
- SNOPKOVÁ P. & SNOPKO L., 1979: Biostratigrafia gelnickej serie v Spišsko-gemerskom rudohorí na základe palinologických výsledkov. Západne Karpáty, séria Geológia, 5, 57-102.
- VOZÁROVÁ A., 1973: Valúnová analýza mladopaleozoických zlepcov Spišsko-gemerskeho rudohoria. Západne Karpáty, 18, 7-98. (Eng. res.)
- VOZÁROVÁ A. & VOZÁR J., 1988: Late paleozoic in West Carpathians. GÚDŠ, Bratislava, 314 p.
- VOZÁR J., TOMEK C., VOZÁROVÁ A. & DVOŘÁKOVÁ V., 1995: Deep seismic profile G: geological interpretation (Inner Western Carpathians, Slovakia), Contrib. of the 3rd Annual meeting of IGCP Project 356. Plate Tectonic Aspects of Alpine Metallogeny in the Carpatho - Balkan Region, 1-3. (In print).
- ZAGORČEV I. S., 1993: The geometrical classification of folds and distribution of fold types in natural rocks. Journal of Struct. Geology, 15, 3-5, 243-251.

Distributed Parameter Model for the Laugarnes Geothermal Field - SW Iceland

MARIÁN FENDEK

Geological Survey of Slovak Republic, Mlynská dolina 1, 817 04 Bratislava

Abstract: The paper describes distributed parameter model of the Laugarnes geothermal field located inside Reykjavík, in south-western Iceland. The model was conceived after adopting the programme AQUA to process 30 years observation of the reservoir response to production. No cooling was observed in wells during the whole period of production. A good fit was achieved with the model for drawdown. The monthly average production of 16 wells measured between 1961 and 1991 was used to calibrate the model. The obtained reservoir parameters were used to predict the future behaviour of the reservoir at three different constant production rates until the year 2012. A constant decline of the water level and silica content has been observed. Based on the trend of the curve for the measured and calculated drawdown obtained from the distributed groundwater flow model it is quite obvious that with present production no steady-state condition in the reservoir will be reached before 2012.

Key words: Iceland, geothermal field, mathematical modelling, hydraulic parameters, prediction

1. Introduction

Iceland lies astride the N-S running Mid -Atlantic Ridge which spans the entire Atlantic Ocean. The surface expressions of the ridge are the so called neovolcanic zones, divided into several branches. In general, the structure of neovolcanic zone is dominated by fissure swarms and central volcanoes. Most fissure swarms are about 10 km wide and 30-100 km long. The rate of spreading of the divergent plates has averaged 2 cm/year over the last four million years (HAMMONS et al., 1991). The neovolcanic zone is flanked by Quaternary rocks characterised by sequences of subaerial lava flows, intercalated by hyaloclastics and morainic horizons, indicative of glacial conditions. The Quaternary formations are flanked by Tertiary floodbasalts (SAEMUNDSSON, 1978).

The thermal gradient is about 50 °C/km in the Tertiary basalts of Iceland farthest from active volcanic zone. It increases toward the volcanic zone and may be as high as 150° C/km near the edge of the volcanic zone (PÁLMASSON et al., 1979). Geothermal activity is widespread in Iceland and most intense near, as well as inside, the volcanic zone. It falls into two main groups based on the temperature at depth in the geothermal systems (BÖDVARSSON, 1961). By definition the temperature is higher than 200 °C in high-temperature

systems and lower than 150 °C in low-temperature systems. High-temperature fields are located inside the active volcanic zones and they can be used to generate electric power. Low-temperature fields are situated on both sides of these zones mostly in lowlands and valleys of the Quaternary and Tertiary strata. About 250 low-temperature fields and about 30 high-temperature are known at the present.

According to a hypothesis by Einarsson the geothermal water should be a part of the general ground-water flow from the highlands to the lowlands, heated due to flowing through hot rocks at depth in the Earth crust. The force driving the water through the crust was the hydrostatic pressure difference between the highlands and lowlands of Iceland (TÓMASSON, 1993). This model was based on the general hydrological considerations and assumed that the source of water supplied to the low-temperature systems was precipitation, infiltrated in the highlands interior. The ÁRNASON's (1977) interpretation of the deuterium content of the mean annual precipitation in Iceland supports Einarsson's model.

In the light of geological, geophysical and geochemical data compiled over the last few decades it is clear that the interpretation of any particular geothermal system has to take into account all available data from the area. This is especially true for the stable isotope interpretation of groundwater flow. It is considered questionable to use deuterium values in present-day precipitation to obtain information on the recharge areas to the various geothermal sites, without taking into account other available hydrogeological data from the area.

Data on permeability and temperature in deep wells in several low-temperature geothermal systems in Iceland indicate that these systems are transient and represent groundwater convection through young fractures. Thus, the heat source to the system is local and the hot rock is made permeable by active fracturing (SVEINBJÖRNSDÓTTIR et al., 1995). This contradicts the general model of the low-temperature geothermal systems described above.

One of the tools to study a geothermal field in detail is reservoir modelling by mathematical models. The optimal production strategy of a geothermal field cannot be obtained without using a good performing reservoir model. It should give a clear picture of all physical and chemical parameters of a reservoir and obtained results should be comparable to the field measurements. The past, present and future exploitation of the geothermal field must comply with the created model. All plans to change the production rate from a reservoir should be carefully confronted with it. The drilling of new boreholes, their situation and casing design, possible reinjection

options for recovering the water level, changes in the chemical concentration and heat losses due to interaction with another aquifer should be taken into consideration, only after addressing the reservoir model. As a final result, it should reward its users giving them the best economical solution.

This paper is a summary of the author's results obtained during geothermal training programme at the United Nations University in Iceland in the field of reservoir engineering.

2. The main features of the Laugarnes geothermal field

2.1. Locality

The Laugarnes low-temperature field is located inside Reykjavik, in SW part of Iceland (Figure 1). The elevation of the area ranges from 15 to 40 m above sea level. It is one of the three major geothermal areas within a radius of 6 kilometres from the centre of Reykjavik. The others are the Ellidaár and Seltjarnarnes fields (Figure 1). Geothermal water from these areas is highly suitable for direct use because of low content of dissolved solids and, therefore, it can be piped directly into radiators for space heating. These three areas have been heavily exploited during the last 20-30 years (TÓMASSON, 1993). During 1991 the average production from the Seltjarnarnes area was about 35 l/s of 105 - 110 °C water, the average production from the Laugarnes area was 167 l/s of 127 °C water and the average production from the Ellidaár area was 113 l/s of 87 °C water. Since 1957 a total of 48 deep wells with depths ranging from 600 to 3 085 m have been drilled in the Reykjavik geothermal areas and in their neighbourhood, in addition to about 70 shallower wells.

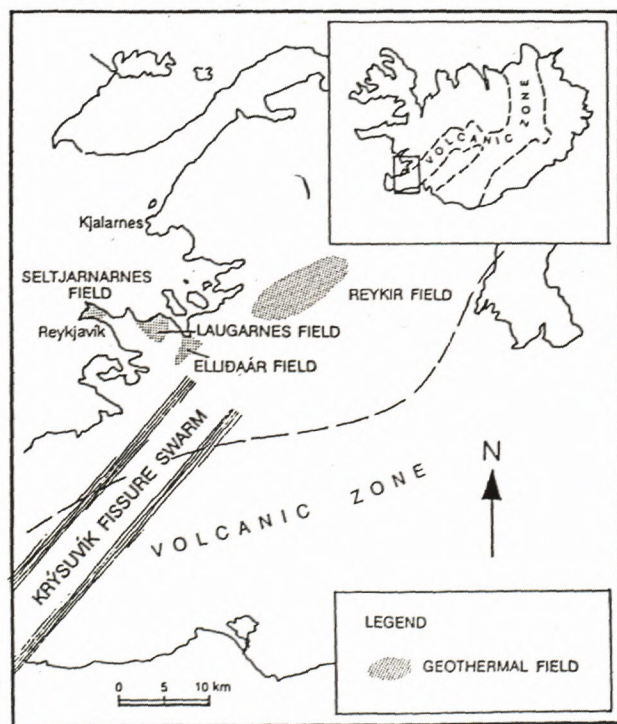


Fig. 1 General location of the Laugarnes geothermal field (KEPINSKA, 1994)

2.2. Hydrogeothermics

The Reykjavik area lies 8-10 km N of the volcanically active Reykjanes rift zone. It is located in Plio-Pleistocene volcanics on the S outskirts of the Kjalarnes central volcano (FRIDLEIFSSON, 1973).

The Reykjavik area is covered by horizontal olivine tholeiite basalts of late interglacial age, down to a depth of 30-50 m (THORSTEINSSON - ELIASSON, 1970).

Underneath this lava flow there are found up to 60 m thick, mostly marine sediments, overlaying a major discordance. Beneath, alternating lavas and hyaloclastites occur. This sequence is of Plio-Pleistocene age. Thick hyaloclastite formations are common in the upper 500 - 1 000 m, but basaltic lavas are predominant in the lower parts of the wells, which are commonly up to 2 km deep.

The Plio-Pleistocene strata in the Laugarnes area appear to dip at 3-12° to the SE (THORSTEINSSON - ELIASSON, 1970). These strata occur at 250 - 300 m lower elevation in wells of the Ellidaár area.

Aquifers are predominantly found where lavas contact hyaloclastites. The Laugarnes geothermal field has been found to be fed by three aquifers (THORSTEINSSON - ELIASSON, 1970). **Aquifer A** with water of 110 - 120 °C extends from 250 - 650 m, **aquifer B** with water of 135 °C from 730 - 1 250 m and **aquifer C** with water temperature of 146 °C, below 2 150 m. Tufts and sediments act as aquicludes between the aquifers while scoriaceous and fractured contacts between individual lava flows are permeable. Because each lava flow is a lens between overlying and underlying flows, the permeable zones within each aquifer are not continuous but may merge with those of adjacent flows. Aquifer B is the main aquifer with a contribution of 80 %. Mixing of these waters yields an average well discharge temperature of 125 - 130 °C.

The recharge area of the Laugarnes field has been mapped by deuterium (ÁRNASSON, 1977). By comparing the deuterium content of the precipitation in Iceland to that of the geothermal water, the Langjökull area has been shown to provide the recharge for the Laugarnes geothermal field.

As in the Laugarnes field, aquifers in the Ellidaár field occur at contacts between hyaloclastites and lavas. The Ellidaár field is fed by at least two different groundwater systems. The N part of the Ellidaár field is probably fed by the same recharge area as the Laugarnes field. The other recharge area for the S part of this geothermal field is most likely E of Reykjavik, at a distance of less than 45 km (ÁRNASSON - TÓMASSON, 1970; TÓMASSON et al., 1975).

TÓMASSON et al. (1975) described the results from measured surface thermal gradients in shallow drillholes in Reykjavik. The high surface thermal gradients inside the thermal areas are due to localised transport of water from the thermal systems at depth to the surface. This is best demonstrated in the Laugarnes field, where the highest surface gradients are measured (400 °C/km). Prior to exploitation about 10 l/s of 88 °C water issued in free flow from thermal springs in that area, whereas, only minor natural thermal activity was found in the other areas in Reykjavik. There is very little, or no transport of water from depths in the rocks between the thermal areas, and the depth of the gradient drill holes (at least down to several hundred meters) has little influence on the measured gradient outside the thermal fields. The

surface gradient of 0 °C/km to the SE of the thermal areas is due to cold groundwater penetrating young volcanic rocks. This cold groundwater zone has been found to reach down to 750 m (measured in a hole 986 m deep) in the volcanic zone 11 km S of the Ellidaár field (PÁLMASSON, 1967).

Outside the thermal fields the thermal gradient is about 100 °C/km. The reverse temperature gradients found in the Ellidaár and Reykir fields can only be accounted for by the circulation of cold water at depth. This cooling effect might be similar to the surface cooling effect observed SE of Reykjavík.

The Reykjavík geothermal fields appear to be separated by hydrogeological barriers. Production from one of the field does not effect the water level in the other two. In addition, the temperature, isotopic composition and the geochemistry of the water differ in the three fields. Shallow wells (less than 300 m deep) between the fields exhibit much lower temperature gradients than those measured within the Reykjavík geothermal fields. The geothermal fields therefore appear as thermal anomalies (TÓMASSON et al., 1975).

2.3. Production history and utilization

The Laugarnes field is the first geothermal field in Iceland utilized for public district heating. Up to 1958 the production was only by free flow from wells but after 1964 the production has been covered entirely by down-hole pumps. The rate of free flow from the field was some 20 - 40 l/s before pumping started but the average production in the years 1965 - 1993 has been about 167 l/s. An enhancement in production by a factor of 4 to 8 was, therefore, obtained by the introduction of down-hole pumps in the Laugarnes field. It should be noted that the production rate during the 30 years of pumping has been relatively constant and that the pressure (water level) in the reservoir has also been relatively stable during the pumping period (STEFÁNSSON et al., 1995).

The exploitation of geothermal water in the Laugarnes field was begun in 1928 - 1930 by the drilling of 14 small diameter wells near the Thvottalaugar hot spring. The depth of the deepest well was 246 m; collectively, the wells yielded 15 - 20 l/s at a temperature of 95 °C, as compared to 5 - 10 l/s previously issuing from the spring.

Drilling was resumed, first in 1940 by drilling of two wells down to 650 and 760 m, respectively, at Thvottalaugar and at Raudará, and again in 1956 - 1959 by drilling of 16 wells, 260 - 696 m deep, 1 - 2 km W of the Thvottalaugar wells. The aggregate flow from these wells in 1959 was about 60 l/s, 90 - 98 °C. During the drilling phase of 1959 - 1963, 22 wells were drilled by the rotary method to depths of 650 - 2 198 m. The individual well flow rates ranged from 1 l/s to more than 50 l/s. Five additional deep wells have since been drilled, in 1968 and 1969, and 1978 - 1982, to depths ranging between 1 359 and 3 085 m, one of them, the RV-34, being the deepest well in Iceland.

The wells are of the open hole type. Casing is cemented in place to a depth required to prevent collapse of unconsolidated shallow formations and exclude surface waters and the hole left open below the casing point. Well data of supply wells and principal observation wells are given in Table 1.

Up to the year 1960, when deep-well turbine pumps were first installed, withdrawal of water from the wells was by flow on the head. Since 1967, however, it has been exclusively through deep-well turbine pumps from 11 supply wells. Prior to 1962, flow rates were estimated

from periodic flow measurements but have since then been metered.

Withdrawal rates were relatively uniform during the period 1957-1962, when the withdrawal was predominantly by flow on the head but those subsequent to 1962 vary according to seasonal demand, being about three times as heavy in the winter season, October until March, than in the warmer season, April until September.

An investigation on the response of the piezometric surface in the area to increased pumping was begun in 1965 and continued through 1969. The investigation was conducted by automatic water stage records and by periodic measurements of water levels in non-pumping observation wells.

The oldest and by far the biggest district heating service in Iceland is Hitaveita Reykjavíkur (Municipal District Heating Service of Reykjavík), which supplies about 60 % of all geothermal water used in Iceland for district heating. Currently it supplies water for space heating and domestic use for Reykjavík and all neighbouring communities (150 000 inhabitants). Hitaveita Reykjavíkur uses three low-temperature fields: the Reykir field about 20 km NE of Reykjavík and two fields inside the town, those of Laugarnes and Ellidaár. Since 1990 Hitaveita Reykjavíkur also utilizes the Nesjavellir high-temperature field, 30 km E of Reykjavík, which currently provides about 18 % of the geothermal energy used by the district heating service.

The Laugarnes field has been exploited by the Hitaveita Reykjavíkur since 1928. Up to the present, more than 50 deep water wells have been drilled in the area producing hot water up to 130 °C. The wells are not all connected to the water supply system due to reasons such as: they are too shallow, the water temperature is too low or the water yield of the wells is too small. Besides, some of the production wells have been taken off-line as an increasing amount of dissolved salts (sea water) in the geothermal water has caused depositions in downhole pumps. The yearly average production from this area since 1962 is shown in Figure 2.

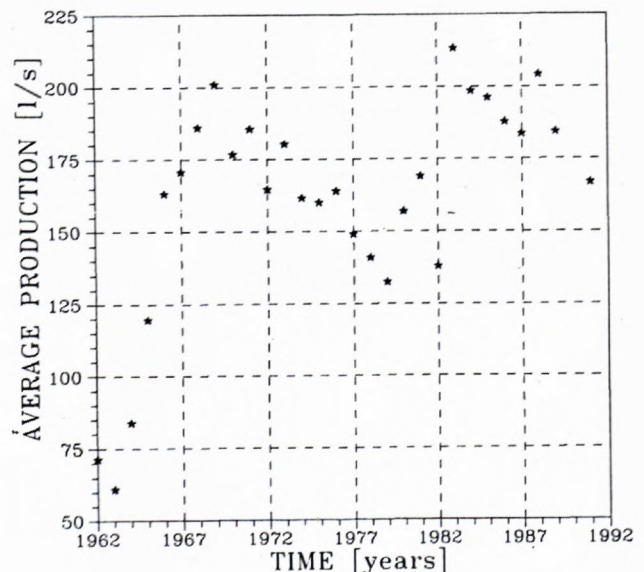


Fig. 2 The yearly average production from the Laugarnes geothermal field

3. Distributed parameter model for the Laugarnes geothermal field

In recent years, particularly during the last decade, the use of geothermal reservoir modelling has grown significantly. Modelling has turned out to be a very effective method for analysing data from geothermal reservoirs, as well as for estimating a geothermal field's future behaviour and its production potential. Numerous quantitative models have been developed for different geothermal fields all over the world (BÖDVARSSON et al., 1986).

In a broad sense, geothermal reservoir models can be divided into two categories:

1. **Simple models** are in many cases adequate idealisation of real situations (GRANT et al., 1982). They have a great advantage of being simple, they do not require the use of large computers and they are inexpensive to use. But simple models can neither consider spatial variation in the properties and parameters of a reservoir nor its internal structure. According to their methods of calculation, simple models can be further divided into two subcategories:

a. **distributed analytical models** in which, for example, the pressure response is given by an analytical function;

b. **lumped parameter models** that use very few blocks to represent the geothermal system. It does not consider the internal distribution of mass and energy. Usually, it is used as a first stage in a modelling process and for

checking the results of more complex modelling. The main disadvantage of the lumped model is that it does not consider fluid flow within the reservoir, and does not consider spatial variations in reservoir properties and conditions. Usually, it is very useful for predicting the reservoir responses of single-phase geothermal fields.

2. **Numerical models** are very general mathematical models that can be used to simulate geothermal reservoirs in as much detail as desired. If only a few grid blocks are used, one has the equivalent of a lumped parameter model, but several hundred or thousand grid blocks can be used to simulate entire geothermal systems. But detailed numerical modelling of a geothermal reservoir is time consuming, costly and requires large amounts of field data. Numerical models can be further divided into two subcategories:

a. **natural-state models** developed for studies of the natural (unexploited) behaviour of geothermal systems;

b. **exploitation models** developed for studies of geothermal reservoirs under exploitation (BÖDVARSSON et al., 1986).

Numerical models allow a much more detailed description of a reservoir system and the different flow regimes that occur in the system. They can be used to simulate the entire geothermal system, including reservoir, caprock, bedrock, shallow cold aquifers, recharge areas, even tectonic structures. In general, it is necessary to use numerical models for a complete, realistic solution of geothermal problems. They are used in the case of two-phase reservoirs and in cases where large variations in temperature, or pressure conditions prevail.

Tab. 1: Well data in the Laugarnes field

| Well no. | Year completed | Elevation [m a.s.l.] | Depth of well [m] | Depth of casing [m] | Temperature of water [°C] |
|----------|----------------|----------------------|-------------------|---------------------|---------------------------|
| RV-01 | 1962 | 12.04 | 1067 | 70 | - |
| RV-02 | 1958 | 20.86 | 650 | 30 | - |
| RV-03 | 1958 | 27.03 | 732 | 71 | - |
| RV-04 | 1959 | 15.48 | 2198 | 69 | 135 |
| RV-05 | 1959 | 15.07 | 741 | 68 | 130 |
| RV-06 | 1959 | 27.63 | 765 | 99 | - |
| RV-07 | 1959 | 16.90 | 752 | 94 | - |
| RV-08 | 1960 | 11.01 | 1397 | 91 | - |
| RV-09 | 1959 | 27.06 | 862 | 90 | 128 |
| RV-10 | 1959 | 15.87 | 1306 | 92 | 130 |
| RV-11 | 1962 | 25.72 | 928 | 112 | 130 |
| RV-12 | 1962 | 17.74 | 1105 | 94 | - |
| RV-13 | 1962 | 17.10 | 975 | 100 | - |
| RV-14 | 1962 | 4.28 | 1026 | 101 | - |
| RV-15 | 1962 | 24.72 | 1014 | 112 | 126 |
| RV-16 | 1962 | 16.78 | 1300 | 256 | - |
| RV-17 | 1963 | 21.59 | 634 | 93 | 122 |
| RV-19 | 1963 | 28.09 | 1239 | 79 | 128 |
| RV-20 | 1963 | 26.11 | 764 | 87 | 129 |
| RV-21 | 1963 | 24.74 | 978 | 112 | 129 |
| RV-22 | 1963 | 30.36 | 1583 | 83 | - |
| RV-25 | 1968 | 29.50 | 1647 | 79 | - |
| RV-32 | 1969 | 42.00 | 1359 | 100 | - |
| RV-34 | 1978 | 33.00 | 3085 | 328 | 123 |
| RV-35 | 1979 | 17.00 | 2857 | 276 | 119 |
| RV-38 | 1982 | 16.50 | 1488 | 325 | 128 |
| H-16 | 1943 | 12.36 | 770 | 17 | - |
| H-18 | 1956 | 8.42 | 697 | 19 | - |
| H-19 | 1956 | 10.20 | 471 | - | - |
| H-27 | 1959 | 14.98 | 403 | 31 | 109 |
| H-29 | 1959 | 19.82 | 249 | 33 | - |
| H-32 | 1961 | 33.27 | 606 | 32 | - |
| H-34 | 1961 | 7.00 | 399 | - | - |

In both cases, the models can only be as good as the data upon which they are based. Substantial monitoring programs are, therefore, essential.

3.1. Results from the calibration

Distributed parameter model for the Laugarnes geothermal field was created by AQUA programme package developed by Vatnaskil Consulting Engineers (1991) to solve the groundwater flow and mass transport by differential equations using the Galerkin finite element method with triangular elements. The model is two dimensional.

The total surface area covered by the mesh is about 67.95 km². The pumping area is located in the middle of the modelling area. The model was created with 1 356 nodes and 2 627 elements. Thus, the boundaries are taken far enough away to avoid their influence on the solution. Boundary conditions for the distributed groundwater flow model are established based on resistivity and

water level measurements. The no-flow boundary was established around the whole Laugarnes area and only a small part in the SE area was used as boundary with constant potential. The boundary conditions which were used for the distributed model are shown in Figure 3. As for the initial state, prior to production it was assumed that the reservoir water head was constant.

The production rates are taken as a monthly average for each supply well from 1962 - 1991. The initial values for transmissivity and storage coefficient are taken from the results of well tests. A number of tests have been made in wells in the Laugarnes area in order to determine values of the aquifer constants, transmissivity and storativity, and to locate impervious boundaries believed to exist between the three hydrothermal systems. The tests were conducted by observations of water levels in observation wells after a supply well was turned off or on, correction being made for previous trends in water levels. Because of variation in demand, the tests are of short duration, usually less than 10 - 20

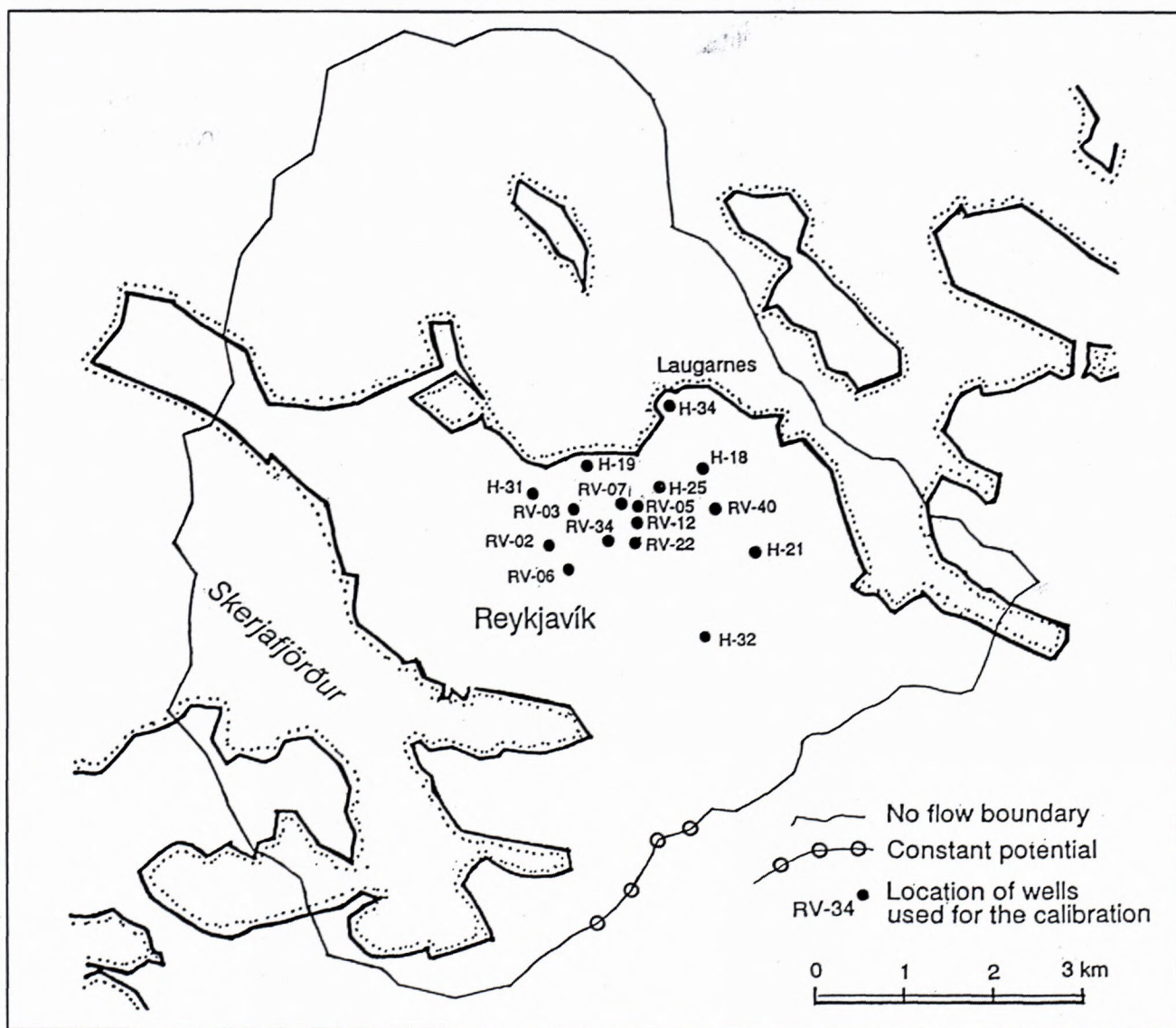


Figure 3: Boundary conditions of the model (FENDEK, 1992)

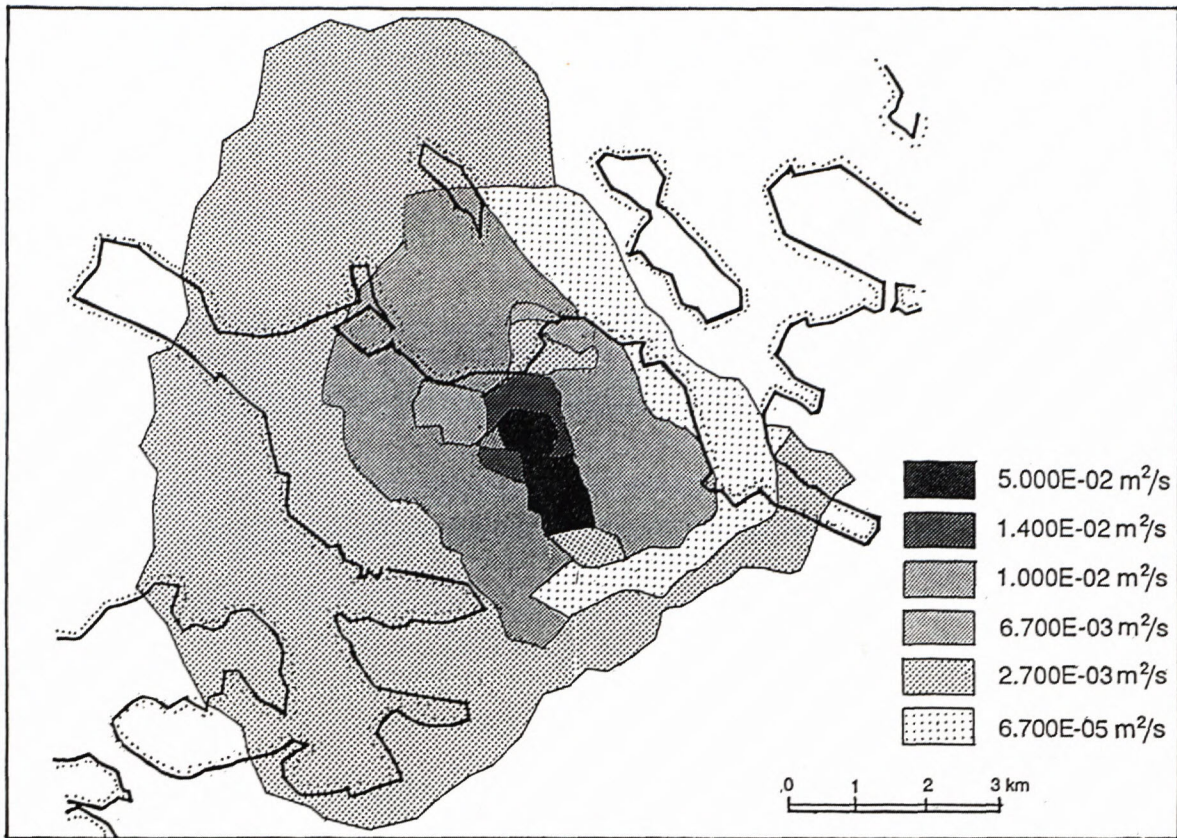


Figure 4: Map of transmissivity in the vicinity of wells (FENDEK, 1992)

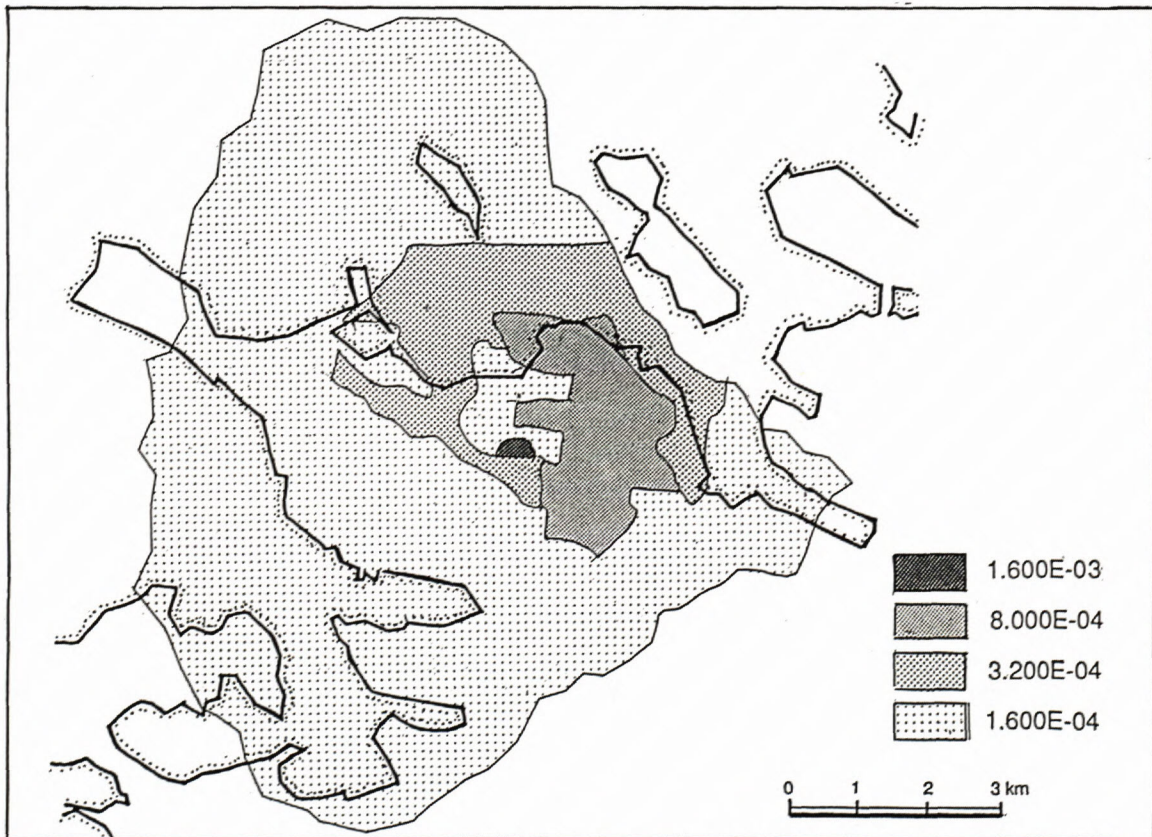


Figure 5: Map of storage coefficient (FENDEK, 1992)

hours and are interfered with by operating supply wells, the discharge of which varies somewhat by variations in water level. Analysed by the THEIS nonequilibrium method, the test data gave values ranging from 3.5×10^{-3} to $8.8 \times 10^{-3} \text{ m}^2/\text{s}$ for the **coefficient of transmissivity** and 3.9×10^{-5} to 3.2×10^{-4} for the **coefficient of storage** (THORSTEINSSON - ELIASSON, 1970).

The transmissivity, storage coefficient, anisotropy and porosity are determined by matching observed and calculated reservoir response. The **transmissivity** in the area covered by the model varies from 5.0×10^{-2} to $6.7 \times 10^{-5} \text{ m}^2/\text{s}$. The low value for transmissivity is obtained along the NE boundaries of Laugarnes area and the highest value is obtained in the centre of this area (Figure 4).

The calibration started with the value of the **storage coefficient** in the range of 1.6×10^{-3} to 1.6×10^{-4} (Figure 5).

The long term effect of the exploitation was analysed, so the elastic storage coefficient and the delayed yield effect were taken into account. It was assumed that **porosity** of the reservoir is in the range of 0.0111-0.0108 and the time constant 6 500 days.

The **leakage coefficient** in the centre area was taken to be in the range of 6×10^{-11} to $9 \times 10^{-12} \text{ s}^{-1}$ and around the main production area the value of zero (0) was used (Figure 6) because almost no influence on temperature from the cold water recharge from above was observed.

Anisotropy is determined by anisotropy angle and by the ratio between transmissivity in x (T_{xx}) and y (T_{yy}) directions equal to 0.0999. **Anisotropy angles** range from 50 degrees in the W and S part of Laugarnes area to 120 degrees in the centre and NE part of the area (FENDEK, 1992).

For the calibration of the model the measured data from 16 wells were used. The areal distribution of these

wells is shown in Figure 3. The example of results from the calibration is shown in Figure 7. The best results were obtained for observation well RV-07. A good fit between measured and calculated drawdown values was obtained with the model for wells which are inside the main production area (RV-05, RV-34, RV-11, RV-22, H-25, H-19, RV-03, RV-06 and RV-02). A slightly worse fit between measured and calculated drawdown values was obtained with the model for wells which are around this production area (H-34, H-18, RV-40, H-21, H-32, H-31) (FENDEK, 1992). The depth of these wells ranges from 249 - 770 m (Table 1 refers), they are relatively shallow and produce geothermal water from the top of the reservoir. This can be the reason why better results are not obtained with the two-dimensional AQUA model for these wells.

Mass transport calculations can be used to estimate leakage coefficient and aquifer thickness. By fitting the calculated and measured values of silica concentration, the above-mentioned parameters can be calculated. Several measurements of silica concentration exist from each production well.

The silica content decreased due to the production (HETTLING, 1984) and the induced leakage from above. The model parameters used for solving the mass transport of silica are as follows:

- average initial concentration: 160 mg/l
- average concentration in the top aquifer: 22 mg/l
- a_T/a_L : 0.16
- longitudinal dispersivity (a_L): 80 m
- molecular diffusion: $10^{-8} \text{ m}^2/\text{s}$
- aquifer thickness: 800 m

The concentration calculated with the model shows the same decreasing trend (Figure 8).

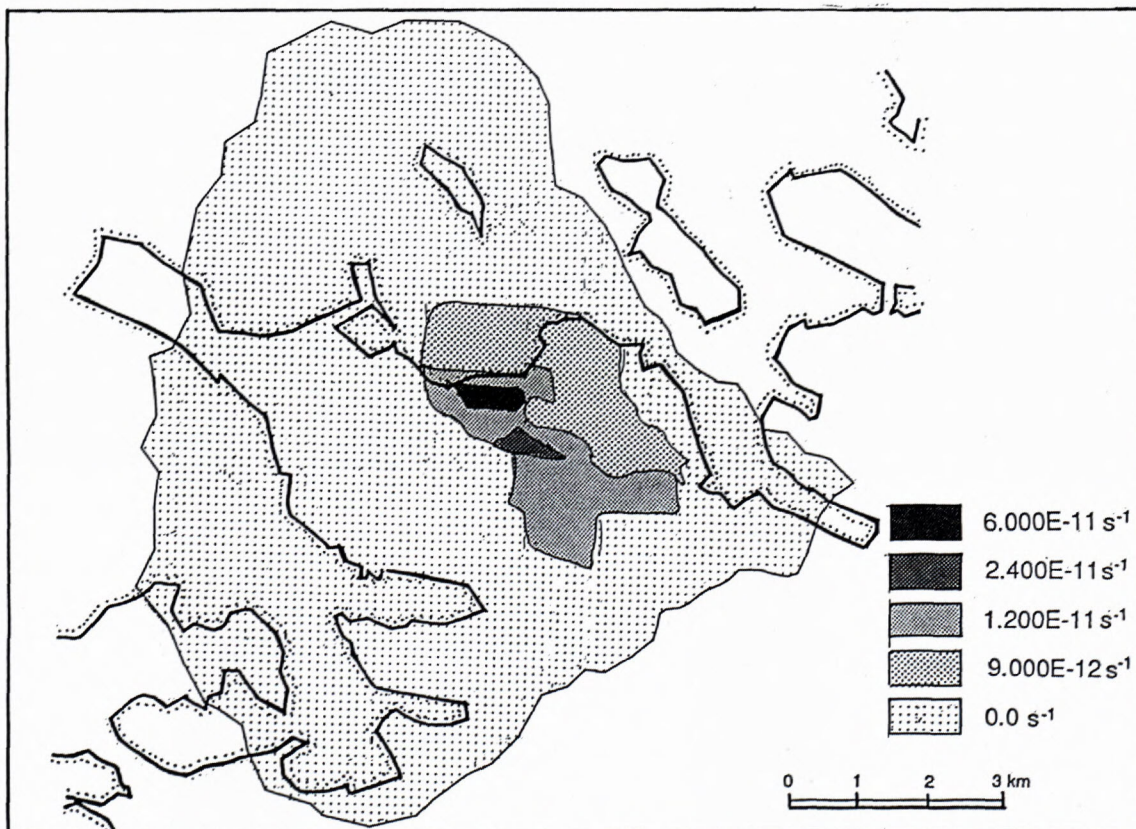


Figure 6: Areal distribution of leakage coefficient (FENDEK, 1992)

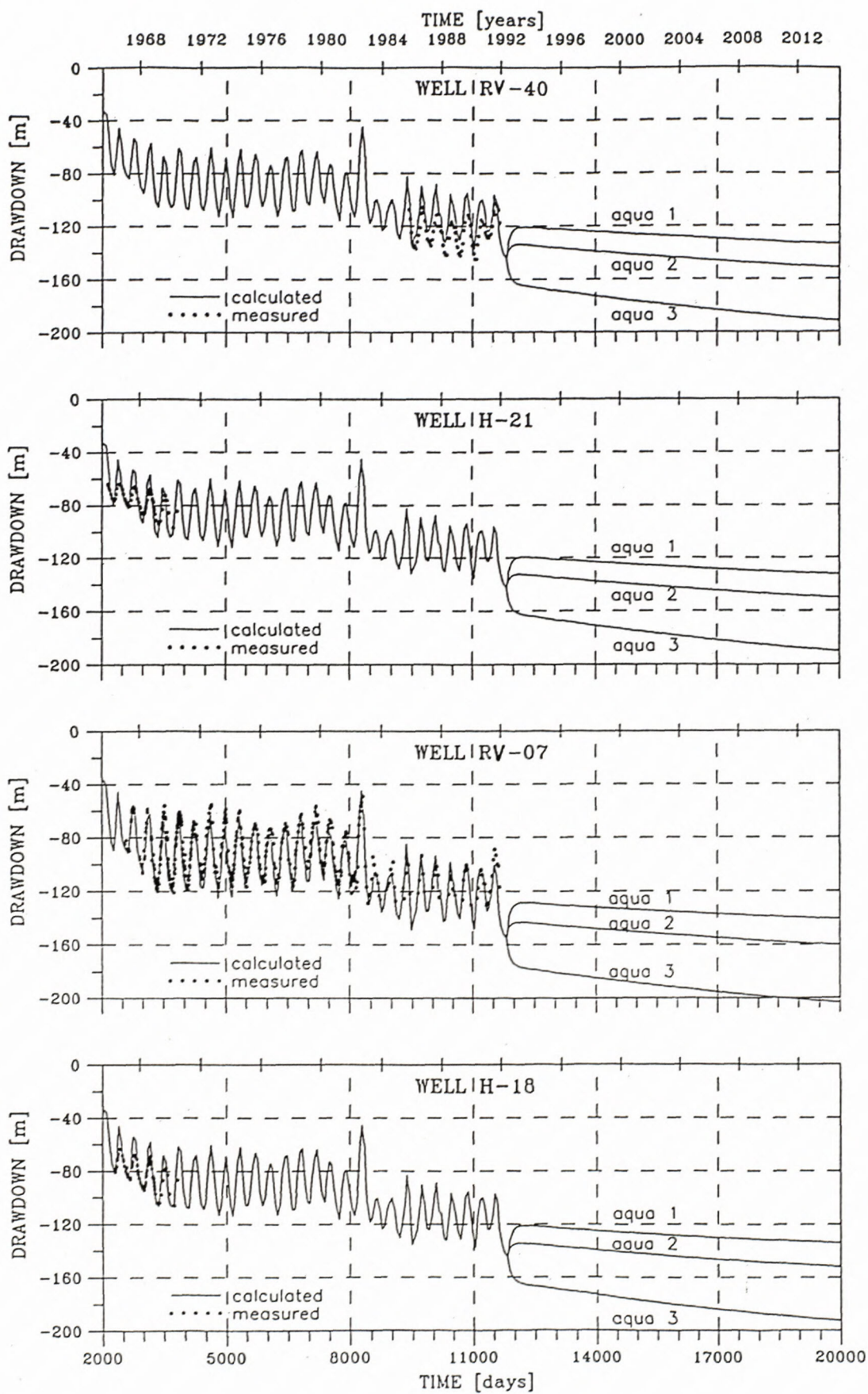


Figure 7: Measured, calculated and prediction drawdown for some wells (FENDEK, 1992)

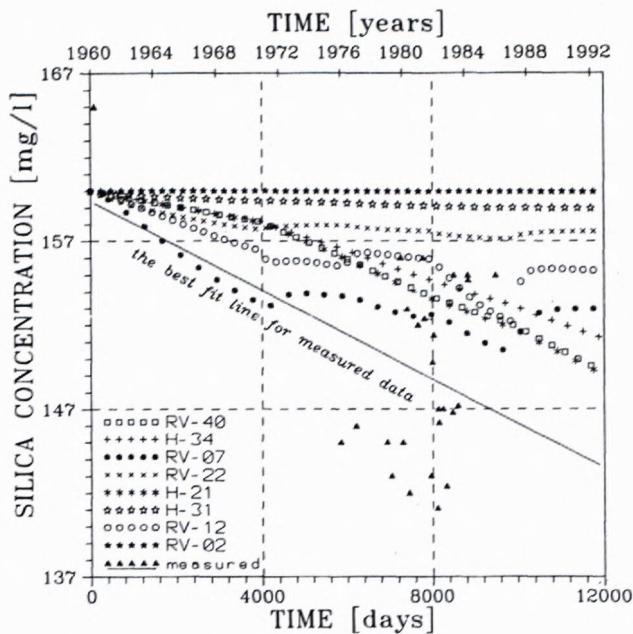


Figure 8: Example of silica concentration decline in some wells (FENDEK, 1992)

3.2. Future prediction of the reservoir response

After calibration, the model was used to calculate the drawdown until the end of the year 2012. As a starting point for future prediction the reservoir state as of 1992 is taken. The calculations were made with three different production rates which are shown in Table 2 for each supply well.

Table 2 : Future predictions for the yearly average production [l/s]

| Well no. | aqua 1 | aqua 2 | aqua 3 |
|----------|--------|--------|--------|
| RV-05 | 53.0 | 53.0 | 65.0 |
| RV-09 | 4.4 | 7.0 | 10.0 |
| RV-10 | 12.5 | 15.0 | 20.0 |
| RV-11 | 20.6 | 25.0 | 30.0 |
| RV-15 | 13.2 | 16.0 | 20.0 |
| RV-17 | 10.9 | 12.0 | 15.0 |
| RV-19 | 21.2 | 25.0 | 30.0 |
| RV-20 | 15.6 | 24.0 | 33.3 |
| RV-21 | 30.8 | 30.0 | 45.0 |
| RV-35 | 7.1 | 7.0 | 11.0 |
| RV-38 | 10.0 | 20.0 | 30.2 |
| Total: | 199.3 | 234.0 | 309.5 |

The production rates under column aqua 1 represent the average production for the last year (1991), which totals 199.3 l/s for all wells. The values under column aqua 2 indicate that the average production is increased by 17.4 % (total of 234 l/s) when compared to that of the actual values in the column under aqua 1. Furthermore, the values under column aqua 3 give the highest values for yearly average production rate and the total of 309.5 l/s is 55.5 % higher than the values in aqua 1. The calculation results for the future predictions are shown in Figure 7. All calculated curves of future drawdown show a lowering trend. The obtained drawdown is between 110 - 190 m with a corresponding total yearly average production of 199.3 -

309.5 l/s respectively. The results mentioned above are yearly average values and do not take into account the seasonal changes in production.

4. Results and conclusions

The prime objective of this paper was to create a model approximating the natural conditions of the Laugarnes geothermal field, using the field data for the last 30 years.

Through this model, the reservoir parameters and features of the field were described and some predictions of its future behaviour were made. All available geological, geophysical and geochemical information, along with field measurement data were collected and carefully studied to understand how all these factors contributed to the overall picture of the geothermal reservoir.

The study of the Laugarnes geothermal reservoir, applying the distributed model, presents results that are very close to the measured field data. This indicates a correct approach and that the model is reliable for similar reservoir modelling and future forecasting. However, as the methods use only linear functions in their mathematical models, the effects of turbulence and skin impact are not taken into account. This means that the drawdown values in close proximity to the pumping wells cannot always be considered accurate.

The measurements from the field indicate higher values of SiO₂ in 1962. Over the production period of 30 years, the effects of water discharge are observed very clearly with a lowering of the water level and decline of the SiO₂ content.

For the calibration of the model, the measured data from 16 wells were used. Good fit with the model for drawdown, using the equation for delayed yield, shows that the reservoir is controlled by two different storage mechanisms. At the start of production, storage is controlled by liquid/formation compressibility with characteristic values for the confined aquifers ranging from 1.6×10^{-3} to 1.6×10^{-4} . In later production, the storage coefficient is controlled by the mobility of the free surface with a value of approximately 0.011, which is near to the effective porosity. The transmissivity in the area covered by the model varies from 5.0×10^{-2} to 6.7×10^{-5} m²/s. The leakage coefficient in the centre area was taken to be in the range of 6.0×10^{-11} to 9.0×10^{-12} s⁻¹ and around the main production area the value of zero was used.

From the trend of the measured and calculated curves for the drawdown obtained from distributed groundwater flow model, it is quite obvious that with present production no steady-state conditions in the reservoir can be reached until the year 2012. The obtained drawdown is between 110 - 190 m with a corresponding total yearly average production of 199.3 - 309.5 l/s respectively. So, the recharge in the system is much less than production for the present drawdown.

Acknowledgements:

The author would like to thank Dr. Ingvar Birgir Fridleifsson, the director of the United Nations University Geothermal Training Programme for providing excellent work conditions during the entire study. The author is grateful to Dr. Snorri Páll Kjaran and Sigurdur Lárus Hólm for supervising his study of reservoir engineering. Finally, the author is grateful to the late Dr. Tomáš Koráb, former director of the Dionýz Štúr Institute of Geology in Bratislava, for giving him the opportunity to participate in the UNU training programme.

References

- ÁRNASON, B. & TÓMASSON, J., 1970: Deuterium and chloride in geothermal studies in Iceland. *Geothermics*, Special issue, Vol.2, 1405-1415.
- ÁRNASON, B., 1977: Hydrogeothermal systems in Iceland traced by deuterium. *Geothermics*, Vol.5, 125-151.
- BÖDVARSSON, G., 1961: Physical characteristic of natural heat resources in Iceland. *Jökull* 11, 29-38.
- BÖDVARSSON, G.S., PRUESS, K. & LIPPMAN, M. J., 1986: Modelling of geothermal systems. *J. Pet. Tech.* (Sept. 1986), 1007-1021.
- FENDEK, M., 1992: Distributed parameter models for the Laugarnes geothermal field, SW-Iceland and the Central depression of Danube basin, S-Slovakia. UNU Geothermal Training Programme, Iceland, Report 5, 41 p.
- FRIDLEIFSSON, I. B., 1973: Petrology and structure of Esja Quaternary volcanic region, SW-Iceland. Unpublished Ph. D. Thesis. Oxford University.
- GRANT, M. A., DONALDSON, I. G. & BIXLEY, P. F., 1982: Geothermal reservoir engineering. Academic Press, New York, 369 p.
- HAMMONS, T. J., PÁLMASSON, G. & THORHALLSSON, S., 1991: Geothermal electric power generation in Iceland for the proposed Iceland/United Kingdom HVDC power link. *IEEE Transactions on energy conversion*. Vol. 6, No. 2, 289-295.
- HETTLING, H. K., 1984: The chemical and isotopic changes in the low temperature areas of Laugarnes, Ellidaár and Reykir. UNU Geothermal Training Programme, Report 3, Reykjavík, 52 p.
- KEPINSKA, B. 1994: The temperature distribution in the Seltjarnarnes field, SW-Iceland; The reservoir temperature in the Podhale field, S-Poland. Reports of the UNU Geothermal Training Programme, 1994, Iceland, Report 7, 151-182.
- PÁLMASSON, G., 1967: On heat flow in Iceland in relation to the Mid-Atlantic Ridge. *Societas Scientiarum Islandica*, Vol. 38, 111-127.
- PÁLMASSON, G., ARNÓRSSON, S., KRISTJÁNSSON, L., FRIDLEIFSSON, I. B., KRISTMANNSDÓTTIR, H., SAEMUNDSSON, K., STEFÁNSSON, V., STEINGRÍMSSON, B. & TÓMASSON, J., 1979: The Iceland crust: Evidence from drillhole data on structure and processes. In: Deep drilling results in the Atlantic ocean: Ocean crust. Maurice Ewig Series, Vol.2, Am. Geophys. Union, 43-65.
- SAEMUNDSSON, K., 1978: Fissure swarms and central volcanoes of the neovolcanic zones of Iceland. *Geol. I. Spec. Iss.* 10, 415-432.
- STEFÁNSSON, V., AXELSSON, G., SIGURDSSON, Ó. & KJARAN, S. P., 1995: Geothermal reservoir management in Iceland. Proceedings of the World Geothermal Congress, Florence, Italy, 1763-1768.
- SVEINBJÖRNSDÓTTIR, A. E., JOHNSEN, S. & ARNÓRSSON, S., 1995: The use of stable isotopes of oxygen and hydrogen in geothermal studies in Iceland. Proceedings of the World Geothermal Congress, Florence, Italy, 1043-1047.
- THORSTEINSSON, T. & ELÍASSON, J., 1970: Geohydrology of the Laugarnes hydrothermal system in Reykjavík, Iceland. *Geothermics*, Special issue, Vol. 2, 1191-1204.
- TÓMASSON, J., 1993: The nature of the Ellidaár geothermal area in SW-Iceland. *Geothermics*, Vol.22, No.4, 329-348.
- TÓMASSON, J., FRIDLEIFSSON, I. B. & STEFÁNSSON, V., 1975: A hydrological model for the flow of thermal water in southwestern Iceland with special reference to the Reykir and Reykjavík thermal areas. Second UN symposium on the development and use of geothermal resources, San Francisco, Proceedings, 643-648.
- Vatnaskil Consulting Engineers, 1991: AQUA user's manual. Vatnaskil, Reykjavík.



Slovenská geologická spoločnosť

Prírodovedecká fakulta Univerzity Komenského

Slovenská akadémia vied

Geologická služba Slovenskej republiky

100th
anniversary

Dimitrij Andrusov

Alpine evolution of the Western Carpathians and related areas

ALEWECA

International conference held at the occasion
of the 100th anniversary of the birth of
Dimitrij Andrusov

Bratislava

September 11-14th 1997

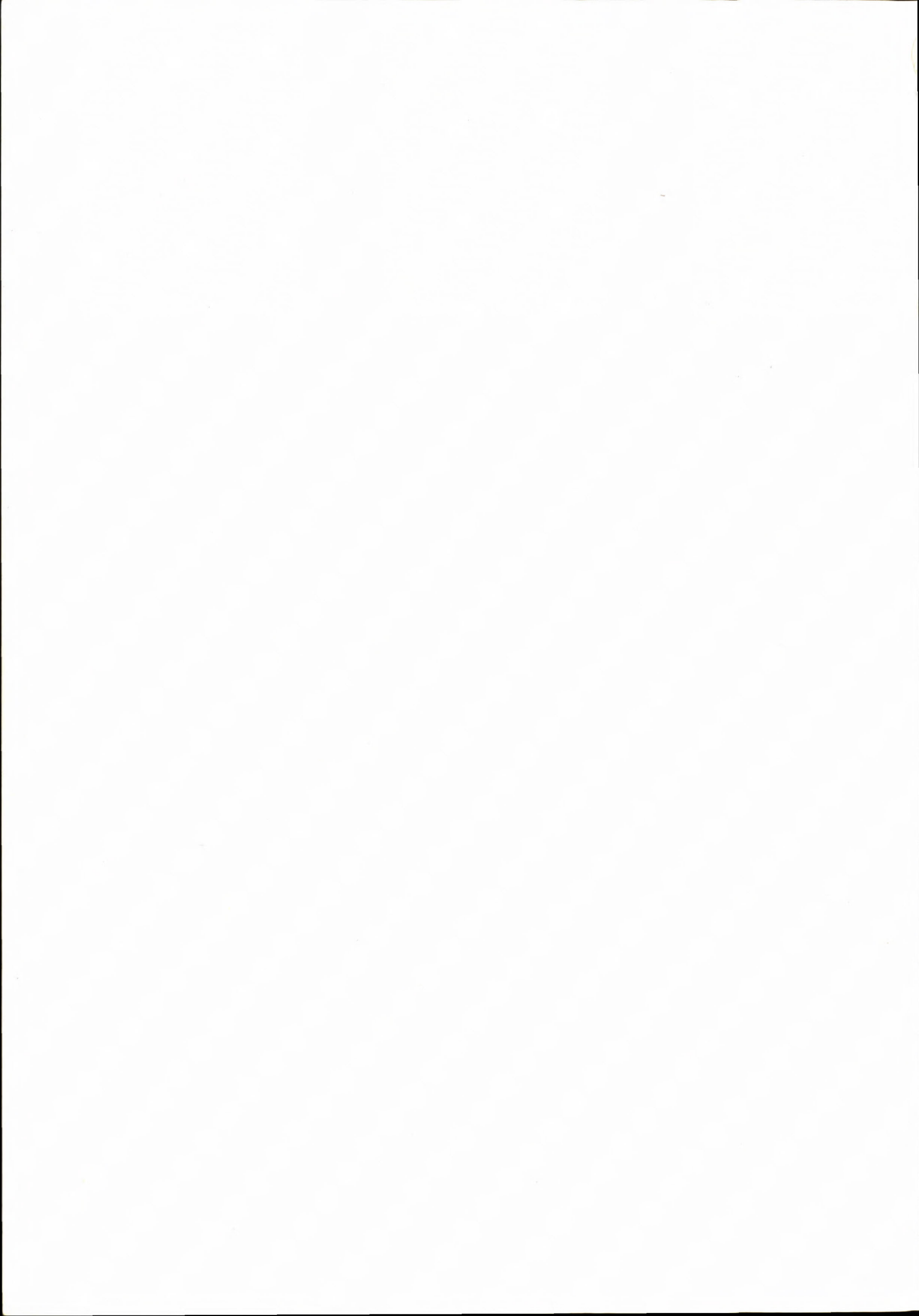
Informations :

Jozef Hók

Mlynská dolina 1

817 04 Bratislava

tel., 07 / 3705119 - fax: 07 / 371940 E-mail : HOK @ GUDS.SANET.SK



Instructions to authors

General instructions

The editorial Board of Geological Survey of Slovak Republic accepts manuscripts in English language.

The Editorial Board accepts or refuses a manuscript with regard to the reviewer's opinion. The author is informed of the refusal within 14 days from the decision of the Editorial Board. Accepted manuscript is prepared for publication in an appropriate issue of the magazine. The author(s) and the publishers enter a contract establishing the rights and duties of both parties during editorial preparation and printing, until the time of publishing of the paper.

Text layout

The text should be arranged as follows: full name of the author(s); title of the paper, number of supplements (in brackets below the title, e.g. 5 figs., 4 tabs.); key words - maximum 5 words arranged successively from general to special terms; abstract (max. 15 lines presenting principal results); in a footnote on the first page, name of the author(s), as well as his (their) professional or private address.

The text of the paper should be logically divided. For the purpose of typology, the author may use a hierarchic division of chapters and sub-chapters, using numbers with their titles. The editorial board reserves the right to adjust the type according to generally accepted rules even if the author has not done this.

Names of cited authors in the text are written without first names or initials (e.g. Štúr, 1868), the names of co-authors are divided (e.g. Mišík & Sýkora, 1981). The name(s) is followed by a comma. If there are more authors, the first one, or the first two only are cited, adding et al. and publication year.

Mathematical and physical symbols of units, such as %, ‰, °C should be preceded by a space, e.g. 60 %, 105 °C etc. Abbreviations of the units such as second, litre etc. should be written without a period. Compass bearings may be substituted by the abbreviations E, W, NW, SSE etc. Brackets (parentheses) are to be indicated as should be printed, i.e. square brackets, parentheses or compound. Dashes should be typed as double hyphens.

If a manuscript is typed, 2 copies are required, including figures. Required is A4 page size, 30 text lines with 60 characters, including spaces, typed with line spacing No. 2. The author should mark these parts of a text which should be printed in different type with a vertical line on the left side of the manuscript. Paragraphs are marked with 1 tab space from the left margin, or by a typographic symbol. Greek characters should be written by hand and followed by their description in parentheses, e.g. (sigma, omega, etc.). Indices and exponents should be properly marked.

If the text is delivered on a diskette (3.5" or 5.25"), it is necessary to send also one hard copy. The publishers shall accept the following text formats:

*.doc (Word for Windows 6.0), *.txt (DOS text formatted or unformatted, T602), *.wp5 (WordPerfect 4.2, 5.0, 5.1), *.wri (Write for Windows), *.602 (T602).

Tables and figures

Tables shall be accepted in a size of up to A4, numbered in the same way as in text.

Tables should be typed on separate sheets of the same size as text, with normal type. The author is asked to mark in the text where the table should be inserted. Short explanations attached to a table, should be included on the same sheet. If the text is longer, it should be typed on a separate sheet.

In contributions delivered on a diskette, tables may be written using a text editor (Word for Windows, Word Perfect, T602), or a spreadsheet (Quattro Pro, Excel) and delivered as a separate file. Characters in the table should not be less than 8 point large.

Figures should be presented in black-and-white, in exceptional cases also in colour. Figures are to be presented by the author

simultaneously with the text of the paper, in two copies, or on a diskette + one hard copy. Graphs, sketches, profiles and maps must be always drawn separately. High-quality copies are accepted as well. Captions should be typed outside the figure. The graphic supplements should be numbered on the reverse side, along with the orientation of the figures. Large-size supplements are accepted only exceptionally. Photographs intended for publishing should be sharp, contrasting, on shiny paper. High quality colour photographs will only be accepted depending on the judgement of the technical editors.

If a picture is delivered in a digital form, the following formats will be accepted: *.cdr, *.dxf, *.bmp, *.tiff, *.wpg, *.hpg. Other formats are to be consulted with the editors.

References

- list of references should only include papers cited in text
 - the items are to be listed alphabetically, with hanging indent in the second and following lines
- authors are to be cited with initials following the family name.

Example

Cícha I. & Seneš J., 1971: Probleme der Beziehung zwischen Bio- und Chronostratigraphie des jungeren Tertiärs. Geol. Zbor. (Bratislava), 56, 2, 529 - 640.

Matula M., 1969: Regional engineering geology of Czechoslovak Carpathians. 1. Ed. Mahel', M., Bratislava, Vyd. Slov. Akad. Vied, 225 p.

Andrusov D., Bystrický J. & Fusán O., 1973: Outline of the Structure of the West Carpathians. Guide-book for geol. exc. X. Congr. CBGA, Geol. Úst. D. Štúra, Bratislava, 5 - 44.

Manuscript

- proceedings should be cited as follows:
 1. family name and initials of author(s)
 2. publication year
 3. title of paper
 4. title of proceedings
 5. editor(s)
 6. place of publishing
 7. publishing house
 8. page range
 9. non published reports should be denoted "manuscript" and the place of archive should be given.

Proofs

The translator as well as the author(s) are obliged to correct the errors which are due to typing and technical arrangements. The first proofs are sent to author(s) as well as to the translator. The second proof is provided only to the editorial office. It will be sent to authors upon request.

The proofs must be marked clearly and intelligibly, to avoid further errors and doubts. Common typographic symbols are to be used, the list and meaning of which will be provided by the editorial office. Each used symbol must also appear on the margin of the text, if possible on the same line where the error occurred. The deadlines and conditions for proof-reading shall be stated in the contract.

Final remarks

These instructions are obligatory to all authors. Exceptions may be permitted by the Editorial Board or the managing editor. Manuscripts not complying with these instructions shall be returned to the authors.

1. Editorial Board reserves the right to publish preferentially invited manuscript and to assemble thematic volumes,

2. Editorial Board sits four times a year and closing dates for individual volumes will be on every 15th day of March, June, September and December.

3. To refer to our Magazine please use the following abbreviations: Slovak Geological Mag. No D. Štúr Publ. Bratislava.

Contents

| | |
|--|-----|
| KATERINOPOULOS A., KOKKINAKIS A. and KYRIAKOPOULOS K.: Mineralogy, Petrology and Chemistry of the Fotino Granitic Rocks, Thessaly, Central Greece _____ | 87 |
| ŠIMON L. and HALOUZKA R.: Pútikov vršok volcano - the youngest volcano in the Western Carpathians _____ | 103 |
| HALÁSOVÁ E., HUDAČKOVÁ N., HOLCOVÁ K., VASS D., ELEČKO M. and PERESZLÉNYI M.: Sea ways connecting the Fil'akovo/Pétervására Basin with the Eggenburgian/Burdigalian open sea ____ | 125 |
| KOVÁČ P. and HÓK J.: Tertiary Development of the Western Part of Klippen Belt _____ | 137 |
| JACKO S., SASVÁRI T., ZACHAROV M., SCHMIDT R. and VOZÁR J.: Contrasting styles of Alpine deformations at the eastern part of the Veporicum and Gemericum units, Western Carpathians ____ | 151 |
| FENDEK M.: Distributed Parameter Model for the Laugarnes Geothermal Field - SW Iceland _____ | 165 |